APPLICATION OF THE METHOD OF PARAMETRIC DIFFERENTIATION TO TWO DIMENSIONAL TRANSONIC FLOWS

by

Woodrow Whitlow, Jr.

S.B., Massachusetts Institute of Technology
(1974)

S.M., Massachusetts Institute of Technology
(1975)

SUBMITTED IN PARTIAL FULFILLMENT
OF THE REQUIREMENTS FOR THE
DEGREE OF DOCTOR OF PHILOSOPHY

at the

MASSACHUSETTS INSTITUTE OF TECHNOLOGY

September 1979

Signature of Author _____
Department of Aeronautics & Astronautics
August 17, 1979

Certified by _____
Thesis Supervisor

Certified by _____
Thesis Supervisor

Certified by _____
Thesis Supervisor

Certified by _____
Thesis Supervisor

Certified by _____
Thesis Supervisor

Accepted by _____
Chairman, Departmental Graduate Committee

APPLICATION OF THE METHOD OF PARAMETRIC DIFFERENTIATION TO TWO DIMENSIONAL TRANSONIC FLOWS

by

Woodrow Whitlow, Jr.

Submitted to the Department of

Aeronautics and Astronautics on August 17, 1979

in partial fulfillment of the requirements for the

degree of Doctor of Philosophy

ABSTRACT

The problem of unsteady, two dimensional transonic flow is investigated. The flow field is modeled using the small perturbation potential equation. Assuming that the unsteadiness can be treated as a linear perturbation about the steady state, the potential is separated into steady and unsteady components. This results in a nonlinear equation for the steady flow and a linear equation, coupled to the steady flow, for the unsteadiness. The problems presented by the nonlinearity of the mean flow are circumvented by differentiating the steady flow equation with respect to either the airfoil thickness ratio or the angle of attack. The nonlinear problem is then reduced to solving a set of ordinary differential equations and a linear partial differential equation with variable coefficients. A relaxation procedure is uniquely combined with predictor-corrector methods to calculate steady transonic flow fields for various airfoil thickness ratios and angles of attack; free stream Mach numbers less than unity are used in all cases. The data obtained using this method compares well with experimental data and data obtained using other prediction techniques. The steady flow data is used to determine the effects of varying the airfoil thickness ratio on the unsteady aerodynamic loads. If shock waves are present in the flow field, a compatability condition is introduced at the mean shock location to account for the effects of moving shock waves. By monitoring the amplitude of the shock motion, I am able to determine when the assumption that the unsteadiness is a linear perturbation about the steady state is violated. I also present analysis which provides me with an estimate of the maximum reduced frequency of the unsteady motion which leads to stable numerical solutions of the unsteady potential equation.

Thesis Supervisor: Wesley L. Harris
Title: Associate Professor of Aeronautics and Astronautics

Thesis Supervisor: Judson R. Baron
Title: Professor of Aeronautics and Astronautics

Thesis Supervisor: Eugene E. Covert
Title: Professor of Aeronautics and Astronautics

Thesis Supervisor: Jack L. Kerrebrock
Title: Professor of Aeronautics and Astronautics

Thesis Supervisor: Marten T. Landahl
Title: Professor of Aeronautics and Astronautics

ACKNOWLEDGEMENTS

The completion of any major project is very seldom the result of the efforts of a single individual, and credit should be given to those who took interest in and assisted the individual whose name adorns the the final report. Many thanks are due Professors Judson R. Baron, Eugene E. Covert, Jack L. Kerrebrock, and Marten T. Landahl for their helpful suggestions and criticisms throughout the course of this research effort. Dr. William T. Thompkins also deserves thanks for his valuable advice on numerical methods.

It is very difficult for a student to make a significant contribution to his field of specialty without a positive force to guide him. In this case, I would like to recognize the support and other intangibles given to me by Professor Wesley L. Harris - a close friend who happened to be my thesis chairman. Space does not permit me to list the many ways in which he has made my MIT experience a more meaningful and enjoyable one.

The role of the family cannot be overlooked, and I would like to begin by thanking my mother and father, Woodrow and Willie Mae Whitlow, for both their moral and financial support. I must give my heartfelt thanks to those who had to endure perhaps more than I - my wife, Michele, and daughters, Mary and Natalie. Michele deserves special praise for her financial and spiritual support and for typing this manuscript.

Special thanks are also due Dr. Jerry Bryant and Earnestine Bryant for helping me to keep the entire MIT experience in perspective. The following friends also deserve mention: Ali Ahmadi, Briggette Bailey,

Dale Carlson, Song Young Chung, Austin Harton, James Hubbard, N. Humbad, Kenneth Leighton, Luiz Lima, Rudolph Martinez, Dr. Tom Matoi, and Karen Scott. Gloria Payne deserves special thanks for her efforts.

The National Aeronautics and Space Administration (NASA) supported this work under NASA Grant NSG 1219, Dr. Samuel Bland, Technical Monitor. The stimulating discussions with NASA employees Dr. E. C. Yates and Dr. Perry Newman are greatly appreciated. Some financial assistance was also obtained from the Office of the Dean of the Graduate School at MIT. All computations were performed at the MIT Information Processing Center as Problem M12702.

TABLE OF CONTENTS

LIST OF SYMBOLS

a - Speed of sound

b - Exponent of M in the nonlinear term of the steady potential equation

c - Airfoil chord length

C_p - Pressure coefficient

C_p^* - Critical pressure coefficient

C_L - Lift coefficient

$C_{m_{LE}}$ - Moment coefficient about the airfoil leading edge

f - $\frac{d\xi}{dx}$

$\mathcal{F}(x)$ - Mean airfoil position

$f_1(x,t)$ - Perturbation about the mean airfoil position

g - $\frac{\partial \phi}{\partial \tau}$ or $\frac{\partial \varphi}{\partial \alpha}$

h - $\frac{d\eta}{dz}$

i - $\sqrt{-1}$

$\hat{i}$ - Unit vector in the streamwise direction

k - $\frac{\omega c}{U}$

$\hat{k}$ - Unit vector in the direction normal to the free stream

M - Free stream Mach number

P - Pressure

Q - Magnitude of the velocity vector

$\bar{Q}$ - Velocity vector

R - Gas constant

S - Specific entropy

T, t - Time

$\underline{T}$ - Temperature

$\bar{u}$ - Velocity vector

U - Free stream velocity

$X, \bar{X}$ - Unstretched coordinates in the streamwise direction

X_s - Instantaneous shock wave position

ΔX_s - Shock excursion amplitude

X_m - Mean shock wave position

z, Z - Unstretched coordinates in the direction normal to the free stream

$\bar{z}$ - βz

α - Angle of attack

α_m - Mean angle of attack

β - $\sqrt{1-M^2}$

γ - Ratio of specific heats

Γ - Circulation

δ - Amplitude of unsteady motion

ϵ - Characterizing parameter

$\Delta\epsilon$ - Increment in ϵ

η - Stretched coordinate in the direction normal to the free stream

$\Delta\eta$ - Coordinate spacing in the η direction

λ_s - Unsteady shock motion

μ - Switching function

$\Delta\xi$ - Coordinate spacing in the streamwise direction

ξ - Stretched coordinate in the streamwise direction

π - 3.14159...

ρ - Density

σ - Measure of camber and angle of attack

τ - Airfoil thickness ratio

$\bar{\Phi}, \tilde{\Phi}$ - Perturbation velocity potential

ϕ - Steady component of Φ

$\hat{\varphi}$ - Unsteady component of Φ

φ - Amplitude of $\hat{\varphi}$

Φ - Velocity potential

ω - Relaxation factor; frequency in the definition of k

$\bar{\omega}$ - Vorticity vector

Subscripts

B - Boundary points

l - Denotes grid row

n - Denotes grid column

∞ - Denotes free stream conditions

T - Trailing edge conditions

CHAPTER I

INTRODUCTION

The aerodynamic forces acting on aircraft operating at transonic speeds are generally greater than those acting on aircraft in subsonic or supersonic flight. When aircraft undergo unsteady motions while operating in the transonic flight regime, disturbances interact and build up, and there may be large phase differences between the aircraft motion and its unsteady aerodynamic loads. These characteristics make it more likely that flutter and other dynamic instabilities will occur in transonic flight. Hence, in this age of high subsonic and supersonic aircraft, the behavior of flight vehicles while operating at transonic speeds is of great concern to aircraft designers.

In order to design a vehicle that can operate safely at the desired flight conditions, we need the ability to determine the steady and unsteady airloads on aircraft in transonic flight. One way to accomplish this is to use the wind tunnel as a design tool, but the cost of models and wind tunnel test time will most likely result in the choice of a configuration that does not possess the optimum aerodynamic characteristics. Consequently, we should seek to develop methods to predict the aerodynamic loads acting on aircraft in transonic flight.

The primary difficulty associated with predicting transonic flow fields is that the governing equations are nonlinear and that, generally, various types of flow regions and shock waves are present in the flow field. Early studies of steady, two dimensional transonic flows avoided

the problem of nonlinearity by using the hodograph method [1]-[3]. The governing equations become linear in the hodograph plane, but the method is limited because of the difficulty of satisfying the boundary conditions for general airfoils. Hence, only simple wedge profiles were considered in those early studies. More recent studies show that hodograph methods are quite useful for treating the inverse problem of transonic airfoil design [4],[5].

Because of the limitations of the hodograph method when applied to direct problems, it was necessary to develop other transonic methods. Spreiter and Alksne [6] developed the method of local linearization to solve the steady, two dimensional, transonic small perturbation potential equation. However, the assumptions upon which that method is based limits its applicability to flows with free stream Mach numbers at or very near unity. Hence, local linearization is restricted to analyzing flows in a narrow portion of the transonic Mach number range.

Landahl [7] described the unsteady transonic flow field with a small perturbation potential equation and separated the potential into steady and unsteady components. He demonstrated that for high frequency motions in near sonic flow the unsteady potential equation is linear and uncoupled from the nonlinear steady flow. In that form, analytic solutions of the unsteady transonic problem were obtained, but, for many problems of engineering interest, low frequency motions must be considered. We are then faced with solving a linear equation with variable coefficients. Additional difficulty arises because those coefficients must be determined from the solutions of the nonlinear steady potential

equation.

One of the most important breakthroughs in transonic flow research was made when Magnus and Yoshihara [8] used a modified Lax-Wendroff difference method to numerically solve the unsteady, two dimensional Euler equations. The steady aerodynamic loads acting on airfoils were then determined by allowing the unsteady solutions to approach a steady state. By obtaining steady state solutions in that manner, it was necessary to solve a hyperbolic equation instead of the more difficult mixed elliptic/hyperbolic equation that results when the steady Euler equations are considered. The computations were lengthy, requiring as much as three and one half hours on a CDC 6400, but the emphasis was on understanding the flow field and not on computational speed. The predicted pressure distributions on a shockless airfoil in supercritical flow showed good agreement with experimental data except near the supersonic flow region. Also, except where the shock wave and boundary layer interact, the predicted pressure distributions on a NACA 64A410 airfoil in supercritical flow showed good agreement with experimental data. Most important was that the great potential of computational fluid dynamics was demonstrated.

The next major breakthrough came when Murman and Cole [9] developed a relaxation method to solve the steady, two dimensional, small perturbation potential equation. That method yielded numerical solutions of mixed transonic flow fields in an order of magnitude less computer time than the method of Magnus and Yoshihara [8]. The Murman-Cole method introduced the concept of type dependent differences, which amounts to

introducing an artificial viscosity into the potential equation at supersonic points. Numerical solutions of the transonic potential equation are continuous throughout the flow field, and shock waves appear as narrow regions with steep gradients. Hence, shock waves are spread over a finite number of grid spaces, and, by allowing the grid spacing to approach zero, the shock thickness can be made arbitrarily small. Murman and Cole [9] calculated pressure distributions on nonlifting circular arc airfoils, and the agreement with experimental data was very good. Unfortunately, there was no attempt to compare with the data generated by Magnus and Yoshihara [8]. The Murman-Cole method [9] does not maintain conservative form immediately downstream of shock waves and does not enforce the theoretical shock jump conditions, but this was corrected when Murman [10] developed a conservative type dependent difference method.

Following the success of Magnus and Yoshihara [8] and Murman and Cole [9], research in the field of transonic aerodynamics intensified, as evidenced by the frequent appearance of review papers in the literature [4],[11]-[14]. Jameson [15] performed a von Neumann test which indicated that the Murman-Cole difference method [9] has a marching instability in the streamwise direction if the flow is not perfectly aligned with the coordinate system (However, the Murman-Cole method has worked extremely well in practice). He then introduced a rotated difference method for solving the full potential equation. This method was unique because no assumptions about the flow direction were made. Jameson [16] later developed a conservative rotated difference

method for the full potential equation which demonstrated excellent agreement with experimental pressure measurements on blunt nosed airfoils.

Another improvement in transonic flow calculations, but not as significant as the breakthroughs of [8],[9] and [15], was made by Ballhaus and Goorjian [17] when they applied an alternating direction implicit (ADI) method to the low frequency small perturbation potential equation. Ballhaus and Goorjian [17] presented results that compare very well with those of Magnus and Yoshihara [8] and require substantially less computer time to obtain.

Following the lead of Landahl [7], several researchers sought solutions of the separated unsteady small perturbation potential equations [18] -[23]. The steady component of the flow field is governed by a nonlinear equation, and the unsteadiness is described by a linear equation which is coupled to the steady flow. Stahara and Spreiter [18], [19] and Isogai [20] have applied the concept of local linearization to the unsteady potential equation, but the analysis restricts the applicability of the unsteady local linearization method to flows with sonic or near sonic free stream velocities. Hence, numerical methods were applied to the separated potential equations.

Ehlers [21] and Traci et al. [22],[23] developed finite difference methods to solve the separated unsteady potential equation, but none of those methods accounted for the effects of unsteady shock wave motions. The experiments of Tijdeman and Zwaan [24],[25] indicate that moving shock waves induce relatively large local pressures on the portion of the

airfoil over which they travel. When the pressure distributions are integrated over the airfoil chord to yield the unsteady aerodynamic loads, the importance of considering the unsteady shock wave motions becomes apparent. Hence, we should hesitate before using the results of [21]-[23] in stability calculations and should seek to improve those methods.

The present research effort is aimed at developing an efficient tool that can be used to predict the onset of flutter and other instabilities. In this study, I employ the concept of a separated small perturbation potential. In order to determine the stability boundaries, many solutions of the nonlinear steady flow equation may be required, and a method to efficiently determine those solutions is needed. Nixon [26],[27] developed a perturbation method which may be used to determine steady flow solutions for various free stream Mach numbers and airfoil conditions. That method is somewhat limited because the steady flow conditions cannot be changed if the change causes the appearance or disappearance of shock waves. Hence, I seek to develop a method which can be used to efficiently determine steady transonic flow fields and not be subject to the type of restrictions that Nixon [26],[27] faces.

To determine the necessary steady flow fields, I employ the method of parametric differentiation, which was first used to predict steady transonic flow fields by Rubbert and Landahl [28]. This method reduces the nonlinear steady potential equation to a set of ordinary differential equations and a linear partial differential equation

describing the rate of change of the nonlinear solution with a chosen physical parameter. By integrating the ordinary differential equations over a range of parameters, I easily obtain a number of solutions of the steady potential equation. The primary difficulty associated with this technique is that I must solve the linear partial differential equation for the rates of change of the steady solution with the chosen parameter.

In this study, I develop a relaxation procedure to determine the rate of change of the steady potential with airfoil thickness ratio and angle of attack. The rates of change of the potential with airfoil thickness ratio and angle of attack are described by the same equation, with only the parameterized tangency condition differing. Thus, the same numerical procedure is used to compute both rates of change of the solution.

At each point in the flow field, the relaxation solutions are uniquely combined with a predictor-corrector method to integrate the steady solution in the direction of the chosen parameter. Nixon's perturbation method [26],[27] differs from this approach in that he expands the potential in a small parameter and obtains an expression relating the velocities for various values of that parameter. However, Nixon is still faced with solving a nonlinear equation for the zeroth order solution; this is not necessary with parametric differentiation. Parametric differentiation also has the advantage of being able to yield both subcritical and supercritical solutions in one integration.

The shock jump conditions in parameter space are satisfied by using conservative type dependent differences. Yu and Seebass [29] and Hafez and Cheng [30] developed shock fitting methods which could give sharp shock wave definition even on coarse grids. They also argue that shock fitting should be used for supercritical flow calculations because the governing equations cannot always be written in conservation form. However, because of the simplicity of the shock capturing method and because the equation describing the rate of change of the steady solution is easily put into conservation form, I satisfy the shock jump conditions by using conservative type dependent differences.

Once the steady solutions are known, the unsteady component of the flow field may be computed. The unsteadiness is assumed to vary harmonically with time which reduces the unsteady problem to a time independent one. Hence, the same relaxation method used to determine the rate of change of the steady solution with the chosen parameter can be used to compute the unsteady component of the flow field. To account for the effects of moving shock waves, I enforce a compatability condition at the mean shock wave location.

In order to demonstrate the present method, the steady forces and moments on lifting and nonlifting biconvex airfoils are computed for free stream Mach numbers less than unity. The computations required to obtain the families of steady solutions are quite reasonable. Having determined the steady state solutions, families of low frequency unsteady solutions are determined. The unsteady solutions allow me to determine

the effects of varying the steady state conditions on the unsteady aerodynamic loads. Hence the methods developed in this study should prove useful as a tool for predicting the occurrence of aerodynamically induced instabilities.

CHAPTER II

FORMULATION OF THE PROBLEM OF UNSTEADY TRANSONIC FLOW PAST AIRFOILS

2.1. Introduction

In order to fully treat unsteady transonic flows, I should be capable of solving for the flow field variables $(p, \rho, \bar{u})$, while considering viscous effects and the fact that transonic flow fields are generally mixed- subsonic and supersonic flow regions coexist. However, instead of solving the full conservation and state equations, we can obtain most of the essential features and much information about the flow field from the solution of a single, nonlinear small perturbation potential equation. This equation is derived, following Ashley and Landahl [31] from the Eulerian gas dynamic equations by satisfying conservation of mass, linear momentum, and energy to lowest order and assuming the flow to be inviscid, isentropic and irrotational. A major advantage in using the idea of small perturbations is that it allows a simplified treatment of the airfoil boundary conditions; the boundary conditions may be applied on a mean profile line and expressed in terms of vertical perturbation velocities and local airfoil slopes. Consequently, no special procedure is required to obtain data on the airfoil boundary.

In this chapter, I derive the nondimensional small perturbation potential equation and the associated initial and boundary

conditions. The problem is then simplified by separating the potential into steady and unsteady components. The limits on the amplitude of the unsteady motion which allow this separation are determined from a dimensional analysis of the unsteady shock motion. The separated potential equations and the associated boundary conditions are presented. Also, limitations of the small perturbation potential approach are discussed.

2.2. Derivation of the Small Perturbation Equation and Airfoil Boundary Conditions

Because of the assumption of inviscid, isentropic, irrotational flow, the unsteady transonic flow problem can be reduced to one of solving a single equation for a velocity potential, Φ. That equation is derived here following the procedure of Ashley and Landahl [31].

From the equations of conservation of mass, linear momentum, and energy, I can deduce Bernoulli's equation

$$\frac{\partial \Phi}{\partial T} + \frac{Q^2 - U^2}{2} + \int_{\rho_\infty}^{\rho} \frac{dp'}{\rho} = 0 \tag{2.1}$$

Using Leibnitz's rule to differentiate the integral term in (2.1) yields

$$\frac{d}{dp} \int_{\rho_\infty}^{\rho} \frac{dp'}{\rho} = \frac{1}{\rho} \tag{2.2}$$

Now, I can write

$$\frac{D}{DT}\int_{P_\infty}^{P}\frac{dp'}{\rho} = \left(\frac{d}{dp}\int_{P_\infty}^{P}\frac{dp'}{\rho}\right)\frac{Dp}{DT} = \frac{a^2}{\rho}\frac{D\rho}{DT} \tag{2.3}$$

where

$$\frac{D}{DT} = \frac{\partial}{\partial T} + \bar{Q}\cdot\nabla$$

and

$$a^2 = a_\infty^2 - (\gamma-1)\left[\bar{\Psi}_T + \frac{1}{2}\left(\bar{\Psi}_X^2 + \bar{\Psi}_Z^2 - U^2\right)\right] \tag{2.4}$$

To complete the derivation, I rewrite Bernoulli's equation as

$$\int_{P_\infty}^{P}\frac{dp'}{\rho} = -\left(\frac{\partial\bar{\Psi}}{\partial T} + \frac{Q^2-U^2}{2}\right)$$

which becomes, when combined with (2.3)

$$\frac{1}{\rho}\frac{D\rho}{DT} = \frac{-1}{a^2}\frac{D}{DT}\left(\frac{\partial\bar{\Psi}}{\partial T} + \frac{Q^2-U^2}{2}\right)$$

$$= \frac{-1}{a^2}\left[\frac{\partial^2\bar{\Psi}}{\partial T^2} + \frac{\partial}{\partial T}Q^2 + \bar{Q}\cdot\nabla\left(\frac{Q^2}{2}\right)\right]$$

Introducing this expression for $\frac{1}{\rho}\frac{D\rho}{DT}$ into the mass conservation equation

$$\frac{1}{\rho}\frac{D\rho}{DT} = -\nabla\cdot\bar{Q} = -\nabla^2\bar{\Psi}$$

I obtain the full potential equation

$$\nabla^2 \Phi - \frac{1}{a^2}\left[\frac{\partial^2 \Phi}{\partial T^2} - \frac{\partial Q^2}{\partial T} + \bar{Q} \cdot \nabla\left(\frac{Q^2}{2}\right) \right] = 0$$

which in expanded form is

$$(a^2 - \Phi_X^2)\Phi_{XX} + (a^2 - \Phi_Z^2)\Phi_{ZZ} - \Phi_{TT}$$

$$- 2(\Phi_X \Phi_Z \Phi_{XZ} + \Phi_X \Phi_{XT} + \Phi_Z \Phi_{ZT}) = 0 \qquad (2.5)$$

I , next, seek to reduce the complexity of this equation.

The full potential equation may be simplified by assuming the velocity field to be the combination of a uniform stream and perturbations upon that stream. Thus, the potential may be written as

$$\Phi(X, Z, T) = U[X + \bar{\Phi}(X, Z, T) + \ldots] \qquad (2.6)$$

where $\bar{\Phi}$ is the perturbation velocity potential. Equations (2.4), (2.5) and (2.6) are then combined to yield the perturbation potential equation

$$(1-M^2)\bar{\Phi}_{XX} + \bar{\Phi}_{ZZ} - 2\frac{M^2}{U}\bar{\Phi}_{XT} - \frac{1}{a_\infty^2}\bar{\Phi}_{TT} =$$

$$M^2\left\{ \left[(\gamma+1)\bar{\Phi}_X + \bar{\Phi}_X^2 \right]\bar{\Phi}_{XX} + \frac{(\gamma-1)}{2}\left(\frac{2}{U}\bar{\Phi}_T + \bar{\Phi}_X^2 + \bar{\Phi}_Z^2\right)\left(\bar{\Phi}_{XX} + \bar{\Phi}_{ZZ}\right) \right.$$

$$\left. + \left[(\gamma-1)\bar{\Phi}_X + \bar{\Phi}_Z^2 \right]\bar{\Phi}_{ZZ} + 2\left[(1+\bar{\Phi}_X)\bar{\Phi}_Z\bar{\Phi}_{XZ} + \frac{1}{U}\left(\bar{\Phi}_X\bar{\Phi}_{XT} + \bar{\Phi}_Z\bar{\Phi}_{ZT}\right) \right] \right\} \qquad (2.7)$$

I may simplify (2.7) by assuming the perturbations to be small enough such that products of perturbation terms may be neglected. However, when the flow is transonic, $1-M^2$ is small,

necessitating the retention of the $M^2(\gamma+1)\bar{\Phi}_{\bar{x}}\bar{\Phi}_{\bar{x}\bar{x}}$ term. When the reduced frequency of the unsteady motion is of order unity, the $\frac{M^2(\gamma-1)}{U}\bar{\Phi}_{\bar{T}}\bar{\Phi}_{\bar{x}\bar{x}}$ term should also be retained. Using the above assumptions, (2.7) is reduced to the transonic small perturbation potential equation

$$\left[1-M^2-\frac{M^2(\gamma-1)}{U}\bar{\Phi}_{\bar{T}}-M^2(\gamma+1)\bar{\Phi}_{\bar{x}}\right]\bar{\Phi}_{\bar{x}\bar{x}}+\bar{\Phi}_{\bar{z}\bar{z}}-2\frac{M^2}{U}\bar{\Phi}_{\bar{x}\bar{T}}-\frac{1}{a_\infty^2}\bar{\Phi}_{\bar{T}\bar{T}}=0$$

Introducing the following nondimensional variables

$$x=\frac{\bar{x}}{c}$$

$$z=\frac{\bar{z}}{c}$$

$$t=\frac{U}{c}\bar{T}$$

$$\Phi=\frac{\bar{\Phi}}{c}$$

I obtain the dimensionless form of the transonic small perturbation potential equation

$$\left[1-M^2-M^2(\gamma-1)\Phi_t-M^2(\gamma+1)\Phi_x\right]\Phi_{xx}+\Phi_{zz}-2M^2\Phi_{xt}-M^2\Phi_{tt}=0 \qquad (2.8)$$

It is essential that any transonic method be capable of accurately predicting mixed flow fields, and even though (2.8) is a simplified flow model, it is capable of yielding mixed flow solutions. However, the small perturbation approach does have some limitations.

One limitation is that the small perturbation assumptions are violated at airfoil leading edges. Ballhaus [14] reports a dependency of numerical solutions on the spacing of the computational grid near

the leading edge. Fortunately, the grid dependency may be confined to a small region near the leading edge by using a fine grid in that region.

A limitation on the geometry of shock waves is seen by considering the curved, adiabatic shock wave of Figure 2.1. Crocco's theorem states

$$\underline{T}\nabla s + \bar{u} \times \bar{\omega} = \bar{u}_t + \nabla h_0$$

where s is the specific entropy, h_0 is the stagnation enthalpy, $\underline{T}$ is temperature, $\bar{u}$ is the velocity vector, and $\bar{\omega}$ is the vorticity vector. If the upstream flow, u_1, is steady and uniform, the local vorticity, ω_s, immediately downstream of the shock wave is

$$\omega_s = -\frac{u_1}{r} \cos\beta' \frac{\rho_1}{\rho_2}\left(\frac{\rho_2}{\rho_1} - 1\right)^2$$

where β' is the local shock inclination, ρ_1 and ρ_2 are the fluid densities upstream and downstream of the shock wave, respectively, and r is the local shock wave radius of curvature. Since ω_s increases with decreasing r, highly curved shock waves cannot be treated with potential flow theory.

Crocco's theorem shows that vorticity is generated in unsteady flows even if there are no entropy gradients. If the velocity field and its rate of change with time are such that significant amounts of vorticity are generated, I can no longer assume potential flow. The actual limitation on the level of unsteadiness can be determined by comparing potential flow data with experimental data or data obtained from a flow model that is valid for both rotational and irrotational flows. When the potential flow data begins to deviate significantly from the experimental data or the data from the rotational flow model, I can assume that the limit on the level of unsteadiness has been reached.

A simple analysis of normal shock waves indicates that any

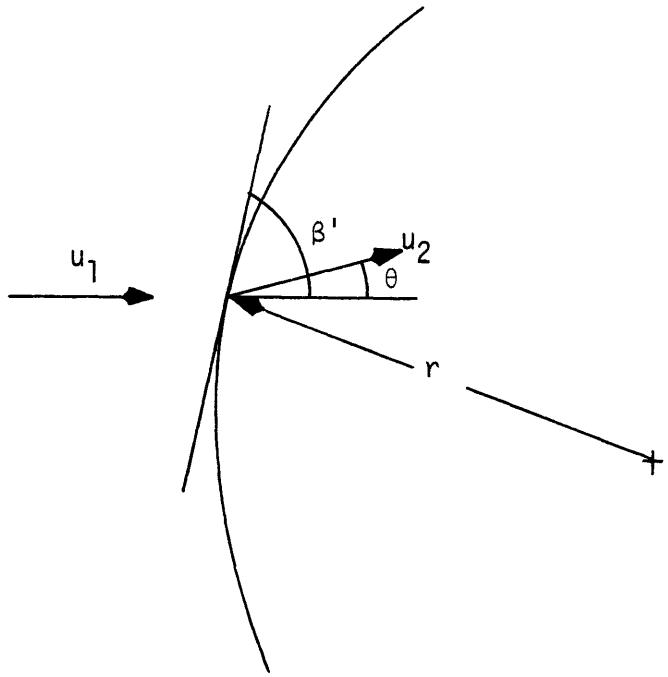

Figure 2.1. Geometry of curved shock waves.

shock waves in the flow field must be sufficiently weak. The increase in entropy, Δs, across a normal shock wave is, [32]

$$\frac{\Delta s}{R} = \frac{2}{3}\frac{\gamma}{(\gamma+1)^2}(M_1^2-1)^3 + O((M_1^2-1)^4) \approx \frac{\gamma+1}{2\gamma^2}\left(\frac{P_2}{P_1}-1\right)^3$$

Usually, when M_1 becomes greater than 1.3, the shock wave separates the boundary layer, and viscous and rotational flow effects must be considered. This result indicates that potential flow models can only be used to compute flows with relatively weak shock waves. The above result also provides an estimate of the entropy jump across shock waves which causes the potential flow assumptions to be violated.

Because the small perturbation equations are derived assuming that M is nearly unity, there are cases when the predicted flow field may be in error. A comparison of the critical pressure coefficient, C_p^*, determined from the exact and small perturbation equations indicate that if M is considerably less than unity, small perturbation theory may predict a completely subsonic flow field when, according to the exact equations, the flow has become supercritical. Krupp [33], for the case of steady flow, has rewritten the coefficient of Φ_{xx} as $1-M^2-M^b(\gamma+1)\Phi_x$, which allows the choice of b such that the small perturbation approximation of either C_p^* or the average pressure across normal shock waves matches the exact quantities. In this study, b has been set at 2, but as M nears unity, the choice of b becomes less important.

The condition which must be satisfied at the airfoil boundary is determined by considering the airfoil as a streamline across which no fluid flows. Therefore, on the airfoil, the fluid velocity

normal to the airfoil must equal the airfoil velocity normal to itself.

If the instantaneous airfoil position is given by

$$B(x,z,t) = 0 \tag{2.9}$$

the fluid velocity normal to the airfoil is $\frac{(1+\Phi_x)B_x + \Phi_z B_z}{\sqrt{B_x^2 + B_z^2}}$,

and the velocity of the body normal to itself is $-\frac{B_t}{\sqrt{B_x^2+B_z^2}}$.

Hence, the airfoil tangency condition is

$$\frac{DB}{Dt} = B_t + (1+\Phi_x)B_x + \Phi_z B_z = 0$$

Generally, for thin bodies Φ_x is much less than unity, and the tangency condition may be reduced to

$$B_t + B_x + \Phi_z B_z = 0 \tag{2.10}$$

Other conditions which must be satisfied are continuous pressure and normal velocity in the wake and the Kutta, shock jump and far field conditions. How these conditions are treated is detailed in the next sections.

Once I solve (2.8) subject to the appropriate conditions, the results are reported in the form of a pressure coefficient, C_p, where

$$C_p = \frac{p - p_\infty}{\frac{1}{2}\rho_\infty U^2}$$

Utilizing the proper isentropic relations, the small perturbation

approximation of C_p becomes

$$C_p = -2(\bar{\Phi}_x + \bar{\Phi}_t) \tag{2.11}$$

The forces and moments acting on the airfoil are then easily found by integrating the profile pressure coefficient over the chord.

2.3. Separation of the Small Perturbation Potential

For some subsonic and supersonic flows, for which the governing equations are linear, the potential may be separated into steady and unsteady components, each independent of the other. The transonic equation is nonlinear and, generally, cannot be separated in that manner. However, if the unsteadiness can be treated as a linear perturbation on the steady flow, the transonic potential may also be separated. Here, I use a dimensional analysis and the experimental results of Tijdeman and Zwaan [24], [25] to determine the conditions under which separation of the transonic potential is allowed.

If I am to be justified in separating the potential in (2.8), the unsteady loads should vary linearly with the amplitude of the unsteady motion, with a phase shift. As a result, I must pay close attention to the motions of imbedded shock waves. Shock waves induce relatively large pressures in the regions over which they travel. Therefore, if the motion of a shock wave carries it over a

significant portion of the airfoil, the aerodynamic loads become a nonlinear function of the unsteady motion. I, then, must examine the factors which contribute to the motion of embedded shock waves.

The parameters governing the ratio of the shock excursion amptitude to chord, $\frac{\Delta x_s}{c}$, illustrated in Figure 2.2 are obtained from a dimensional analysis. I write Δx_s as a function of the dimensional physical parameters which describe the flow field

$$\Delta x_s = f(c^b, \omega^d, v^e, a_\infty^f, \rho_\infty^g, T^h, \delta^i, P_\infty^j, \alpha_m^k)$$

where in the above equation, T represents the maximum airfoil thickness. In terms of basic quantities, the shock excursion amplitude becomes

$$L = f(L^b, t^{-d}, L^e t^{-e}, L^f t^{-f}, m^g L^{-3g}, L^h, L^i, m^j L^{-j} t^{-2j})$$

from which I obtain the following relationships

$$\begin{aligned} b + e + f - 3g + h + i - j &= 1 \\ d + e + f \qquad\quad + 2j &= 0 \\ g \qquad\quad + j &= 0 \end{aligned}$$

Using the above equations to eliminate two of the variables and then grouping terms with like exponents, the dimensionless dependence of the shock excursion amplitude is formed

$$\frac{\Delta x_s}{c} = f\left[\left(\frac{\omega c}{v}\right)^d, \left(\frac{a_\infty}{v}\right)^f, \left(\frac{T}{c}\right)^h, \left(\frac{\delta}{c}\right)^i, \left(\frac{P_\infty}{\rho_\infty v^2}\right)^j, \alpha_m^k\right] \qquad (2.12)$$

where δ is the amplitude of the unsteady motion.

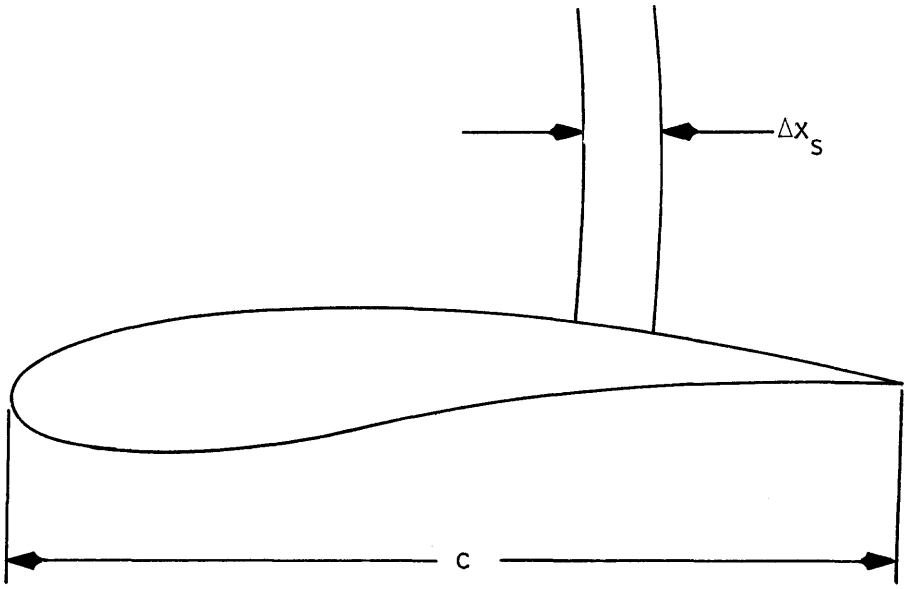

Figure 2.2. Region traversed by imbedded shock wave.

Equation (2.12) is rewritten as

$$\frac{\Delta x_s}{c} \propto k^d M^{-f} \tau^h \left(\frac{\xi}{c}\right)^i \gamma^{-j} \alpha_m^K$$

where $\frac{\gamma p_\infty}{\rho_\infty} = a_\infty^2$ has been used. The experiments reported in [24] and [25] may be used to determine the effect of the various nondimensial parameters on $\frac{\Delta x_s}{c}$.

The experiments of Tijdeman and Zwaan show that the shock motion increases when the motion frequency decreases. The shock excursion to chord ratio is then written as

$$\frac{\Delta x_s}{c} = C M^{-f} \gamma^{-j} \frac{\tau^h \alpha_m^K}{k^{|i|}} \left(\frac{\xi}{c}\right)^i \tag{2.13}$$

where C is a proportionality constant. I may thus conclude that given the free stream conditons and fluid properties, I must require $\frac{\xi}{c} << \tau, \alpha_m$ if the unsteadiness is to be treated as a linear perturbation about the steady state. When $\frac{\xi}{c} = O(\tau, \alpha_m)$, the transonic potential cannot be separated unless some additional constraint, such as high frequency, is met.

Considering unsteady motions for which $\frac{\xi}{c} << \tau, \alpha_m$, the equations governing each component of the flow field are obtained by separating the potential in the following manner

$$\Phi(x, z, t) = \phi(x, z) + \hat{\varphi}(x, z, t) \tag{2.14}$$

assuming that ϕ and its derivatives are much larger than $\hat{\varphi}$ and its derivatives. Substitution of (2.14) into (2.8) and grouping terms of similar order leads to

$$[1-M^2-M^2(\gamma+1)\phi_x]\phi_{xx}+\phi_{zz}=0 \tag{2.15}$$

$$[1-M^2-M^2(\gamma+1)\phi_x]\hat{\varphi}_{xx}-M^2(\gamma+1)\phi_{xx}\hat{\varphi}_x+\hat{\varphi}_{zz}$$

$$-M^2(\gamma-1)\phi_{xx}\hat{\varphi}_t-2M^2\hat{\varphi}_{xt}-M^2\hat{\varphi}_{tt}=0 \tag{2.16}$$

The effects of thickness, camber, and mean angle of attack may be found from (2.15), while (2.16) represents the effects of the unsteady motion.

Although (2.14) is allowable only if $\frac{\delta}{c} \ll \bar{\tau}, \alpha_m$, solutions of (2.15) and (2.16) may be used in problems of engineering interest. For example, flutter prediction requires the analysis of unsteady motions of infinitesimal amplitude. However, because the unsteady flow is coupled to the steady flow, it may be required to obtain a large number of steady flow solutions to predict the stability boundaries. I now proceed to

specify the complete boundary value problems for each flow component.

2.4. Definition of the Boundary Value Problems

2.4.1. Steady Component

As a consequence of (2.14), the instantaneous airfoil position may be written as

$$z = \mathcal{F}(x) + f_1(x,t)$$

with $\mathcal{F}, \mathcal{F}_x >> f_1, f_{1x}$. Figure 2.3 shows a typical perturbation about some mean position. Equation (2.9) becomes

$$B(x,z,t) = z(x,t) - \mathcal{F}(x) - f_1(x,t) = 0$$

and the tangency condition which must be satisfied by the mean flow is

$$\phi_z = \mathcal{F}'(x) \qquad (z = \mathcal{F}(x))$$

Generally, for thin airfoils, the boundary doesn't vary significantly from the chord, and the tangency condition may be applied on the mean profile line. Thus, the tangency condition is simplified to

$$\phi_z = \mathcal{F}'(x) \qquad (z = 0) \tag{2.17}$$

The condition that the perturbation velocities vanish in the far field is

$$\lim_{x^2+z^2 \to \infty} \phi_x, \phi_z = 0 \tag{2.18}$$

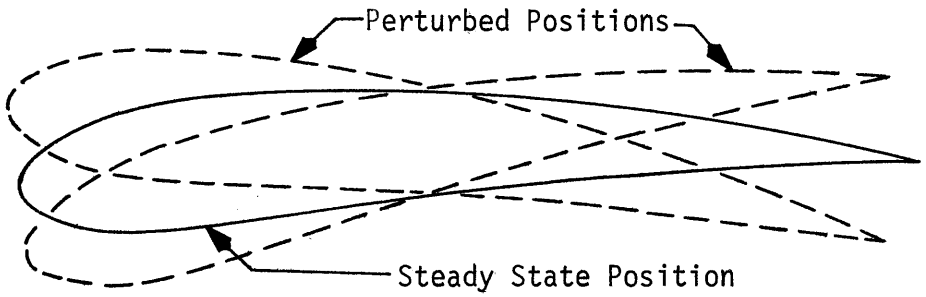

Figure 2.3. Typical perturbations about the steady state airfoil position.

The conditions expressed in (2.17) and (2.18) aren't sufficient to make ϕ single valued. Hence, another condition is required.

The insertion of an airfoil into the flow field converts it to a doubly connected region, and a cyclic constant is needed to make ϕ single valued. I introduce a cut along the x-axis downstream of the trailing edge (see Figure 2.4). The cyclic constant to be specified is the circulation, Γ, which is the jump in ϕ across the cut. The circulation must be chosen such that the fluid velocity at sharp trailing edges is finite, producing a smooth joining of the upper and lower portions of the flow. Continuous motion can only occur if there is no pressure discontinuity at subsonic trailing edges. This is simply a statement of the Kutta condition. From (2.11), the steady, small perturbation approximation to the Kutta condition is

$$\Delta \phi_x = 0 \qquad (x = c, z = 0) \tag{2.19}$$

where Δ represents the jump in a quantity across the line $z = 0$. Because there is no mechanism by which oncoming supersonic flow can adjust itself to the presence of the trailing edge, the pressure is not required to be continuous at supersonic trailing edges.

Across the cut in the flow field, pressure and normal velocity must be continuous. These conditions take the form

$$\Delta \phi_x = 0 \qquad (x > c, z = 0) \tag{2.20}$$

$$\Delta \phi_z = 0 \qquad (x > c, z = 0) \tag{2.21}$$

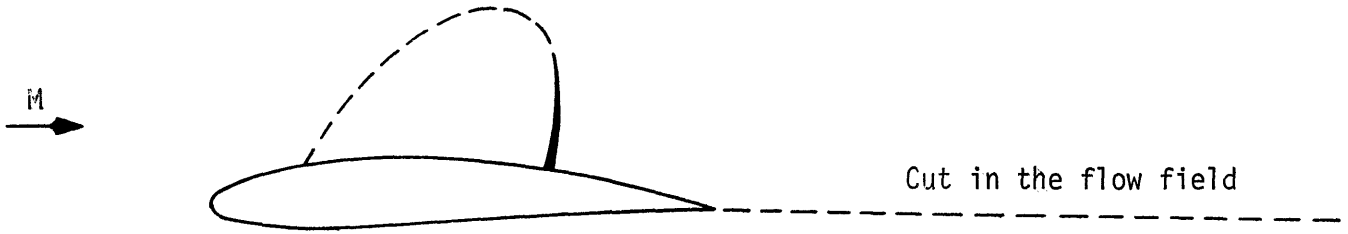

Figure 2.4. Location of the cut in the flow field.

Using (2.20) and (2.21), I can write

$$\Delta\phi(x>c, z=0) = \Delta\phi_T \tag{2.22}$$

where the subscript T represents quantities at the trailing edge. If the flow is supersonic at the trailing edge, I require

$$\Delta\phi(x>c, z=0) = \Delta\phi(x=c^+, z=0) \tag{2.23}$$

Where c^+ is the location infinitesimally downstream of the trailing edge.

The conditions expressed in (2.17)- (2.23) are sufficient to uniquely determine the flow field in the absence of imbedded shock waves. The appearance of shock waves in the flow field, which is illustrated in Figure 2.5, requires me to ensure the continuity of ϕ across the shock wave and that the small pertubation approximation to the Rankine-Hugoniot conditions is satisfied. Murman and Cole [9] have shown that those conditions are already contained in (2.15). By writing (2.15) in the conservation form

$$\left[(1-M^2)\phi_x - M^2(\gamma+1)\frac{\phi_x^2}{2}\right]_x + (\phi_z)_z = 0$$

and integrating across the shock wave, the shock jump condition

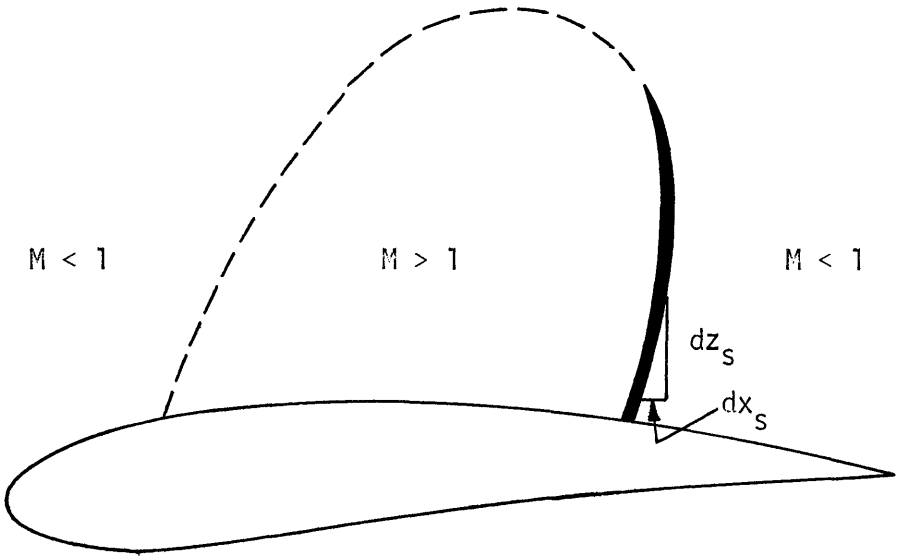

Figure 2.5. Imbedded supersonic region and shock wave in a transonic flow field.

is found to be,

$$\left\langle (1-M^2)\phi_x - M^2(\gamma+1)\frac{\phi_x^2}{2} \right\rangle \left(\frac{dz}{dx}\Big|_s\right) - \langle \phi_z \rangle = 0 \qquad (2.24)$$

where $\langle\ \rangle$ represents the jump in a quantity across the shock wave.

2.4.2. Unsteady Component of the Flow

At the airfoil, the condition which must be satisfied by the unsteady potential is

$$\hat{\varphi}_z = f_{1x} + f_{1t} \qquad (2.25)$$

In the far field, I require the disturbances to propagate outward without reflection, and at subsonic trailing edges, the Kutta condition requires that

$$\Delta(\hat{\varphi}_x + \hat{\varphi}_t) = 0 \qquad (x=c, z=0) \qquad (2.26)$$

For unsteady motions of high reduced frequencies, experiments have shown that the unsteady pressure at the trailing edge is nonzero [34], [35]; this nonzero trailing edge loading has been attributed to viscous effects [35]. However, for the reduced frequencies under consideration in the present work, experiments support the validity of using (2.26). Again, if the flow is supersonic at the trailing edge, there is no requirement of continuous pressure.

Across the wake, the unsteady pressure and normal velocity must be continuous. Assuming the unsteady motion to be small enough such that I can satisfy the wake conditions along the line downstream of the mean trailing edge location, those conditions become

$$\Delta(\hat{\varphi}_x + \hat{\varphi}_t) = 0 \tag{2.27}$$

$$\Delta\hat{\varphi}_z = 0 \tag{2.28}$$

Equations (2.27) and (2.28) imply a discontinuity in $\hat{\varphi}$ in the wake. If the trailing edge flow is subsonic, that discontinuity is determined such that the unsteady Kutta condition is satisfied.

The conditions which must be satisfied across imbedded shock waves are detailed in Chapter five.

2.5. Summary

The conservation and state equations have been reduced to a single small perturbation potential equation. The perturbation potential has been separated into steady and unsteady components, with appropriate boundary conditions specified for each component. From (2.16), it is seen that the unsteady component of the flow field is coupled to the mean flow. Hence, many steady solutions may be required to predict stability boundaries. The major difficulty in solving for the steady flow is that a nonlinear partial differential equation must be solved. This nonlinearity is essential if mixed flows are to be computed. I have also recognized some of the limitations of the small perturbation approach and presented possible methods to ease those limitations.

CHAPTER III

ANALYSIS OF STEADY, TWO-DIMENSIONAL, TRANSONIC FLOWS

3.1. Introduction

As shown in Chapter two, the separation of the potential simplifies the mathematical complexity of the transonic problem, but many steady state solutions may be needed to fully predict the unsteady responses of bodies in transonic flow. As a result, we would be required to repeatedly solve a nonlinear partial differential equation, subject to various steady state boundary conditions. Thus, I seek a method which will allow us to easily calculate steady transonic flows over a wide range of conditions. One such method is the method of parametric differentiation.

Parametric differentiation is a procedure by which certain nonlinear problems, which are characterized by some physical parameter, may be transformed into linear problems by considering the perturbations about a known base solution due to small changes in that parameter. The effects of large parameter changes are found by repeatedly incrementing the parameter in small amounts. Hence, from the linear equations, I may obtain many nonlinear solutions as a function of the physical parameter. The chosen parameter may appear in the governing equations and/or the boundary or initial conditions.

The concept of parametric differentiation is well established

and has been previously applied to a wide range of problems in fluid dynamics. Rubbert and Landahl applied the method to the Falkner-Skan boundary layer problem and to the problem of steady transonic flow past nonlifting airfoils [28],[36], Whitlow and Harris [37], [38] calculated unsteady, internal, transonic flow fields using parametric differentiation, and Jischke and Baron [39] used the method to solve problems in radiative gasdynamics. In the field of acoustics, Harris [40] used parametric differentiation to predict far field noise propagation in a lossless and dissipative medium.

In this chapter, I outline the method of parametric differentiation and present the formulation of the steady transonic boundary value problem in parameter space. I demonstrate that application of parametric differentiation to the transonic problem reduces it to a set of linear, independent first order ordinary differential equations with the base solution as an initial condition. A technique for solving ordinary differential equations is then employed to extend and determine the potential for various values of the parameter of interest. I also present a procedure for determining the base solution.

3.2 The Method of Parametric Differentiation

In order to understand the concept of parametric differentiation, consider a function, $\phi(\bar{x},t;\epsilon)$, which is governed by a nonlinear ordinary or partial differential equation

$$N[\phi(\bar{x},t;\epsilon)] = 0 \tag{3.1}$$

and satisfies the boundary conditions

$$a\,\phi(\bar{x}_B,t;\epsilon) + b\frac{\partial\phi}{\partial n}(\bar{x}_B,t;\epsilon) = a\,\phi_B + b\left(\frac{\partial\phi}{\partial n}\right)_B \tag{3.2}$$

where N is a nonlinear differential operator, $\bar{x}_B$ is the boundary location, and ϵ is a characterizing parameter. By differentiating (3.1) and (3.2) with respect to ϵ , I obtain the equivalent linear problem

$$L[q(\bar{x},t;\epsilon)] = 0 \tag{3.3}$$

$$a\,q(\bar{x}_B,t;\epsilon) + b\frac{\partial q}{\partial n}(\bar{x}_B,t;\epsilon) = a\,q_B + b\left(\frac{\partial q}{\partial n}\right)_B \tag{3.4}$$

where L is a linear differential operator, and q , the increment in the solution due to a small change in the parameter is defined as $\frac{\partial\phi}{\partial\epsilon}$. Generally, the linear operator will have variable coefficients involving ϕ and its derivatives, thus the primary difficulty becomes to solve a linear equation with variable coefficients.

The method of parametric differentiation is not the ideal method for all nonlinear problems, and before I decide to apply the method to any problem, I should be certain of the following

(a) The governing equations become linear

(b) The results are physically plausible

(c) The method is cost effective

(d) Extended solutions are weak functions of the base solution

This final point is particularly important. For most problems, a base solution is easily obtained, but in some cases, the perturbations about the base solution may be singular. In such cases, Rubbert and Landahl [28] suggest starting from an assumed solution for $\epsilon = \epsilon_0 + \Delta\epsilon$. Even though that starting solution may be slightly incorrect, if the extended solutions are indeed weak functions of the base solution, we will obtain the correct solution when ϵ becomes only slightly different from its starting value.

3.3. The Steady Transonic Problem as an Ordinary Differential Equation

Upon application of the method of parametric differentiation, at every point in space, the steady transonic flow problem is reduced to the initial value problem

$$\frac{d\phi}{d\epsilon} = g(\epsilon) \quad , \quad \phi(\epsilon_0) = \phi_0 \tag{3.5}$$

where ϕ_0 is the base solution. Numerical techniques for solving ordinary differential equations may be applied to (3.5), and entire flow fields for various values of ϵ are obtained in one integration of the differential equation.

Some of the most successful and widely used techniques for integrating ordinary differential equations are the Runge-Kutta methods. To determine $\phi(\epsilon_1 + \Delta\epsilon)$ using the Runge-Kutta

methods, it is required that g be known in the interval $\epsilon_1 \le \epsilon \le \epsilon_1 + \Delta\epsilon$. Because it is inconvenient to obtain data in the interval $\epsilon_1 \le \epsilon \le \epsilon_1 + \Delta\epsilon$, I chose not to use Runge-Kutta methods to solve (3.5). One method which does not require knowldege of g in the aforementioned interval is the Euler, or tangent line method

$$\phi(\epsilon_1 + \Delta\epsilon) = \phi(\epsilon_1) + \Delta\epsilon\, g(\epsilon_1) \tag{3.6}$$

This method assumes that, throughout the interval $\Delta\epsilon$, the solution follows a linear path tangent to $\phi(\epsilon_1)$, and its error is proportional to $\Delta\epsilon^2$. Since Euler's method extends the solutions using a linear approximation and its error term is relatively large, the solutions would have to be extended in relatively small increments to maintain accuracy. Hence, Euler's method is not used to solve (3.5), and a desirable multistep method is sought.

Equation (3.5) is integrated using a fifth order predictor-corrector method [41]. The procedure is to start the solution with the lower order methods given in Appendix A and predict the next solution with Milne's predictor

$$p(\epsilon+\Delta\epsilon) = \phi(\epsilon-3\Delta\epsilon) + \frac{4}{3}\Delta\epsilon\left[2g(\epsilon) - g(\epsilon-\Delta\epsilon) + 2g(\epsilon-2\Delta\epsilon)\right]$$

$$+\frac{14}{45}\Delta\epsilon^5 \frac{d^4 g}{d\epsilon^4} \tag{3.7}$$

The predicted soultions are then modified with the relationship

$$m(\epsilon+\Delta\epsilon) = p(\epsilon+\Delta\epsilon) + \frac{112}{121}\left[c(\epsilon) - p(\epsilon)\right] \tag{3.8}$$

where $c(\epsilon)$ is the corrected potential at the previous integration step. The values of m from (3.8) are used as potentials to define the coefficients in (3.3) making it possible to determine $g(\epsilon+\Delta\epsilon)$.

then correct the solution with

$$c(\epsilon+\Delta\epsilon) = \frac{1}{3}[\phi(\epsilon)+\phi(\epsilon-\Delta\epsilon)+\phi(\epsilon-2\Delta\epsilon)]$$

$$+\frac{\Delta\epsilon}{36}[13g(\epsilon+\Delta\epsilon)+39g(\epsilon)+15g(\epsilon-\Delta\epsilon)+5g(\epsilon-2\Delta\epsilon)]-\frac{\Delta\epsilon^5}{40}\frac{d^4g}{d\epsilon^4} \quad (3.9)$$

(Equation (3.9) is termed the "one-third" corrector and is used instead of Milne's corrector because of its more desirable stability characteristics. The final solutions are obtained from the modified corrector

$$\phi(\epsilon+\Delta\epsilon) = c(\epsilon+\Delta\epsilon) - \frac{9}{121}[c(\epsilon+\Delta\epsilon)-p(\epsilon+\Delta\epsilon)] \quad (3.10)$$

The solution process for a family of airfoils is summarized in Figure 3.1.

In order to apply the method discussed in this section, I must be able to determine the rate of change of the solution throughout the flow field. The governing equations and boundary conditions to be satisfied by g are detailed in the next section.

3.4. Formulation of the Linear Boundary Value Problem

The linear boundary value problem for g is determined by

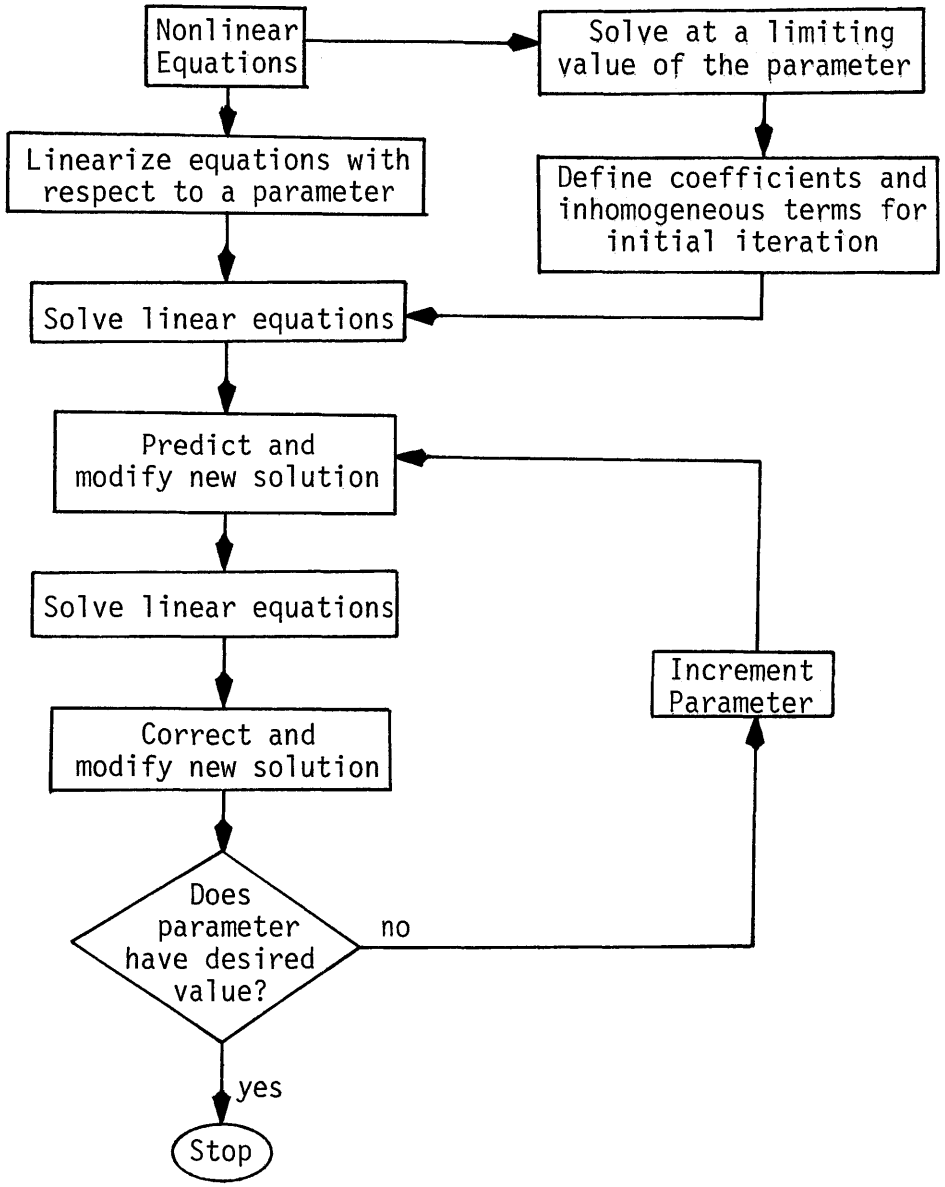

Figure 3.1. Solution procedure using the method of parametric differentiation.

differentiating (2.15) and (2.17)-(2.23) with respect to a characterizing parameter. The chosen parameters are the airfoil thickness ratio, τ , which characterizes nonlifting flows and the measure of camber and angle of attack, σ , which characterizes lifting flows. The free stream Mach number is another possible parameter but is not used as such here.

It should be noted that neither τ nor σ appears in (2.15). This is advantageous because the governing equations for both lifting and nonlifting flows are identical and may be solved by the same numerical technique. This would not be the case if Mach number was chosen as a parameter.

Differentiating (2.15) with respect to τ or σ , I obtain the linear equation

$$[1-M^2-M^2(\gamma+1)\phi_x]g_{xx}-M^2(\gamma+1)\phi_{xx}g_x+g_{zz}=0 \qquad (3.11)$$

An important characteristic of (3.11) is that it switches type - the quantity $1-M^2-M^2(\gamma+1)\phi_x$ changes sign - at the same points in the flow field as the nonlinear potential equation.

If the mean airfoil position is defined as

$$\mathcal{F}(x) = \pm\tau F(x) + \sigma G(x)$$

the conditions to be satisfied on the boundaries of nonlifting and lifting airfoils are, respectively

$$g_z = \pm F'(x) \qquad (z=0) \tag{3.12}$$

$$g_z = G'(x) \qquad (z=0) \tag{3.13}$$

At subsonic trailing edges I require that

$$\Delta g_x = 0 \qquad (x=c,\ z=0) \tag{3.14}$$

and along the cut in the flow field

$$\Delta g_x = 0 \qquad (x>c,\ z=0) \tag{3.15}$$

$$\Delta g_z = 0 \qquad (x>c,\ z=0) \tag{3.16}$$

Equations (3.14)-(3.16) lead to the requirements that

$$\Delta g(x>c,\ z=0) = \Delta g_T \tag{3.17}$$

downstream of subsonic trailing edges, and

$$\Delta g(x>c,\ z=0) = \Delta g(x=c^+,\ z=0) \tag{3.18}$$

downstream of supersonic trailing edges, where Δg_T is the jump in g across the trailing edge. Completing the problem specification for shockless flows is the condition that

$$\lim_{x^2+z^2\to\infty} q_x, q_z = 0 \tag{3.19}$$

When the flow becomes supercritical, additional conditions must be satisfied at any shock wave that appears in the flow field. Those conditions are easily obtained by following the technique of Murman and Cole [9]. I begin by writing (3.11) in the conservation form

$$\nabla\cdot\left\{\left[1-m^2-m^2(\gamma+1)\phi_x\right]q_x\,\hat{i} + q_z\hat{k}\right\} = 0 \tag{3.20}$$

The integral of (3.20) over the entire flow field is then converted to the line integral

$$\int_C \left\{\left[1-m^2-m^2(\gamma+1)\phi_x\right]q_x\hat{i} + q_z\hat{k}\right\}\cdot\hat{n}\,ds \tag{3.21}$$

which, when integrated across a discontinuity, yields the parametric shock jump conditions

$$\left\langle\left[1-m^2-m^2(\gamma+1)\phi_x\right]q_x\right\rangle\left(\frac{dz}{dx}\right)_s - \langle q_z\rangle = 0 \tag{3.22}$$

Having properly posed the linear boundary value problem, steady transonic flow solutions may be obtained. However, a base solution of the nonlinear problem is needed to initialize the solution procedure. One possibility is to solve the potential equation for a starting solution, but other realistic solutions may be easily obtained. The conditions for which those solutions are valid are outlined below.

3.5. Formulation of Base Solutions

Miles [42] and Lin, et. al. [43], by scaling the variables of (2.18) in the following manner

$$\xi = x$$

$$\eta = z$$

$$\phi = \bar{\epsilon} f^* , \quad f^* = O(1)$$

and ordering terms, have shown that the flow field is transonic if

$$1 - M^2 = O(\tau^{2/3}, \sigma^{2/3})$$

and is subsonic or supersonic if

$$|1-M^2| \gg \bar{\tau}^{2/3}, \sigma^{2/3}$$

Since I only consider flows that are subsonic at infinity, if $\bar{\tau}$ and σ are sufficiently small, the base solution will satisfy Laplace's equation

$$\phi_{xx} + \phi_{\bar{z}\bar{z}} = 0$$

Consequently, the base solutions may be obtained from elementary singularity distributions.

Considering the lift to be due to an angle of attack, α, the starting lifting solution, ϕ^L, may be obtained by distributing a line of vortices along the airfoil chord. Extending the incompressible vorticity distribution, derived in [31], to compressible flows, ϕ^L becomes

$$\phi^L(x,\bar{z};\alpha_0) = \frac{\alpha}{\pi} \int_{chord} \sqrt{\frac{c-\xi^*}{\xi^*}} \tan^{-1}\left(\frac{\bar{z}}{x-\xi^*}\right) d\xi^* \qquad (3.23)$$

The nonlifting contribution is represented by the following distribution of sources and sinks along the airfoil chord

$$\phi^t(x,z;\tau_0) = \frac{I}{2\pi B}\int_{chord} F'(\xi)\ln\left[(x-\xi)^2+\bar{z}^2\right]d\xi \tag{3.24}$$

In Appendix B, (3.24) has been integrated to yield the base solution for nonlifting biconvex airfoils.

3.6. Summary

I have used the method of parametric differentiation to linearize the steady, small perturbation transonic flow problem. A predictor-corrector method for extending the solution was presented, and the boundary value problem for lifting and nonlifting flows, including flows with imbedded shock waves, have been specified. A base solution is required to initialize the solution procedure, and conditions for which relatively simple linear base solutions may be used for this purpose are presented. These base solutions are then represented by singularity distributions.

CHAPTER IV

DETERMINATION OF THE RATE OF CHANGE OF THE STEADY POTENTIAL AND RESULTS FOR STEADY FLOWS

4.1. Introduction

In order to determine the rate of change of the steady potentials with the chosen parameter, I must solve a linear partial differential equation with variable coefficients. Because of the variable coefficients, any solution technique that is used must be capable of admitting elliptic, hyperbolic, and discontinuous solutions. In this work, finite difference methods are applied, with appropriate difference operators being employed in the various regions of the flow field. Those operators are constructed to allow signals to propagate in the upstream and downstream directions in subsonic (elliptic) regions and only in the downstream direction in supersonic (hyperbolic) regions.

The correct direction of signal propagation and the calculation of the parametric shock jump conditions are ensured by applying the concept of conservative type dependent differencing to (3.11). This type of differencing is equivalent to adding, at all points in supersonic flow regions, an artificial viscosity of the order of the grid spacing in the streamwise direction. Derivatives in the streamwise direction are approximated with

centered differences in subsonic flow regions and with backward (upwind) differences in supersonic flow regions, and derivatives normal to the free stream are always approximated with centered differences. Where the flow accelerates through sonic velocity, a parabolic difference operator is used, and immediately downstream of imbedded shock waves, I employ a combination of centered and backward differences.

In the numerical procedure, special measures are taken to satisfy the boundary conditions. Dirichlet conditions are satisfied by setting g along the appropriate boundary at the prescribed value, and Neumann and Robbin conditions are specified midway between grid points. Neumann and Robbin boundary conditions are then easily incorporated into the difference equations.

Having differenced the equation governing g in the manner described above, I obtain an implicit set of simultaneous equations. Starting from the upstream boundary, I proceed downstream calculating the flow field using a column relaxation method. The entire process is repeated until, throughout the flow field, the magnitude of the difference of the value of g for successive iterations and the change in Δg_7 over a given number of iterations are less than predetermined constants. All computations are carried out in a coordinate system that has been stretched to infinity. That stretching increases the density of grid points near the airfoil and requires the computation of

relatively fewer points in the far field.

In the remainder of this chapter, I present the numerical procedure used to solve (3.11) subject to the appropriate conditions; that procedure is detailed in Appendix C. Also, I present families of steady state loads on lifting and nonlifting airfoils, the convergence histories of the solutions, and some comparisons of my data with that obtained by other researchers.

4.2. Coordinate System

At large distances from the airfoil, far field boundary conditions are to be specified, and if the computational region is extended sufficiently far, the relatively simple boundary conditions at infinity may be utilized. Here, I use the coordinate transformation introduced by Carlson [44] which maps an infinite physical region into a finite computational domain and distributes the grid points more densely in the neighborhood of the airfoil. The infinite physical region may now be computed with a reasonable number of grid points.

The physical plane is separated into the three regions shown in Figure 4.1, and the coordinates are transformed in the following manner

$$z = a_1 \tan\left(\frac{\pi}{2}\eta\right) \qquad |\eta| \le 1 \tag{4.1}$$

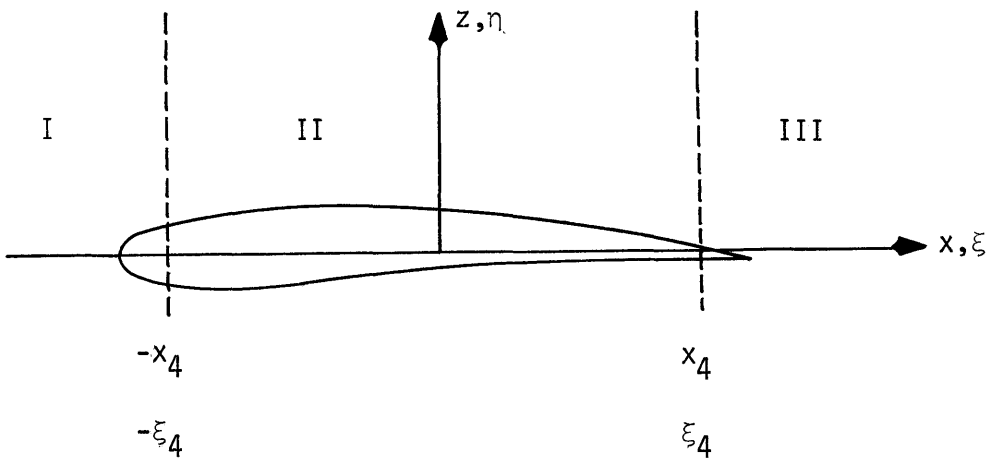

Figure 4.1. Regions of the physical plane.

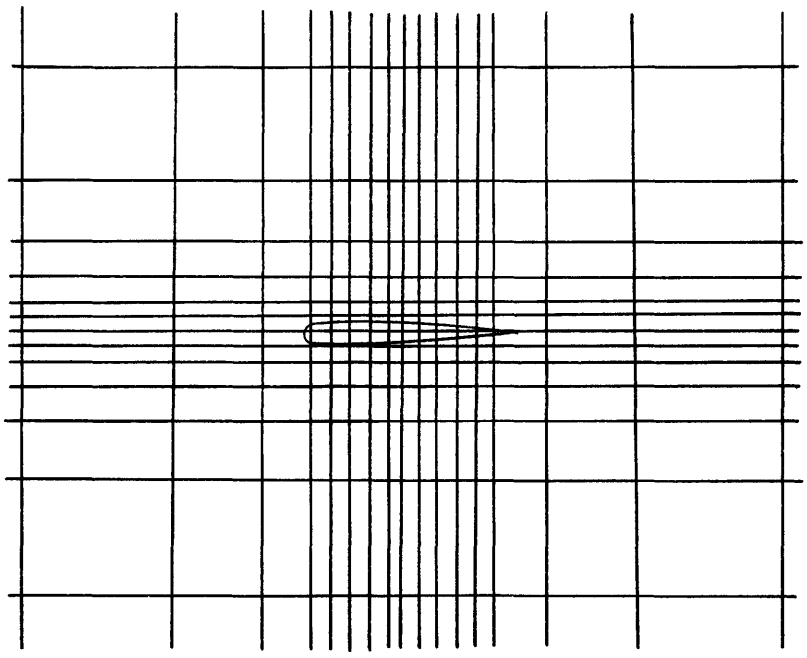

Figure 4.2. Typical transformed coordinate system.

$$x_I = -x_4 + a_2 \tan\left[\frac{\pi}{2}(\xi+\xi_4)\right] + a_3 \tan\left[\frac{\pi}{2}(\xi+\xi_4)^3\right] \qquad -(1+\xi_4) \le \xi \le -\xi_4 \qquad (4.2)$$

$$x_{II} = \xi(a_4 + b\xi^2) \qquad |\xi| \le \xi_4 \qquad (4.3)$$

$$x_{III} = x_4 + a_2 \tan\left[\frac{\pi}{2}(\xi-\xi_4)\right] + a_3 \tan\left[\frac{\pi}{2}(\xi-\xi_4)^3\right] \qquad \xi_4 \le \xi \le (1+\xi_4) \qquad (4.4)$$

Hence, the infinite physical region is transformed into the finite computational plane $|\xi| \le (1+\xi_4)$, $|\eta| \le 1$. The constants a_1, a_2, a_3, x_4 and ξ_4 are predetermined, and a_4 and b are determined by requiring continuity of x and $\frac{dx}{d\xi}$ at $\xi = \pm\xi_4$.

In region II, the transformed coordinate is then

$$x_{II} = \xi\left[\left(\frac{6x_4 - \pi a_2 \xi_4}{4\xi_4}\right) + \left(\frac{\pi a_2 \xi_4 - 2x_4}{4\xi_4^3}\right)\xi^2\right] \qquad |\xi| \le \xi_4$$

We should also note that the coordinate stretching is symmetric and that the airfoil should be centered at the origin of the coordinate system. The airfoil chord then varies from $-\frac{c}{2}$ to $\frac{c}{2}$.

A typical transformed coordinate system is shown in Figure 4.2.

4.3. Treatment of the Boundary Conditions

In the transformed coordinates, (3.11) becomes

$$[1-m^2-m^2(\gamma+1)f\phi_\xi]f(fg_\xi)_\xi - m^2(\gamma+1)f(f\phi_\xi)_\xi f g_\xi$$

$$+h(hg_\eta)_\eta = 0 \qquad (4.5)$$

where $f = \frac{d\xi}{dx}$ and $h = \frac{d\eta}{dz}$ in regions I, II, and III are

$$h = \frac{2}{\pi a_1}\cos^2\left(\frac{\pi}{2}\eta\right)$$

$$f_I = \frac{2}{\pi}\left\{a_2\sec^2\left[\frac{\pi}{2}(\xi+\xi_4)\right] + 3a_3(\xi+\xi_4)^2\sec^2\left[\frac{\pi}{2}(\xi+\xi_4)^3\right]\right\}^{-1}$$

$$f_{II} = (a_4 + 3b\xi^2)^{-1}$$

$$f_{III} = \frac{2}{\pi}\left\{a_2\sec^2\left[\frac{\pi}{2}(\xi-\xi_4)\right] + 3a_3(\xi-\xi_4)^2\sec^2\left[\frac{\pi}{2}(\xi-\xi_4)^3\right]\right\}^{-1}$$

For nonlifting and lifting airfoils, respectively, the tangency conditions become

$$hg_\eta = \pm F'(x(\xi)) \qquad (4.6)$$

$$hg_\eta = \zeta_\eta'(x(\xi)) \qquad (4.7)$$

Downstream of subsonic trailing edges

$$\Delta\varphi\left(X(\xi) > \frac{c}{2}\,,\ \eta = 0\right) = \Delta\varphi_T \tag{4.8}$$

and if the trailing edge flow is supersonic

$$\Delta\varphi\left(X(\xi) > \frac{c}{2}\,,\ \eta = 0\right) = \Delta\varphi\left(X(\xi) = \frac{c}{2}^{+},\ \eta = 0\right) \tag{4.9}$$

In order to more easily incorporate the far field conditions into the numerical procedure, the conditions that are actually used are slightly different from those in (3.19). Along the lateral boundaries of the computational plane, the potential is represented as that due to a point vortex located at $(\xi, \eta) = (0,0)$. Consequently,

$$\phi(\xi, \pm 1) = -\frac{\Delta\phi_T}{2\pi}\,\theta_v \tag{4.10}$$

which in the parametric problem becomes

$$\varphi(\xi, \pm 1) = -\frac{\Delta\varphi_T}{2\pi}\,\theta_v \tag{4.11}$$

where θ_v is the polar angle measured in the counter-

clockwise direction. At points that are midway between the first and second grid columns, I impose the condition that the perturbation velocity in the streamwise direction must vanish. In the parametric problem, this condition becomes

$$f_{\xi} = 0 \qquad \xi = -(1+\xi_4) + \frac{\Delta\xi}{2} \tag{4.12}$$

Similarly, downstream of the airfoil

$$f_{\xi} = 0 \qquad \xi = 1+\xi_4 - \frac{\Delta\xi}{2} \tag{4.13}$$

The full plane boundary value problem is shown in Figure 4.3.

If the flow is nonlifting, symmetry is used to reduce the computational requirements. I consider the flow in only the upper half of the flow field and enforce the condition that, except along the airfoil chord, there is no vertical velocity component along the line of symmetry. This condition is

$$h_{\eta} = 0 \qquad |x(\xi)| > \frac{c}{2}\ , \ \eta = 0 \tag{4.14}$$

If the flow is nonlifting, conditions (4.8) and 4.9) are automatically satisfied. Figure 4.4 illustrates the half plane boundary value problem.

4.4. Finite Difference Equations for the Linearized Problem

The correct direction of signal propagation throughout the

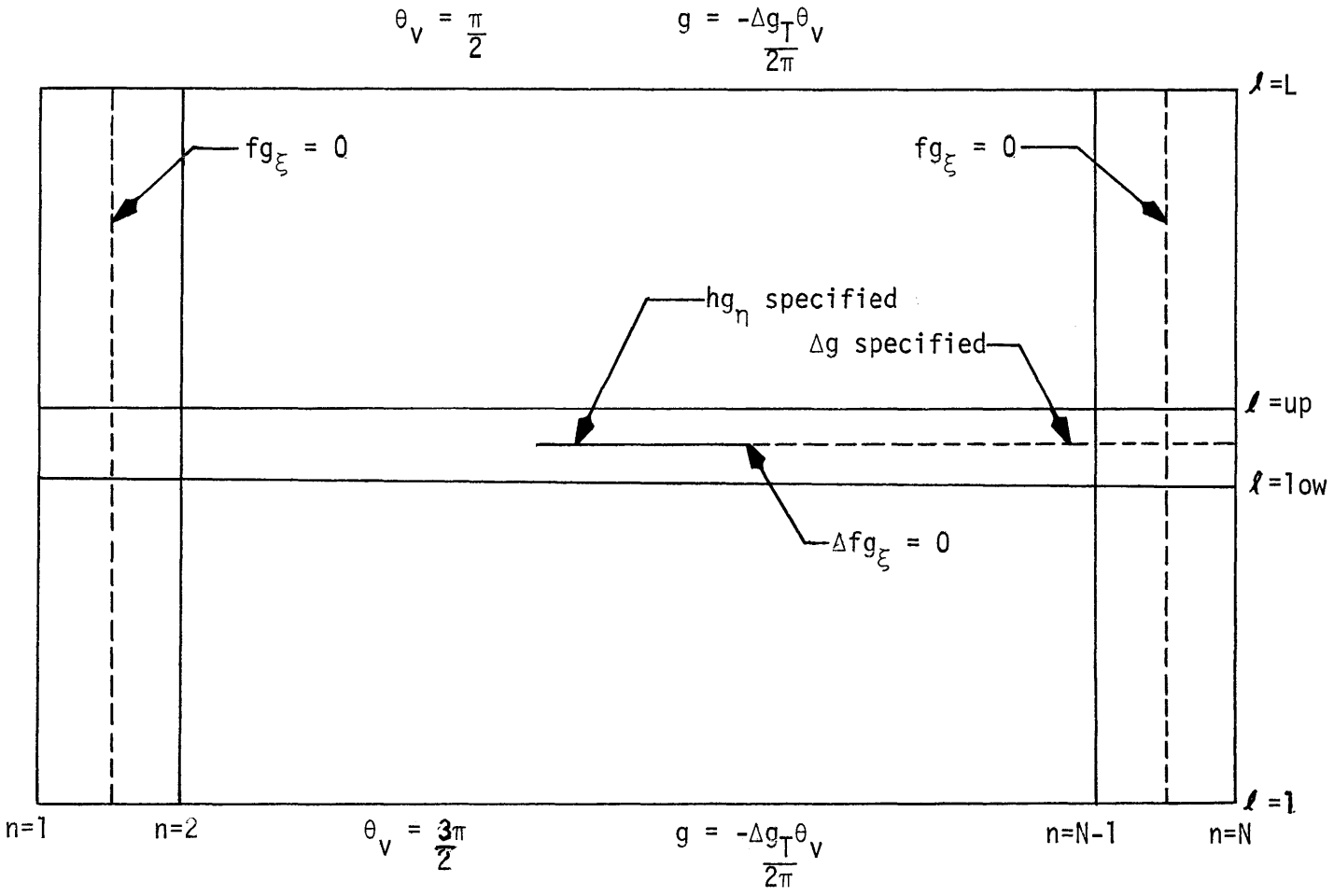

ıre 4.3. Full plane boundary value problem.

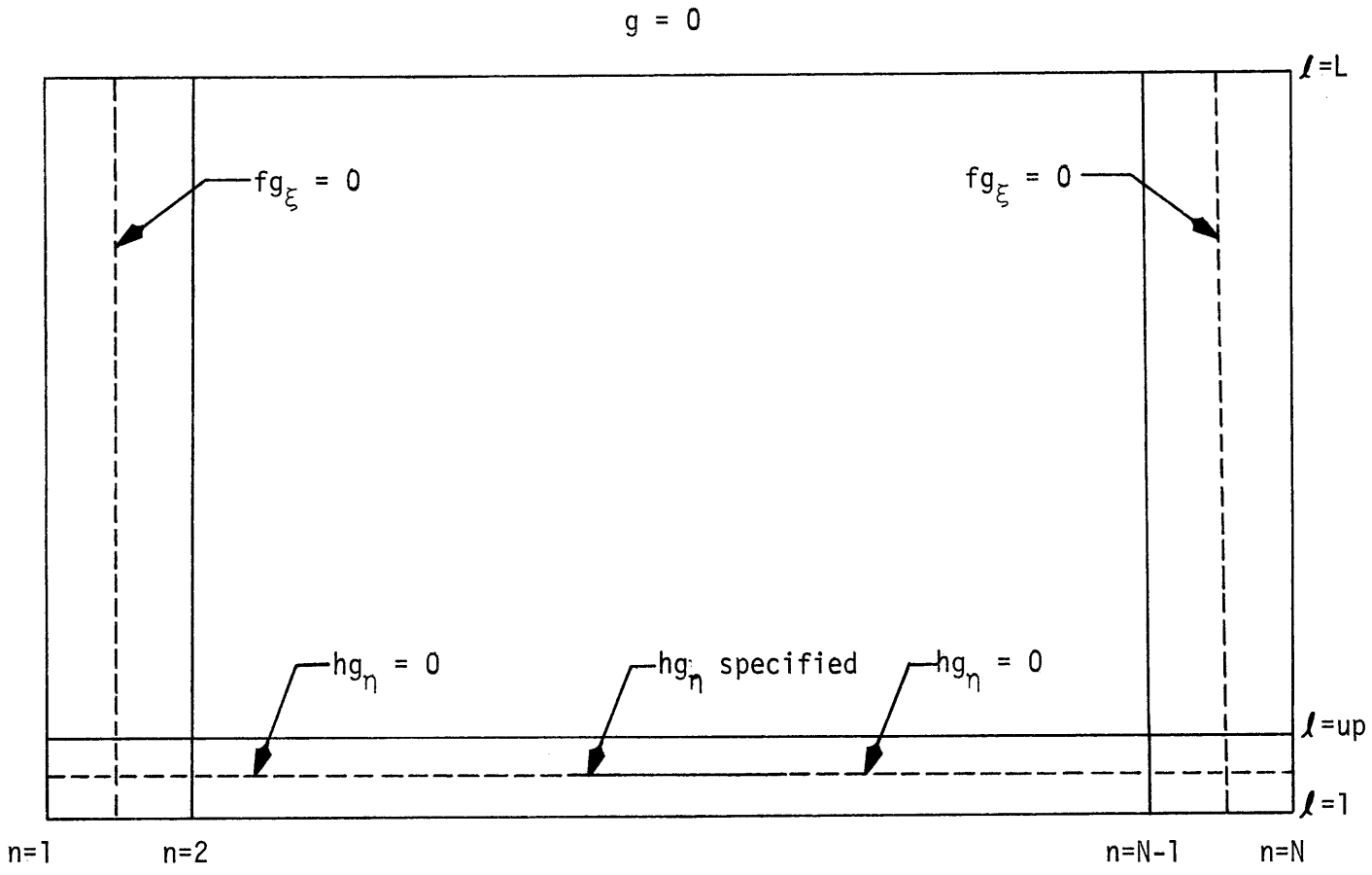

re 4.4. Half plane boundary value problem.

flow field and the calculation of the parametric shock jump conditions are ensured by using a conservative type dependent difference method. Defining $\tilde{a}$ and $\tilde{b}$ as

$$\tilde{a} \equiv \frac{f}{h}\left[1-M^2-M^2(\gamma+1)f\phi_\xi\right]g_\xi$$

$$\tilde{b} = \frac{h}{f}\,g_\eta$$

the divergence form of (4.5) is

$$\nabla\cdot(\tilde{a}\,\hat{i}+\tilde{b}\,\hat{k}) = 0 \tag{4.15}$$

By integrating (4.15) over the shaded element of area in Figure 4.5, I obtain

$$\frac{\tilde{a}_{n+1/2,\ell}-\tilde{a}_{n-1/2,\ell}}{\Delta\xi} + \frac{\tilde{b}_{n,\ell+1/2}-\tilde{b}_{n,\ell-1/2}}{\Delta\eta} = 0 \tag{4.16}$$

The substitution of (C.3)-(C.6) and (C.9)-(C.12) into (4.16) then leads to the conservative finite difference representation of (4.5)

$$(1-\mu_{n,\ell})\left\{\alpha_1\left[g_{n+1,\ell}-\frac{g^+_{n,\ell}}{\omega}-\left(1-\frac{1}{\omega}\right)g_{n,\ell}\right]-\alpha_2\left[\frac{g^+_{n,\ell}}{\omega}+\left(1-\frac{1}{\omega}\right)g_{n,\ell}-g^+_{n-1,\ell}\right]\right\}$$

$$+\mu_{n-1,\ell}\left[\alpha_2(g_{n,\ell}-g_{n-1,\ell})-\alpha_3(g_{n-1,\ell}-g_{n-2,\ell})\right]$$

$$+\frac{h_\ell}{\Delta\eta^2}\left[h_{\ell+1/2}(g^+_{n,\ell+1}-g^+_{n,\ell})-h_{\ell-1/2}(g^+_{n,\ell}-g^+_{n,\ell-1})\right]=0 \tag{4.17}$$

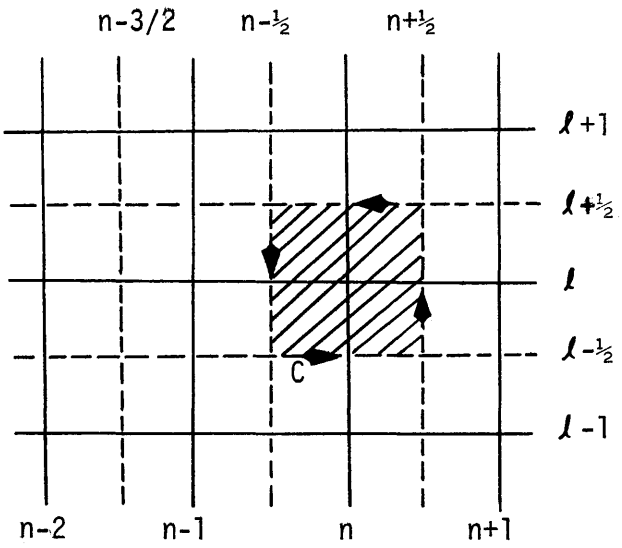

Figure 4.5. Element of area in the computational plane.

where the superscript + denotes data from the current iteration, and the nonsubscripted variables are from the previous iteration.

In supersonic flow regions, it is necessary to add additional terms to (4.17) to maintain numerical stability. The reason for this becomes clear when I do a timelike analysis of (4.17). Treating the difference between iterations, $g^{+}_{n,\ell} - g_{n,\ell}$, as a time derivative, at subsonic points the actual equation being solved is

$$f\{[1-m^2-m^2(\gamma+1)f\phi_\xi]fg_\xi\}_\xi + h(hg_\eta)_\eta$$

$$-\alpha_2 \Delta t \Delta\xi g_{\xi t} - \left[\frac{\alpha_1}{\omega} - \alpha_2\left(1-\frac{1}{\omega}\right)\right]\Delta t\, g_t = 0 \qquad (4.18)$$

and at supersonic points I solve

$$f\{[1-m^2-m^2(\gamma+1)f\phi_\xi]fg_\xi\}_\xi + h(hg_\eta)_\eta = 0 \qquad (4.19)$$

The characteristics of (4.19) are the curves

$$\frac{d\xi}{d\eta} = \pm\frac{f}{h}\sqrt{-[1-m^2-m^2(\gamma+1)f\phi_\xi]}$$

which are real. Consequently, (4.19) is hyperbolic with ξ as the timelike direction. As the solution approaches its converged value, the timelike derivatives in (4.18) vanish and we obtain solutions to the original steady state equation. However, from (4.18) and (4.19) it is evident that at the beginning of the

iteration process, the time dependent terms may not match near the sonic line, so I add the term $-\epsilon^* f_n f_{n-1/2} \frac{\Delta t}{\Delta \xi} g_{\xi t}$ to (4.19).

Since ξ is the timelike direction in the steady supersonic problem, I should take steps to ensure that it remains the timelike direction in the unsteady problem. The analysis of (C.17)-(C.19) demonstrates that the proper choice of ϵ^* ensures that ξ remains the timelike direction when $-\epsilon^* f_n f_{n-1/2} \frac{\Delta t}{\Delta \xi} g_{\xi t}$ is added to (4.19). In this work I use $\epsilon^* = .6$, and the choice of $\epsilon^* \leq 0$ results in numerical instabilities. With the inclusion of the additionalterm,the form of the finite difference representation of (4.5) becomes

$$
\begin{aligned}
&(1-\mu_{n,\ell})\left\{ d_1 \left[g_{n+1,\ell} - \frac{g^+_{n,\ell}}{\omega} - \left(1-\frac{1}{\omega}\right) g_{n,\ell} \right] - d_2 \left[\frac{g^+_{n,\ell}}{\omega} + \left(1-\frac{1}{\omega}\right) g_{n,\ell} - g^+_{n-1,\ell} \right] \right\} \\
&+ \mu_{n-1,\ell} \left[d_2 (g_{n,\ell} - g_{n-1,\ell}) - d_3 (g_{n-1,\ell} - g_{n-2,\ell}) \right] \\
&+ \frac{h_\ell}{\Delta \eta^2} \left[h_{\ell+1/2} (g^+_{n,\ell+1} - g^+_{n,\ell}) - h_{\ell-1/2} (g^+_{n,\ell} - g^+_{n,\ell-1}) \right] \\
&- \mu_{n,\ell} \epsilon^* f_n f_{n-1/2} \frac{}{\Delta \xi^2} (g^+_{n,\ell} - g_{n,\ell} - g^+_{n-1,\ell} + g_{n-1,\ell}) = 0
\end{aligned}
\tag{4.20}
$$

That using the conservative differencing scheme amounts to adding an artificial viscosity of order $\Delta \xi$ to the equations at

supersonic points is seen by writing (4.17) in the form

$$\left\{\left[\frac{f}{h}\left(1-M^2-M^2(\gamma+1)f\phi_\xi\right)g_\xi\right]_\xi\right\}_{n,\ell} + \left[\left(\frac{h}{f}g_\eta\right)_\eta\right]_{n,\ell}$$

$$-\left\{\mu\left[\frac{f}{h}\left(1-M^2-M^2(\gamma+1)f\phi_\xi\right)g_\xi\right]_\xi\right\}_{n,\ell} + \left\{\mu\left[\frac{f}{h}\left(1-M^2-M^2(\gamma+1)f\phi_\xi\right)g_\xi\right]_\xi\right\}_{n-1,\ell} = 0 \tag{4.21}$$

The last two terms in (4.21) are a difference approximation of $-D_\xi\left\{\mu\left[\frac{f}{h}\left(1-M^2-M^2(\gamma+1)f\phi_\xi\right)g_\xi\right]_\xi\right\}_\xi$ which is taken to be an artificial viscosity. In the limit of vanishing grid spacing, the artificial viscosity vanishes.

Equation (4.20) is referred to as the interior point difference equation because it is valid at points away from the boundaries of the computational region. Near the boundaries, the difference equation is altered to satisfy the boundary conditions. The following sections describe the methods used to satisfy conditions (4.6)-(4.8) and (4.11)-(4.14).

4.5. Numerical Treatment of the Boundary Conditions

On the upper and lower boundaries of the computational region, (4.11) is used to specify the values of $g(\xi,1)$, and the other boundary conditions are satisfied by altering the form of the difference equations at the appropriate points. The upstream and downstream conditions, (4.12) and (4.13), are satisfied by setting $(fg_\xi)_{n-1/2,\ell} = 0$ along n = 2

and by setting $(fg_\xi)_{n+1/2,\ell} = 0$ along n = N-1. When these conditions are substituted into (4.17), I obtain the finite difference equations given in (C.38) and (C.47). Satisfying (4.12) and (4.13) in the above manner implies an algebraic relationship between $g_{1,\ell}$ and $g_{2,\ell}$ and between $g_{N-1,\ell}$ and $g_{N,\ell}$, and it is not necessary to determine $g_{1,\ell}$ and $g_{N,\ell}$.

The airfoil tangency condition and the symmetry condition are incorporated into the difference equations by altering the form of the derivatives in the η direction. The tangency condition is satisfied on the slit $|x(\xi)| \le \frac{c}{2}$ midway between the rows ℓ = up and ℓ = low (See Figures 4.3 and 4.4). When $|x(\xi)| \le \frac{c}{2}$, $(hg_\eta)_{n,up-1/2}$ and $(hg_\eta)_{n,low+1/2}$ are prescribed from the upper and lower boundary tangency conditions. In the nonlifting problem, I must satisfy the condition

$$(hg_\eta)_{n,up-1/2} = 0 \qquad |x(\xi)| > \frac{c}{2}$$

When the above derivatives are substituted into

$$h(hg_\eta)_\eta = \frac{h_\ell}{\Delta\eta}\left[(hg_\eta)_{n,\ell+1/2} - (hg_\eta)_{n,\ell-1/2}\right] \tag{4.22}$$

at the appropriate grid points, conditions (4.6), (4.7) and (4.14) are satisfied.

4.6. Numerical Treatment of the Subsonic Trailing Edge Condition and the Conditions Along the Cut in the Flow Field

The conditions at subsonic trailing edges and on the cut in the flow field are also incorporated into the difference equations by altering (4.22). Because q is discontinuous along the slit downstream of the trailing edge, values of q along ℓ=up are larger, by the amount $\Delta\tilde{q}$, than the values I would obtain by expanding in a Taylor series from ℓ=low to ℓ=up. To offset this discontinuity, I add $\Delta\tilde{q}$ to $q_{n,low}$, and η derivatives on the slit become

$$(hq_\eta)_{n,up-1/2} = (hq_\eta)_{n,low+1/2} = \frac{h_{up+1/2}}{\Delta\eta}\left[q_{n,up} - (q_{n,low}+\Delta\tilde{q})\right] \tag{4.23}$$

The conditions at the trailing edge and on the slit are then incorporated into the difference equations by substituting, in (4.22), the right side of (4.23) for $(hq_\eta)_{n,\ell-1/2}$ along ℓ=up and for $(hq_\eta)_{n,\ell+1/2}$ along ℓ=low. Equation (4.8) indicates that $\Delta\tilde{q}$ should have the value of Δq_T, hence I need a method to determine the appropriate jump in q along the cut in the flow field.

Throughout the iteration procedure, Δq_T is an unknown quantity which must be calculated simultaneously with the solution of (4.5). To determine the correct value of Δq_T, we extend, to the present problem, the method applied by Ballhaus and Bailey [45] to the potential equation. We update $\Delta\tilde{q}$

using the relaxation formula

$$\Delta\tilde{g}^{+} = \Delta\tilde{g} - \omega_r(\Delta\tilde{g} - \Delta g_T) \tag{4.24}$$

where ω_r is an under relaxation factor - usually near 0.2. I then substitute $\Delta\tilde{g}^{+}$ for Δg_T in (4.11) and solve the finite difference equations. The value of Δg_T is then calculated and the process repeated until a converged solution is found. As the solution converges, $\Delta\tilde{g}$ and $\Delta\tilde{g}^{+}$ approach Δg_T. Condition (4.8) is satisfied, and g takes on its theoretical values along $\eta = \pm 1$. The finite difference equations adjacent to the cut in the flow field are given in (C.56)-(C.71).

The jump in g across the airfoil is evaluated using a second order extrapolation procedure. From (C.76) and (C.81) that jump is found to be

$$\Delta g_n = \frac{9}{8}(g_{n,up} - g_{n,low}) - \frac{1}{8}(g_{n,up+1} - g_{n,low-1}) - \frac{3}{8}\Delta\eta\left[(g_\eta^u)_n + (g_\eta^l)_n\right] \tag{4.25}$$

where g_η^u and g_η^l are known from the upper and lower boundary tangency conditions, respectively. Generally, the trailing edge is not located at a mesh point, thus the linear extrapolation, detailed in (C.83)-(C.87), is used to derive the following expression for Δg_T

$$\Delta g_T = \left(1 + \frac{3}{2}\frac{\Delta\xi_T}{\Delta\xi}\right)\Delta g_{-T1} - 2\frac{\Delta\xi_T}{\Delta\xi}\Delta g_{-T2} + \frac{\Delta\xi_T}{2\Delta\xi}\Delta g_{-T3} \qquad (4.26)$$

where the subscripts are explained in Figure 4.6.

4.7. Results and Discussions

At each point (n,ℓ), (4.20) is written in the form

$$-A_\ell g^+_{n,\ell-1} + B_\ell g^+_{n,\ell} - C_\ell g^+_{n,\ell+1} = D_\ell$$

where the vectors A, B, C and D throughout the flow field are given in Appendix C. I then apply the solution procedure of Apendix G to determine $g(x,z;\epsilon)$. Those calculations were carried out, for biconvex airfoils, on a grid with 51 columns and 22 rows. The constants a_1, a_2, a_3, ξ_4 and x_4 were set at 1, .3, 2, 1 and .493, respectively, and $\Delta\xi$ was chosen to be .08. This choice of constants produces a grid with 25 points on the airfoil. I set $\Delta\eta$ at .09524, and when solving only for the upper half of the flow field I chose $\Delta\eta$ =.04878 with the first grid row located at η =-.02439. $|\eta| \le 1$ and $|\xi| \le 2$, which for my choice of constants, stretches the grid to infinity in both directions. Numerical solutions of (3.11) were considered to have converged, for nonlifting flows, when $\left|\frac{g^+_{n,\ell} - g_{n,\ell}}{\omega}\right| \le 2\cdot10^{-5}$ and for lifting flow, when $\left|\frac{g^+_{n,\ell} - g_{n,\ell}}{\omega}\right| \le .0015$ which corresponds to Δg_T changing by less

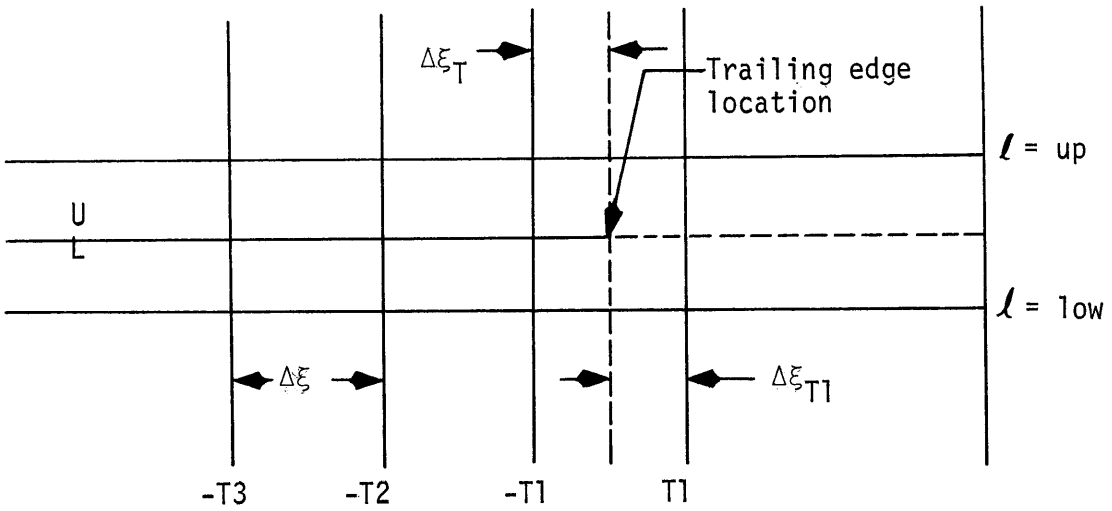

Figure 4.6. Grid spacing near the airfoil trailing edge.

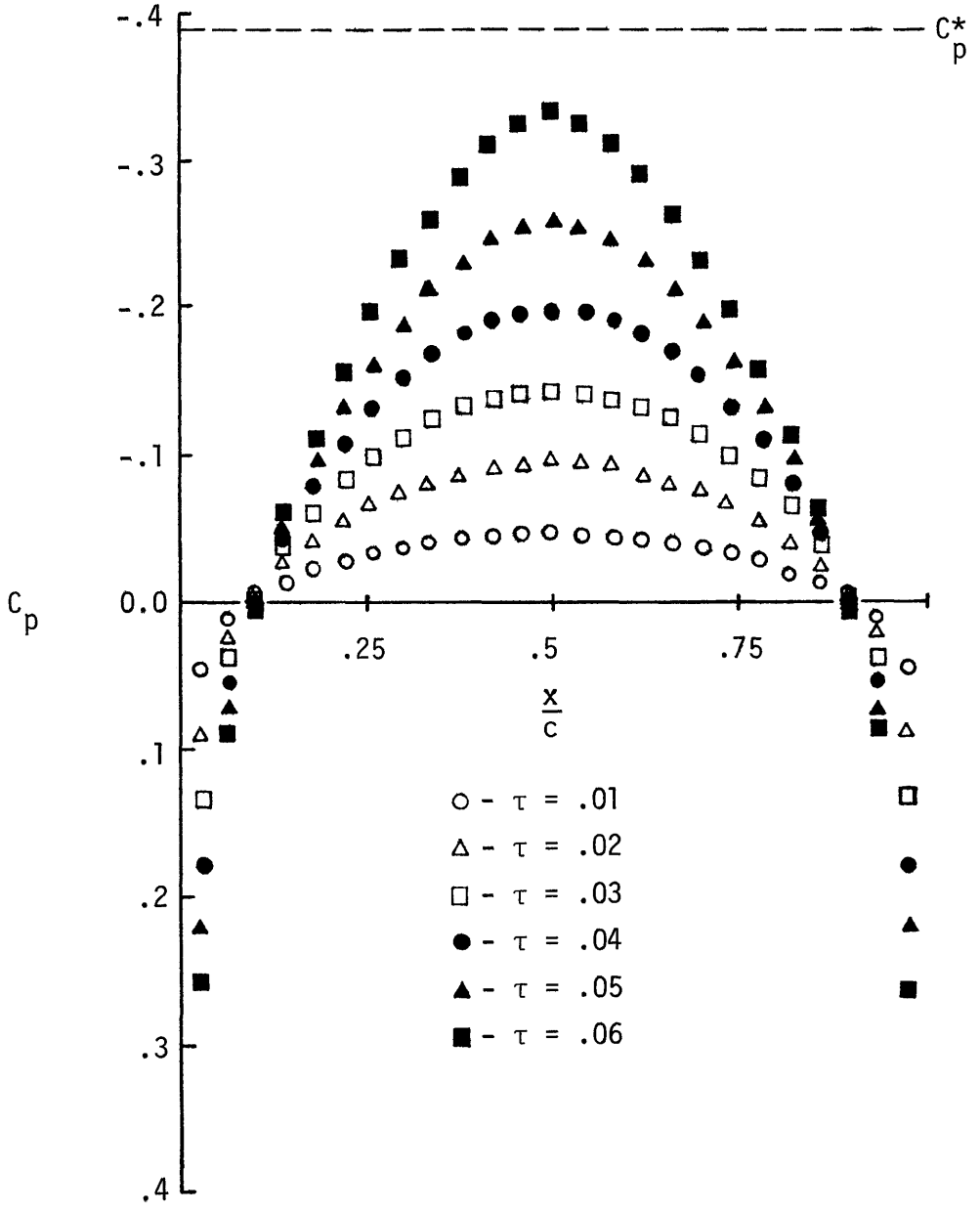

Figure 4.7. Pressure distributions on nonlifting parabolic arc airfoils at M = .825.

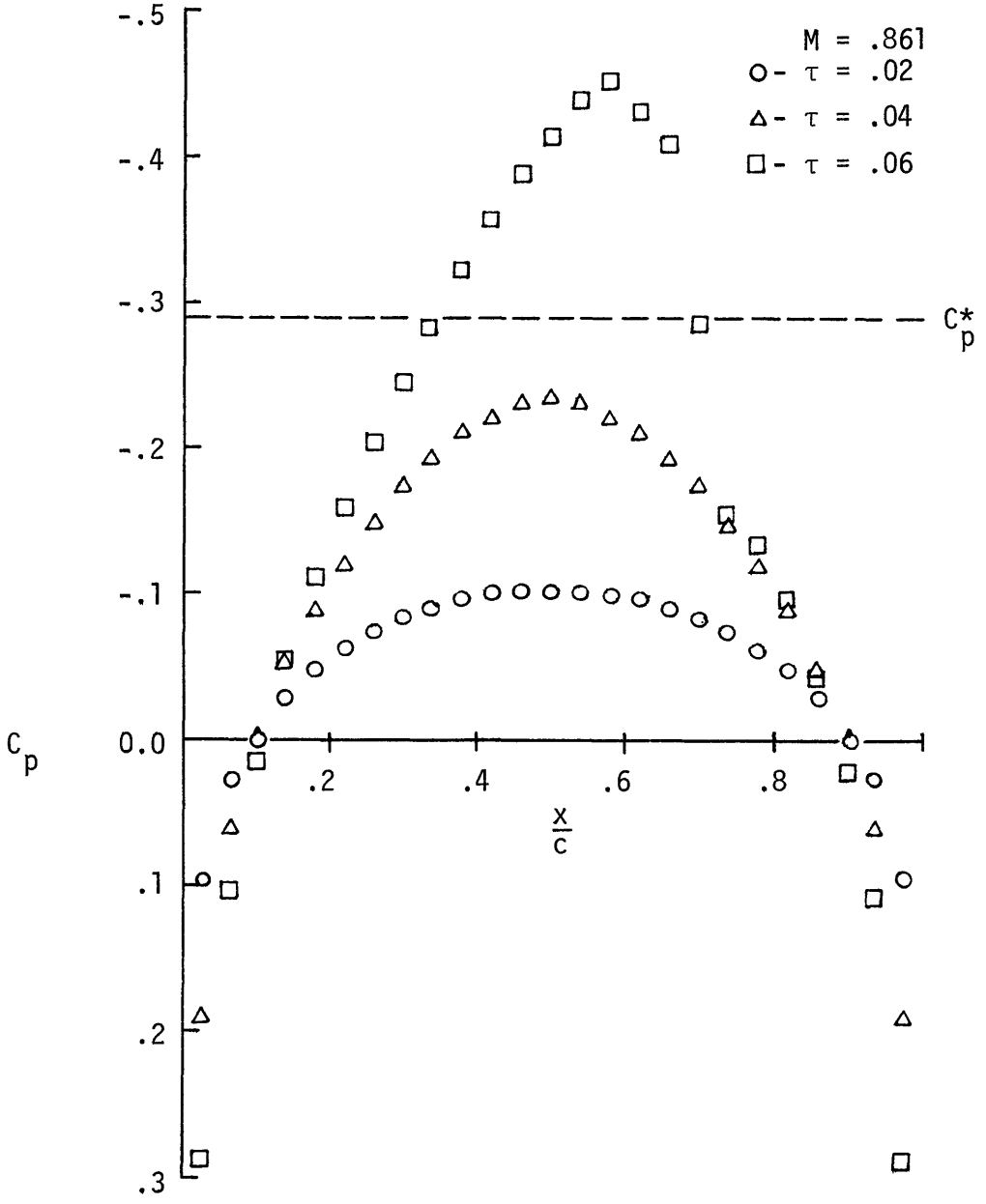

Figure 4.8. Pressure distributions on nonlifting circular arc airfoils.

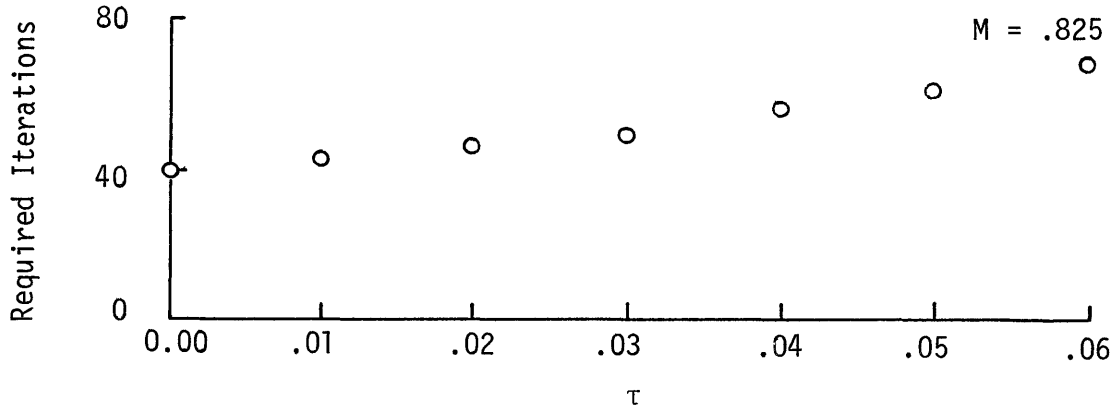

Figure 4.9. Computational requirements for nonlifting parabolic arc airfoils.

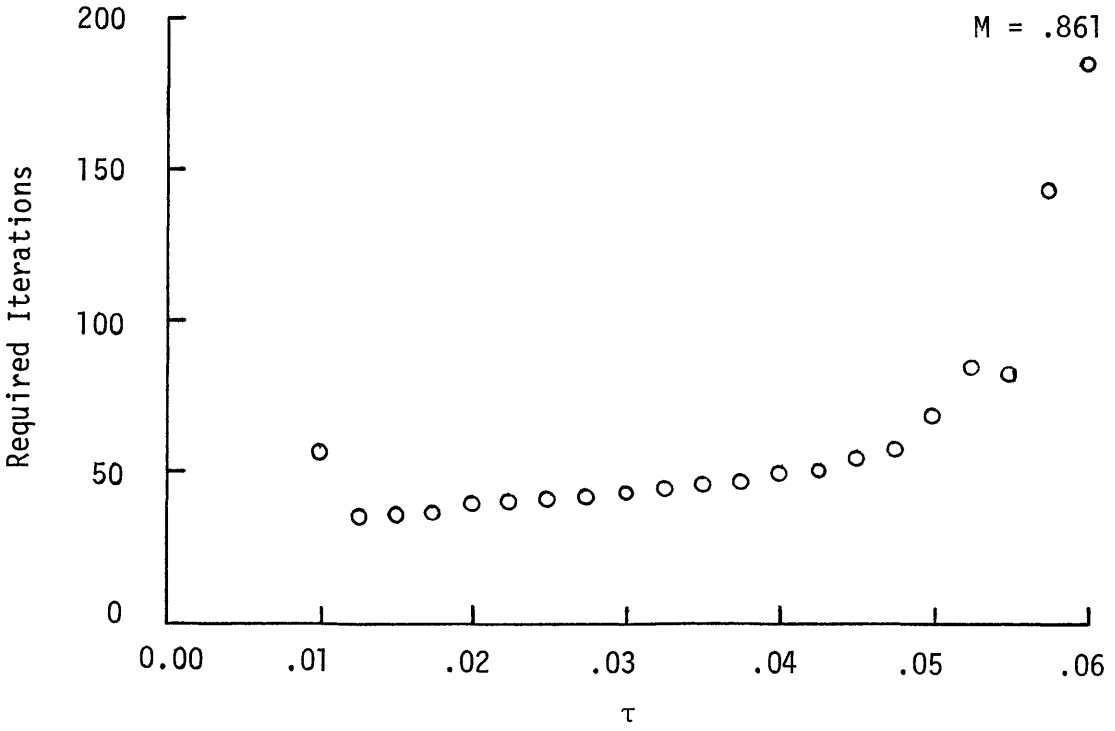

Figure 4.10. Computational requirements for nonlifting circular arc airfoils.

than 0.02% between successive iterations.

When the finite difference methods used to determine $g(x,z;\epsilon)$ are combined with the predictor-corrector methods of Section 3.3, I obtain families of steady flow solutions (The computer program is listed in Appendix H). A typical set of solutions for nonlifting subcritical airfoils is shown in Figure 4.7, where I have chosen $\tau_0 = 0$ and $\Delta\tau = .01$. Figure 4.8 shows part of the family of solutions that result when increasing the airfoil thickness ratio caused the flow to become supercritical; those solutions were obtained using $\tau_0 = .01$ and $\Delta\tau = .0025$. For the examples described above, the computations required to determine g at the various values of τ are summarized in Figures 4.9 and 4.10. For subcritical flows, the required computations increase slightly with increasing τ, and when supersonic flow regions appear, the computational requirements show a relatively sharp increase as τ increases. The previous solution of (3.11) is used as the initial estimate of the new solution, and the sharp increase in required computations could be due to the failure of that initial estimate to adequately approximate the new solution near shock waves.

To obtain the six solutions in Figure 4.7 and the 21 solutions from which I obtain Figure 4.8 requires one minute and 3.42 minutes of CPU time, respectively, on an IBM 370/168. The initial computational requirements are substantially reduced by differentiating (B.4) with respect to τ and using that result as the initial estimate of the solution at $\tau = \tau_0$. When that procedure is followed, the determination of $g(x,z;\tau_0)$ for M=.806 and M=.825 requires 38 and 39 iterations, respectively. In contrast, 219 and 225 iterations are required if I make an initial estimate of $g = 0$.

Figures 4.11 and 4.12 show that the solutions are indeed weak functions of the base solution. The pressure distributions were determined using as base solutions, first, $\phi = 0$ everywhere (a nonlifting flat plate) and then the solution given by (B.4) for $\tau = .01$. A lack of resources prevented a similar comparison for supercritical flows, but the result is expected to be the same.

By varying first the airfoil thickness ratio and then its angle of attack, I obtained families of lifting solutions. Pressure distributions on a six percent thick circular arc airfoil at angles of attack $.5^0$ and 1^0 are shown in Figure 4.13; I have chosen $\tau_0 = 0$, $\Delta\tau = .01$, $\alpha_0 = 0^0$ and $\Delta\alpha = .5^0$. Comparisons of the lift coefficient and the moment coefficient about the leading edge with those predicted by thin airfoil theory are shown in Figure 4.14. The determination of $g(x,z;\alpha_0)$ requires a relatively large amount of computations, but the computational speed may be increased. Values of $g(x,z;\tau=.06)$ were used as the initial estimate of $g(x,z;\alpha_0)$, but since g represents the rate of change of the solution in the direction of each parameter, that is not a good initial estimate of $g(x,z;\alpha_0)$. Hence, a relatively high number of iterations is needed to determine $g(x,z;\alpha_0)$. I expect that using the derivative of (3.23) with respect to α as the initial estimate would increase the convergence rate. Once the initial solution is known, the computational requirements decrease sharply, and other lifting solutions are computed very quickly. Figure 4.15 summarizes the computations required to determine the solutions of Figure 4.13; it requires 2.9 minutes of CPU time on an IBM 370/168 to compute the six nonlifting and two lifting solutions. As

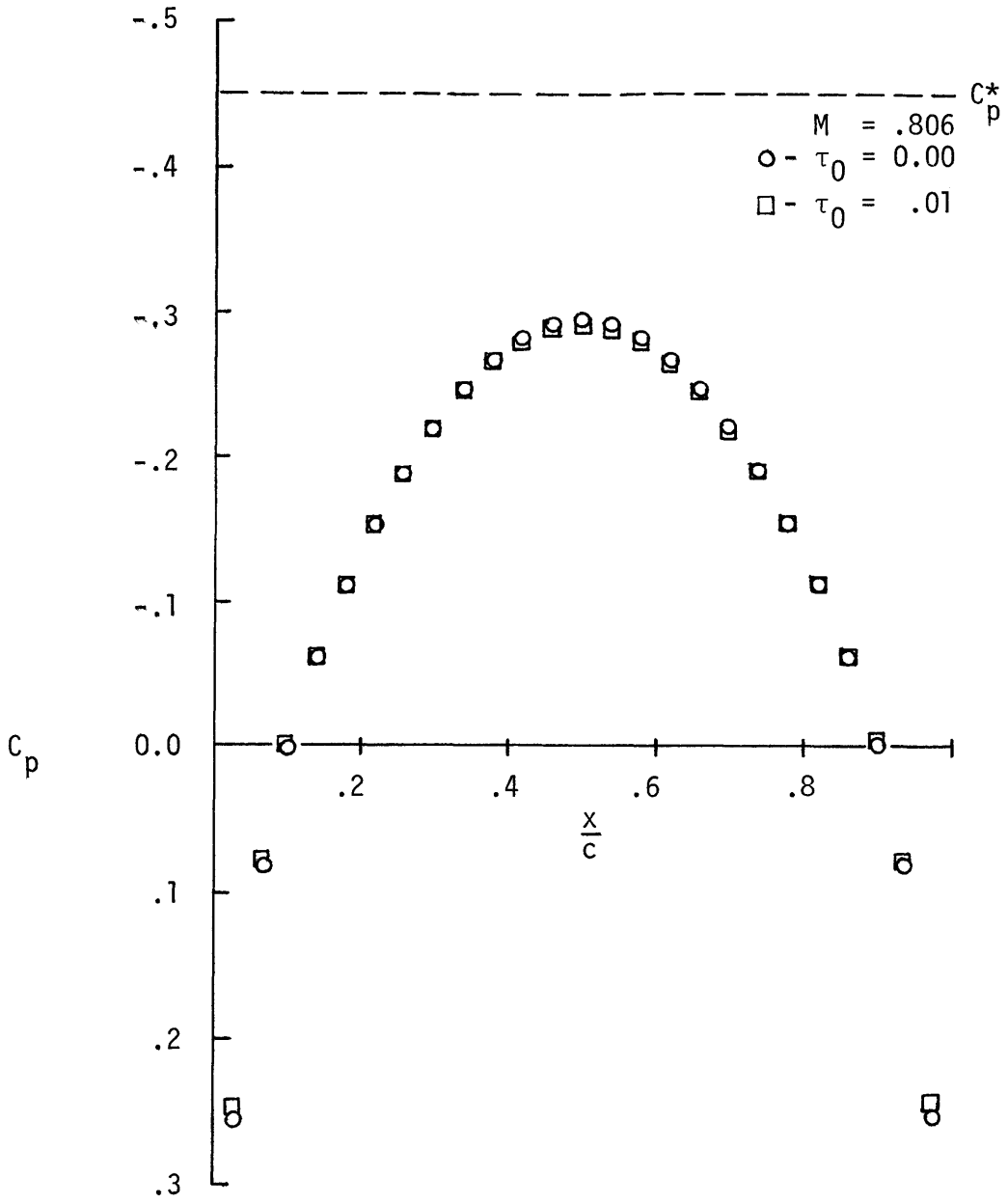

Figure 4.11. Pressure distributions on a six percent thick, nonlifting circular arc airfoil.

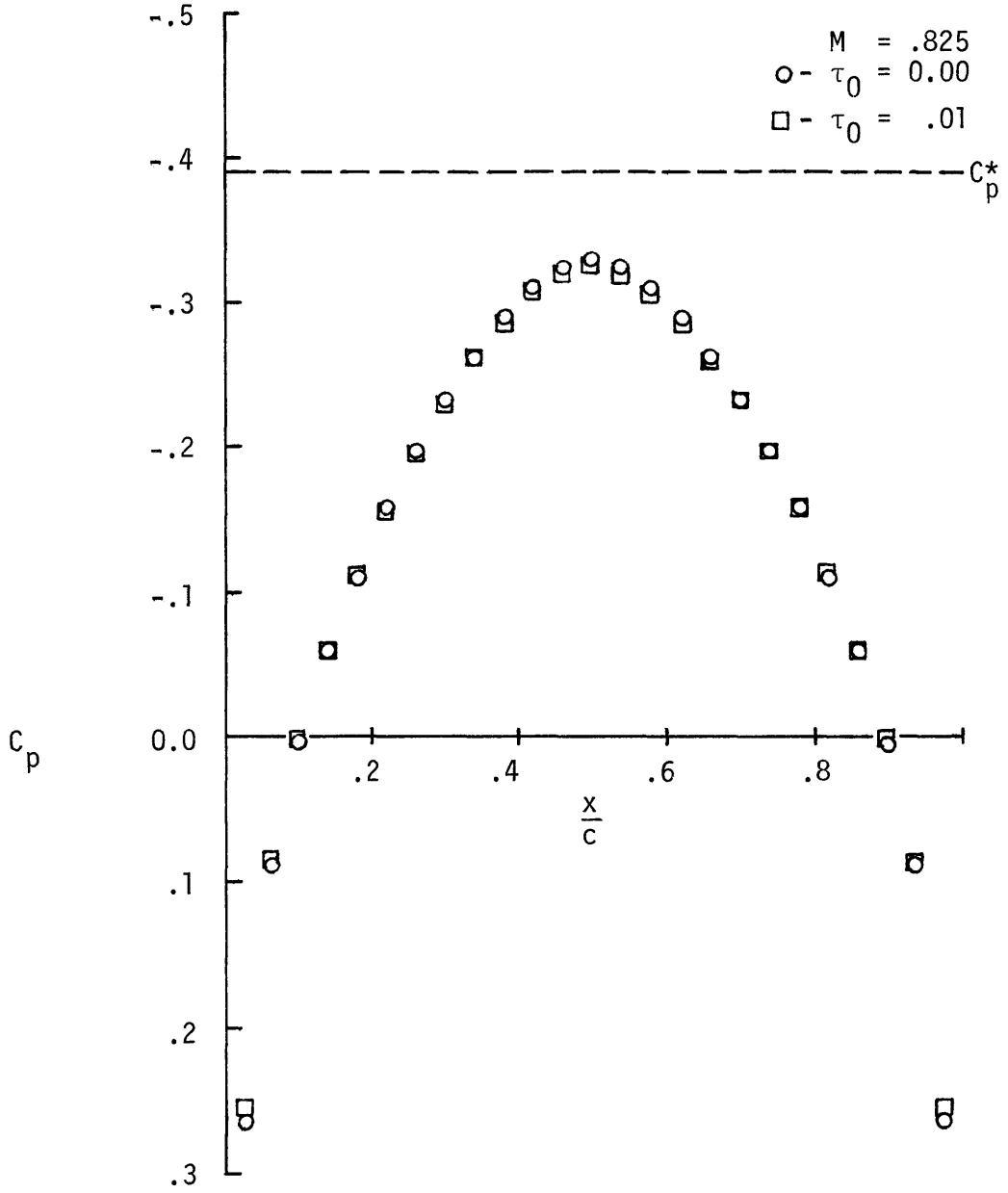

Figure 4.12. Pressure distributions on a six percent thick, nonlifting parabolic arc airfoil.

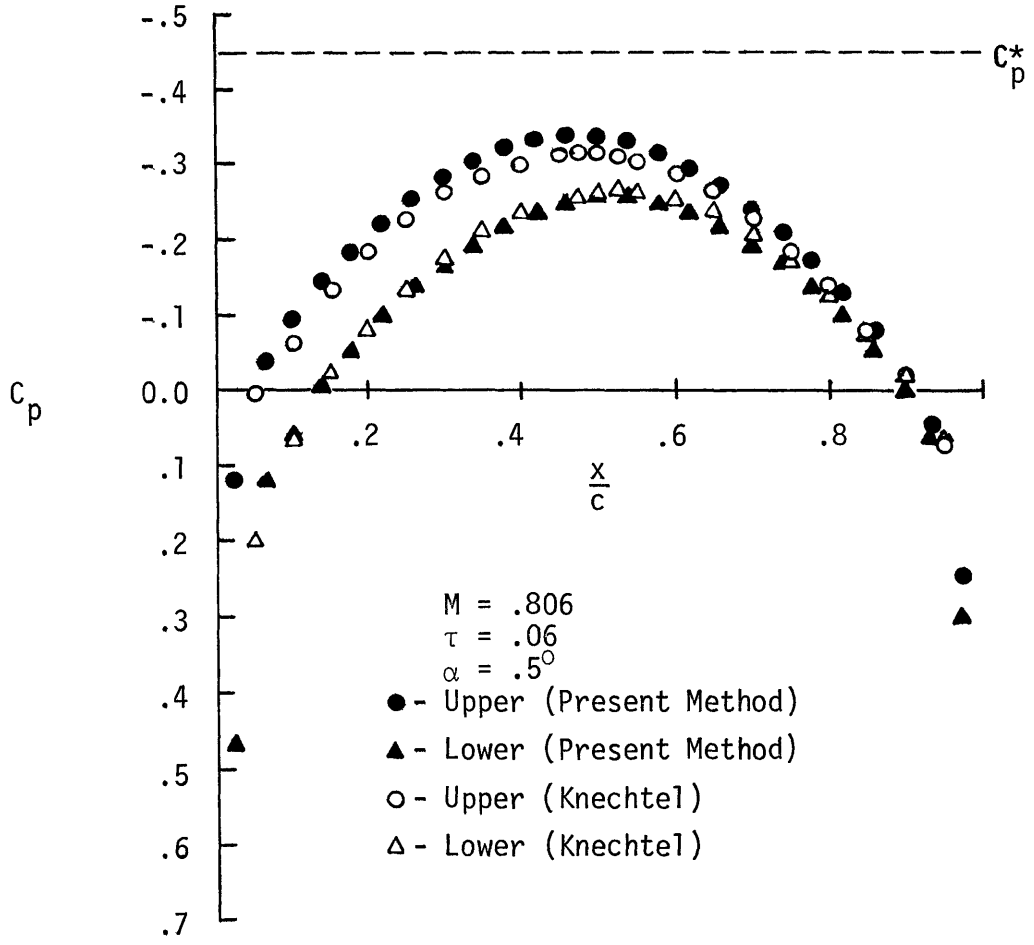

Figure 4.13a. Pressure distributions on a lifting circular arc airfoil.

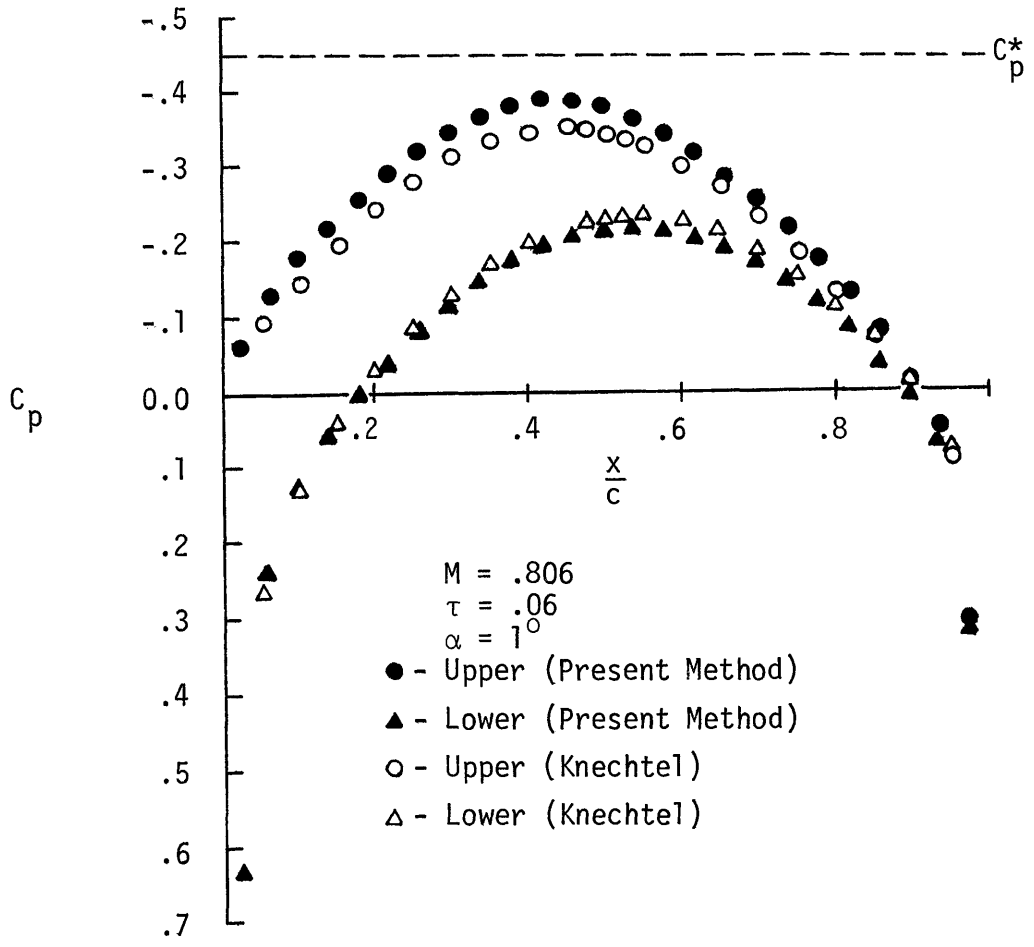

Figure 4.13b. Pressure distributions on a lifting circular arc airfoil.

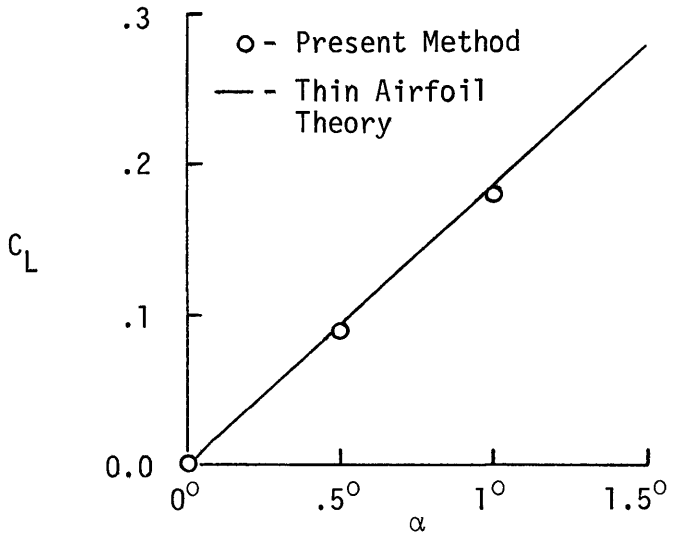

Figure 4.14a. Lift coefficients on a six percent thick circular arc airfoil at M = .806.

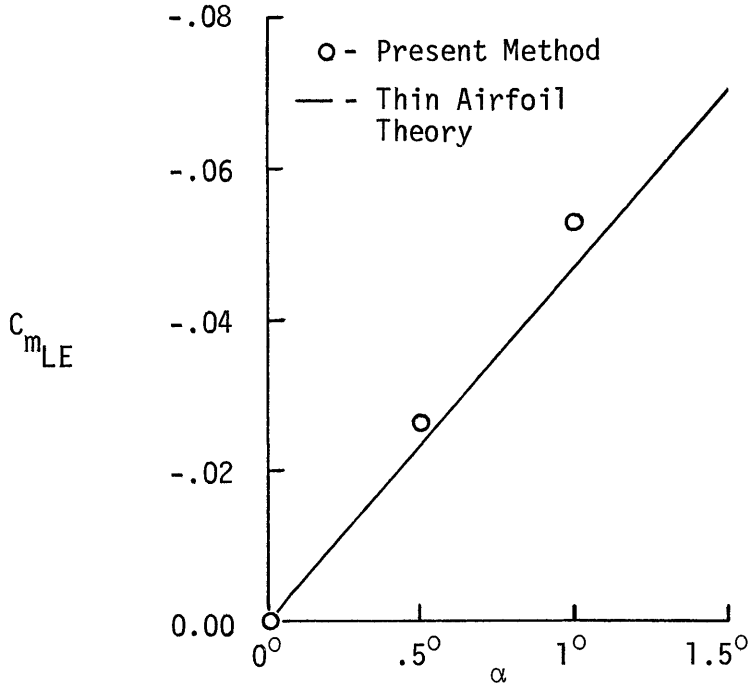

Figure 4.14b. Moment coefficients about the leading edge of a six percent thick circular arc airfoil at M = .806.

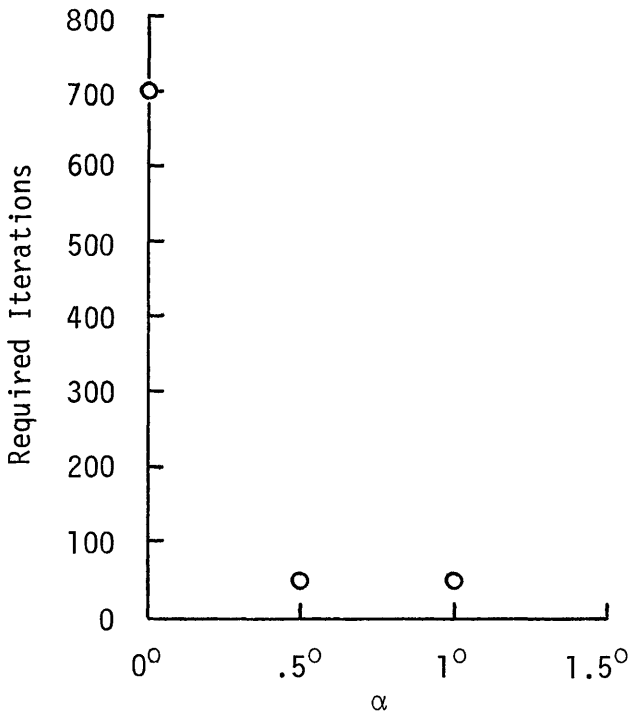

Figure 4.15. Computational requirements for lifting circular arc airfoils at M = .806.

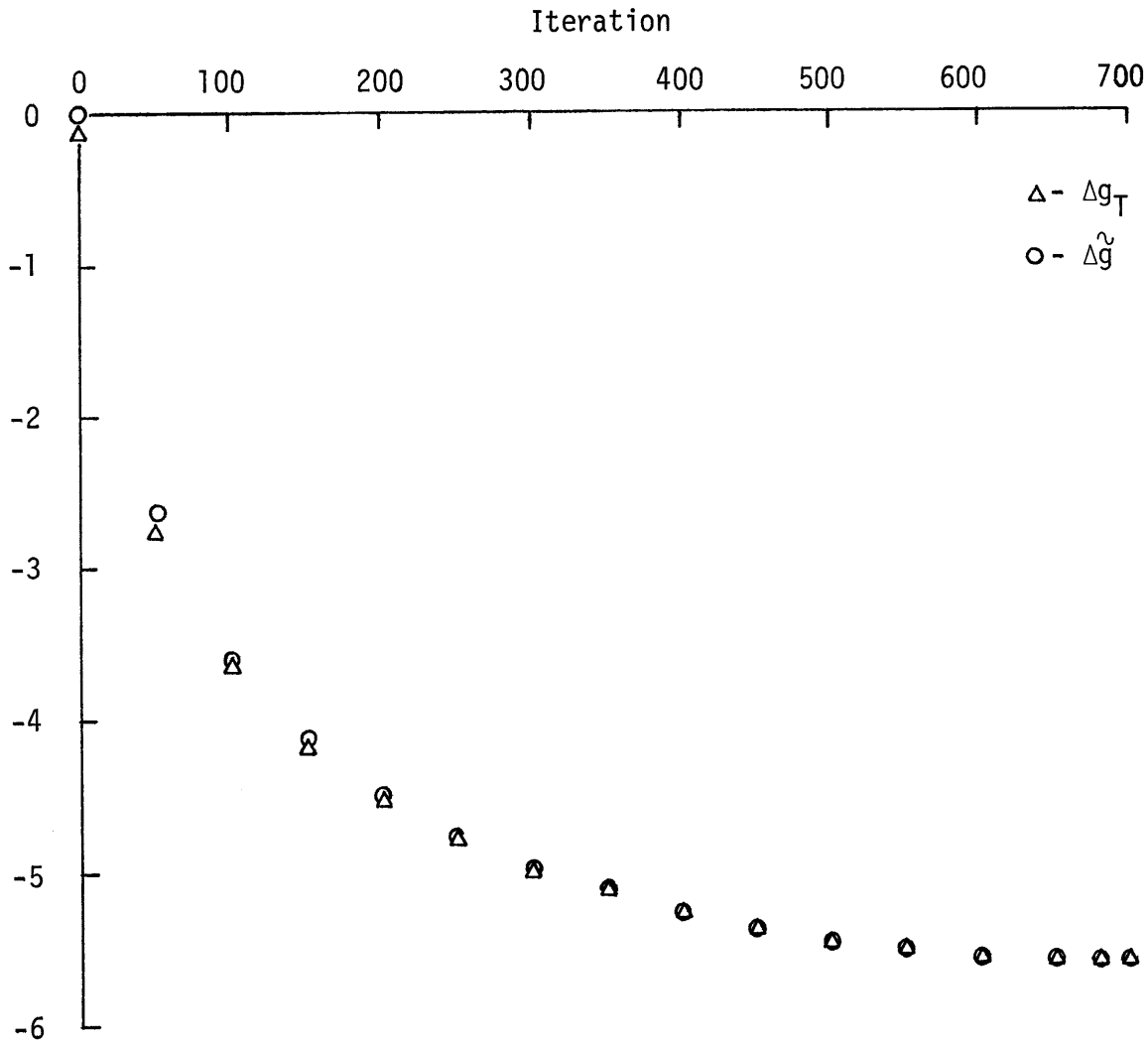

Figure 4.16a. The jump in g at the airfoil trailing edge and the jump in g used to evaluate the far field; M = .806, $\alpha = 0^{o}$.

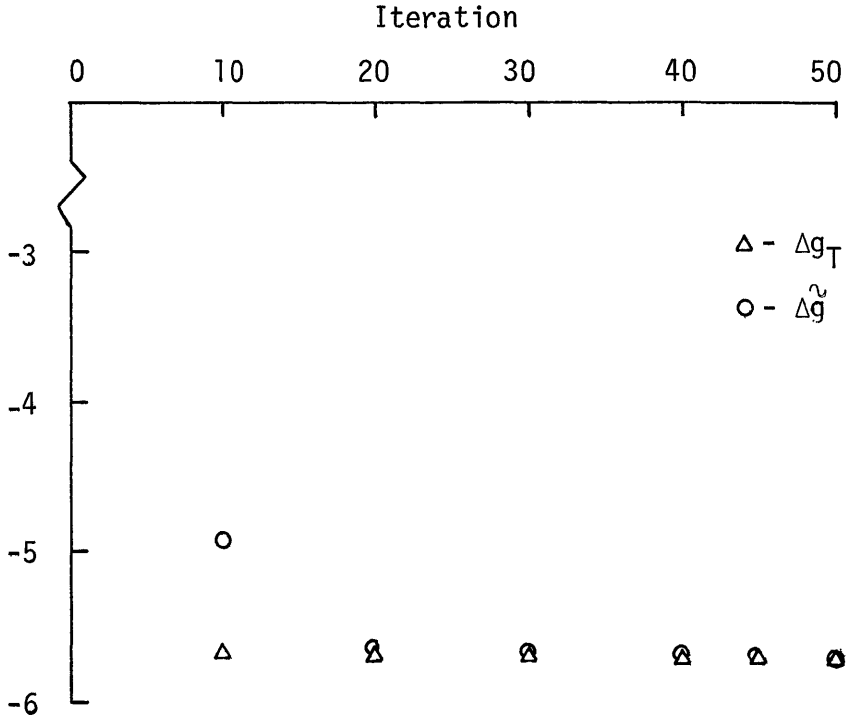

Figure 4.16b. The jump in g at the airfoil trailing edge and the the jump in g used to evaluate the far field; M = .806, $\alpha = .5^{\circ}$.

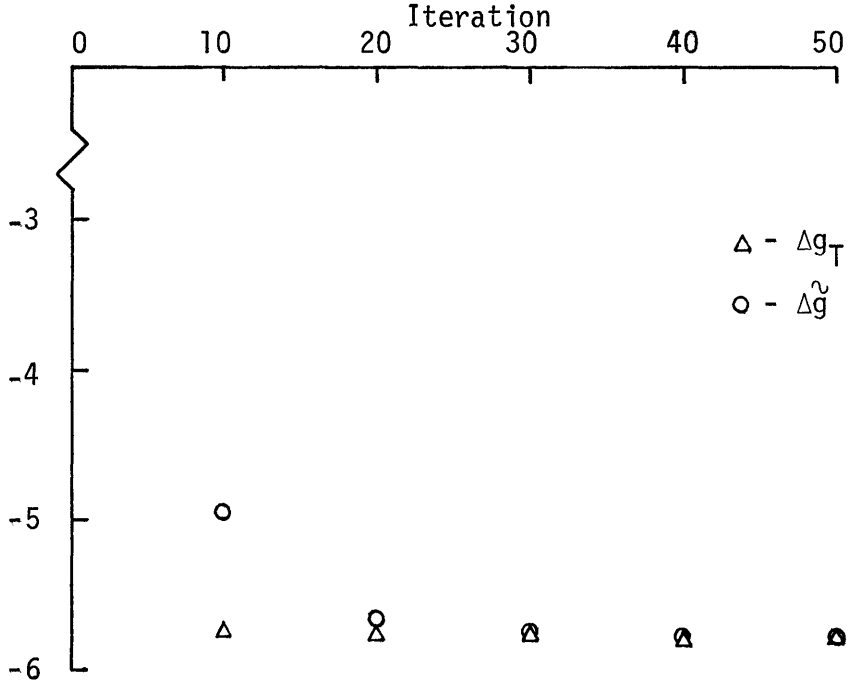

Figure 4.16c. The jump in g at the airfoil trailing edge and the the jump in g used to evaluate the far field; M = .806, $\alpha = 1^{\circ}$.

solutions of (3.11) converge, how Δq_T and $\Delta \tilde{q}$ stabilize and approach each other is shown in Figure 4.16.

When using parametric differentiation to analyze lifting flows, it is essential to be consistent in defining the sign of all angles. For example, the mean airfoil position, $\mathcal{F}(x)$, may be written as

$$\mathcal{F}(x) = \pm \tau F(x) \pm \alpha x$$

depending on how α is defined. Hence, the tangency conditions becomes

$$q_z = \pm 1$$

Since, in the far field, I define positive angles in the counter-clockwise direction, I must define $\mathcal{F}(x)$ and the tangency condition as

$$\mathcal{F}(x) = \pm \tau F(x) + \alpha x$$

$$q_z = 1$$

with negative values of α producing positive lift. Defining $\mathcal{F}(x)$ as $\pm\tau F(x) - \alpha x$, with $\alpha > 0$ for positive lift is contrary to the definition of θ_v and leads to numerical instabilities.

Having determined families of steady solutions, I next compare my results with data obtained by other means. Figure 4.17 shows a comparison of nonlifting, subcritical pressure distributions obtained using the present method with those obtained by Rubbert [46], using parametric differentiation, and the experiments of Knechtel [47]. There is good agreement between between all three sets of data, especially between the present method and the experimental data. A comparison of nonlifting, subcritical data with the integral equation method (IEM) of Ogana [48] is shown in Figure 4.18, and Figure 4.19 shows a comparison of current supercritical results with those obtained from a finite difference

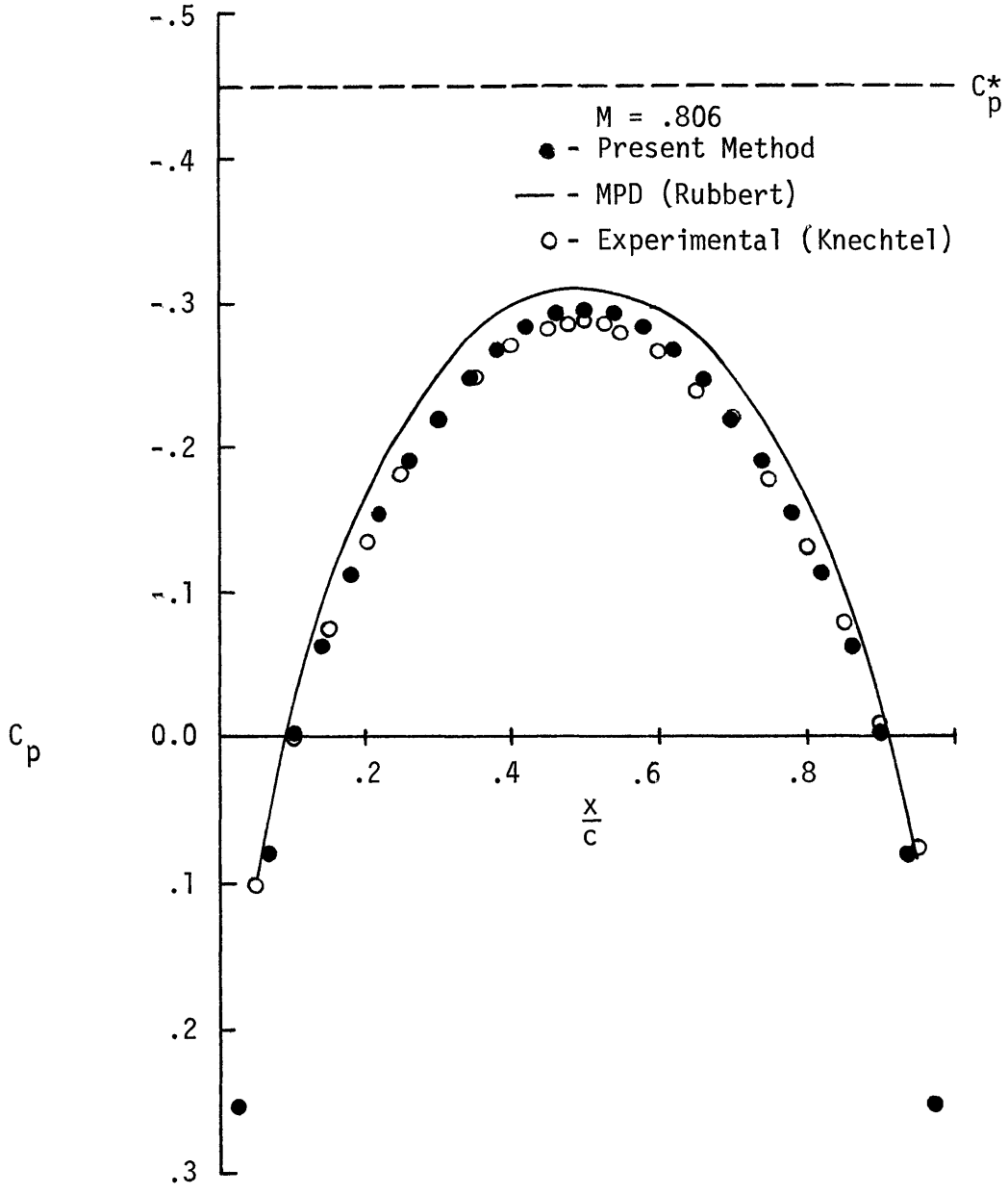

Figure 4.17. Pressure distributions on a six percent thick circular arc airfoil.

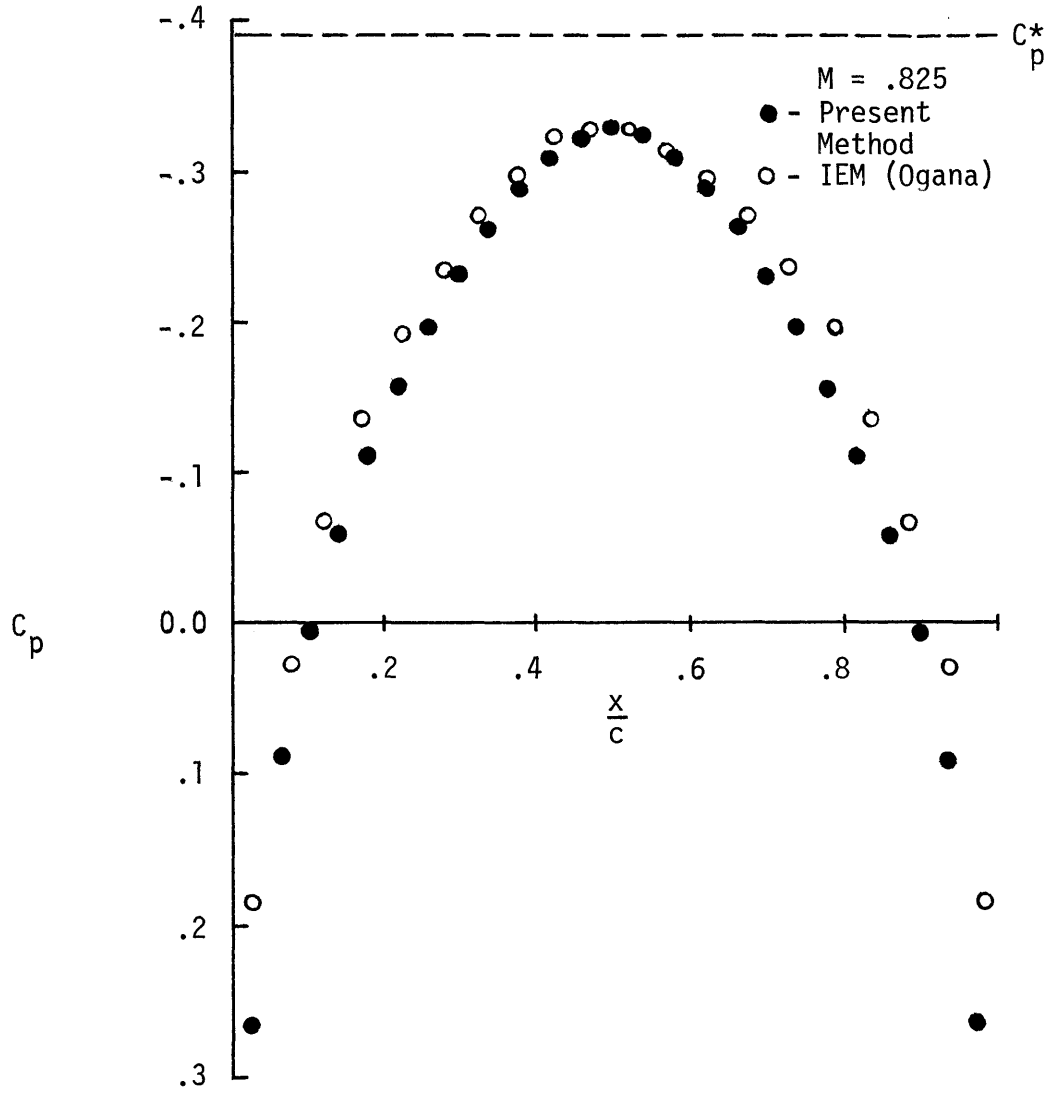

Figure 4.18. Pressure distributions on a six percent thick parabolic arc airfoil.

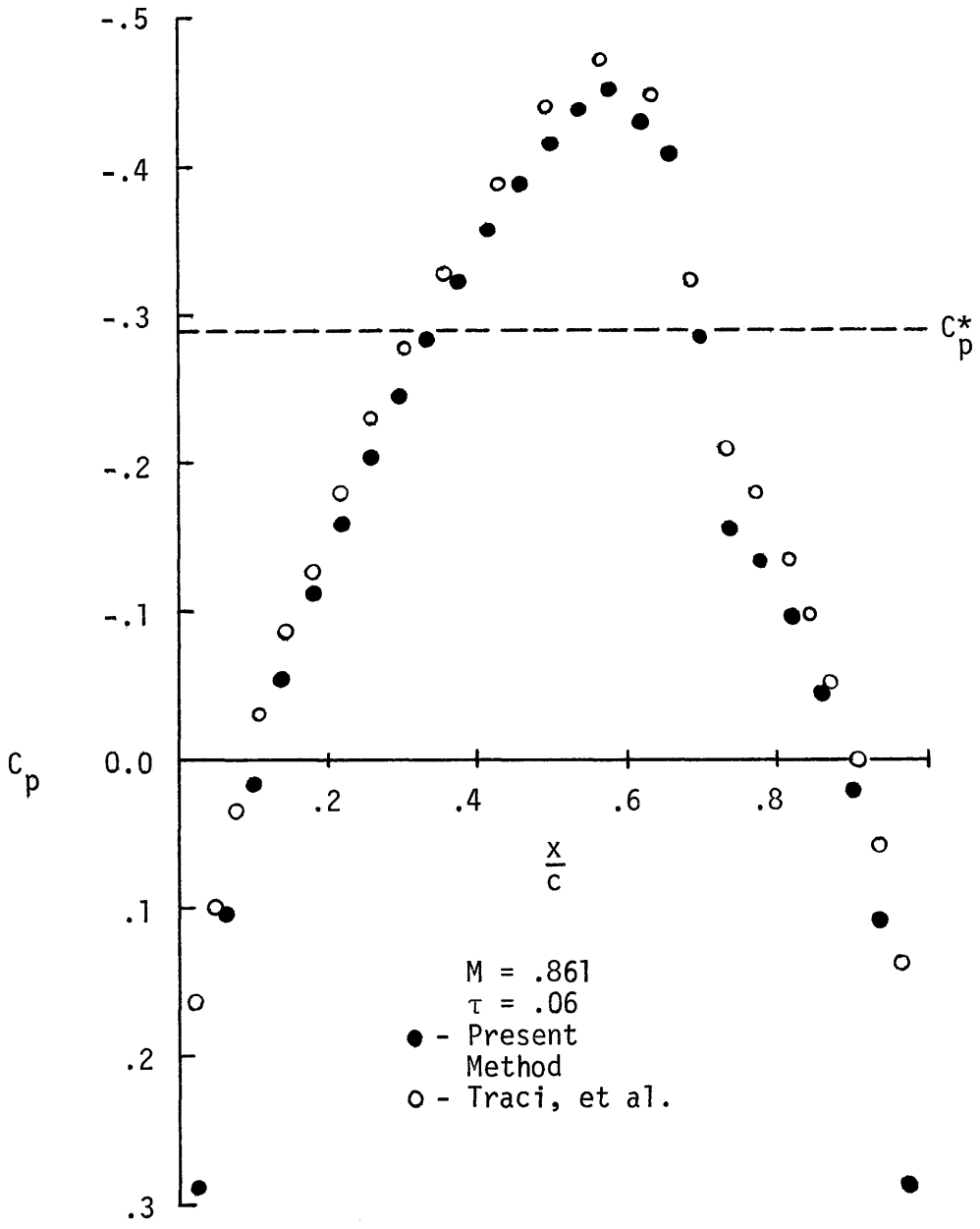

Figure 4.19. Pressure distributions on a six percent thick circular arc airfoil.

solution of the potential equation [23]. In both cases, the agreement is very good. Figure 4.13 shows relatively good agreement between the present lifting results and the experiments of Knechtel [47], with the differences probably due to the effects of viscosity on the measured data. Sivaneri [49] applied integral equation techniques to (3.11), and Figure 4.20 shows that there is very good agreement between the integral equation and finite difference methods.

4.8. Summary

A finite difference method has been developed to determine the rate of change of the steady potential with the airfoil thickness ratio and angle of attack. That method has been combined with the predictor-corrector methods of Section 3.3 to obtain families of lifting and non-lifting solutions. Those solutions were presented, and the computational requirements were summarized. The data obtained using the present method was seen to compare favorably with data obtained by other means.

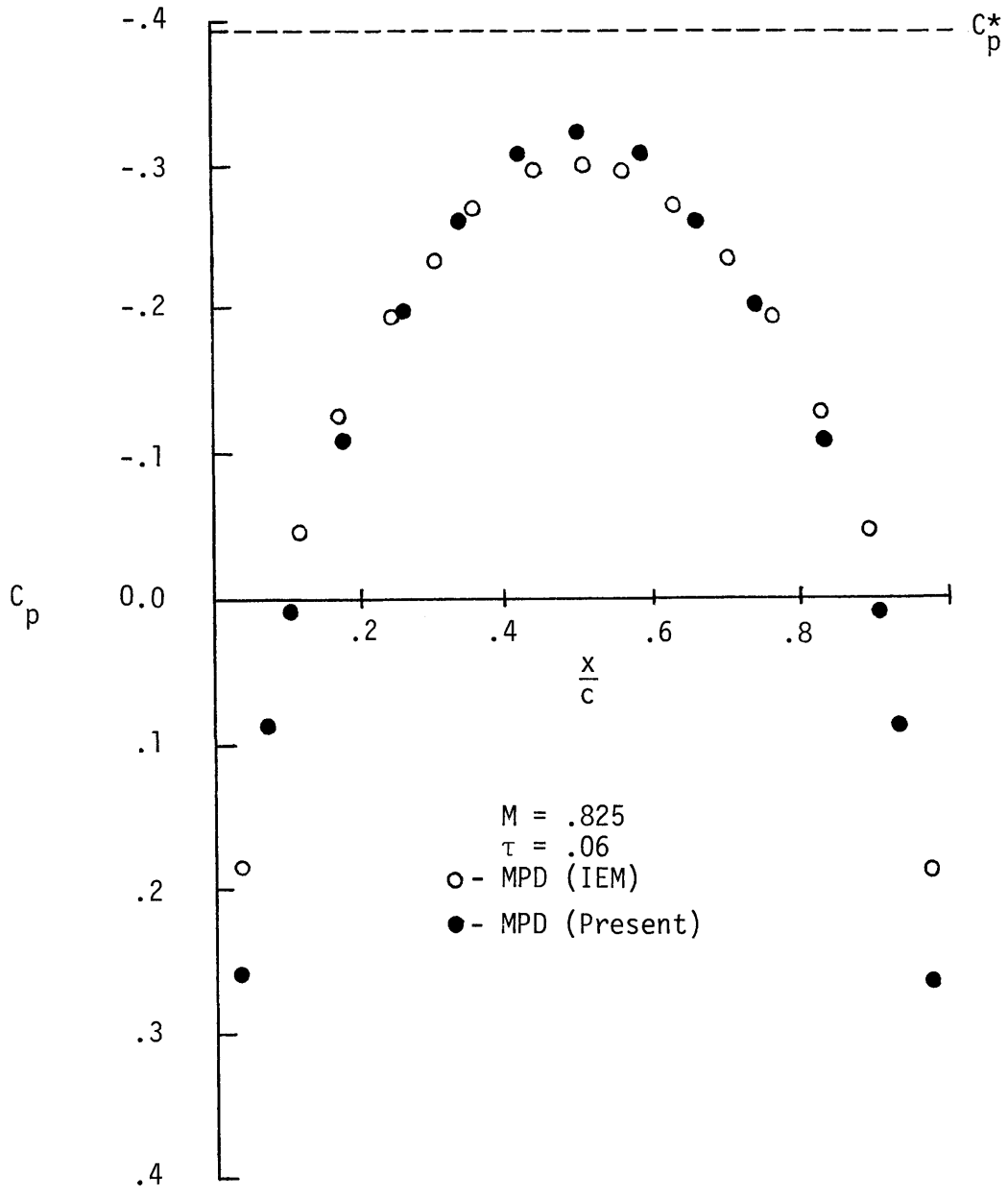

Figure 4.20. Pressure distributions on a six percent thick parabolic arc airfoil.

CHAPTER V

SOLUTION PROCEDURE AND RESULTS FOR UNSTEADY FLOWS

5.1. Introduction

Employing a relaxation procedure similar to that of [21]-[23], the families of steady state solutions are used to help determine families of unsteady pressure distributions. I consider oscillatory airfoil motions and, thus, assume that the unsteady potential varies harmonically with time. Equation (2.16) is then reduced to a time independent equation for the amplitude of the unsteady potential. That amplitude is generally complex and allows me to compute phase shifts between the airfoil motion and the aerodynamic loads. Finite difference techniques, similar to those of Chapter four, are utilized to solve for the amplitude of the unsteady potential.

The stability analysis of an oscillating flat plate indicates that relaxation methods will not yield converged solutions when the reduced frequency of the unsteady motion exceeds a limiting value; those limiting frequencies are inversely proportional to the size of the computational region. In an attempt to increase the maximum allowable frequency, I reduce the size of the computational region. That corresponds to placing the boundaries at finite distances from the airfoil, and the Klunker-type far field conditions [21] are prescribed on the boundaries (The unsteady potential is prescribed on the lateral boundaries, and the unsteady pressure

coefficient is prescribed on the upstream and downstream boundaries). Radiation conditions may also be used, but because their use resulted in relatively slow convergence of the numerical solutions, the Klunker-type conditions were used in all computations.

Differencing the equation governing the amplitude of the unsteady potential leads to a set of implicit simultaneous equations. Starting at the upstream boundary and marching downstream, those equations are solved using a column relaxation procedure. That process is repeated until the change in the amplitude of the unsteady potential for successive iterations is less than a predetermined constant. In the computational procedure, measures similar to those of sections 4.5 and 4.6 are taken to satisfy the boundary conditions. The jump in the unsteady potential across the wake is written to satisfy the Kutta condition, and I account for the effects of oscillating shock waves by imposing a compatability condition at their mean positions.

In the remainder of Chapter five, I present the procedure that is used to solve for the unsteady flow field perturbations. Examples of the unsteady loads are presented, and in cases where the flow has become supercritical, the motions of imbedded shock waves are calculated.

5.2. Formulation of the Boundary Value Problem for Harmonically Oscillating Airfoils

When analyzing airfoils undergoing harmonic oscillations, the deviation of the airfoil from its mean position and the unsteady po-

tential may be written, respectively, as

$$f_1(x,t) = RP\{\bar{f}(x)e^{ikt}\}$$

$$\varphi(x,z,t) = RP\{\varphi(x,z)e^{ikt}\}$$

where RP denotes the real part of a complex quantity. In the stretched coordinate system, (2.16) becomes

$$[1-m^2-m^2(\gamma+1)f\phi_\xi]f(f\varphi_\xi)_\xi + h(h\varphi_\eta)_\eta - m^2(\gamma+1)f(f\phi_\xi)_\xi f\varphi_\xi$$

$$-2ikm^2f\varphi_\xi + m^2[k^2-ik(\gamma-1)f(f\phi_\xi)_\xi]\varphi = 0 \qquad (5.1)$$

and the tangency and Kutta conditions become, respectively

$$h\varphi_\eta = f\bar{f}_\xi + ik\bar{f} \qquad |x(\xi)| \le \frac{c}{2}, \ \eta = 0 \qquad (5.2)$$

$$\Delta(f\varphi_\xi + ik\varphi) = 0 \qquad x(\xi) = \frac{c}{2}, \ \eta = 0 \qquad (5.3)$$

In terms of unstretched variables, the wake conditions are

$$\Delta(\varphi_x + ik\varphi) = 0 \qquad x(\xi) > \frac{c}{2}, \ \eta = 0 \qquad (5.4)$$

$$\Delta\varphi_z = 0 \qquad x(\xi) > \frac{c}{2}, \ \eta = 0 \qquad (5.5)$$

Equation (5.4) and (5.5) are combined to yield

$$\Delta\varphi = \Delta\varphi_1 e^{-ik[x(\xi)-x_1(\xi)]} \quad , \quad x(\xi) > \frac{c}{2} \quad , \quad \eta = 0 \qquad (5.6)$$

where the subscript 1 denotes quantities immediately downstream of the trailing edge. The constant of integration, $\Delta\varphi_1$, is chosen to satisfy the Kutta condition, and how that is done is detailed in the next section.

The stability analysis shown in Appendix F yields the condition

$$k^2 + 4\pi \frac{f_n}{a_\xi} k \leq 4\pi^2 \frac{(1-m^2)}{m^2} \left[\frac{f_n^2}{a_\xi^2} + \frac{h_\ell^2}{(1-m^2)c_\eta^2} \right] \qquad (5.7)$$

where a_ξ and c_η are the extents of the computational region in the ξ and η directions, respectively. While (5.7) is valid only for a flat plate, it provides an estimate of the maximum reduced frequency for which relaxation methods will yield converged solutions. In an attempt to increase the limiting frequency, the size of the computational region is reduced. This amounts to placing the physical boundaries at finite distances from the airfoil, and the Klunker type far field conditions [21] are used to specify data on the boundaries of the computational region. I chose $|\xi| \leq 1.84$ and $|\eta| \leq .905$, which corresponds to $|x| \leq 4.35$ and $|z| \leq 6.63$.

On the lateral boundaries, the amplitude of the unsteady potential is given by

$$\varphi(x(\xi),z(\eta)) = \frac{1}{\beta}\left\{\iint [m^2(\gamma+1)\psi_x \phi_{x'}\varphi_{x'} + ikm^2(\gamma-1)\psi\phi_{x'x'}\varphi]\,dx'dz'\right.$$

$$\left. + \psi_z \int_{-\frac{c}{2}}^{\frac{c}{2}} \Delta\varphi\, dx' + \psi \int_{-\frac{c}{2}}^{\frac{c}{2}} \Delta\varphi_{z'}\, dx' + \Delta\varphi_T \int_{\frac{c}{2}}^{\infty} e^{-ik(x'-\frac{c}{2})}\psi_z\, dx'\right\} \qquad (5.8)$$

where ψ is given in (E.10). At the upstream and downstream boundaries, I prescribe the pressure function, P, where

$$P(x(\xi),z(\eta)) = f\varphi_\xi + ik\varphi = \frac{1}{\beta}\left\{\iint [m^2(\gamma+1)\chi_x \phi_{x'}\varphi_{x'} + ikm^2(\gamma-1)\chi\phi_{x'x'}\varphi]\,dx'dz'\right.$$

$$\left. + \chi_z \int_{-\frac{c}{2}}^{\frac{c}{2}} \Delta\varphi\, dx' + \chi \int_{-\frac{c}{2}}^{\frac{c}{2}} \Delta\varphi_{z'}\, dx' + \Delta\varphi_T\, \psi_z\left(x(\xi) - \tfrac{c}{2}, \beta z(\eta)\right)\right. \qquad (5.9)$$

where

$$\chi = \psi_x + ik\psi$$

Equations (5.8) and (5.9) may be simplified by noting that $\Delta\varphi_z = 0$. Also, Weatherill et al. [50] have found that the area integrals are not significant and need not be retained.

Since the wake integral in (5.8) is slow to converge, (5.8) is used to evaluate φ only at $x(\xi)=\frac{c}{2}$ on the upper and lower boundaries. By integrating $(\varphi e^{ikx})_x = P e^{ikx}$, I obtain a recursion formula which is used to determine φ at all points on the lateral boundaries. At $x(\xi)=\frac{c}{2}$, the wake integral is

$$\Delta\varphi_T \int_{\frac{c}{2}}^{\infty} e^{ik(x'-\frac{c}{2})} \psi_z \, dx' = i\frac{\pi}{2} kM z(\gamma) \Delta\varphi_T \left\{ i \int_0^{\frac{\pi}{2}} e^{-\frac{kz(\gamma)}{\beta}\cos\theta} J_1\left(\frac{kM}{\beta} z(\gamma) \sin\theta\right) d\theta \right.$$

$$+ \int_0^{\frac{\pi}{2}} \left[e^{-\frac{kz(\gamma)}{\beta}\cos\theta} Y_1\left(\frac{kM}{\beta} z(\gamma) \sin\theta\right) + \frac{2}{\pi} e^{-\frac{kz(\gamma)}{\beta}\cosh\theta} K_1\left(\frac{kM}{\beta} z(\gamma) \sinh\theta\right) \right] d\theta$$

$$\left. + \frac{2}{\pi} \int_{\pi/2}^{\infty} e^{-\frac{kz(\gamma)}{\beta}\cosh\theta} K_1\left(\frac{kM}{\beta} z(\gamma) \sinh\theta\right) d\theta \right\} \qquad (5.10)$$

Figure 5.1 summarizes the unsteady boundary value problem.

5.3. Procedure for Calculating the Unsteady Perturbations

Solutions of (5.1) are obtained using a conservative finite difference method. Because the difference equations are developed using the procedure of Section 4.4, I simply present the interior point finite difference representation of (5.1)

$$(1-\mu_{n,\ell}) \left\{ d_1 \left[\varphi_{n+1,\ell} - \frac{\varphi^+_{n,\ell}}{\omega} - \left(1-\frac{1}{\omega}\right)\varphi_{n,\ell} \right] - d_2 \left[\frac{\varphi^+_{n,\ell}}{\omega} + \left(1-\frac{1}{\omega}\right)\varphi_{n,\ell} - \varphi^+_{n-1,\ell} \right] \right.$$

$$\left. - \frac{ikM^2 f_n}{\Delta\xi} \left(\varphi_{n+1,\ell} - \varphi^+_{n-1,\ell}\right) + d_4 \left[\frac{\varphi^+_{n,\ell}}{\omega} + \left(1-\frac{1}{\omega}\right)\varphi_{n,\ell} \right] \right\} +$$

$$\mu_{n-1,\ell} \left[d_2 \left(\varphi_{n,\ell} - \varphi_{n-1,\ell}\right) - d_3 \left(\varphi_{n-1,\ell} - \varphi_{n-2,\ell}\right) - \frac{ikM^2 f_n}{\Delta\xi} \left(\varphi_{n,\ell} - \varphi_{n-2,\ell}\right) \right]$$

$$+ \mu_{n,\ell} d_5 \varphi_{n,\ell} + \frac{h_\ell}{\Delta\eta^2} \left[h_{\ell+1/2} \left(\varphi^+_{n,\ell+1} - \varphi^+_{n,\ell}\right) - h_{\ell-1/2} \left(\varphi^+_{n,\ell} - \varphi^+_{n,\ell-1}\right) \right]$$

$$- \mu_{n,\ell} \epsilon^* \frac{f_n f_{n-1/2}}{\Delta\xi^2} \left(\varphi^+_{n,\ell} - \varphi_{n,\ell} - \varphi^+_{n-1,\ell} + \varphi_{n-1,\ell}\right) = 0 \qquad (5.11)$$

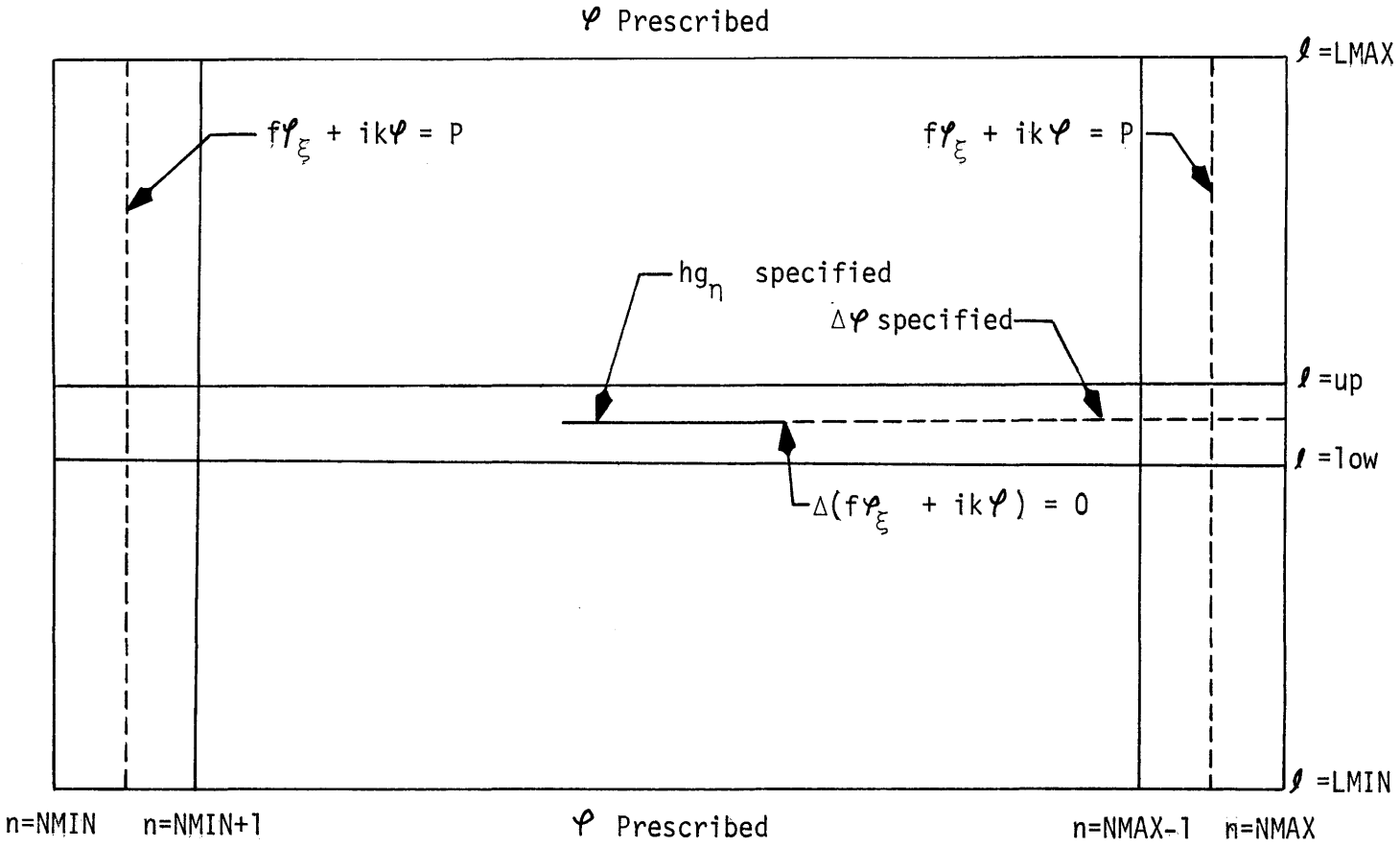

Figure 5.1. Unsteady boundary value problem.

where α_4 and α_5 are defined in (D.10) and (D.11), respectively.

The derivation of (5.10) may be found in Appendix D. Equation (5.10) is altered at the appropriate grid points to satisfy the boundary conditions.

The condition at the upstream boundary is incorporated directly into (5.11) by replacing $\varphi_{NMIN,\ell}$ with

$$\varphi_{NMIN,\ell} = \alpha_6 \varphi_{NMIN+1,\ell} - \alpha_7 P$$

where α_6 and α_7 are defined in (D.32) and (D.33), respectively.

Similarly, at the downstream boundary, I substitute, from (D.38)

$$\varphi_{NMAX,\ell} = \alpha_8 \varphi_{NMAX-1} - \alpha_9 P$$

The unsteady tangency condition is satisfied by altering the difference equations at points adjacent to the mean airfoil position. When $|x(\xi)| \leq \frac{c}{2}$, $(h\varphi_\eta)_{n,up-1/2}$ and $(h\varphi_\eta)_{n,low+1/2}$ are prescribed from the unsteady, upper and lower boundary tangency conditions. By substituting those derivatives into

$$h(h\varphi_\eta)_\eta = \frac{h\ell}{\Delta\eta}\left[(h\varphi_\eta)_{n,\ell+1/2} - (h\varphi_\eta)_{n,\ell-1/2}\right] \tag{5.12}$$

at the proper grid points, I ensure that the unsteady tangency condition is satisfied.

I also satisfy the unsteady Kutta condition by altering the form of (5.12) at the appropriate grid points. When $x(\xi) > \frac{c}{2}$ and

ℓ=up, the jump in the unsteady potential across the wake is accounted for by writing $h(h\varphi_\eta)_\eta$ as

$$h(h\varphi_\eta)_\eta = \frac{h_{up}}{\Delta\eta^2}\left[h_{up+1/2}(\varphi^+_{n,up+1}-\varphi^+_{n,up}) - h_{up-1/2}(\varphi^+_{n,up}-\varphi^+_{n,up-1}-\Delta\varphi_n)\right] \tag{5.13}$$

and when $x(\xi)>\frac{c}{2}$ and ℓ=low,

$$h(h\varphi_\eta)_\eta = \frac{h_{low}}{\Delta\eta^2}\left[h_{low+1/2}(\varphi_{n,low+1}-\varphi_{n,low}-\Delta\varphi_n) - h_{low-1/2}(\varphi_{n,low}-\varphi_{n,low-1})\right] \tag{5.14}$$

By choosing $\Delta\varphi_n$ in the proper manner, when (5.13) and (5.14) are substituted into (D.8), I am assured that the unsteady Kutta condition is satisfied.

The proper choice of $\Delta\varphi_n$ is determined by differencing $f\Delta\varphi_\xi + ik\Delta\varphi = 0$ at the trailing edge. Using the notation of Figure 4.6 the expansions

$$\Delta\varphi_{T1} = \Delta\varphi_T + \Delta\xi_{T1}(\Delta\varphi_\xi)_T + \frac{\Delta\xi_{T1}^2}{2}(\Delta\varphi_{\xi\xi})_T + O(\Delta\xi_{T1}^3)$$

$$\Delta\varphi_{-T2} = \Delta\varphi_T - (\Delta\xi+\Delta\xi_T)(\Delta\varphi_\xi)_T + \frac{(\Delta\xi+\Delta\xi_T)^2}{2}(\Delta\varphi_{\xi\xi})_T + O((\Delta\xi+\Delta\xi_T)^3)$$

are combined to yield

$$(\Delta\varphi_\xi)_T = \frac{(\Delta\xi+\Delta\xi_T)}{2\Delta\xi\Delta\xi_{T1}}\Delta\varphi_{T1} - \frac{\Delta\xi_{T1}}{2\Delta\xi(\Delta\xi+\Delta\xi_T)}\Delta\varphi_{-T2} - \frac{(\Delta\xi+\Delta\xi_T-\Delta\xi_{T1})}{\Delta\xi_{T1}(\Delta\xi+\Delta\xi_T)}\Delta\varphi_T \tag{5.15}$$

when (5.15) is substituted into (5.3), I find that the unsteady Kutta condition requires that $\Delta\varphi_n$ take the form

$$\Delta\varphi_n = \left\{\left(\frac{\Delta\xi_{T1}}{\Delta\xi+\Delta\xi_T}\right)^2 \Delta\varphi_{T2} + \left[1-\left(\frac{\Delta\xi_{T1}}{\Delta\xi+\Delta\xi_T}\right)^2 - 2ik\frac{\Delta\xi\,\Delta\xi_{T1}}{f_T(\Delta\xi+\Delta\xi_T)}\right]\Delta\varphi_T\right\} e^{-ik[x(\xi)-x_1(\xi)]} \tag{5.16}$$

The values of $\Delta\varphi$ along the airfoil and at the trailing edge are obtained from procedures similar to that of (C.72)-C.87). Hence

$$\Delta\varphi = \frac{9}{8}(\varphi_{n,up} - \varphi_{n,low}) - \frac{1}{8}(\varphi_{n,up+1} - \varphi_{n,low-1}) - \frac{3}{8}\Delta\gamma(\varphi_\gamma^u + \varphi_\gamma^\ell) \tag{5.17}$$

$$\Delta\varphi_T = \left(1+\frac{3}{2}\frac{\Delta\xi_T}{\Delta\xi}\right)\Delta\varphi_{T1} - 2\frac{\Delta\xi_T}{\Delta\xi}\Delta\varphi_{T2} + \frac{\Delta\xi_T}{2\Delta\xi}\Delta\varphi_{T3} \tag{5.18}$$

5.4. Motion of Imbedded Shock Waves

In previous studies, methods which treat the unsteadiness as a linear perturbation upon the steady state account for the presence of imbedded shock waves but do not consider the effects of their unsteady motions [21]-[23]. The experiments of Tijdeman and Zwann [24],[25] indicate that the periodical motion of imbedded shock waves induce relatively large local pressures which may have a significant effect on the unsteady forces and moments. Hence, I deem it essential to include the effects of moving shock waves in the solution procedure.

Tijdeman and Zwaan [24],[25] observed three types of periodical shock wave motion. In what they have termed as type A motion, the shock wave oscillates almost sinusoidally with phase shifts between

the airfoil motion and shock position and between the strength of the shock wave and its position. In type B motion, the shock wave again oscillates sinusoidally but disappears during part of the cycle, and in type C motion, a shock wave periodically propagates off of the airfoil leading edge. Here I only consider shock movements that resemble type A motions, and the assumptions under which separated the potential limits the amplitudes of shock oscillation to relatively small values. Clearly, type C motions, which carry the shock waves over relatively large portions of the airfoil, cannot be treated using the current approach.

The effects of type A shock motions are determined by imposing a compatability condition, detailed by Cunningham [51], at the mean shock position. This shock condition is similar to that of Landahl [7] but is valid for all frequencies. I assume periodic motions and write the instantaneous shock position, x_s , as

$$x_s = x_m + RP\{\lambda_s(z)e^{ikt}\}$$

where x_m is the shock wave's steady state position. The requirement that the tangential velocity be continuous across the shock wave yields, upon integration around the finite shock path,

$$\bar{\mathcal{I}}^+ = \bar{\mathcal{I}}^- \tag{5.19}$$

where the superscripts + and - represent quantities immediately downstream and upstream of the instantaneous shock positon, respectively.

Expanding the perturbation potential in a Taylor series about the mean shock position and retaining only first order terms in λ_s yields

$$\bar{\Phi}^+(x_s) = \phi^+(x_m) + \lambda_s e^{ikt}\phi_x^+(x_m) + \varphi^+(x_m)e^{ikt}$$

$$\bar{\Phi}^-(x_s) = \phi^-(x_m) + \lambda_s e^{ikt}\phi_x^-(x_m) + \varphi^-(x_m)e^{ikt}$$

where I have assumed that ϕ is analytically continuous on both sides of the shock wave. From (5.19) I then obtain the shock motion necessary to maintain equality of the total potential across the shock wave

$$\lambda_s = -\frac{\varphi^+ - \varphi^-}{\phi_x^+ - \phi_x^-} \tag{5.20}$$

Assuming that the inclination of the shock wave is small, a second condition is found by imposing the Rankine-Hugoniot condition for normal shock waves [32]

$$u^- - u^+ = \frac{2u^-}{\gamma+1}\left[1 - \left(\frac{a^-}{u^-}\right)^2\right] \tag{5.21}$$

where u is the velocity in the streamwise direction. Using the relations

$$(a^-)^2 = \frac{1}{m^2} - (\gamma-1)(\bar{\Phi}_x^- + \bar{\Phi}_t^-)$$

$$u^- = 1 + \bar{\Phi}_x^- - ik\lambda_s e^{ikt}$$

$$u^+ = 1 + \bar{\Phi}_x^+ - ik\lambda_s e^{ikt}$$

(5.21) becomes

$$\bar{\Phi}_x^+ + \mu^* \bar{\Phi}_x^- + 2\left(\frac{\gamma-1}{\gamma+1}\right)\bar{\Phi}_t^- - \frac{4ik}{\gamma+1}\lambda_s e^{ikt} = -\frac{2}{\gamma+1}\left(1-\frac{1}{m^2}\right)$$

where

$$\mu^* = \frac{\gamma-1}{\gamma+1} + \frac{2}{m^2(\gamma+1)}$$

Writing the derivatives as

$$\bar{\Phi}_x^-(x_s) = \phi_x^-(x_m) + \lambda_s e^{ikt}\phi_{xx}^-(x_m) + \varphi_x^-(x_m)e^{ikt}$$

$$\bar{\Phi}_x^+(x_s) = \phi_x^+(x_m) + \lambda_s e^{ikt}\phi_{xx}^+(x_m) + \varphi_x^+(x_m)e^{ikt}$$

$$\bar{\Phi}_t^-(x_m) = ike^{ikt}(\lambda_s\phi_x^- + \varphi^-)$$

and equating terms proportional to e^{ikt} yields the shock movement necessary to satisfy the Rankine-Hugoniot condition

$$\lambda_s = -\frac{\varphi_x^+ + \mu^*\varphi_x^- + 2ik\left(\frac{\gamma-1}{\gamma+1}\right)\varphi^-}{\phi_{xx}^+ + \mu^*\phi_{xx}^- + 2ik\left(\frac{\gamma-1}{\gamma+1}\right)\phi_x^- - \frac{4ik}{\gamma+1}} \tag{5.22}$$

By requiring the equality of shock motions given by (5.20) and (5.21), the following compatability condition is obtained

$$\varphi_x^+ - K^*\varphi^+ = -\mu^*\varphi_x^- - \left[2ik\left(\frac{\gamma-1}{\gamma+1}\right) + K^*\right]\varphi^- \tag{5.23}$$

where

$$K^n = \frac{\phi_{xx}^+ + \mu\phi_{xx}^- + 2ik\left(\frac{\gamma-1}{\gamma+1}\right)\phi_x^- - \frac{4ik}{\gamma+1}}{\phi_x^+ - \phi_x^-}$$

To satisfy (5.23), I assume that the shock wave is located midway between the two grid points where switching function, μ, switches from unity to zero. Using the notation of Figure 5.2, the derivatives in (5.23) are evaluated with backward differences at grid points immediately adjacent to the assumed shock location. Immediately downstream of the shock wave, I require that

$$\varphi_{n,\ell}^+ = \frac{1}{(f_n - 2\Delta\xi K^n)}\left\{-\left[2\Delta\xi K^n + \mu^n f_{n-1} + 4ik\Delta\xi\left(\frac{\gamma-1}{\gamma+1}\right)\right]\varphi_{n-1,\ell}^+ + f_n\varphi_{n-2,\ell}^+ + \mu^n f_{n-1}\varphi_{n-3,\ell}^+\right\} \tag{5.24}$$

The derivative terms that comprise K^n are approximated with centered difference formulas. Hence

$$K^n = 2\Delta\xi\left\{\frac{f_n}{\Delta\xi^2}\left[f_{n+1/2}(\phi_{n+1,\ell} - \phi_{n,\ell}) - f_{n-1/2}(\phi_{n,\ell} - \phi_{n-1,\ell})\right]\right.$$

$$- \mu^n\frac{f_{n-1}}{\Delta\xi^2}\left[f_{n-1/2}(\phi_{n,\ell} - \phi_{n-1,\ell}) - f_{n-3/2}(\phi_{n-1,\ell} - \phi_{n-2,\ell})\right] - \frac{4ik}{\gamma+1}$$

$$\left. + 2ik\left(\frac{\gamma-1}{\gamma+1}\right)\frac{f_{n-1}}{2\Delta\xi}(\phi_{n,\ell} - \phi_{n-2,\ell})\right\}\left[f_n(\phi_{n+1,\ell} - \phi_{n-1,\ell}) - f_{n-1}(\phi_{n,\ell} - \phi_{n-2,\ell})\right]^{-1}$$

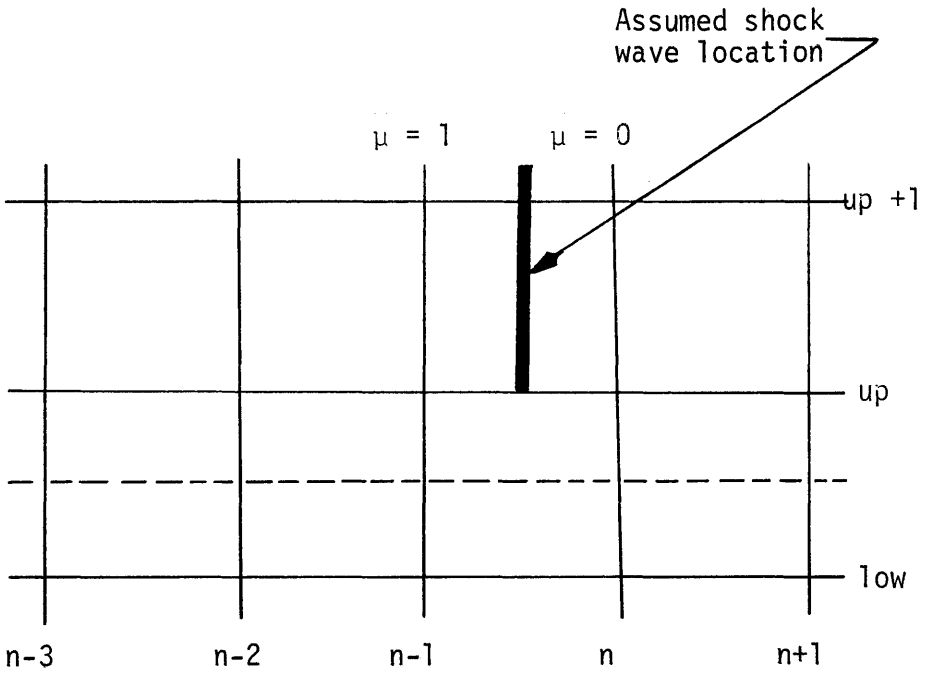

Figure 5.2. Location of the imbedded shock wave, relative to the computational grid.

By imposing condition (5.23) in the solution procedure the effects of oscillating shock waves are included in the solution. The shock excursion, λ_s , is complex which allows me to calculate any phase shift between the airfoil and shock wave motion. Also, by monitoring the amplitude of λ_s for various unsteady motions, I get an idea of when the assumption of linear unsteady perturbations is violated.

5.5. Results and Discussions

The finite difference representation of (5.1) is written in tridiagonal form, with the tridiagonal coefficients given in Appendix D. Employing the solution procedure of Appendix G, I am able to compute the unsteady component of the flow field for various steady state conditions; a computer program which performs that task is listed in Appendix H. Unsteady loads for two types of motions, heaving oscillations and pitch about the midchord, are calculated, but the program is capable of treating pitching motions about any point and oscillating flaps with arbitrary hinge locations. Numerical solutions of (5.1) were considered to have converged when $\left| \frac{\varphi^{+}_{n,\ell} - \varphi_{n,\ell}}{\omega} \right| \leq 2 \cdot 10^{-5}$ for heaving motions and when $\left| \frac{\varphi^{+}_{n,\ell} - \varphi_{n,\ell}}{\omega} \right| \leq 10^{-4}$ for pitching motions.

Figure 5.3 shows the unsteady lift distributions on subcritical, parabolic arc airfoils of various thickness ratios undergoing heaving

oscillations of amplitude, δ , .01c. The effects of varying the airfoil thickness ratio on the unsteady lift coefficient and moment coefficient about the leading edge is shown in Figure 5.4; both increase in magnitude with increasing τ , with slight changes in phase. The cases τ = 0, .03 and .06 require 1.5, 1.7 and 1.8 minutes of CPU time, respectively, on an IBM 370/168.

The unsteady lift distributions on subcritical parabolic arc airfoils pitching about the midchord, with an amplitude of one degree, are shown in Figure 5.5, and Figure 5.6 shows how the unsteady lift and moment about the leading edge vary with τ . As in the case of heaving oscillations, the magnitude of unsteady lift and moment increases with τ, and the phase shifts remain almost constant.

The unsteady lift distributions on a supercritical circular arc airfoil undergoing heaving oscillations, with $\frac{\delta}{c}$ = .01, is shown in Figure 5.7. The spikes in the lift distributions are due to the presence of the imbedded shock wave in the flow field. There is a waviness in the lift distributions upstream of the shock wave for which I can offer no plausible physical explanation. However, similar trends are observed in the data obtained by others [23],[52]. At points nearest the upper and lower boundaries of the airfoil, the shock excursion amplitudes are .032c and .039c, respectively, and the requirement that the shock wave travel over a small portion of the airfoil chord is satisfied. The computed values of λ_s at all shock points are presented in Table I.

Figure 5.8 shows the unsteady lift distributions that result when the supercritical circular arc airfoil oscillates in pitch about its

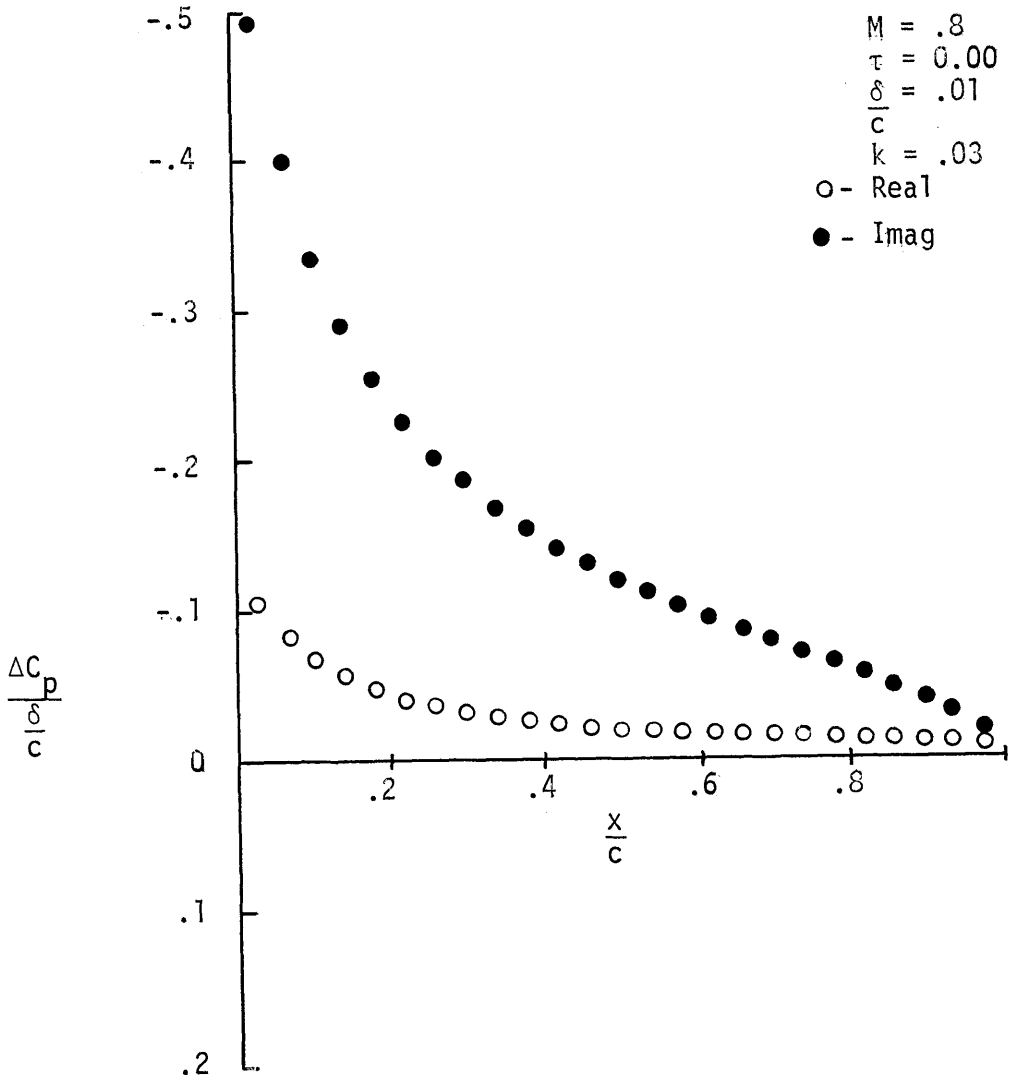

Figure 5.3a. Unsteady lift distribution on a flat plate oscillating in heave.

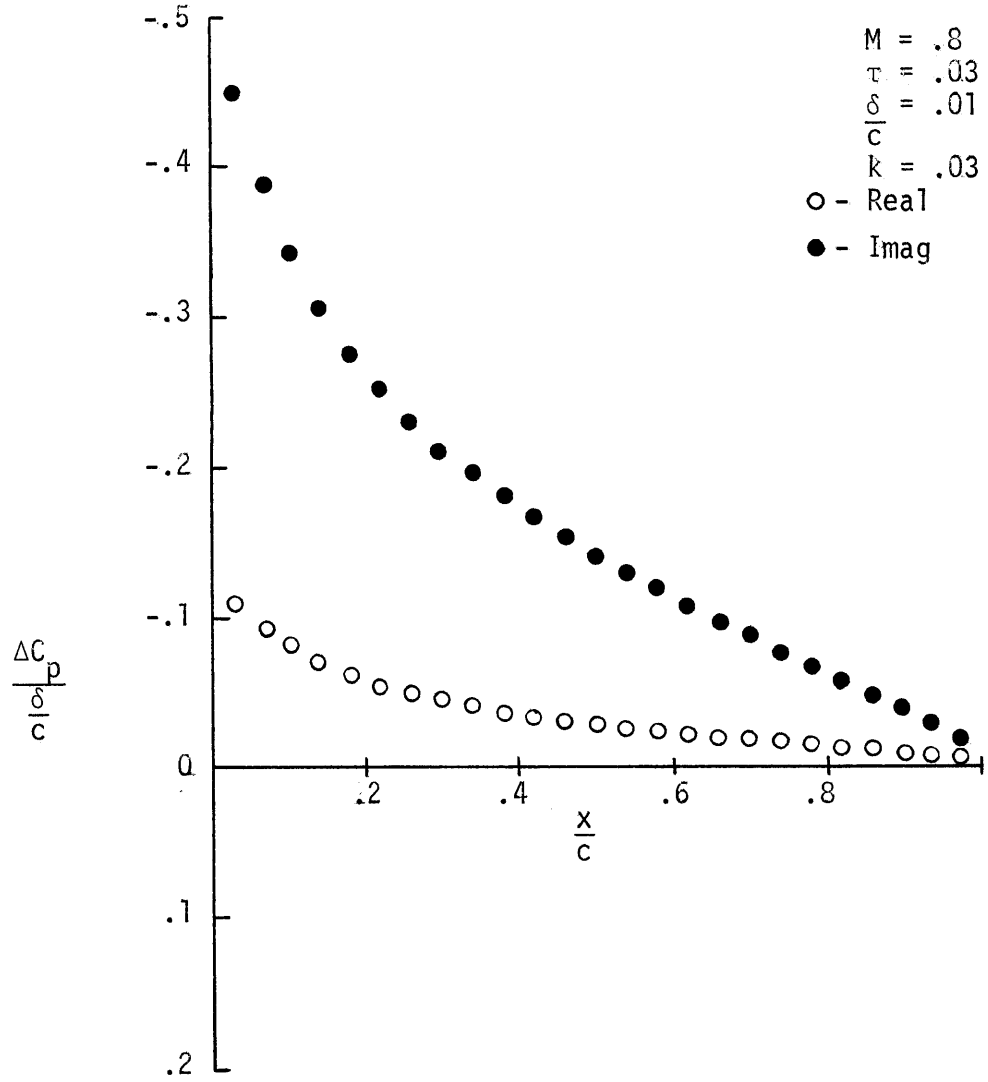

Figure 5.3b. Unsteady lift distribution on a parabolic arc airfoil oscillating in heave.

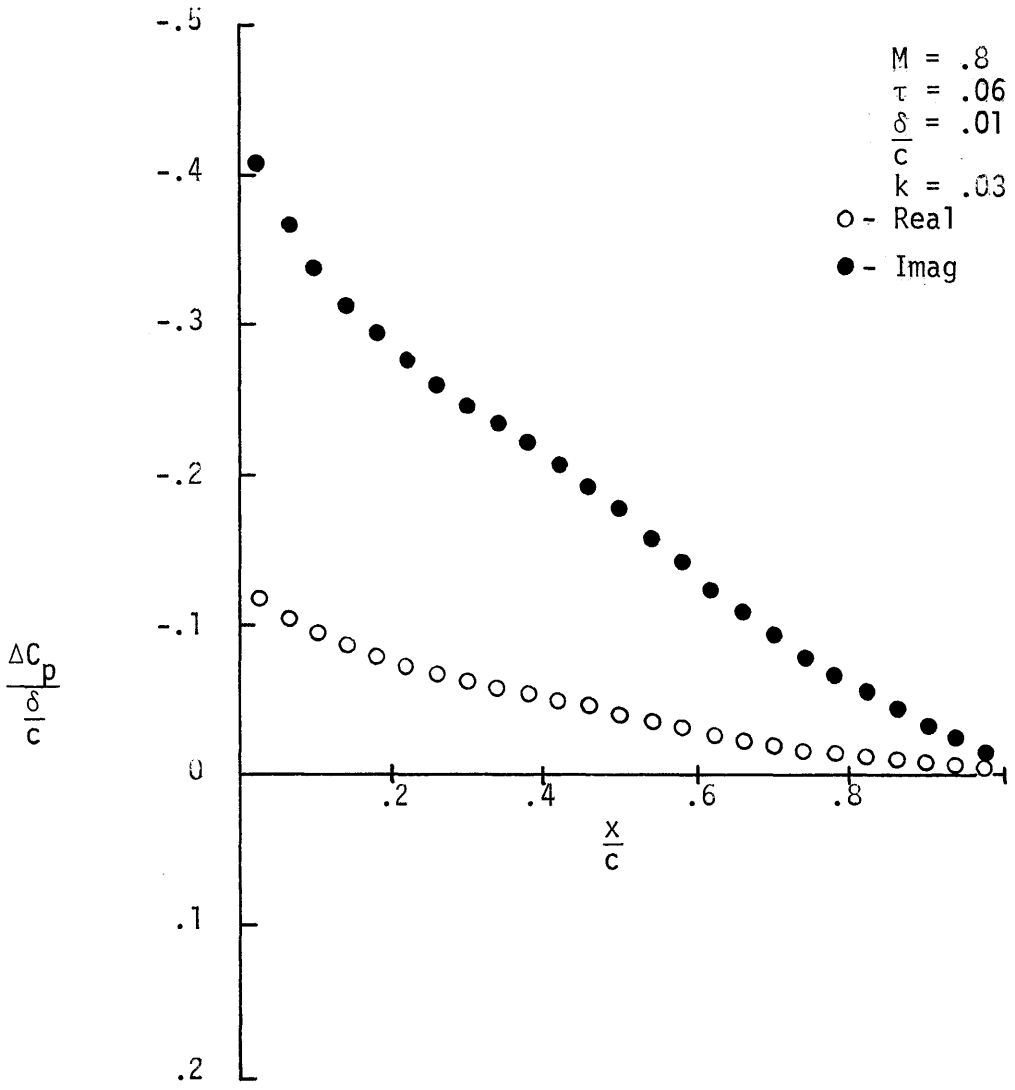

Figure 5.3c. Unsteady lift distribution on a parabolic arc airfoil oscillating in heave.

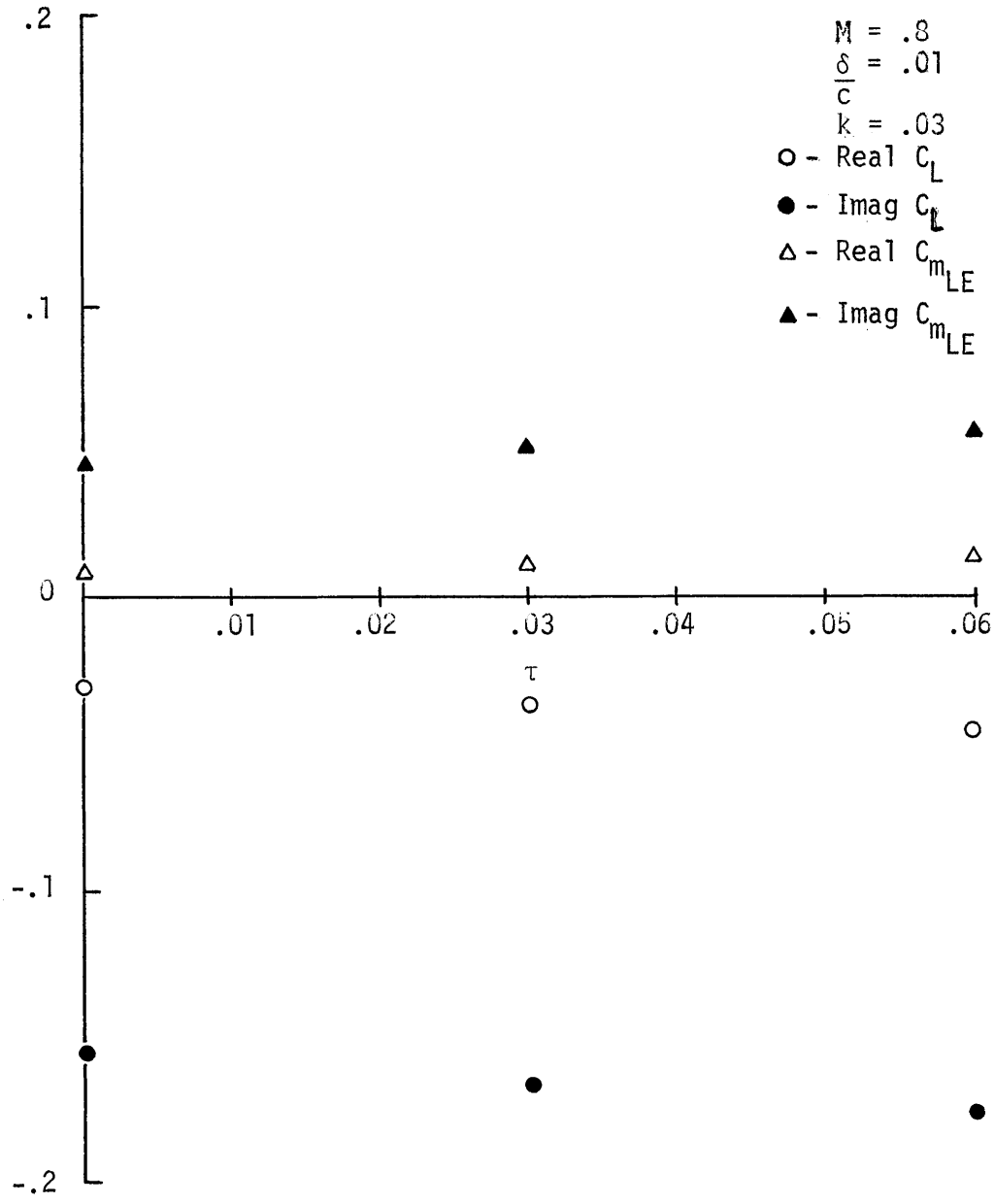

Figure 5.4. Unsteady lift coefficients and moment coefficients about the leading edge divided by the amplitude of oscillation for parabolic arc airfoils oscillating in heave.

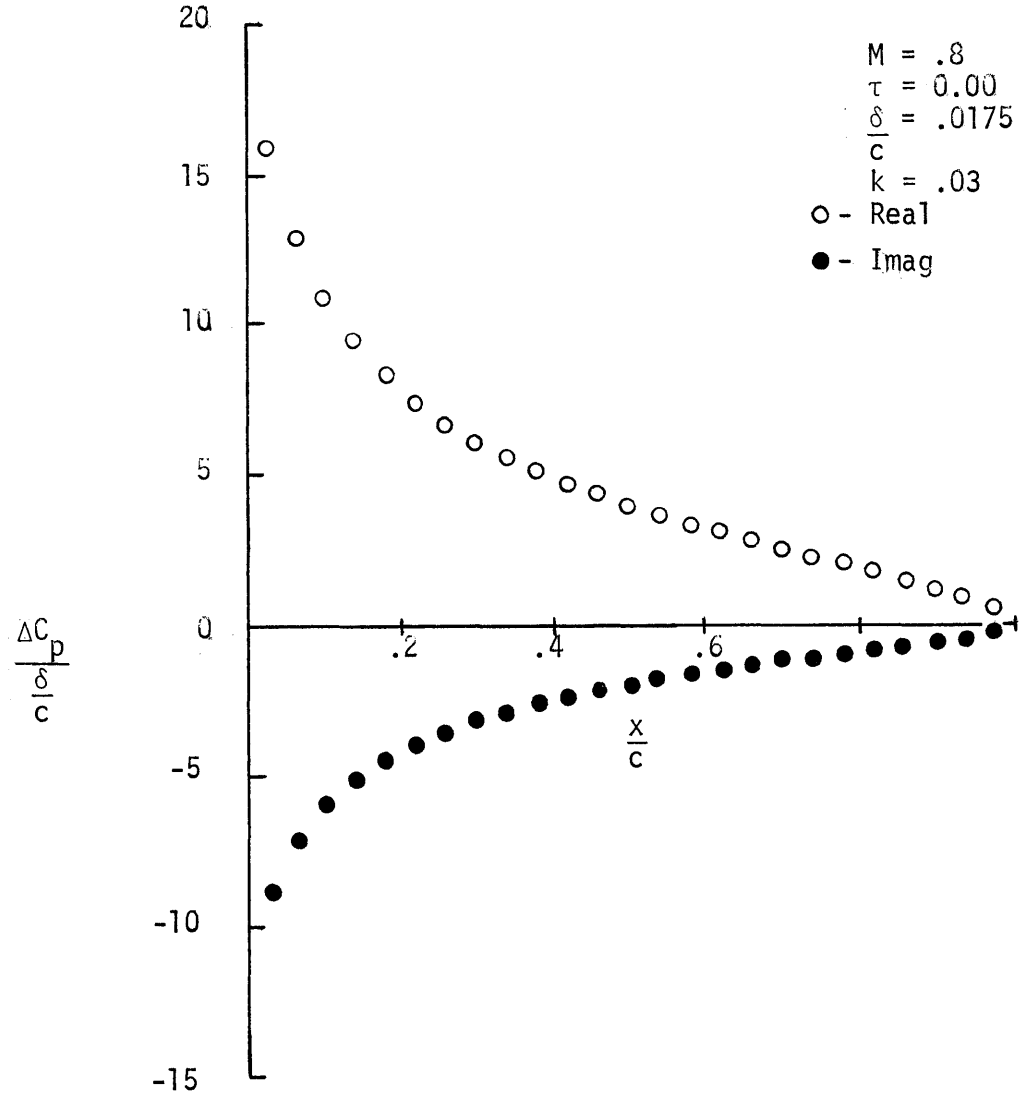

Figure 5.5a. Unsteady lift distribution on a flat plate oscillating in pitch about its midchord.

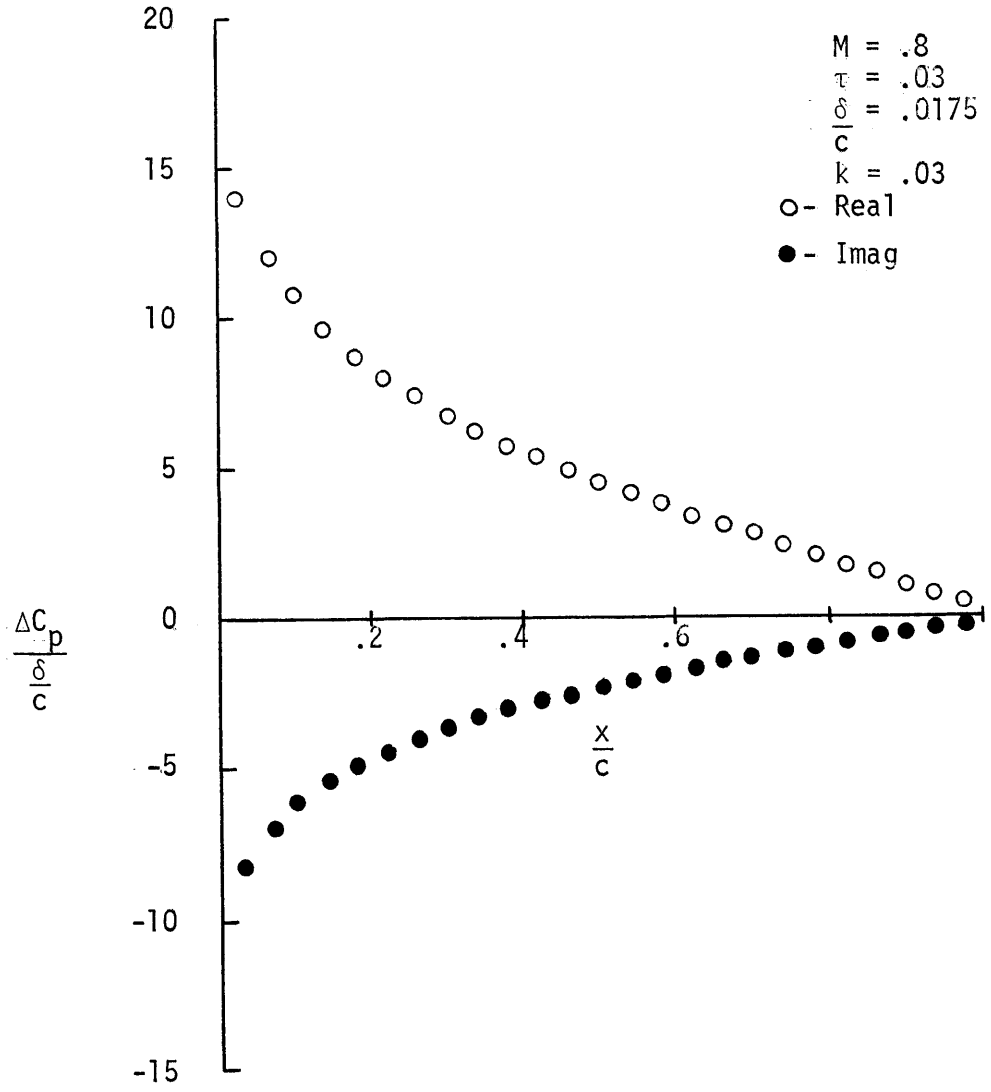

Figure 5.5b. Unsteady lift distribution on a parabolic arc airfoil oscillating in pitch about its midchord.

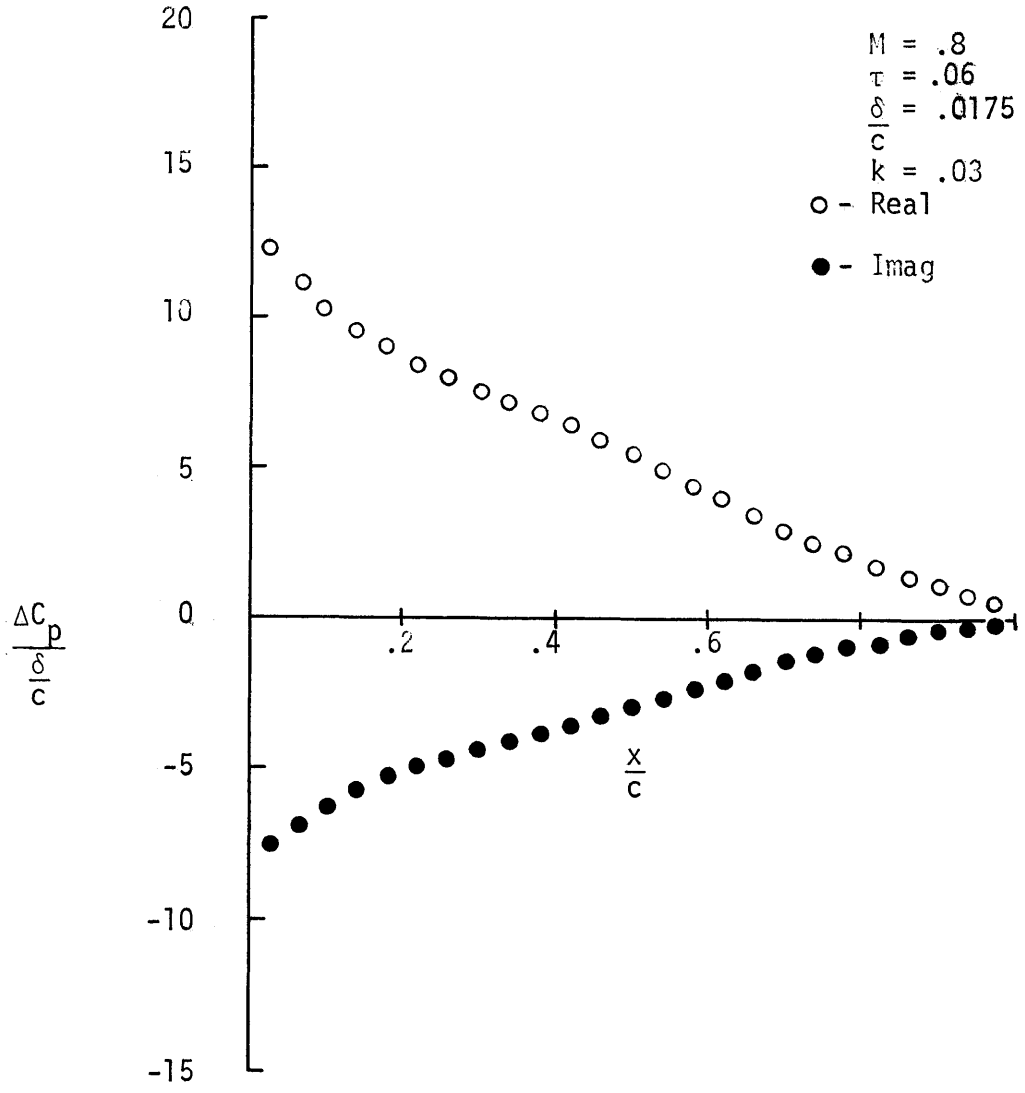

Figure 5.5c. Unsteady lift distribution on a parabolic arc airfoil oscillating in pitch about its midchord.

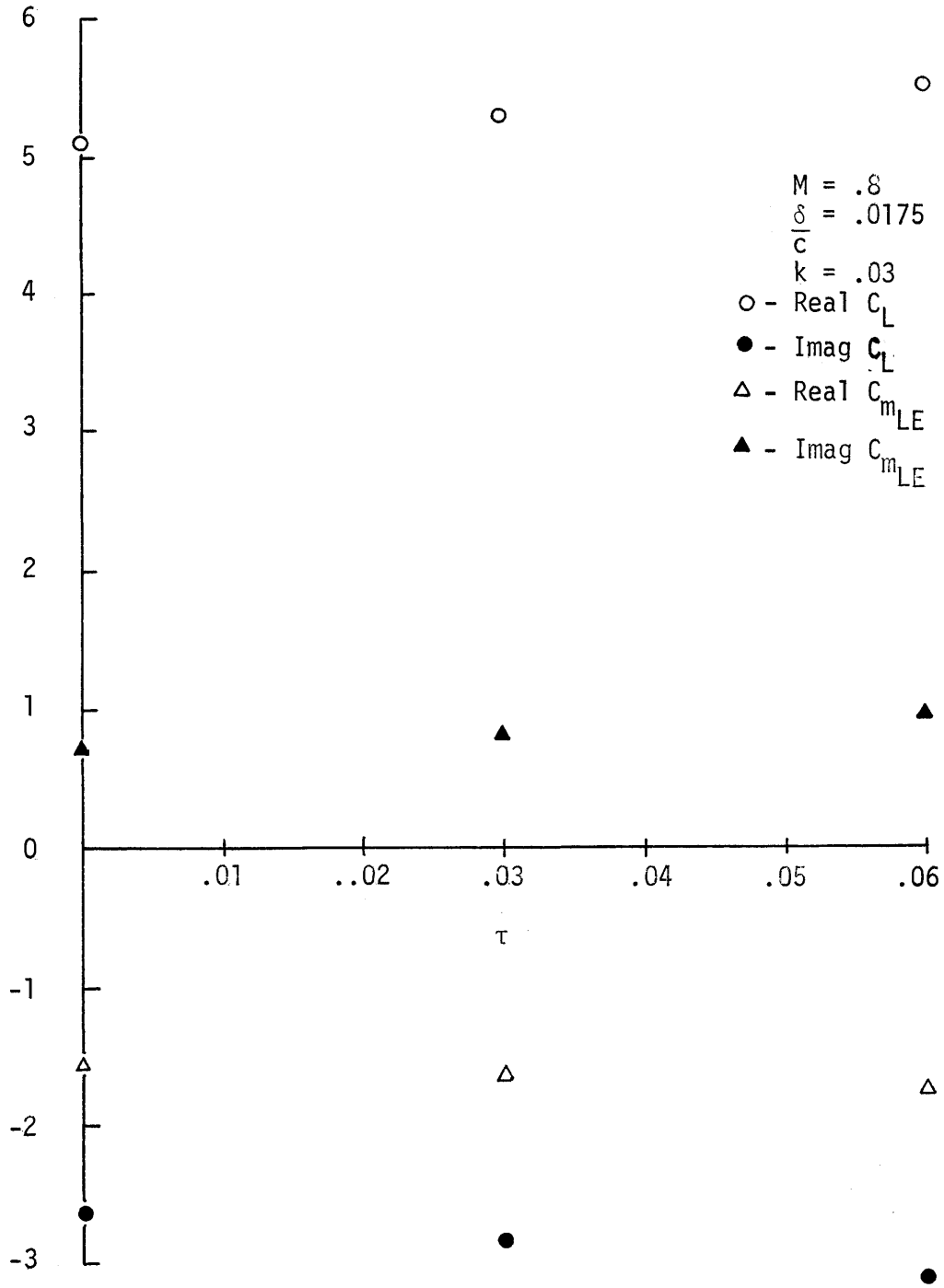

Figure 5.6. Unsteady lift coefficients and moment coefficients about the leading edge divided by the amplitude of oscillation for parabolic arc airfoils oscillating in pitch about the midchord.

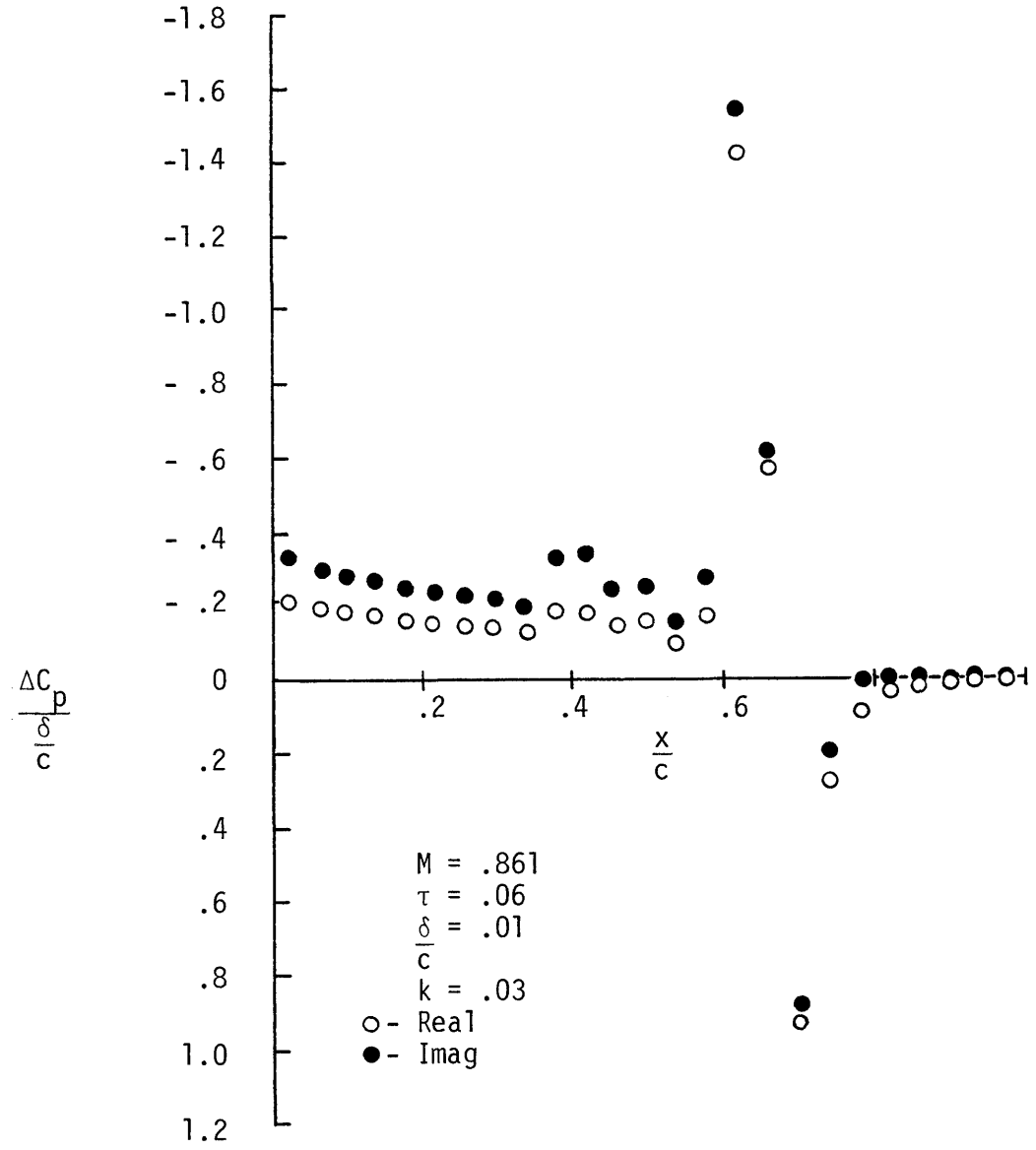

Figure 5.7. Unsteady lift distribution on a circular arc airfoil oscillating in heave.

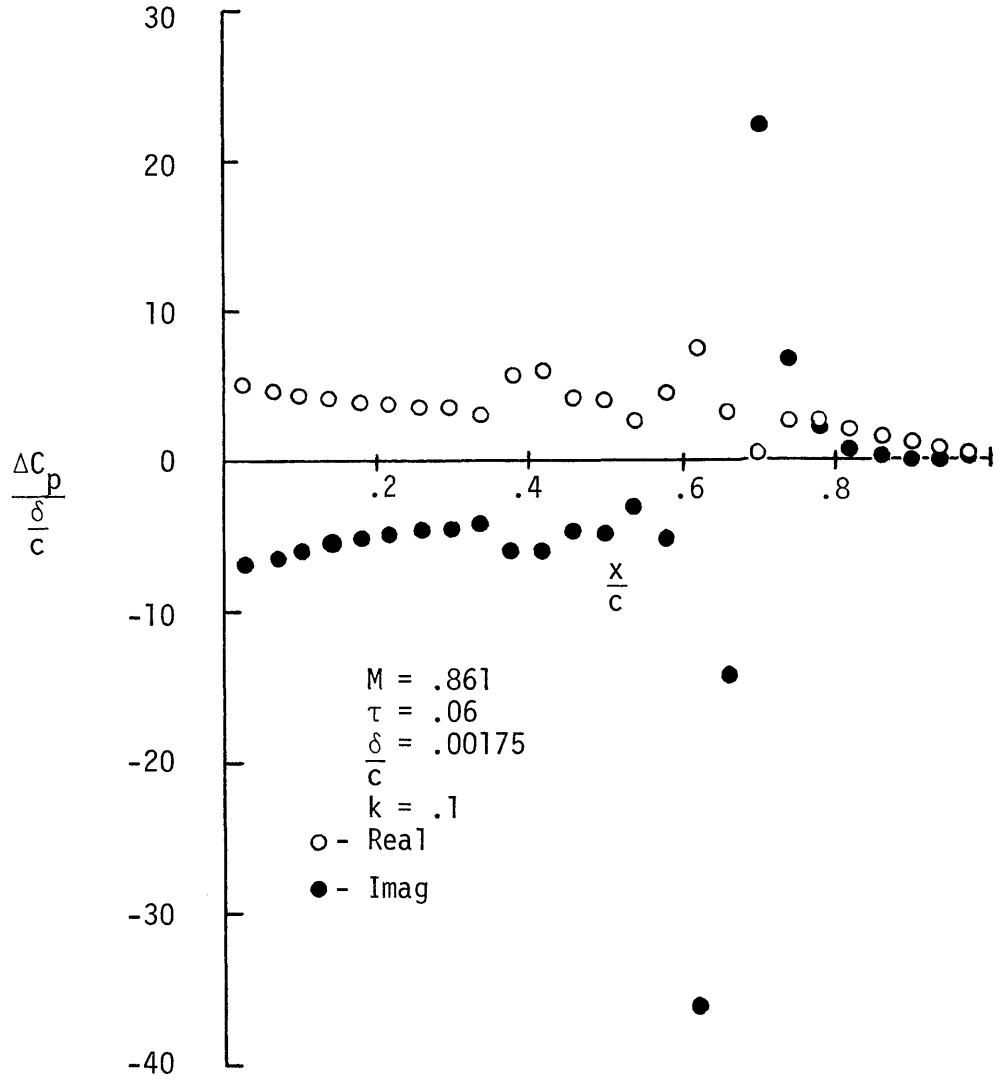

Figure 5.8. Unsteady lift distribution on a circular arc airfoil oscillating in pitch about its midchord.

midchord. At points nearest the upper and lower airfoil boundaries, λ_s=.138c and .15c, respectively (See Table II). When I chose $\frac{\xi}{c}$ to be one degree, $|\lambda_s|$ becomes of the order of the airfoil chord. This indicates that the conditions for which separation of the potential is allowable are not met, and a check of the flow field reveals that, at some locations, $|\varphi| > |\phi|$. Consequently, I do not expect the data for this case to be very reliable. I should anticipate this result because the analysis of Section 2.3 shows that I should have $\frac{\xi}{c} << \tau, \alpha_m$, but a one degree pitch amplitude is approximately $.3\tau$. Table III summarizes the shock motions for the one degree pitch case.

The unsteady lift distributions shown in Figure 5.8 are for k =.1. When I set k =.2, the numerical solutions began to converge and then diverged. No attempt was made to calculate the flow field for $.1 < k < .2$, but such calculations would provide an estimate of the frequency limitation at M = .861.

5.6. Summary

A finite difference method has been developed which is used to compute the unsteady component of the flow field. Steady state solutions, obtained using the finite difference and predictor-corrector methods, are used to determine the effects of varying the airfoil thickness ratio on the unsteady lift and moment about the airfoil leading edge. If shock waves are present in the flow field, a shock compatability condition is introduced into the numerical procedure. That condition allows me to calculate the motion of shock waves, and, by monitoring the amplitude of the shock motion, I am able to determine when the assumption that the unsteadiness is a linear perturbation upon the steady flow breaks down.

Table I

Motion	$\frac{\delta}{c}$	k	$\frac{x_m}{c}$	z	$\frac{\lambda_s}{c}$	$\frac{\lvert\lambda_s\rvert}{c}$
Heave	.01	.03	.641	-.228	-.014-.01i	.017
Heave	.01	.03	.641	-.075	.036+.013i	.038
Heave	.01	.03	.641	.075	.031+.008i	.032
Heave	.01	.03	.641	.228	-.013-.008l	.015

Table II

Motion	$\frac{\delta}{c}$	k	$\frac{x_m}{c}$	z	$\frac{\lambda_s}{c}$	$\frac{\lvert\lambda_s\rvert}{c}$
Pitch	.00175	.1	.641	-.228	-.006-.077i	.077
Pitch	.00175	.1	.641	-.075	.119+.089i	.149
Pitch	.00175	.1	.641	.075	.121+.067i	.138
Pitch	.00175	.1	.641	.228	-.015-.070i	.072

Table III

Motion	$\frac{\delta}{c}$	k	$\frac{x_m}{c}$	z	$\frac{\lambda_s}{c}$	$\frac{\lvert\lambda_s\rvert}{c}$
Pitch	.0175	.1	.641	-.228	.045-.657i	.659
Pitch	.0175	.1	.641	-.075	.888+.894i	1.26
Pitch	.0175	.1	.641	.075	.931_.696i	1.16
Pitch	.0175	.1	.641	.228	-.423-.607i	.74

CHAPTER VI

CONCLUSIONS AND RECOMMENDATIONS

In this study, I sought to develop a tool which would be useful in predicting the onset of aerodynamically induced instabilities. The unsteady, transonic small perturbation potential equation is used to describe the flow field, and the unsteadiness is treated as a linear perturbation about the steady state. This assumption restricts me to analyzing unsteady motions of infinitesimal amplitude. Nevertheless, because flutter prediction requires the analysis of infinitesimal amplitude motion, the methods developed in this study should prove to be a valuable design tool.

Since the equation governing the unsteady potential is coupled to the steady flow field, many steady solutions may be required to predict the occurrence of instabilities. Consequently, a major difficulty was to repeatedly solve a nonlinear partial differential equation. The problem of nonlinearity was avoided by differentiating the steady flow equation with respect to a characterizing physical parameter. The primary difficulty was then reduced to solving a linear equation for the rate of change of the steady potential with the chosen parameter.

I developed a single relaxation method that determines the rate of change of the steady potential with airfoil thickness ratio and angle of attack for subcritical and supercritical flows. That relaxation method is a significant improvement on the parametric

differentiation method of Rubbert and Landahl [28]. They developed several approximate analytic solutions of the linear equation governing the rate of change of the steady velocity with airfoil thickness ratio, but each solution is applicable to only certain types of flows. The method developed here makes no assumptions about the rate of change of the potential and may be applied to all types of flows.

To demonstrate the present method, I uniquely combined the relaxation method with predictor-corrector methods to obtain families of steady state nonlifting and lifting solutions. Obtaining the lifting solutions represents another significant improvement on the method of [28] because Rubbert and Landahl were unable to predict the pressure distributions on lifting airfoils.

Parametric differentiation, applied in the present form, also represents a significant improvement on the perturbation method of Nixon [26],[27]. Nixon's method is also capable of treating the effects of several parameter variations, but the method is limited because it cannot treat variations that cause shock waves to be lost or generated. The results presented in Figure 4.8 show that parametric differentiation does not have that limitation.

That the present method is accurate is seen by comparing my results with those obtained by other researchers. I showed that pressure data obtained using parametric differentiation compares favorably with that obtained from experiments, from relaxation solutions of the potential equation, and from integral equation solutions of the potential and parameterized equations.

The computational efficiency of the present method also appears to compare favorably with relaxation solutions of the potential equation. Although differences in computers, types of airfoils considered, and number of grid points used prevent direct comparisons, the relative efficiency of the present method can be determined from a study conducted by Ballhaus, Jameson, and Albert [53]. That study showed that using line relaxation, approximately 350 iterations were required to obtain the pressure distribution on a 10 percent thick parabolic arc airfoil, with M = .7 (subcritical flow). Extrapolating the curve of Figure 4.9 to τ = .10 suggests that the computational efficiency of the present methods compares favorably with relaxation solutions of the potential equation. While the total number of iterations required to obtain the parametric differentiation solution may be greater, parametric differentiation also provides the solutions for $\tau_0 \leq \tau \leq .10$. One numerical advantage of using parametric differentiation is that the initial estimate of the solution at $\epsilon = \epsilon_1 + \Delta\epsilon$ takes into account the slope of the previous solution. Conversely, using $\phi(\epsilon_1)$ as the initial estimate of the solution of (2.15) for $\epsilon = \epsilon_1 + \Delta\epsilon$ should prove to be a poorer estimate, and more iterations may be required to obtain converged solutions.

If I wish to predict the onset of aerodynamically induced instabilities, the effects of the nonlinear steady flow on the unsteady forces and moments must be considered. As an example, I used families of subcritical, nonlifting steady solutions to determine the effects of varying the airfoil thickness ratio on the

unsteady lift and moment about the leading edge, and those quantities show increasing magnitude, with slight phase changes as τ increases. That I was able to determine the effects of airfoil thickness ratio on the unsteady aerodynamic loads suggest that I can generate the information necessary to predict the onset of instabilities.

An assumption under which the velocity potential was separated into steady and unsteady components is that imbedded shock waves do not travel over large portions of the airfoil chord. For supercritical flows, I introduced a compatability condition at the mean shock location which allowed me to account for the effects of moving shock waves and determine the amplitude of the unsteady shock motion. Hence, I was able to determine when the assumption that the unsteadiness is a linear perturbation upon the steady state is violated. The unsteady shock wave motions summarized in Tables I and II indicate that the associated airfoil motions do not violate the linear perturbation assumption. When the pitch amplitude was increased to 30 percent of the airfoil thickness ratio, the shock excursion amplitude indicated a violation of the linear perturbation assumption (See Table III). The shock compatability condition assumes normal shock waves, but the data of Tables I-III indicate that the shock waves actually tilt slightly. A two dimensional condition, such as that presented in [55], would be a more accurate shock condition.

I have also performed a stability analysis on the unsteady finite difference equations. The results of that analysis allow me to estimate the reduced frequency beyond which relaxation solutions

will not converge. Numerical experiments could then be used to determine the exact frequency limitation.

The results presented in this study give an indication of the great potential of the method of parametric differentiation in analyzing transonic flow problems. Families of steady and unsteady flow solutions were obtained for reasonable amounts of computations. All partial differential equations were solved using relaxation methods, which are among the simplest but not the most efficient numerical methods. Ballhaus, Jameson, and Albert [53] have presented approximate factorization methods for solving the small perturbation potential equation; those methods greatly reduced the computations required to compute steady two dimensional flow fields. Applying such a factorization scheme to (3.11) should make parametric differentiation an even more attractive transonic method. The computer program developed for the present study varies the second parameter only after the first has reached its maximum value. Any program developed in the future should have the capability of varying any parameter at any time.

The development of any transonic method should be done so with the ultimate goal of extending that method to three dimensions. Parametric differentiation would then be even more effective because of the additional parameters that may be considered; such parameters could be wing sweep and the twist of the wing. Extension of the relaxation and predictor-corrector methods to three dimensions should not pose any great difficulties.

APPENDIX A

PREDICTOR-CORRECTOR METHODS FOR GENERATING STARTING SOLUTIONS

Initially the starting data necessary for use in (3.7) and (3.9) is unavailable. Consequently, less accurate methods are employed until that data is obtained. To determine solutions at $\epsilon = \epsilon_0 + \Delta\epsilon$, I use the second order predictor and corrector

$$p(\epsilon_0+\Delta\epsilon) = \phi(\epsilon_0) + \Delta\epsilon g(\epsilon_0) + \frac{\Delta\epsilon^2}{2}\frac{dg}{d\epsilon} \tag{A.1}$$

$$c(\epsilon_c+\Delta\epsilon) = \phi(\epsilon_0) + \Delta\epsilon g(\epsilon_0+\Delta\epsilon) - \frac{\Delta\epsilon^2}{2}\frac{dg}{d\epsilon} \tag{A.2}$$

where p and c are the predicted and corrected potentials, respectively.

The error terms, $\pm \frac{\Delta\epsilon^2}{2}\frac{dg}{d\epsilon}$, are not evaluated, but they are compensated for by modifying (A.1) and (A.2). The deviation of the predicted and corrected potentials from the exact values are

$$\phi(\epsilon_0+\Delta\epsilon) - p(\epsilon_0+\Delta\epsilon) = \frac{\Delta\epsilon^2}{2}\frac{dg}{d\epsilon}$$

$$\phi(\epsilon_0+\Delta\epsilon) - c(\epsilon_0+\Delta\epsilon) = -\frac{\Delta\epsilon^2}{2}\frac{dg}{d\epsilon}$$

which, assuming that $\frac{dg}{d\epsilon}$ is constant over the interval, yields the relation

$$\Delta\epsilon^2 \frac{dy}{d\epsilon} = c(\epsilon_0+\Delta\epsilon) - p(\epsilon_0+\Delta\epsilon) \tag{A.3}$$

By introducing (A.3) into (A.1) and (A.2), I eliminate most of the second order error. Generally, c-p varies slowly from step to step, thus in (A.1) I use

$$\Delta\epsilon^2 \frac{dy}{d\epsilon} = c(\epsilon_0) - p(\epsilon_0)$$

The modified predicted and corrected solutions then become, respectively

$$m(\epsilon_0+\Delta\epsilon) = p(\epsilon_0+\Delta\epsilon) + \frac{1}{2}[c(\epsilon_0) - p(\epsilon_0)] \tag{A.4}$$

$$\phi(\epsilon_0+\Delta\epsilon) = c(\epsilon_0+\Delta\epsilon) - \frac{1}{2}[c(\epsilon_0+\Delta\epsilon) - p(\epsilon_0+\Delta\epsilon)] \tag{A.5}$$

With the potential known at an additional value of ϵ, the order of the quadrature method is increased. I use the predictor-corrector formulas

$$p(\epsilon_0+2\Delta\epsilon) = \phi(\epsilon_0) + 2\Delta\epsilon\, y(\epsilon_0+\Delta\epsilon) + \frac{\Delta\epsilon^3}{3}\frac{d^2y}{d\epsilon^2} \tag{A.6}$$

$$c(\epsilon_0+2\Delta\epsilon) = \phi(\epsilon_0+\Delta\epsilon) + \frac{\Delta\epsilon}{2}[y(\epsilon_0+2\Delta\epsilon) + y(\epsilon_0+\Delta\epsilon)] - \frac{\Delta\epsilon^3}{12}\frac{d^2y}{d\epsilon^2} \tag{A.7}$$

Following the above procedure, I obtain

$$\Delta\epsilon^3 \frac{d^2y}{d\epsilon^2} = \frac{12}{5}[c(\epsilon_0+2\Delta\epsilon) - p(\epsilon_0+2\Delta\epsilon)]$$

and the modified predictor and corrector become

$$m(\epsilon_0+2\Delta\epsilon) = p(\epsilon_0+2\Delta\epsilon) + \frac{4}{5}[c(\epsilon_0+\Delta\epsilon) - p(\epsilon_0+\Delta\epsilon)] \tag{A.8}$$

$$\phi(\epsilon_0+2\Delta\epsilon) = c(\epsilon_0+2\Delta\epsilon) - \frac{1}{5}[c(\epsilon_0+2\Delta\epsilon) - p(\epsilon_0+2\Delta\epsilon)] \tag{A.9}$$

Increasing the order of the quadrature again, for $\epsilon = \epsilon_0 + 3\Delta\epsilon$, I use

$$p(\epsilon_0+3\Delta\epsilon) = \phi(\epsilon_0+2\Delta\epsilon) + \phi(\epsilon_0+\Delta\epsilon) - \phi(\epsilon_0) + 2\Delta\epsilon[g(\epsilon_0+2\Delta\epsilon) - g(\epsilon_0+\Delta\epsilon)] + \frac{\Delta\epsilon^4}{3}\frac{d^3g}{d\epsilon^3} \tag{A.10}$$

$$c(\epsilon_0+3\Delta\epsilon) = \phi(\epsilon_0+2\Delta\epsilon) + \frac{\Delta\epsilon}{12}[5g(\epsilon_0+3\Delta\epsilon) + 8g(\epsilon_0+2\Delta\epsilon) - g(\epsilon_0+\Delta\epsilon)] - \frac{\Delta\epsilon^4}{24}\frac{d^3g}{d\epsilon^3} \tag{A.11}$$

The error is

$$\Delta\epsilon^4\frac{d^3g}{d\epsilon^3} = \frac{24}{9}[c(\epsilon_0+3\Delta\epsilon) - p(\epsilon_0+3\Delta\epsilon)]$$

which leads to the modified predictor-corrector

$$m(\epsilon_0+3\Delta\epsilon) = p(\epsilon_0+3\Delta\epsilon) + \frac{8}{9}[c(\epsilon_0+2\Delta\epsilon) - p(\epsilon_0+2\Delta\epsilon)] \tag{A.12}$$

$$\phi(\epsilon_0+3\Delta\epsilon) = c(\epsilon_0+3\Delta\epsilon) - \frac{1}{9}[c(\epsilon_0+3\Delta\epsilon) - p(\epsilon_0+3\Delta\epsilon)] \tag{A.13}$$

With the starting data determined from (A.1)-(A.13), solutions at all subsequent values of ϵ are obtained using the fifth order

predictor-corrector

$$p(\epsilon_0+n\Delta\epsilon) = \phi(\epsilon_0+(n-4)\Delta\epsilon) + \frac{4}{3}\Delta\epsilon\,[2g(\epsilon_0+(n-1)\Delta\epsilon) - g(\epsilon_0+(n-2)\Delta\epsilon) + 2g(\epsilon_0+(n-3)\Delta\epsilon)] + \frac{14}{45}\Delta\epsilon^5\frac{d^4g}{d\epsilon^4} \quad (A.14)$$

$$c(\epsilon_0+n\Delta\epsilon) = \frac{1}{3}[\phi(\epsilon_0+(n-1)\Delta\epsilon) + \phi(\epsilon_0+(n-2)\Delta\epsilon + \phi(\epsilon_0+(n-3)\Delta\epsilon)]$$

$$+ \frac{\Delta\epsilon}{36}[13g(\epsilon_0+n\Delta\epsilon) + 39g(\epsilon_0+(n-1)\Delta\epsilon) + 15g(\epsilon_0+(n-2)\Delta\epsilon)$$

$$+ 5g(\epsilon_0+(n-3)\Delta\epsilon)] - \frac{\Delta\epsilon^5}{40}\frac{d^4g}{d\epsilon^4} \quad (A.15)$$

The modified potential used to find $g(\epsilon_0+n\Delta\epsilon)$ is

$$m(\epsilon_0+n\Delta\epsilon) = p(\epsilon_0+n\Delta\epsilon) + \frac{112}{121}[c(\epsilon_0+(n-1)\Delta\epsilon) - p(\epsilon_0+(n-1)\Delta\epsilon)] \quad (A.16)$$

and to determine the final values of the potential, I use

$$\phi(\epsilon_0+n\Delta\epsilon) = c(\epsilon_0+n\Delta\epsilon) - \frac{9}{121}[c(\epsilon_0+n\Delta\epsilon) - p(\epsilon_0+n\Delta\epsilon)] \quad (A.17)$$

I should point out that $p-c$ is initially set at zero and that each time the order of the predictor-corrector is changed, it is reset to zero.

APPENDIX B

BASE SOLUTION FOR NONLIFTING BICONVEX AIRFOILS

When $|1-m^2| >> \tau^{2/3}, \alpha^{2/3}$, (2.15) may be reduced to the linear equation

$$(1-m^2)\phi_{xx} + \phi_{\bar{z}\bar{z}} = 0 \tag{B.1}$$

Thus, if the initial thickness ratio or angle of attack is sufficiently small, the base solution may be obtained from Laplace's equation

$$\phi_{xx} + \phi_{\bar{z}\bar{z}} = 0 \tag{B.2}$$

The initial nonlifting airfoil is represented by a distribution of sources and sinks along its chord, the corresponding velocity potential, with U normalized to unity, is

$$\phi(x,\bar{z}) = \frac{1}{2\beta\pi}\int_{-\frac{c}{2}}^{\frac{c}{2}} \frac{dz_s}{dx_1}\ln\left[(x-x_1)^2+\bar{z}^2\right]dx_1 \tag{B.3}$$

Since for small thickness ratios, circular arc airfoils reduce to parabolic arcs, I define the airfoil boundary as

$$z_s(x_1) = \pm 2\tau\left[\left(\frac{c}{2}\right)^2 - x_1^2\right]$$

The potential then becomes

$$\phi(x,z) = \mp \frac{2\tau}{\beta\pi} \int_{-\frac{c}{2}}^{\frac{c}{2}} x_1 \ln\left[(x-x_1)^2 + \bar{z}^2\right] dx_1$$

or, upon the substitution $\sigma = x - x_1$,

$$\phi(x,z) = \mp \frac{2\tau}{\beta\pi} \left[\int_{x+\frac{c}{2}}^{x-\frac{c}{2}} \sigma \ln(\sigma^2 + \bar{z}^2)\, d\sigma - x \int_{x+\frac{c}{2}}^{x-\frac{c}{2}} \ln(\sigma^2 + \bar{z}^2)\, d\sigma \right]$$

Employing the integration formulas

$$\int_{x+\frac{c}{2}}^{x-\frac{c}{2}} \sigma \ln(\sigma^2 + \bar{z}^2)\, d\sigma = \frac{1}{2}\left\{ \left[\left(x-\frac{c}{2}\right)^2 + \bar{z}^2\right] \ln\left[\left(-\frac{c}{2}\right)^2 + \bar{z}^2\right] - \left[\left(x+\frac{c}{2}\right)^2 + \bar{z}^2\right] \ln\left[\left(x+\frac{c}{2}\right)^2 + \bar{z}^2\right] \right.$$

$$\int_{x+\frac{c}{2}}^{x-\frac{c}{2}} \ln(\sigma^2 + \bar{z}^2)\, d\sigma = \left(x-\frac{c}{2}\right) \ln\left[\left(x-\frac{c}{2}\right)^2 + \bar{z}^2\right] - \left(x+\frac{c}{2}\right) \ln\left[\left(x+\frac{c}{2}\right)^2 + \bar{z}^2\right]$$

$$\left. + 2\bar{z}\left[\tan^{-1}\left(\frac{x-c/2}{\bar{z}}\right) - \tan^{-1}\left(\frac{x+c/2}{\bar{z}}\right)\right] + 2C \right\}$$

I obtain the base solution for nonlifting biconvex airfoils

$$\phi(x,z) = \frac{\tau}{\beta\pi} \left\{ \left[x^2 - \left(\frac{c}{2}\right)^2 - \bar{z}^2\right] \ln\left[\frac{(x-c/2)^2 + \bar{z}^2}{(x^2+c/2) + \bar{z}^2}\right] \right.$$

$$\left. + 4x\bar{z}\left[\tan^{-1}\left(\frac{x-c/2}{\bar{z}}\right) - \tan^{-1}\left(\frac{x+c/2}{\bar{z}}\right)\right] + 2cx \right\} \qquad \text{(B.4)}$$

APPENDIX C

FINITE DIFFERENCE EQUATIONS FOR THE RATE OF CHANGE OF THE STEADY POTENTIAL

In this appendix, I develop the conservative finite difference equations used to determine the rate of change of the steady potential with the chosen parameter. The conservative difference representation of (4.5) is obtained by integrating (4.15) over the shaded area of Figure 4.5. Application of the divergence theorem in that integration leads to

$$\iint \nabla\cdot(\tilde{a}\hat{i}+\tilde{b}\hat{k})\,dA = \oint (\tilde{a}\hat{i}+\tilde{b}\hat{k})\cdot\hat{n}\,ds = 0 \qquad \text{(C.1)}$$

or

$$(\tilde{a}_{n+1/2,\ell}-\tilde{a}_{n-1/2,\ell})\Delta\eta + (\tilde{b}_{n,\ell+1/2}-\tilde{b}_{n,\ell-1/2})\Delta\xi = 0$$

Division by the area of integration yields the difference formula

$$\frac{\tilde{a}_{n+1/2,\ell}-\tilde{a}_{n-1/2,\ell}}{\Delta\xi} + \frac{\tilde{b}_{n,\ell+1/2}-\tilde{b}_{n,\ell-1/2}}{\Delta\eta} = 0 \qquad \text{(C.2)}$$

The fluxes in (C.2) are then represented as

$$\tilde{a}_{n+1/2,\ell} = (1-\mu_{n,\ell}) \left\{ \frac{f}{h} \left[1-m^2-m^2(\gamma+1)+\phi_\xi \right] g_\xi \right\}_{n+1/2,\ell}$$

$$+\mu_{n,\ell} \left\{ \frac{f}{h} \left[1-m^2-m^2(\gamma+1)+\phi_\xi \right] g_\xi \right\}_{n-1/2,\ell} \qquad \text{(C.3)}$$

$$\tilde{a}_{n-1/2,\ell} = (1-\mu_{n-1,\ell}) \left\{ \frac{f}{h} \left[1-m^2-m^2(\gamma+1)+\phi_\xi \right] g_\xi \right\}_{n-1/2,\ell}$$

$$+\mu_{n-1,\ell} \left\{ \frac{f}{h} \left[1-m^2-m^2(\gamma+1)+\phi_\xi \right] g_\xi \right\}_{n-3/2} \qquad \text{(C.4)}$$

$$\tilde{b}_{n,\ell+1/2} = \left(\frac{h}{f} g_\eta \right)_{n,\ell+1/2} \qquad \text{(C.5)}$$

$$\tilde{b}_{n,\ell-1/2} = \left(\frac{h}{f} g_\eta \right)_{n,\ell-1/2} \qquad \text{(C.6)}$$

where μ is a switching function defined as

$$\mu_{n,\ell} = \begin{cases} 0, & 1-m^2-m^2(\gamma+1)+\phi_\xi > 0 \\ 1, & 1-m^2-m^2(\gamma+1)+\phi_\xi < 0 \end{cases}$$

Combining (C.2)-(C.6), I obtain the conservative difference formula

$$(1-\mu_{n,\ell})\frac{f_n}{\Delta\xi}\left|\{[1-m^2-m^2(\gamma+1)f\phi_\xi]fg_\xi\}_{n+1/2,\ell}-\{[1-m^2-m^2(\gamma+1)f\phi_\xi]fg_\xi\}_{n-1/2,\ell}\right|$$

$$+\mu_{n-1,\ell}\frac{f_n}{\Delta\xi}\left|\{[1-m^2-m^2(\gamma+1)f\phi_\xi]fg_\xi\}_{n-1/2,\ell}-\{[1-m^2-m^2(\gamma+1)f\phi_\xi]fg_\xi\}_{n-3/2,\ell}\right|$$

$$+\frac{h_\ell}{\Delta\eta}\left[(hg_\eta)_{n,\ell+1/2}-(hg_\eta)_{n,\ell-1/2}\right]=0 \qquad (C.7)$$

The effect of the switching function is to represent the derivatives in the streamwise direction with centered differences where the flow is subsonic and with backward differences in supersonic flow regions. Where the flow accelerates through sonic velocity, $\mu_{n,\ell}=1$ and $\mu_{n-1,\ell}=0$, a parabolic difference operator is used, and immediately downstream of the supersonic region, $\mu_{n,\ell}=0$ and $\mu_{n-1,\ell}=1$, a combination of centered and backward differences is used.

The evaluation of each term in (C.7) with centered differences yields

$$(1-\mu_{n,\ell})f_n\left\{\frac{f_{n+1/2}}{\Delta\xi^2}\left[1-m^2-m^2(\gamma+1)\frac{f_{n+1/2}}{\Delta\xi}(\phi_{n+1,\ell}-\phi_{n,\ell})\right](\tilde{g}_{n+1,\ell}-\tilde{g}_{n,\ell})\right.$$

$$\left.-\frac{f_{n-1/2}}{\Delta\xi}\left[1-m^2-m^2(\gamma+1)\frac{f_{n-1/2}}{\Delta\xi}(\phi_{n,\ell}-\phi_{n-1,\ell})\right](\tilde{g}_{n,\ell}-\tilde{g}_{n-1,\ell})\right\}$$

$$+\mu_{n-1,\ell}f_n\left\{\frac{f_{n-1/2}}{\Delta\xi^2}\left[1-m^2-m^2(\gamma+1)\frac{f_{n-1/2}}{\Delta\xi}(\phi_{n,\ell}-\phi_{n-1,\ell})\right](\tilde{g}_{n,\ell}-\tilde{g}_{n-1,\ell})\right.$$

$$-\frac{f_{n-3/2}}{\Delta\xi^2}\left[1-m^2-m^2(\gamma+1)\frac{f_{n-3/2}}{\Delta\xi}(\phi_{n-1,\ell}-\phi_{n-2,\ell})\right](\tilde{g}_{n-1,\ell}-\tilde{g}_{n-2,\ell})$$

$$+\frac{h_\ell}{\Delta\eta^2}\left[h_{\ell+1/2}(\tilde{g}_{n,\ell+1}-\tilde{g}_{n,\ell})-h_{\ell-1/2}(\tilde{g}_{n,\ell}-\tilde{g}_{n,\ell-1})\right]=0 \qquad \text{(C.8)}$$

where the $\tilde{g}$'s are the intermediate values of g. The final values, g^+, are obtained from

$$g^+_{n,\ell}=g_{n,\ell}+\omega(\tilde{g}_{n,\ell}-g_{n,\ell})$$

where ω is a relaxation factor. If the flow is subsonic, $1\le\omega\le 2$, and in supersonic regions, $0\le\omega<1$. I then eliminate $\tilde{g}$ from (3.8) by substituting into (C.8)

$$\tilde{g}_{n,\ell}=\frac{g^+_{n,\ell}}{\omega}+\left(1-\frac{1}{\omega}\right)g_{n,\ell} \qquad \text{(C.9)}$$

but (C.9) is not applied at all points.

To evaluate streamwise derivatives at subsonic points, I use current values of $g_{n-1,\ell}$, previous values of $g_{n+1,\ell}$, and (C.9) at the midpoint. Streamwise derivatives at supersonic points are evaluated with data from the previous iteration, and to avoid a discontinuity in $h(hg_\eta)_\eta$ as I cross the sonic line, that term is evaluated with current data at all points. Defining α_1, α_2, and α_3 as

$$\alpha_1 \equiv \frac{f_n f_{n+1/2}}{\Delta\xi^2}\left[1-m^2-m^2(\gamma+1)\frac{f_{n+1/2}}{\Delta\xi}(\phi_{n+1,\ell}-\phi_{n,\ell})\right] \tag{C.10}$$

$$\alpha_2 \equiv \frac{f_n f_{n-1/2}}{\Delta\xi^2}\left[1-m^2-m^2(\gamma+1)\frac{f_{n-1/2}}{\Delta\xi}(\phi_{n,\ell}-\phi_{n-1,\ell})\right] \tag{C.11}$$

$$\alpha_3 \equiv \frac{f_n f_{n-3/2}}{\Delta\xi^2}\left[1-m^2-m^2(\gamma+1)f_{n-3/2}(\phi_{n-1,\ell}-\phi_{n-2,\ell})\right] \tag{C.12}$$

the conservative finite difference approximation of (4.5) becomes

$$\begin{aligned}(1-\mu_{n,\ell})\left\{\alpha_1\left[g_{n+1,\ell}-\frac{g^+_{n,\ell}}{\omega}-\left(1-\frac{1}{\omega}\right)g_{n,\ell}\right]-\alpha_2\left[\frac{g^+_{n,\ell}}{\omega}+\left(1-\frac{1}{\omega}\right)g_{n,\ell}-g^+_{n-1,\ell}\right]\right\}\\ +\mu_{n-1,\ell}\left[\alpha_2(g_{n,\ell}-g_{n-1,\ell})-\alpha_3(g_{n-1,\ell}-g_{n-2,\ell})\right]\\ +\frac{h_\ell}{\Delta\eta^2}\left[h_{\ell+1/2}(g^+_{n,\ell+1}-g^+_{n,\ell})-h_{\ell-1/2}(g^+_{n,\ell}-g^+_{n,\ell-1})\right]=0\end{aligned} \tag{C.13}$$

Treating the difference in g between iterations as the pseudo time derivative

$$g^+_{n,\ell}-g_{n,\ell}=\Delta t\, g_t \tag{C.14}$$

reveals that varying the iteration number of the difference operators introduces timelike derivatives into the original differential equation. Isolation of the timelike terms in the subsonic

difference equation yields

$$\alpha_1 (g_{n+1,\ell} - g_{n,\ell}) - \alpha_2 (g_{n,\ell} - g_{n,\ell-1}) - \frac{\alpha_1}{\omega} (g^+_{n,\ell} - g_{n,\ell})$$

$$+\alpha_2 \left(1 - \frac{1}{\omega}\right)(g^+_{n,\ell} - g_{n,\ell}) - \alpha_2 (g^+_{n,\ell} - g_{n,\ell} - g^+_{n-1,\ell} + g_{n-1,\ell})$$

$$+\frac{h_\ell}{\Delta\eta^2}\left[h_{\ell+1/2}(g_{n,\ell+1} - g_{n,\ell}) - h_{\ell-1/2}(g_{n,\ell} - g_{n,\ell-1})\right]$$

$$+\frac{h_\ell}{\Delta\eta^2}\left[h_{\ell+1/2}(g^+_{n,\ell+1} - g_{n,\ell+1} - g^+_{n,\ell} + g_{n,\ell}) - h_{\ell-1/2}(g^+_{n,\ell} - g_{n,\ell} - g^+_{n,\ell-1} + g_{n,\ell-1})\right] = 0 \tag{C.15}$$

Utilizing (C.14), the subsonic differential equation becomes

$$f\{[1 - m^2 - m^2(\gamma+1) f \phi_\xi] f g_\xi\}_\xi + h(h g_\eta)_\eta - \alpha_2 \Delta t \Delta\xi g_{\xi t}$$

$$-\left[\frac{\alpha_1}{\omega} - \left(1 - \frac{1}{\omega}\right)\alpha_2\right]\Delta t g_t - h_\ell \frac{\Delta t}{\Delta\eta}\left[(h g_{\eta t})_{n,\ell+1/2} - (h g_{\eta t})_{n,\ell-1/2}\right] = 0$$

which as the mesh spacing approaches zero, reduces to

$$f\{[1 - m^2 - m^2(\gamma+1) f \phi_\xi] f g_\xi\}_\xi + h(h g_\eta)_\eta - \alpha_2 \Delta t \Delta\xi g_{\xi t} - \left[\frac{\alpha_1}{\omega} - \left(1 - \frac{1}{\omega}\right)\alpha_2\right]\Delta t g_t = 0 \tag{C.16}$$

As the solution of (C.16) converges, the additional time derivatives vanish, and the solution of the original equation is obtained. At supersonic points, I have

$$\alpha_2(g_{n,\ell}-g_{n-1,\ell})-\alpha_3(g_{n-1,\ell}-g_{n-2,\ell})+\frac{h_\ell}{\Delta\eta^2}\left[h_{\ell+1/2}(g_{n,\ell+1}-g_{n,\ell})\right.$$

$$\left.-h_{\ell-1/2}(g_{n,\ell}-g_{n,\ell-1})\right]+\frac{h_\ell}{\Delta\eta^2}\left[h_{\ell+1/2}(g^+_{n,\ell+1}-g_{n,\ell+1}-g^+_{n,\ell}+g_{n,\ell})\right.$$

$$\left.-h_{\ell-1/2}(g^+_{n,\ell}-g_{n,\ell}-g^+_{n,\ell-1}+g_{n,\ell-1})\right]=0$$

or, as the mesh spacing vanishes

$$f\{f[1-m^2-m^2(\gamma+1)f\phi_\xi]g_\xi\}_\xi+h(hg_\eta)_\eta=0 \qquad \text{(C.17)}$$

During the initial iterations, there is the possibility of a mismatch in the time dependent terms near the sonic line, but I correct this situation by adding a term of the form $g_{\xi t}$ to (C.17). Since in the steady, supersonic problem ξ is the timelike direction, the coefficient of $g_{\xi t}$ should be such that it is the timelike direction in the unsteady problem.

Defining u^* as

$$u^*\equiv f[1-m^2-m^2(\gamma+1)f\phi_\xi]$$

and adding to (C.17) the term $\epsilon^* u^* f\frac{\Delta t}{\Delta\xi}g_{\xi t}$, the supersonic differential equation becomes

$$f(u^*g_\xi)_\xi+h(hg_\eta)_\eta+\epsilon^* u^* f\frac{\Delta t}{\Delta\xi}g_{\xi t}=0 \qquad \text{(C.18)}$$

Introducing the new coordinate

$$\tau^* = t + a^*\xi$$

(C.18) is transformed into

$$f(u^*g_\xi)_\xi + h(hg_\eta)_\eta + u^*f\left(2a^* + \epsilon^*\frac{\Delta t}{\Delta\xi}\right)g_{\xi\tau^*}$$

$$+ u^*f\left(a^{*2} + \epsilon^*a^*\frac{\Delta t}{\Delta\xi}\right)g_{\tau^*\tau^*} + \text{lower derivatives} = 0$$

Elimination of $g_{\xi\tau^*}$ requires $a^* = -\frac{\epsilon^*}{2}\frac{\Delta t}{\Delta\xi}$ which leads to

$$f(u^*g_\xi)_\xi + h(hg_\eta)_\eta - \epsilon^{*2}\frac{u^*f}{4}\frac{\Delta t^2}{\Delta\xi^2}g_{\tau^*\tau^*}$$

$$+ \text{lower derivatives} = 0 \qquad \text{(C.19)}$$

Since u^* is negative in supersonic zones, the ξ direction is indeed the timelike direction in the unsteady supersonic problem.

Having shown that choosing the appropriate coefficient of the additional $g_{\xi t}$ term ensures that ξ is the timelike direction in the unsteady supersonic problem I simplify matters in practice by actually adding the term $-\epsilon^* f_n f_{n-1/2}\frac{\Delta t}{\Delta\xi}g_{\xi t}$ to (C.17). The value of ϵ^* is then chosen to give the partial differential equation the desired properties.

With the additional term, the final form of the finite difference equation becomes

$$(1-u_{n,\ell})\left\{\alpha_1\left[g_{n+1,\ell}-\frac{g^+_{n,\ell}}{\omega}-\left(1-\frac{1}{\omega}\right)g_{n,\ell}\right]-\alpha_2\left[\frac{g^+_{n,\ell}}{\omega}+\left(1-\frac{1}{\omega}\right)g_{n,\ell}-g^+_{n-1,\ell}\right]\right\}$$

$$+u_{n-1,\ell}\left[\alpha_2\left(g_{n,\ell}-g_{n-1,\ell}\right)-\alpha_3\left(g_{n-1,\ell}-g_{n-2,\ell}\right)\right]$$

$$+\frac{h_\ell}{\Delta\eta^2}\left[h_{\ell+1/2}\left(g^+_{n,\ell+1}-g^+_{n,\ell}\right)-h_{\ell-1/2}\left(g^+_{n,\ell}-g^+_{n,\ell-1}\right)\right]$$

$$-u_{n,\ell}\epsilon^*\frac{f_n f_{n-1/2}}{\Delta\xi^2}\left(g^+_{n,\ell}-g_{n,\ell}-g^+_{n-1,\ell}+g_{n-1,\ell}\right)=0 \qquad \text{(C.20)}$$

The tridiagonal coefficients are easily recognized by writing (C.20) in the form

$$-\frac{h_\ell h_{\ell-1/2}}{\Delta\eta^2}g^+_{n,\ell-1}+\left[\frac{h_\ell}{\Delta\eta^2}\left(h_{\ell+1/2}+h_{\ell-1/2}\right)+(1-u_{n,\ell})\frac{(\alpha_1+\alpha_2)}{\omega}+u_{n,\ell}\epsilon^*\frac{f_n f_{n-1/2}}{\Delta\xi^2}\right]g^+_{n,\ell}$$

$$-\frac{h_\ell h_{\ell+1/2}}{\Delta\eta^2}g^+_{n,\ell+1}=(1-u_{n,\ell})\alpha_1 g_{n+1,\ell}-\left[(1-u_{n,\ell})(\alpha_1+\alpha_2)\left(1-\frac{1}{\omega}\right)\right.$$

$$\left.-u_{n,\ell}\epsilon^*\frac{f_n f_{n-1/2}}{\Delta\xi^2}-u_{n-1,\ell}\alpha_2\right]g_{n,\ell}+\left[(1-u_{n,\ell})\alpha_2+u_{n,\ell}\epsilon^*\frac{f_n f_{n-1/2}}{\Delta\xi^2}\right]g^+_{n-1,\ell}$$

$$-\left[u_{n,\ell}\epsilon^*\frac{f_n f_{n-1/2}}{\Delta\xi^2}+u_{n-1,\ell}(\alpha_2+\alpha_3)\right]g_{n-1,\ell}+u_{n-1,\ell}\alpha_3 g_{n-2,\ell}=0 \qquad \text{(C.21)}$$

A comparison of (C.21) with (G.1) reveals that

$$A_i=\frac{h_\ell h_{\ell-1/2}}{\Delta\eta^2} \qquad \text{(C.22)}$$

$$B_i = \frac{h_\ell}{\Delta\eta^2}\left(h_{\ell+1/2} + h_{\ell-1/2}\right) + \left(1-u_{n,\ell}\right)\left(\alpha_1+\alpha_2\right) + u_{n,\ell}\,\epsilon^2 f_n f_{n-1/2} \qquad \text{(C.23)}$$

$$C_i = \frac{h_\ell h_{\ell+1/2}}{\Delta\eta^2} \qquad \text{(C.24)}$$

$$D_i = \left(1-u_{n,\ell}\right)\alpha_1 g_{n+1,\ell} - \left[\left(1-u_{n,\ell}\right)\left(\alpha_1+\alpha_2\right)\left(1-\frac{1}{\omega}\right) - u_{n,\ell}\,\epsilon^2 f_n f_{n-1/2}\right.$$

$$\left. - u_{n-1,\ell}\,\alpha_2\right] g_{n,\ell} + \left[\left(1-u_{n,\ell}\right)\alpha_2 + u_{n,\ell}\,\epsilon^2 f_n f_{n-1/2}\right] g^*_{n-1,\ell}$$

$$- \left[u_{n,\ell}\,\epsilon^2 f_n f_{n-1/2} + u_{n-1,\ell}\left(\alpha_2+\alpha_3\right)\right] g_{n-1,\ell} + u_{n-1,\ell}\,\alpha_3\, g_{n-2,\ell} \qquad \text{(C.25)}$$

where the i subscript denotes interior points of the computational domain.

If $|\chi(\xi)| \le \frac{c}{2}$, $(h g_\eta)_{n,vp-1/2}$ is prescribed from the tangency condition, and

$$h\left(h g_\eta\right)_\eta = \frac{h_{vp}}{\Delta\eta}\left[\frac{h_{vp+1/2}}{\Delta\eta}\left(g^*_{n,vp+1} - g^*_{n,vp}\right) - \left(h g_\eta\right)_{n,vp-1/2}\right]$$

As a result, the tridiagonal coefficients become

$$A_{vp} = 0 \qquad \text{(C.26)}$$

$$B_{up} = B_i - \frac{h_{up}\, h_{up-1/2}}{\Delta\eta^2} \tag{C.27}$$

$$C_{up} = C_i \tag{C.28}$$

$$D_{up} = D_i - \frac{h_{up}\,(hg_\eta)_{n,up-1/2}}{\Delta\eta} \tag{C.29}$$

Similarly, at ℓ =low, $(hg_\eta)_{n,\ell+1/2}$ is prescribed and

$$h(hg_\eta)_\eta = \frac{h_{low}}{\Delta\eta}\left[(hg_\eta)_{n,low+1/2} - \frac{h_{low-1/2}}{\Delta\eta}\left(g^+_{n,low} - g^+_{n,low-1}\right)\right]$$

In this case, the tridiagonal coefficients are

$$A_{low} = A_i \tag{C.30}$$

$$B_{low} = B_i - \frac{h_{low}\, h_{low+1/2}}{\Delta\eta^2} \tag{C.31}$$

$$C_{low} = 0 \tag{C.32}$$

$$D_{low} = D_i + \frac{h_{low}\,(hg_\eta)_{n,low+1/2}}{\Delta\eta} \tag{C.33}$$

If the flow is nonlifting and $|X(\xi)| > \frac{c}{2}$, $(hg_\eta)_{n,up-1/2} = 0$, and

$$h(hg_\eta)_\eta = \frac{h_{up}\, h_{up+1/2}}{\Delta\eta^2}\left(g^+_{n,up+1} - g^+_{n,up}\right)$$

The tridiagonal coefficients are then

$$A_{vp} = 0 \tag{C.34}$$

$$B_{vp} = B_i - \frac{h_{vp} h_{vp-1/2}}{\Delta\eta^2} \tag{C.35}$$

$$C_{vp} = C_i \tag{C.36}$$

$$D_{vp} = D_i \tag{C.37}$$

Along the column n=2, $(f g_\xi)_{n-1/2,\ell} = 0$, and because the flow is subsonic at infinity, I write the difference equation as

$$\frac{f_n}{\Delta\xi}\left\{\left[1-m^2-m^2(\gamma+1)f\phi_\xi\right]f g_\xi\right\}_{n+1/2,\ell} + h(h g_\eta)_\eta = 0$$

or

$$\alpha_1\left[g_{n+1,\ell} - \frac{g^+_{n,\ell}}{\omega} - \left(\frac{1-\alpha_1}{\omega}\right) g_{n,\ell}\right] + \frac{h_\ell}{\Delta\eta^2}\left[h_{\ell+1/2}\left(g^+_{n,\ell+1} - g^+_{n,\ell}\right) - h_{\ell-1/2}\left(g^+_{n,\ell} - g^+_{n,\ell-1}\right)\right] = 0 \tag{C.38}$$

The tridiagonal coefficients are

$$A_u = \frac{h_\ell h_{\ell-1/2}}{\Delta\eta^2} \tag{C.39}$$

$$B_u = \frac{h_\ell\left(h_{\ell+1/2} + h_{\ell-1/2}\right)}{\Delta\eta^2} + \frac{\alpha_1}{\omega} \tag{C.40}$$

$$C_u = \frac{h_\ell h_{\ell+1/2}}{\Delta\eta^2} \tag{C.41}$$

$$D_u = a_1\left[g_{n+1,\ell} - \left(1-\frac{1}{\omega}\right)g_{n,\ell}\right] \tag{C.42}$$

where the u subscript denotes quantities at the upstream boundary. If the flow is nonlifting, at the point n=2 , ℓ =up

$$A = 0 \tag{C.43}$$

$$B = B_u - \frac{h_{up}h_{up-1/2}}{\Delta\eta^2} \tag{C.44}$$

$$C = C_u \tag{C.45}$$

$$D = D_u \tag{C.46}$$

Along n=N-1 , $(fg_\xi)_{n+1/2,\ell}$ =0 , and I have

$$-\frac{f_n}{\Delta\xi}\left\{\left[1-m^2-m^2(\gamma+1)f\phi_\xi\right]fg_\xi\right\}_{n-1/2,\ell} + h(hg_\eta)_\eta = 0$$

which is expressed as

$$-a_2\left[\frac{g^+_{n,\ell}}{\omega} + \left(1-\frac{1}{\omega}\right)g_{n,\ell} - g^+_{n-1,\ell}\right] + \frac{h_\ell}{\Delta\eta^2}\left[h_{\ell+1/2}(g_{n,\ell+1}-g_{n,\ell})\right.$$

$$\left. - h_{\ell-1/2}(g_{n,\ell}-g_{n,\ell-1})\right] = 0 \tag{C.47}$$

The tridiagonal coefficients are

$$A_d = \frac{h_\ell h_{\ell-1/2}}{\Delta\eta^2} \tag{C.48}$$

$$B_d = \frac{h_\ell (h_{\ell-1/2} + h_{\ell+1/2})}{\Delta\eta^2} + \frac{d_2}{\omega} \tag{C.49}$$

$$C_d = \frac{h_\ell h_{\ell+1/2}}{\Delta\eta^2} \tag{C.50}$$

$$D_d = d\left[g^+_{n-1,\ell} - \left(1-\frac{1}{\omega}\right) g_{n,\ell}\right] \tag{C.51}$$

where the d subscript denotes quantities at the downstream boundary. If the flow is nonlifting, at n=N-1, ℓ =up the coefficients are

$$A = 0 \tag{C.52}$$

$$B = B_d - \frac{h_{up} h_{up-1/2}}{\Delta\eta^2} \tag{C.53}$$

$$C = C_d \tag{C.54}$$

$$D = D_d \tag{C.55}$$

When $x(\xi) > \frac{c}{2}$ and ℓ =up

$$h(hg_\eta)_\eta = h_{up}\left[h_{up+1/2}\left(g^+_{n,up+1} - g^+_{n,up}\right) - h_{up-1/2}\left(g^+_{n,up} - g^+_{n,up-1} - \Delta\bar{g}^+\right)\right]$$

and the tridiagonal coefficients are

$$A_{up} = A_i \tag{C.56}$$

$$B_{up} = B_i \tag{C.57}$$

$$C_{up} = C_i \tag{C.58}$$

$$D_{up} = D_i + \frac{h_{up} h_{up-1/2}}{\Delta\eta^2} \Delta\tilde{g}^+ \tag{C.59}$$

At the point n=N-1, ℓ =up

$$A = A_d \tag{C.60}$$

$$B = B_d \tag{C.61}$$

$$C = C_d \tag{C.62}$$

$$D = D_d + \frac{h_{up} h_{up-1/2}}{\Delta\eta^2} \Delta\tilde{g}^+ \tag{C.63}$$

Similarly, along ℓ=low downstream of the trailing edge

$$h(hg_\eta)_\eta = \frac{h_{low}}{\Delta\eta^2}\left[h_{low+1/2}\left(g^+_{n,low+1} - g^+_{n,low} - \Delta\tilde{g}^+\right) - h_{low-1/2}\left(g^+_{n,low} - g^+_{n,low-1}\right)\right]$$

and

$$A_{low} = A_i \tag{C.64}$$

$$B_{low} = B_i \tag{C.65}$$

$$C_{low} = C_i \tag{C.66}$$

$$D_{low} = D_i - \frac{h_{low}}{\Delta\eta^2} h_{low+1/2}\, \Delta\tilde{g}^+ \tag{C.67}$$

and at n=N-1, ℓ=low

$$A = A_d \tag{C.68}$$

$$B = B_d \tag{C.69}$$

$$C = C_d \tag{C.70}$$

$$D = D_d - \frac{h_{low}}{\Delta\eta^2} h_{low+1/2}\, \Delta\tilde{g}^+ \tag{C.71}$$

The tridiagonal coefficients developed in (C.22)-(C.21) are introduced into (G.1), and the solution procedure outlined in Appendix G is employed.

Since the airfoil does not lie on a grid row, a second order extrapolation procedure is used to determine the value of g on the airfoil boundaries and, subsequently, the jump in g across the airfoil. Expanding in a Taylor series, g on the upper boundary, g^u_n, expressed as

$$q_n^w = q_{n,vp} - \frac{\Delta\eta}{2}(q_\eta)_{n,vp} + \frac{\Delta\eta^2}{8}(q_{\eta\eta})_{n,vp} - O(\Delta\eta^3) \tag{C.72}$$

I then determine a second order difference approximation of $(q_\eta)_{n,vp}$ by writing the expansion for $q_{n,vp+1}$

$$q_{n,vp+1} = q_{n,vp} + \Delta\eta(q_\eta)_{n,vp} + \frac{\Delta\eta^2}{2}(q_{\eta\eta})_{n,vp} + O(\Delta\eta^3) \tag{C.73}$$

Eliminating $(q_{\eta\eta})_{n,vp}$ from (C.72) and (C.73), I obtain

$$(q_\eta)_{n,vp} = \frac{1}{3\Delta\eta}(q_{n,vp+1} - 4q_n^w) + \frac{q_{n,vp}}{\Delta\eta} \tag{C.74}$$

The second derivative, $(q_{\eta\eta})_{n,vp}$, is expressed as

$$(q_{\eta\eta})_{n,vp} = \frac{1}{\Delta\eta}\left[(q_\eta)_{n,vp+1/2} - (q_\eta)_{n,vp-1/2}\right]$$

or

$$(q_{\eta\eta})_{n,vp} = \frac{1}{\Delta\eta}\left[\frac{q_{n,vp+1} - q_{n,vp}}{\Delta\eta} - (q_\eta^w)_n\right] \tag{C.75}$$

where q_η^w is prescribed from the tangency condition. Combining (C.72)-(C.75), I get

$$g_n^u = \frac{9}{8} g_{n,up} - \frac{1}{8} g_{n,up+1} - \frac{3}{8} \Delta\eta (g_\eta^u)_n \tag{C.76}$$

Similarly, on the lower boundary

$$g_n^l = g_{n,low} + \frac{\Delta\eta}{2} (g_\eta)_{n,low} + \frac{\Delta\eta^2}{8} (g_{\eta\eta})_{n,low} + O(\Delta\eta^3) \tag{C.77}$$

A second order approximation of $(g_\eta)_{n,low}$ is obtained from (C.77) and the Taylor expansion

$$g_{n,low-1} = g_{n,low} - \Delta\eta (g_\eta)_{n,low} + \frac{\Delta\eta^2}{2} (g_{\eta\eta})_{n,low} - O(\Delta\eta^3) \tag{C.78}$$

Elimination of $(g_{\eta\eta})_{n,low}$ from (C.77) and (C.78) then yields

$$(g_\eta)_{n,low} = \frac{1}{3\Delta\eta} (4 g_n^l - g_{n,low-1}) - \frac{g_{n,low}}{\Delta\eta} \tag{C.79}$$

Similar to the above procedure, I express $(g_{\eta\eta})_{n,low}$ as

$$(g_{\eta\eta})_{n,low} = \frac{1}{\Delta\eta} \left[(g_\eta^l)_n - \frac{g_{n,low} - g_{n,low-1}}{\Delta\eta} \right] \tag{C.80}$$

Introducing (C.79) and (C.80) into (C.77), the lower boundary

value of g becomes

$$g_n^L = \frac{9}{8} g_{n,low} - \frac{1}{8} g_{n,low-1} + \frac{3}{8} \Delta\eta (g_\eta^L)_n \tag{C.81}$$

Defining Δg_n as $g_n^U - g_n^L$, I use (C.76) and (C.81) to arrive at

$$\Delta g_n = \frac{9}{8} (g_{n,up} - g_{n,low}) - \frac{1}{8} (g_{n,up+1} - g_{n,low-1}) - \frac{3}{8} \Delta\eta \left[(g_\eta^U)_n - (g_\eta^L)_n \right] \tag{C.82}$$

Because a grid column generally does not intersect the trailing edge, a first order extrapolation is used to define the jump in g at the trailing edge. I use the following Taylor expansion to express Δg_T

$$\Delta g_T = \Delta g_{-T1} + \Delta\xi_T (\Delta g_\xi)_{-T1} + O(\Delta\xi_T^2) \tag{C.83}$$

A backward difference representation of $(\Delta g_\xi)_{-T1}$ is developed from the series

$$\Delta g_{-T2} = \Delta g_{-T1} - \Delta\xi (\Delta g_\xi)_{-T1} + \frac{\Delta\xi^2}{2} (\Delta g_{\xi\xi})_{-T1} - O(\Delta\xi^3) \tag{C.84}$$

$$\Delta g_{-T3} = \Delta g_{-T1} - 2\Delta\xi (\Delta g_\xi)_{-T1} + 2\Delta\xi^2 (\Delta g_{\xi\xi})_{-T1} - O(\Delta\xi^3) \tag{C.85}$$

Eliminating $(g_{\xi\xi})_{-T1}$ from (C.84) and (C.85), I arrive at the approximation of $(\Delta g_\xi)_{-T1}$

$$(\Delta g_\xi)_{-T1} = \frac{3\Delta g_{-T1} - 4\Delta g_{-T2} + \Delta g_{-T3}}{2\Delta\xi} \tag{C.86}$$

which when combined with (C.83) yields

$$\Delta g_T = \left(1+\frac{3}{2}\frac{\Delta\xi_T}{\Delta\xi}\right)\Delta g_{-T1} - 2\frac{\Delta\xi_T}{\Delta\xi}\Delta g_{-T2} + \frac{\Delta\xi_T}{2\Delta\xi}\Delta g_{-T3} \qquad \text{(C.87)}$$

APPENDIX D

FINITE DIFFERENCE EQUATIONS FOR THE UNSTEADY PERTUBATIONS

In this appendix, I develop the finite difference equations used to calculate the unsteady component of the flow field. Here I also use the concept of conservative type dependent differencing. Equation (5.1) is then written as

$$\nabla\cdot\left|\frac{1}{h}\left\{\left[1-m^2-m^2(\gamma+1)f\phi_\xi\right]f\varphi_\xi-2ikm^2\varphi\right\}\hat{i}+\frac{h}{f}\varphi_\eta\,\hat{k}\right|$$

$$+\frac{m^2}{hf}\left[k^2-ik(\gamma-1)f(f\phi_\xi)_\xi\right]\varphi$$

$$=\nabla\cdot(\bar{a}\hat{i}+\bar{b}\hat{k})+g\varphi=0 \qquad (D.1)$$

Integration of (D.1) over the shaded area of Figure 4.5 and division by that area yields

$$\frac{\bar{a}_{n+1/2,\ell}-\bar{a}_{n-1/2,\ell}}{\Delta\xi}+\frac{\bar{b}_{n,\ell+1/2}-\bar{b}_{n,\ell-1/2}}{\Delta\eta}+g_{n,\ell}\varphi_{n,\ell}=0 \qquad (D.2)$$

The fluxes are represented as

$$\bar{a}_{n+1/2}=\left(1-\frac{u_{n,\ell}}{h}\right)\left\{\left[1-m^2-m^2(\gamma+1)f\phi_\xi\right]f\varphi_\xi-2ikm^2\varphi\right\}_{n+1/2,\ell}$$

$$+\frac{u_{n,\ell}}{h}\left\{\left[1-m^2-m^2(\gamma+1)f\phi_\xi\right]f\varphi_\xi-2ikm^2\varphi\right\}_{n-1/2,\ell} \qquad (D.3)$$

$$\bar{a}_{n-1/2,\ell} = \left(\frac{1-u_{n-1,\ell}}{h}\right)\left\{\left[1-m^2-m^2(\gamma+1)f\phi_\xi\right]f\varphi_\xi - 2ikm^2\varphi\right\}_{n-1/2,\ell}$$

$$+\frac{u_{n-1,\ell}}{h}\left\{\left[1-m^2-m^2(\gamma+1)f\phi_\xi\right]f\varphi_\xi - 2ikm^2\varphi\right\}_{n-3/2,\ell} \qquad (D.4)$$

$$\bar{b}_{n,\ell+1/2} = \left(\frac{h}{f}\varphi_\eta\right)_{n,\ell+1/2} \qquad (D.5)$$

$$\bar{b}_{n,\ell-1/2} = \left(\frac{h}{f}\varphi_\eta\right)_{n,\ell-1/2} \qquad (D.6)$$

The coefficient of the source term is also evaluated using type dependent differences and becomes

$$g_{n,\ell} = (1-u_{n,\ell})\frac{m^2}{h_\ell f_n}\left\{k^2 - ik(\gamma-1)f_n\left[(f\phi_\xi)_{n+1/2,\ell} - (f\phi_\xi)_{n-1/2,\ell}\right]\right\}$$

$$+u_{n,\ell}\frac{m^2}{h_\ell f_n}\left\{k^2 - ik(\gamma-1)f_n\left[(f\phi_\xi)_{n-1/2,\ell} - (f\phi_\xi)_{n-3/2,\ell}\right]\right\} \qquad (D.7)$$

Substituting (D.3)-(D.7) into (D.2), I obtain the conservative difference approximation of (5.1)

$$(1-u_{n,\ell})\frac{f_n}{\Delta\xi}\left|\left\{\left[1-m^2-m^2(\gamma+1)f\phi_\xi\right]f\varphi_\xi - 2ikm^2\varphi\right\}_{n+1/2,\ell} - \left\{\left[1-m^2-m^2(\gamma+1)f\phi_\xi\right]f\varphi_\xi\right.\right.$$

$$\left.\left. - 2ikm^2\varphi\right\}_{n-1/2,\ell}\right| + u_{n-1,\ell}\frac{f_n}{\Delta\xi}\left|\left\{\left[1-m^2-m^2(\gamma+1)f\phi_\xi\right]f\varphi_\xi - 2ikm^2\varphi\right\}_{n-1/2,\ell}\right.$$

$$\left. - \left\{\left[1-m^2-m^2(\gamma+1)f\phi_\xi\right]f\varphi_\xi - 2ikm^2\varphi\right\}_{n-3/2,\ell}\right| + \frac{h_\ell}{\Delta\eta}\left[(h\varphi_\eta)_{n,\ell+1/2} - (h\varphi_\eta)_{n,\ell-1/2}\right]$$

$$+m^2(1-u_{n,\ell})\left\{k^2 - ik(\gamma-1)\frac{f_n}{\Delta\xi}\left[(f\phi_\xi)_{n+1/2,\ell} - (f\phi_\xi)_{n-1/2,\ell}\right]\right\}\varphi_{n,\ell}$$

$$+m^2u_{n,\ell}\left\{k^2 - ik(\gamma-1)\frac{f_n}{\Delta\xi}\left[(f\phi_\xi)_{n-1/2,\ell} - (f\phi_\xi)_{n-3/2,\ell}\right]\right\}\varphi_{n,\ell} = 0 \qquad (D.8)$$

Using centered differences to evaluate each term in (D.8), and evaluating quantities midway between grid lines as

$$\varphi_{n\pm1/2,\ell} = \frac{\varphi_{n,\ell} + \varphi_{n\mp1,\ell}}{2}$$

I obtain the finite difference equation

$$(1-\mu_{n,\ell}) f_n \left\{ \frac{f_{n+1/2}}{\Delta\xi^2}\left[1-m^2-m^2(\gamma+1)\frac{f_{n+1/2}}{\Delta\xi}(\phi_{n+1,\ell}-\phi_{n,\ell})\right](\tilde\varphi_{n+1,\ell}-\tilde\varphi_{n,\ell}) \right.$$

$$\left. -\frac{f_{n-1/2}}{\Delta\xi^2}\left[1-m^2-m^2(\gamma+1)\frac{f_{n-1/2}}{\Delta\xi}(\phi_{n,\ell}-\phi_{n-1,\ell})\right](\tilde\varphi_{n,\ell}-\tilde\varphi_{n-1,\ell}) - \frac{ikm^2}{\Delta\xi}(\tilde\varphi_{n+1,\ell}-\tilde\varphi_{n-1,\ell})\right\}$$

$$+\mu_{n-1,\ell} f_n \left\{ \frac{f_{n-1/2}}{\Delta\xi^2}\left[1-m^2-m^2(\gamma+1)\frac{f_{n-1/2}}{\Delta\xi}(\phi_{n,\ell}-\phi_{n-1,\ell})\right](\tilde\varphi_{n,\ell}-\tilde\varphi_{n-1,\ell}) \right.$$

$$\left. -\frac{f_{n-3/2}}{\Delta\xi^2}\left[1-m^2-m^2(\gamma+1)\frac{f_{n-3/2}}{\Delta\xi}(\phi_{n-1,\ell}-\phi_{n-2,\ell})\right](\tilde\varphi_{n-1,\ell}-\tilde\varphi_{n-2,\ell}) - \frac{ikm^2}{\Delta\xi}(\tilde\varphi_{n,\ell}-\tilde\varphi_{n-2,\ell})\right\}$$

$$+\frac{h_\ell}{\Delta\eta^2}\left[h_{\ell+1/2}(\tilde\varphi_{n,\ell+1}-\tilde\varphi_{n,\ell}) - h_{\ell-1/2}(\tilde\varphi_{n,\ell}-\tilde\varphi_{n,\ell-1})\right]$$

$$+m^2(1-\mu_{n,\ell})\left\{k^2 - ik(\gamma-1)\frac{f_n}{\Delta\xi^2}\left[f_{n+1/2}(\phi_{n+1,\ell}-\phi_{n,\ell}) - f_{n-1/2}(\phi_{n,\ell}-\phi_{n-1,\ell})\right]\right\}\tilde\varphi_{n,\ell}$$

$$+m^2\mu_{n,\ell}\left\{k^2 - ik(\gamma-1)\frac{f_n}{\Delta\xi^2}\left[f_{n-1/2}(\phi_{n,\ell}-\phi_{n-1,\ell}) - f_{n-3/2}(\phi_{n-1,\ell}-\phi_{n-2,\ell})\right]\right\}\tilde\varphi_{n,\ell} = 0 \tag{D.9}$$

In subsonic regions, current values of $\varphi_{n-1,\ell}$ and previous values of $\varphi_{n+1,\ell}$ are used to evaluate derivatives in the ξ direction. At the midpoint and in the source term, I use the combination

$$\tilde\varphi_{n,\ell} = \frac{\varphi^+_{n,\ell}}{\omega} + \left(1-\frac{1}{\omega}\right)\varphi_{n,\ell}$$

In supersonic flow regions, streamwise derivatives and the source term are evaluated with previous data, and, at all points, derivatives in the η direction are evaluated using current information. Using the definitions of α_1, α_2 and α_3 from (C.10)-(C.12) and defining α_4 and α_5 as

$$\alpha_4 = m^2\left\{k^2 - ik(\gamma-1)\frac{f_n}{\Delta\xi^2}\left[f_{n+1/2}(\phi_{n+1,\ell}-\phi_{n,\ell}) - f_{n-1/2}(\phi_{n,\ell}-\phi_{n-1,\ell})\right]\right\} \quad (D.10)$$

$$\alpha_5 = m^2\left\{k^2 - ik(\gamma-1)\frac{f_n}{\Delta\xi^2}\left[f_{n-1/2}(\phi_{n,\ell}-\phi_{n-1,\ell}) - f_{n-3/2}(\phi_{n-1,\ell}-\phi_{n-2,\ell})\right]\right\} \quad (D.11)$$

the finite difference representation of (5.1) becomes

$$(1-\mu_{n,\ell})\left\{\alpha_1\left[\varphi_{n+1,\ell} - \frac{\varphi^+_{n,\ell}}{\omega} - \left(1-\frac{1}{\omega}\right)\varphi_{n,\ell}\right] - \alpha_2\left[\frac{\varphi^+_{n,\ell}}{\omega} + \left(1-\frac{1}{\omega}\right) - \varphi^+_{n-1,\ell}\right]\right.$$

$$\left. - i\frac{km^2}{\Delta\xi}f_n(\varphi_{n+1,\ell} - \varphi^+_{n-1,\ell}) + \alpha_4\left[\frac{\varphi^+_{n,\ell}}{\omega} + \left(1-\frac{1}{\omega}\right)\varphi_{n,\ell}\right]\right\} +$$

$$+\mu_{n-1,\ell}\left[\alpha_2(\varphi_{n,\ell} - \varphi_{n-1,\ell}) - \alpha_3(\varphi_{n-1,\ell} - \varphi_{n-2,\ell}) - i\frac{km^2}{\Delta\xi}f_n(\varphi_{n,\ell} - \varphi_{n-2,\ell})\right]$$

$$+\mu_{n,\ell}\alpha_5\varphi_{n,\ell} + \frac{h_\ell}{\Delta\eta^2}\left[h_{\ell+1/2}(\varphi^+_{n,\ell+1} - \varphi^+_{n,\ell}) - h_{\ell-1/2}(\varphi^+_{n,\ell} - \varphi^+_{n,\ell-1})\right] = 0 \quad (D.12)$$

Isolation of the timelike terms in subsonic regions yields

$$f\left\{\left[1-m^2-m^2(\gamma+1)f\phi_\xi\right]f\varphi_\xi - 2ikm^2\varphi\right\}_\xi + h(h\varphi_\eta)_\eta$$

$$+m^2\left[k^2 - ik(\gamma-1)f(f\phi_\xi)_\xi\right]\varphi + \left[\alpha_2 - (\alpha_1+\alpha_2) + i\frac{km^2}{\Delta\xi}f_n + \frac{\alpha_4}{\omega}\right]\Delta t\varphi_t$$

$$-\left(\alpha_2 - \frac{ikm^2 f_n}{\Delta\xi}\right)\Delta t\,\Delta\xi\, q_{\xi t} = 0 \tag{D.13}$$

and in supersonic regions, I have

$$f\left\{\left[1-m^2-m^2(\gamma+1)f\phi_\xi\right]f\varphi_\xi - 2ikm^2\varphi\right\}_\xi + h(h\varphi_\eta)_\eta$$

$$+m^2\left[k^2 - ik(\gamma-1)f(f\phi_\xi)_\xi\right]\varphi = 0 \tag{D.14}$$

Adding the term $-\epsilon^* u^* f \frac{\Delta t}{\Delta\xi} q_{\xi t}$ to (D.14) and introducing the coordinate

$$\tau^* = t - \frac{\epsilon^*}{2}\frac{\Delta t}{\Delta\xi}$$

I obtain the canonical form

$$f\left\{\left[1-m^2-m^2(\gamma+1)f\phi_\xi\right]f\varphi_\xi - 2ikm^2\varphi\right\}_\xi + h(h\varphi_\eta)_\eta$$

$$+ m^2\left[k^2 - ik(\gamma-1)f(f\phi_\xi)_\xi\right]\varphi - \frac{\epsilon^{*2}}{4}\frac{\Delta t^2}{\Delta\xi^2}f^2\left[1-m^2-m^2(\gamma+1)f\phi_\xi\right]\varphi_{\tau^*\tau^*}$$

$$+ \text{lower derivatives} = 0 \tag{D.15}$$

Again, this assures that in supersonic regions, ξ will be the time-like direction in the unsteady problem. In practice, I add to (D.14) the term $-\epsilon^* f_n f_{n-1/2}\frac{\Delta t}{\Delta\xi}\varphi_{\xi t}$ and choose ϵ^* such that the

the resulting equation has the desired properties. At interior points, the final form of the finite difference equations for the unsteady potential is

$$(1-\mu_{n,\ell})\left\{\alpha_1\left[\varphi_{n+1,\ell}-\frac{\varphi^+_{n,\ell}}{\omega}-\left(1-\frac{1}{\omega}\right)\varphi_{n,\ell}\right]-\alpha_2\left[\frac{\varphi^+_{n,\ell}}{\omega}+\left(1-\frac{1}{\omega}\right)\varphi_{n,\ell}-\varphi^+_{n-1,\ell}\right]\right.$$

$$\left.-\frac{ik\epsilon m^2 f_n}{\Delta\xi}\left(\varphi_{n+1,\ell}-\varphi^+_{n-1,\ell}\right)+\alpha_4\left[\frac{\varphi^+_{n,\ell}}{\omega}+\left(1-\frac{1}{\omega}\right)\varphi_{n,\ell}\right]\right\}+$$

$$+\mu_{n-1,\ell}\left[\alpha_2\left(\varphi_{n,\ell}-\varphi_{n-1,\ell}\right)-\alpha_3\left(\varphi_{n-1,\ell}-\varphi_{n-2,\ell}\right)-\frac{ik\epsilon m^2 f_n}{\Delta\xi}\left(\varphi_{n,\ell}-\varphi_{n-2,\ell}\right)\right]$$

$$+\mu_{n,\ell}\alpha_5\varphi_{n,\ell}+\frac{h_\ell}{\Delta\eta^2}\left[h_{\ell+1/2}\left(\varphi^+_{n,\ell+1}-\varphi^+_{n,\ell}\right)-h_{\ell-1/2}\left(\varphi^+_{n,\ell}-\varphi^+_{n,\ell-1}\right)\right]$$

$$-\mu_{n,\ell}\epsilon^2\frac{f_n f_{n-1/2}}{\Delta\xi^2}\left(\varphi^+_{n,\ell}-\varphi_{n,\ell}-\varphi^+_{n-1,\ell}+\varphi_{n-1,\ell}\right)=0 \qquad \text{(D.16)}$$

Writing (D.16) in the form

$$-\frac{h_\ell h_{\ell-1/2}}{\Delta\eta^2}\varphi^+_{n,\ell-1}+\left[\frac{h_\ell}{\Delta\eta^2}\left(h_{\ell+1/2}+h_{\ell-1/2}\right)+(1-\mu_{n,\ell})\frac{(\alpha_1+\alpha_2-\alpha_4)}{\omega}+\mu_{n,\ell}\epsilon^2\frac{f_n f_{n-1/2}}{\Delta\xi^2}\right]\varphi^+_{n,\ell}$$

$$-\frac{h_\ell h_{\ell+1/2}}{\Delta\eta^2}\varphi^+_{n,\ell+1}=(1-\mu_{n,\ell})\left(\alpha_1-\frac{ik\epsilon m^2 f_n}{\Delta\xi}\right)\varphi_{n+1,\ell}$$

$$-\left[(1-\mu_{n,\ell})(\alpha_1+\alpha_2-\alpha_4)\left(1-\frac{1}{\omega}\right)-\mu_{n,\ell}\left(\alpha_5+\epsilon^2\frac{f_n f_{n-1/2}}{\Delta\xi^2}\right)-\mu_{n-1,\ell}\left(\alpha_2-\frac{ik\epsilon m^2 f_n}{\Delta\xi}\right)\right]\varphi_{n,\ell}$$

$$+\left[(1-\mu_{n,\ell})\left(\alpha_2+\frac{ik\epsilon m^2 f_n}{\Delta\xi}\right)+\mu_{n,\ell}\epsilon^2\frac{f_n f_{n-1/2}}{\Delta\xi^2}\right]\varphi^+_{n-1,\ell}$$

$$-\left[\mu_{n-1,\ell}(\alpha_2+\alpha_3)+\mu_{n,\ell}\epsilon^2\frac{f_n f_{n-1/2}}{\Delta\xi^2}\right]\varphi_{n-1,\ell}+\mu_{n-1,\ell}\left(\alpha_3+\frac{ik\epsilon m^2 f_n}{\Delta\xi}\right)\varphi_{n-2,\ell} \qquad \text{(D.17)}$$

shows that

$$A_i = \frac{h_\ell h_{\ell-1/2}}{\Delta\eta^2} \tag{D.18}$$

$$B_i = \frac{h_\ell (h_{\ell+1/2} + h_{\ell-1/2})}{\Delta\eta^2} + (1-\alpha_{m,\ell})\frac{(d_1+d_2-d_4)}{\omega} + \alpha_{m,\ell}\epsilon^2 f_m \frac{f_{m-1/2}}{\Delta\xi^2} \tag{D.19}$$

$$C_i = \frac{h_\ell h_{\ell+1/2}}{\Delta\eta^2} \tag{D.20}$$

$$D_i = (1-\alpha_{m,\ell})\left(d_1 - \frac{ik\epsilon m^2 f_m}{\Delta\xi}\right)\varphi_{m+1,\ell} + \left[(1-\alpha_{m,\ell})\left(d_2 + \frac{ik\epsilon m^2 f_m}{\Delta\xi}\right) + \alpha_{m,\ell}\epsilon^2 f_m \frac{f_{m-1/2}}{\Delta\xi^2}\right]\varphi^+_{m-1,\ell}$$

$$-\left[(1-\alpha_{m,\ell})(d_1+d_2-d_4)\left(1-\frac{1}{\omega}\right) - \alpha_{m,\ell}\left(d_5 + \epsilon^2 f_m \frac{f_{m-1/2}}{\Delta\xi^2}\right) - \alpha_{m-1,\ell}\left(d_2 - \frac{ik\epsilon m^2 f_m}{\Delta\xi}\right)\right]\varphi_{m,\ell}$$

$$-\left[\alpha_{m-1,\ell}(d_2+d_3) + \alpha_{m,\ell}\epsilon^2 f_m \frac{f_{m-1/2}}{\Delta\xi^2}\right]\varphi_{m-1,\ell} + \alpha_{m-1,\ell}\left(d_3 + \frac{ik\epsilon m^2 f_m}{\Delta\xi^2}\right)\varphi_{m-2,\ell} \tag{D.21}$$

When $|X(\xi)| \le \frac{c}{2}$ and ℓ =up $(h\varphi_m)_{m,\ell-1/2}$ is specified from the the tangency condition, and the tridiagonal coefficients become

$$A_{up} = 0 \tag{D.22}$$

$$B_{up} = B_i - \frac{h_{up} h_{up-1/2}}{\Delta\eta^2} \tag{D.23}$$

$$C_{up} = C_i \tag{D.24}$$

$$D_{up} = D_i - \frac{h_{up}(h\varphi_m)_{m,\ell-1/2}}{\Delta\eta} \tag{D.25}$$

Similarly, when $|X(\xi)| \le \frac{c}{2}$ and ℓ =low, $(h\varphi_m)_{m,\ell+1/2}$ is prescribed

and the coefficients are

$$A_{low} = A_i \tag{D.26}$$

$$B_{low} = B_i - \frac{h_{low}}{\Delta\eta^2} h_{low+1/2} \tag{D.27}$$

$$C_{low} = 0 \tag{D.28}$$

$$D_{low} = D_i + \frac{h_{low}}{\Delta\eta} (h\varphi_\eta)_{n,low+1/2} \tag{D.29}$$

If Klunker type boundary conditions are used, I have on the upstream and downstream boundaries

$$f\varphi_\xi + ik\varphi = P \tag{D.30}$$

Along n= NMIN+1, this condition is incorporated directly into the difference equations by approximating (D.30) as

$$\frac{f_n}{\Delta\xi}(\varphi_{n,\ell} - \varphi_{n-1,\ell}) + \frac{ik}{2}(\varphi_{n,\ell} + \varphi_{n-1,\ell}) = P$$

I then obtain the relation

$$\varphi_{NMIN,\ell} = \alpha_6 \varphi_{NMIN+1,\ell} - \alpha_7 P \tag{D.31}$$

where

$$\alpha_6 \equiv \frac{4f_{n-1/2}^2 - k^2\Delta\xi^2 + 4ikf_{n-1/2}\Delta\xi}{4f_{n-1/2}^2 + k^2\Delta\xi^2} \tag{D.32}$$

$$\alpha_7 \equiv 2\Delta\xi\left(\frac{2f_{n-1/2} + ik\Delta\xi}{4f_{n-1/2}^2 + k^2\Delta\xi^2}\right) \tag{D.33}$$

Substituting (D.31) for $\varphi_{n-1,\ell}$ in (D.16) and assuming subsonic free stream velocity, the tridiagonal coefficients become

$$A_u = \frac{h_\ell h_{\ell-1/2}}{\Delta\eta^2} \tag{D.34}$$

$$B_u = \frac{h_\ell}{\Delta\eta^2}(h_{\ell+1/2} + h_{\ell-1/2}) + \frac{(\alpha_1 + \alpha_2 - \alpha_4)}{\omega} - \alpha_6\left(\alpha_2 + i\frac{km^2 f_n}{\Delta\xi}\right) \tag{D.35}$$

$$C_u = \frac{h_\ell h_{\ell+1/2}}{\Delta\eta^2} \tag{D.36}$$

$$D_u = \left(\alpha_1 - i\frac{km^2 f_n}{\Delta\xi}\right)\varphi_{n+1,\ell} - (\alpha_1 + \alpha_2 - \alpha_4)\left(1 - \frac{1}{\omega}\right)\varphi_{n,\ell} - \alpha_7\left(\alpha_2 + i\frac{km^2 f_n}{\Delta\xi}\right)P \tag{D.37}$$

Similarly, along n = NMAX-1,

$$\varphi_{NMAX,\ell} = \alpha_8\,\varphi_{NMAX-1,\ell} - \alpha_9\,P \tag{D.38}$$

where

$$\alpha_8 \equiv \frac{4f_{n+1/2}^2 - k^2\Delta\xi^2 - 4ikf_{n+1/2}\Delta\xi}{4f_{n+1/2}^2 + k^2\Delta\xi^2}$$

$$\alpha_9 \equiv 2\Delta\xi\left(\frac{2f_{n+1/2} - ik\Delta\xi}{4f_{n+1/2}^2 + k^2\Delta\xi^2}\right)$$

Combining (D.38) and (D.16), I obtain

$$A_d = \frac{h_\ell h_{\ell-1/2}}{\Delta\eta^2} \tag{D.39}$$

$$B_d = \frac{h_\ell}{\Delta\eta^2}\left(h_{\ell+1/2} + h_{\ell-1/2}\right) + \frac{\alpha_1 + \alpha_2 - \alpha_4}{\omega} \tag{D.40}$$

$$C_d = \frac{h_\ell h_{\ell+1/2}}{\Delta\eta^2} \tag{D.41}$$

$$D_d = -\left[(\alpha_1 + \alpha_2 - \alpha_4)\left(1 - \frac{1}{\omega}\right) - \alpha_3\left(\alpha_1 - i\frac{km^2 f_n}{\Delta\xi}\right)\right]\varphi_{n,\ell} + \left(\alpha_2 + i\frac{km^2 f_n}{\Delta\xi}\right)\varphi^+_{n-1,\ell}$$

$$- \alpha_4\left(\alpha_1 - i\frac{km^2 f_n}{\Delta\xi}\right)P \tag{D.42}$$

At ℓ =LMAX-1, $\varphi_{n,\ell+1}$ is prescribed, and

$$A = A_{\ell,u,d} \tag{D.43}$$

$$B = B_{\ell,u,d} \tag{D.44}$$

$$C = 0 \tag{D.45}$$

$$D = D_{\ell,u,d} + \frac{h_\ell}{\Delta\eta^2} h_{\ell+1/2}\, \varphi^+_{n,\ell max} \tag{D.46}$$

and at ℓ= LMIN+1, $\varphi_{n,\ell min}$ is prescribed from the boundary condition,

hence,

$$A = 0 \tag{D.47}$$

$$B = B_{i,u,d} \tag{D.48}$$

$$C = C_{i,u,d} \tag{D.49}$$

$$D = D_{i,u,d} + \frac{h_\ell}{\Delta\eta^2} h_{\ell-1/2}\, \varphi^+_{n,\ell max} \tag{D.50}$$

If the radiation conditions are used in the far field, at n= NMIN+1,

$$\varphi_{NMIN,\ell} = \alpha_6\, \varphi_{NMIN+1,\ell}$$

where

$$\alpha_6 \equiv \frac{1 - \left[\frac{km\Delta\xi}{2f_{n-1/2}(1-m)}\right]^2 - \frac{ikm\Delta\xi}{f_{n-1/2}(1-m)}}{1 + \left[\frac{km\Delta\xi}{2f_{n-1/2}(1-m)}\right]^2}$$

and

$$A_u = \frac{h_\ell}{\Delta\eta^2} h_{\ell-1/2} \tag{D.51}$$

$$B_u = \frac{h_\ell}{\Delta\eta^2}(h_{\ell+1/2} + h_{\ell-1/2}) + \left(\frac{d_1 + d_2 - d_4}{\omega}\right) \tag{D.52}$$

$$C_u = \frac{h_\ell h_{\ell+1/2}}{\Delta\eta^2} \tag{D.53}$$

$$D_u = \left(\alpha_1 - i\frac{km^2 f_n}{\Delta\xi}\right)\varphi_{n+1,\ell} - (\alpha_1 + \alpha_2 - \alpha_4)\left(1 - \frac{1}{\omega}\right)\varphi_{n,\ell} \tag{D.54}$$

At n= NMAX-1,

$$\varphi_{NMAX,\ell} = \alpha_7\, \varphi_{NMAX-1,\ell}$$

where

$$\alpha_7 \equiv \frac{1 - \left[\frac{km\Delta\xi}{2f_{n+1/2}(1+m)}\right]^2 - \frac{ikm\Delta\xi}{f_{n+1/2}(1+m)}}{1 + \left[\frac{km\Delta\xi}{2f_{n+1/2}(1+m)}\right]^2}$$

and the tridiagonal coefficients are

$$A_d = \frac{h_\ell}{\Delta\eta^2} h_{\ell-1/2} \tag{D.55}$$

$$B_d = \frac{h_\ell}{\Delta\eta^2}(h_{\ell+1/2} + h_{\ell-1/2}) + \frac{(\alpha_1 + \alpha_2 - \alpha_4)}{\omega} \tag{D.56}$$

$$C_d = \frac{h_\ell}{\Delta\eta^2} h_{\ell+1/2} \tag{D.57}$$

$$D_d = \left(\alpha_2 + i\frac{km^2 f_n}{\Delta\xi}\right)\varphi^+_{n-1,\ell} + \left[\alpha_7\left(\alpha_1 - i\frac{km^2 f_n}{\Delta\xi}\right) - (\alpha_1 + \alpha_2 - \alpha_4)\left(1 - \frac{1}{\omega}\right)\right]\varphi_{n,\ell} \tag{D.58}$$

Adjacent to the upper boundary, ℓ= LMAX-1, the difference form of (E.15) is

$$\varphi_{n,LMAX} = \alpha_8\, \varphi_{n,LMAX-1}$$

with

$$\alpha_8 \equiv \frac{1 - \left(\frac{km\Delta\eta}{2\beta h_{\ell+1/2}}\right)^2 - i\frac{km\Delta\eta}{\beta h_{\ell+1/2}}}{1 + \left(\frac{km\Delta\eta}{2\beta h_{\ell+1/2}}\right)^2}$$

The tridiagonal coefficients are then

$$A = A_{c,u,d} \tag{D.59}$$

$$B = B_{c,u,d} \tag{D.60}$$

$$C = 0 \tag{D.61}$$

$$D = D_{c,u,d} + \alpha_8 \frac{h_\ell h_{\ell+1/2}}{4\eta^2} \varphi_{n,\ell} \tag{D.62}$$

Adjacent to the lower boundary, ℓ = LMIN+1,

$$\varphi_{n,LMIN} = \alpha_9 \varphi_{n,LMIN+1}$$

with

$$\alpha_9 \equiv \frac{1 - \left(\frac{km\Delta\eta}{2\beta h_{\ell-1/2}}\right)^2 - i\frac{km\Delta\eta}{\beta h_{\ell-1/2}}}{1 + \left(\frac{km\Delta\eta}{2\beta h_{\ell-1/2}}\right)^2}$$

and the coefficients are

$$A = 0 \tag{D.63}$$

$$B = B_{i,u,d} \tag{D.64}$$

$$C = C_{i,u,d} \tag{D.65}$$

$$D = D_{i,u,d} + \frac{h_\ell}{\Delta y^2} h_{\ell-1/2}\, d_q\, \varphi_{n,\ell} \tag{D.66}$$

Along ℓ =up,downstream of the trailing edge,

$$h(h\varphi_y)_y = \frac{h}{\Delta y^2}\left[h_{\ell+1/2}(\varphi^+_{n,\ell+1} - \varphi^+_{n,\ell}) - h_{\ell-1/2}(\varphi^+_{n,\ell} - \varphi^+_{n,\ell-1} - \Delta\varphi_n)\right]$$

where $\Delta\varphi_n$ is given in (5.16). The tridiagonal coefficeints are

$$A = A_{i,d} \tag{D.67}$$

$$B = B_{i,d} \tag{D.68}$$

$$C = C_{i,d} \tag{D.69}$$

$$D = D_{i,d} + \frac{h_\ell}{\Delta y^2} h_{\ell-1/2}\, \Delta\varphi_n \tag{D.70}$$

Along ℓ=low

$$h(h\varphi_y)_y = \frac{h}{\Delta y^2}\left[h_{\ell+1/2}(\varphi^+_{n,\ell+1} - \varphi^+_{n,\ell} - \Delta\varphi_n) - h_{\ell-1/2}(\varphi^+_{n,\ell} - \varphi^+_{n,\ell-1})\right]$$

and

$$A = A_{i,d} \tag{D.71}$$

$$B = B_{i,d} \tag{D.72}$$

$$C = C_{i,d} \tag{D.73}$$

$$D = D_{i,d} - \frac{h_i h_{i+1/2} \Delta \rho_n}{\Delta z^2} \tag{D.74}$$

APPENDIX E

FAR FIELD CONDITIONS AND EVALUATION OF THE WAKE INTEGRAL

Because of an error in the formulation of the adjoint equation in [21], the expression for $\psi(x,z)$ to be used in the Klunker type far field condition is rederived here. Also, the derivation of the Sommerfeld radiation conditions and the methods used to evaluate the wake integrals are presented.

A. Far Field Conditions: Green's Function Method

Rewriting (5.1) in the form

$$\varphi_{xx} + \varphi_{\bar{z}\bar{z}} - \frac{2ikm^2}{1-m^2}\varphi_x + \frac{k^2m^2}{1-m^2}\varphi = \frac{m^2(\gamma+1)}{1-m^2}(\varphi_x\varphi_x)_x + \frac{ikm^2(\gamma-1)}{1-m^2}\varphi_{xx}\varphi \qquad (E.1)$$

and defining a linear operator, $L(\varphi)$ as

$$L(\varphi) = \varphi_{xx} + \varphi_{\bar{z}\bar{z}} - \frac{2ikm^2}{1-m^2}\varphi_x + \frac{k^2m^2}{1-m^2}\varphi$$

an integral equation for φ is obtained by evaluating $\iint \psi L(\varphi)\,dA$. Intergrating, by parts, each term of $\psi L(\varphi)$ over the areas of Figures E.1a and E.1b, I obtain

$$\iint \psi\varphi_{xx}\,dA = \int_{-z_1}^{z_2}(\psi\varphi_x - \psi_x\varphi)\Big|_{x_1(z)}^{x_2(z)}dz + \iint \varphi\psi_{xx}\,dA$$

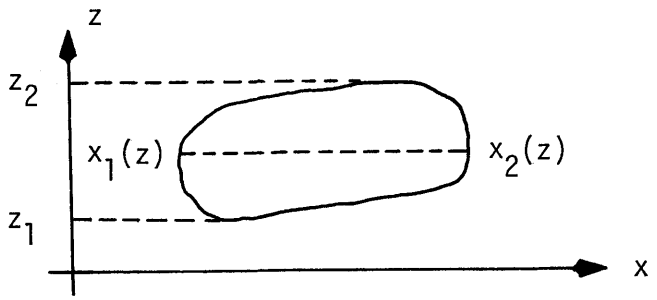

Figure E.1a. Area and path of integration.

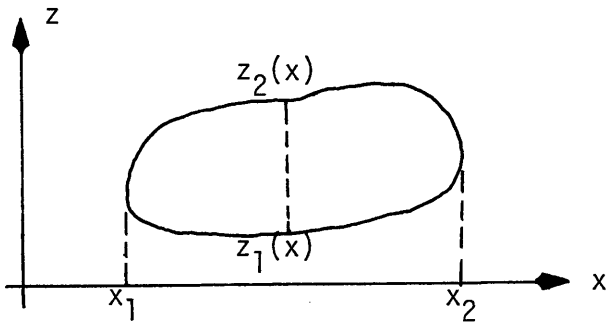

Figure E.1b. Area and path of integration.

Figure E.1c. Local normal along path of integration.

$$\iint \psi \varphi_{\bar{z}\bar{z}}\, dA = \int_{x_1}^{x_2} (\psi \varphi_{\bar{z}} - \psi_{\bar{z}} \varphi) \Big|_{z_1(x)}^{z_2(x)} dx + \iint \varphi \psi_{\bar{z}\bar{z}}\, dA$$

$$-\frac{2ikm^2}{1-m^2} \iint \psi \varphi_x\, dA = -\frac{2ikm^2}{1-m^2} \left\{ \int_{z_1}^{z_2} \psi \varphi \Big|_{x_1(z)}^{x_2(z)} dz - \iint \varphi \psi_x\, dA \right\}$$

$$\frac{k^2 m^2}{1-m^2} \iint \psi \varphi\, dA = \frac{k^2 m^2}{1-m^2} \iint \psi \varphi\, dA$$

which combines to yield

$$\begin{aligned} \iint \psi L(\varphi)\, dA = \iint \varphi \Big(\psi_{xx} + \psi_{\bar{z}\bar{z}} + \frac{2ikm^2}{1-m^2} \psi_x + \frac{k^2 m^2}{1-m^2} \psi \Big)\, dA \\ + \int_{z_1}^{z_2} \Big(\psi \varphi_x - \psi_x \varphi - \frac{2ikm^2}{1-m^2} \psi \varphi \Big) \Big|_{x_1(z)}^{x_2(z)} dz \\ + \int_{x_1}^{x_2} (\psi \varphi_{\bar{z}} - \psi_{\bar{z}} \varphi) \Big|_{z_1(x)}^{z_2(x)} dx \end{aligned} \qquad \text{(E.2)}$$

The final two integrals in (E.2) reduce to a single line integral along the curve enclosing the area of interest. Noting from Figure E.1c that

$$dz = ds \cos\theta = \hat{\imath} \cdot \hat{n}$$

$$dx = ds \sin\theta = \hat{k} \cdot \hat{n}$$

I can write for any quantity, Q^*

$$\int_{z_1}^{z_2} Q^* \Big|_{x_1(z)}^{x_2(z)} dz = \int_{z_1}^{z_2} \left\{ Q^*(x_2(z)) - Q^*(x_1(z)) \right\} dz = \oint_C Q^* \hat{i} \cdot \hat{n} \, ds \tag{E.3}$$

$$\int_{x_1}^{x_2} Q^* \Big|_{z_1(x)}^{z_2(x)} dx = \int_{x_1}^{x_2} \left\{ Q^*(z_2(x)) - Q^*(z_1(x)) \right\} dx = \oint_C Q^* \hat{k} \cdot \hat{n} \, ds \tag{E.4}$$

Utilizing (E.3) and (E.4), I have

$$\int_{z_1}^{z_2} \left(\psi \varphi_x - \psi_x \varphi - \frac{2ikm^2}{1-m^2} \psi \varphi \right) \Big|_{x_1(z)}^{x_2(z)} dz = \oint_C \left(\psi \varphi_x - \psi_x \varphi - \frac{2ikm^2}{1-m^2} \psi \varphi \right) \hat{i} \cdot \hat{n} \, ds \tag{E.5}$$

$$\int_{x_1}^{x_2} (\psi \varphi_{\bar{z}} - \psi_{\bar{z}} \varphi) \Big|_{z_1(x)}^{z_2(x)} dx = \oint_C (\psi \varphi_{\bar{z}} - \psi_{\bar{z}} \varphi) \hat{k} \cdot \hat{n} \, ds \tag{E.6}$$

Equations (E.5) and (E.6) are then introduced into (E.2) to yield the following integral equation for φ

$$\iint \left\{ \psi L(\varphi) - \varphi L^*(\psi) \right\} dA = \oint_C \left(\varphi \psi_n - \psi \varphi_n + \frac{2ikm^2}{1-m^2} \psi \varphi \hat{i} \cdot \hat{n} \right) ds \tag{E.7}$$

where $\hat{n}$ is the unit normal that points into the flow field and $L^*(\psi)$ is the adjoint operator

$$L^*(\psi) = \psi_{xx} + \psi_{\bar{z}\bar{z}} + \frac{2ikm^2}{1-m^2} \psi_x + \frac{k^2 m^2}{1-m^2} \psi$$

Ehlers [21] assumes that the operator, $L(\varphi)$, is self adjoint, but for an operator of the form

$$L(\varphi) = \nabla^2 \varphi + a \varphi_x + b \varphi_{\bar{z}} + c \varphi$$

the adjoint operator should be

$$L^*(\psi) = \nabla^2\psi - (a\psi)_x - (b\psi)_{\bar{z}} + c\psi$$

To define ψ, I assume that it is a Green's function which satisfies

$$\psi_{xx} + \psi_{\bar{z}\bar{z}} + \frac{2ikm^2}{1-m^2}\psi_x + \frac{k^2m^2}{1-m^2}\psi = \delta(x-x')\delta(\bar{z}-\bar{z}') \tag{E.8}$$

Writing ψ as $\psi_0 e^{\frac{-ikm^2}{1-m^2}x}$ (E.8) becomes

$$\psi_{0xx} + \psi_{0\bar{z}\bar{z}} + \left(\frac{km}{1-m^2}\right)^2\psi_0 = e^{\frac{ikm^2}{1-m^2}x}\delta(x-x')\delta(\bar{z}-\bar{z}') \tag{E.9}$$

Solutions of (E.9) are obtained using Fourier transform techniques [54], where the transform pair is defined as

$$\bar{\psi}(k_x, k_{\bar{z}}) = \frac{1}{2\pi}\int_{-\infty}^{\infty}\int e^{i(k_x x + k_{\bar{z}}\bar{z})}\psi_0(x,\bar{z})\,dx\,d\bar{z}$$

$$\psi_0(x,\bar{z}) = \frac{1}{2\pi}\int_{-\infty}^{\infty}\int e^{-i(k_x x + k_{\bar{z}}\bar{z})}\bar{\psi}(k_x, k_{\bar{z}})\,dk_x\,dk_{\bar{z}}$$

Taking the Fourier transform of (E.9), I obtain

$$\left\{k_x^2 + k_{\bar{z}}^2 - \left(\frac{km}{1-m^2}\right)^2\right\}\bar{\psi}(k_x, k_{\bar{z}}) = -e^{\frac{ikm^2}{1-m^2}x'}e^{i(k_x x' + k_{\bar{z}}\bar{z}')}$$

or

$$\bar{\psi}(k_x, k_{\bar{z}}) = -e^{\frac{ikm^2}{1-m^2}x'} \frac{e^{i(k_x x' + k_{\bar{z}}\bar{z}')}}{k_x^2 + k_{\bar{z}}^2 - \left(\frac{km}{1-m^2}\right)^2}$$

Hence,

$$\psi_0(x, \bar{z}) = \frac{e^{\frac{-ikm^2}{1-m^2}x'}}{2\pi} \int_{-\infty}^{\infty}\int \frac{e^{-i[k_x(x-x') + k_{\bar{z}}(\bar{z}-\bar{z}')]}}{k_x^2 + k_{\bar{z}}^2 - \left(\frac{km}{1-m^2}\right)^2} dk_x dk_{\bar{z}}$$

Making the substitutions

$$x - x' = \rho\cos\Omega$$

$$\bar{z} - \bar{z}' = \rho\sin\Omega$$

$$k_x = r\cos\theta$$

$$k_{\bar{z}} = r\sin\theta$$

ψ_0 becomes

$$\psi_0(x, \bar{z}) = -e^{\frac{ikm^2}{1-m^2}x'} \int_0^{\infty} \frac{r\,dr}{r^2 - \left(\frac{km}{1-m^2}\right)^2} \int_0^{2\pi} e^{-ir\rho\cos(\theta-\Omega)} d\theta$$

which may be rewritten as

$$\psi_0(x,\bar{z}) = -e^{i\frac{km^2}{1-m^2}x'} \int_0^\infty \frac{r J_0(\rho r)}{r^2 - \left(\frac{km}{1-m^2}\right)^2} dr$$

Utilizing the relationships

$$\int_0^\infty \frac{r J_0(ar)}{r^2-b^2} dr = K_0(ipb)$$

$$K_n(y) = -i\frac{\pi}{2} e^{-in\frac{\pi}{2}} H_n^{(2)}(-iy)$$

I obtain

$$\psi_0(x,\bar{z}) = i\frac{\pi}{2} e^{i\frac{km^2}{1-m^2}x'} H_0^{(2)}\left(\frac{km}{1-m^2}\sqrt{(x-x')^2+(\bar{z}-\bar{z}')^2}\right)$$

Interchanging the primed and unprimed variables, the adjoint function is, in terms of original variables

$$\psi(x,z) = i\frac{\pi}{2} e^{i\frac{km^2}{1-m^2}(x-x')} H_0^{(2)}\left(\frac{km}{1-m^2}\sqrt{(x-x')^2+\beta^2(z-z')^2}\right) \quad \text{(E.10)}$$

It should be noted that the above expression for ψ represents outgoing waves at infinity.

B. Far Field Conditions: Sommerfeld Radiation Formulation

Other types of boundary conditions that may be used are the Sommerfeld radiation conditions. Far from the airfoil, I

assume the steady state perturbation velocities and their derivatives to be small and consider the unsteady potential equation

$$\varphi_{xx} + \varphi_{\bar{z}\bar{z}} - \frac{2ikm^2}{1-m^2}\varphi_x + \frac{k^2m^2}{1-m^2}\varphi = 0 \tag{E.11}$$

Writing φ as

$$\varphi(x,\bar{z}) = e^{\frac{ikm^2}{1-m^2}x}\varphi_0(x,\bar{z})$$

(E.11) is transformed into Helmholtz's equation

$$\varphi_{0xx} + \varphi_{0\bar{z}\bar{z}} + \left(\frac{km}{1-m^2}\right)^2\varphi_0 = 0 \tag{E.12}$$

Since I have written $\hat{\varphi}$ as φe^{ikt}, the solution of (E.12) which represents outgoing waves at infinity is

$$\varphi_0 = H_0^{(2)}\left(\frac{km}{1-m^2}r\right)$$

where

$$r = \sqrt{x^2+\bar{z}^2}$$

Hence

$$\hat{\varphi}(x,\bar{z},t) = e^{ikt}\varphi(x,\bar{z}) = e^{ik\left(t+\frac{m^2}{1-m^2}x\right)}H_0^{(2)}\left(\frac{km}{1-m^2}r\right)$$

In the far field, the asymptotic approximation of the Hankel

function allows me to represent $\hat{\varphi}(x,z,t)$ as

$$\hat{\varphi}(x,z,t) \sim \sqrt{\frac{2\beta^2}{\pi k m r}}\, e^{ik\left(t+\frac{m^2}{1-m^2}x-\frac{mr}{1-m^2}\right)-i\frac{\pi}{4}}$$

At the upstream boundary, $r \to -x$ and

$$\hat{\varphi} \sim \sqrt{\frac{2\beta^2}{-\pi k m x}}\, e^{ik\left(t+\frac{m^2}{1-m^2}x+\frac{mx}{1-m^2}\right)-i\frac{\pi}{4}}$$

$$\hat{\varphi}_r = -\hat{\varphi}_x = \left(\frac{1}{2x} - \frac{ikm}{1-m}\right)\hat{\varphi}$$

In the limit $x \to -\infty$, I obtain the radiation condition

$$\hat{\varphi}_x - \frac{ikm}{1-m}\hat{\varphi} = 0 \qquad , \qquad x \to -\infty$$

or

$$\varphi_x - \frac{ikm}{1-m}\varphi = 0 \qquad , \qquad x \to -\infty \tag{E.13}$$

Similarly, at the downstream boundary, $r = x$, and the radiation condition becomes

$$\varphi_x + \frac{ikm}{1+m}\varphi = 0 \qquad , \qquad x \to \infty \tag{E.14}$$

On the upper lateral boundary, $r = \bar{z}$, and

$$\hat{\varphi} \sim \sqrt{\frac{2\beta^2}{\pi k m \bar{z}}}\, e^{ik\left(t+\frac{m^2}{1-m^2}x-\frac{m}{1-m^2}\bar{z}\right)-i\frac{\pi}{4}}$$

$$\hat{\varphi}_r = \hat{\varphi}_{\bar{z}} = -\left(\frac{1}{2\bar{z}} + \frac{ikm}{1-m^2}\right)\hat{\varphi}$$

In the limit $z \to \infty$ the radiation condition is

$$\varphi_z + \frac{ikm}{\sqrt{1-m^2}}\varphi = 0 \quad , \quad z \to \infty \tag{E.15}$$

Similarly, on the lower boundary, where $r = -\bar{z}$, I have

$$\varphi_z - \frac{ikm}{\sqrt{1-m^2}}\varphi = 0 \quad , \quad z \to -\infty \tag{E.16}$$

C. Evaluation of the Wake Integrals

Next, I present a method to evaluate the wake integrals of (5.10)

$$I_1 = \int_0^{\pi/2} e^{-\frac{kz}{\beta}\cos\theta} J_1\left(\frac{km}{\beta} z\sin\theta\right) d\theta$$

$$I_2 = \int_0^{\pi/2} \left\{ e^{-\frac{kz}{\beta}\cos\theta} Y_1\left(\frac{km}{\beta} z\sin\theta\right) + \frac{2}{\pi} e^{-\frac{kz}{\beta}\cosh\theta} K_1\left(\frac{km}{\beta} z\sinh\theta\right) \right\} d\theta$$

$$I_3 = \int_{\pi/2}^{\infty} e^{-\frac{kz}{\beta}\cosh\theta} K_1\left(\frac{km}{\beta} z\sinh\theta\right) d\theta$$

The integrands of I_1 and I_3 are well behaved over their respective

ranges of integration, but Y_1 and K_1 each have singularities at $\theta = 0$. As $\theta \to 0$, the integrand of I_2 reduces to $e^{-\frac{kz}{\beta}}\left\{ Y_1\left(\frac{km}{\beta} z\theta\right) + \frac{2}{\pi} K_1\left(\frac{km}{\beta} z\theta\right)\right\}$. For small arguments,

$$Y_1\left(\frac{km}{\beta} z\theta\right) \sim \frac{2}{\pi}\left\{ \frac{km}{2\beta} z\theta \left(\log \frac{km}{2\beta} z\theta + \nu\right) - \frac{\beta}{km z\theta}\right\}$$

$$K_1\left(\frac{km}{\beta} z\theta\right) \sim \frac{\beta}{km z\theta}$$

where ν is Euler's constant, and the integrand of I_2 is the well behaved function $\frac{km}{\beta\pi} z\theta\, e^{-\frac{kz}{\beta}}\left(\log \frac{km}{2\beta} z\theta + \nu\right)$.

Legendre-Gauss quadrature is used to evaluate I_1 and I_2, the standard Legendre-Gauss form is

$$\int_{-1}^{1} f(x)\,dx \cong \sum_{i=1}^{n} w_i f(x_i)$$

where the abscissas, x_i, are the zeros of the Legendre polynomials, $P_n(x)$, and the weights, w_i, are

$$w_i = \frac{2(1-x_i^2)}{(n+1)^2 [P_{n+1}(x_i)]^2}$$

When the integration is to be taken over an arbitrary finite interval, the transformation $y = \left(\frac{b-a}{2}\right)x + \frac{b+a}{2}$ is used to convert the integral $\int_a^b f(y)\,dy$ to $\frac{b-a}{2}\int_{-1}^{1} f\left(\frac{b-a}{2} x + \frac{b+a}{2}\right)$; the integral is then evaluated as

$$\int_a^b f(y)\,dy \cong \frac{b-a}{2}\sum_{i=1}^{n} w_i\, f\left(\frac{b-a}{2}x_i + \frac{b+a}{2}\right) \qquad \text{(E.17)}$$

Utilizing (E.17), I_1 and I_2 are approximated as

$$\int_0^{\pi/2} e^{-\frac{kz}{\beta}\cos\theta} J_1\left(\frac{km}{\beta} z\sin\theta\right) d\theta \cong \frac{\pi}{4}\sum_{i=1}^{n} w_i\, e^{-i\frac{kz}{\beta}\cos\theta_i} J_1\left(\frac{km}{\beta} z\sin\theta_i\right)$$

$$\int_0^{\pi/2}\left\{e^{-\frac{kz}{\beta}\cos\theta} Y_1\left(\frac{km}{\beta} z\sin\theta\right) + \frac{2}{\pi} e^{-\frac{kz}{\beta}\cosh\theta} K_1\left(\frac{km}{\beta} z\sinh\theta\right)\right\} d\theta \cong$$

$$\frac{\pi}{4}\sum_{i=1}^{n} w_i\left\{e^{-\frac{kz}{\beta}\cos\theta_i} Y_1\left(\frac{km}{\beta} z\sin\theta_i\right) + \frac{2}{\pi} e^{-\frac{kz}{\beta}\cosh\theta_i} K_1\left(\frac{km}{\beta} z\sinh\theta_i\right)\right\}$$

where

$$\theta_i = \frac{\pi}{4}(x_i + 1)$$

Gauss-Laguerre integration is used to evaluate I_3. The standard form of Gauss-Laguerre integration is

$$\int_0^{\infty} e^{-x} f(x)\,dx \cong \sum_{i=1}^{n} w_i\, f(x_i)$$

where X_i are the zeros of the Laguerre polynomials, $L_n(X)$, and w_i are defined as

$$w_i = \frac{x_i}{(n+1)^2 [L_{n+1}(x_i)]^2}$$

To get I_3 in the standard Gauss-Laguerre form, I first make the substitution $\theta = \cosh^{-1}\left(\frac{\beta\tau}{kz} + \cosh\frac{\pi}{2}\right)$ to obtain

$$I_3 = e^{-\frac{kz}{\beta}\cosh\frac{\pi}{2}} \int_0^\infty e^{-\tau} \frac{K_1\left(\frac{km}{\beta}z\sqrt{\left(\frac{\beta}{kz}\right)^2\tau\left(\tau+2\frac{kz}{\beta}\cosh\frac{\pi}{2}\right)+\sinh^2\frac{\pi}{2}}\right)}{\sqrt{\tau\left(\tau+2\frac{kz}{\beta}\cosh\frac{\pi}{2}\right)+\left(\frac{kz}{\beta}\right)^2\sinh^2\frac{\pi}{2}}}\, d\tau$$

Hence,

$$\int_{\pi/2}^\infty e^{-\frac{kz}{\beta}\cosh\theta} K_1\left(\frac{km}{\beta}z\sinh\theta\right) d\theta \cong$$

$$e^{-\frac{kz}{\beta}\cosh\frac{\pi}{2}} \sum_{i=1}^{n} w_i \frac{K_1\left(\frac{km}{\beta}z\sqrt{\left(\frac{\beta}{kz}\right)^2\tau_i\left(\tau_i+2\frac{kz}{\beta}\cosh\frac{\pi}{2}\right)+\sinh^2\frac{\pi}{2}}\right)}{\sqrt{\tau_i\left(\tau_i+2\frac{kz}{\beta}\cosh\frac{\pi}{2}\right)+\left(\frac{kz}{\beta}\right)^2\sinh^2\frac{\pi}{2}}}$$

To ensure that the Gaussian quadrature formulas yield accurate results, the integrals are first evaluated for an initial number of data points, n; the number of points over the interval is then increased and the integrals reevaluated. This process is repeated unitl the difference in the values of the integrals obtained using the larger and smaller number of points reaches a predetermined small number. This process is shown in Figure E.2.

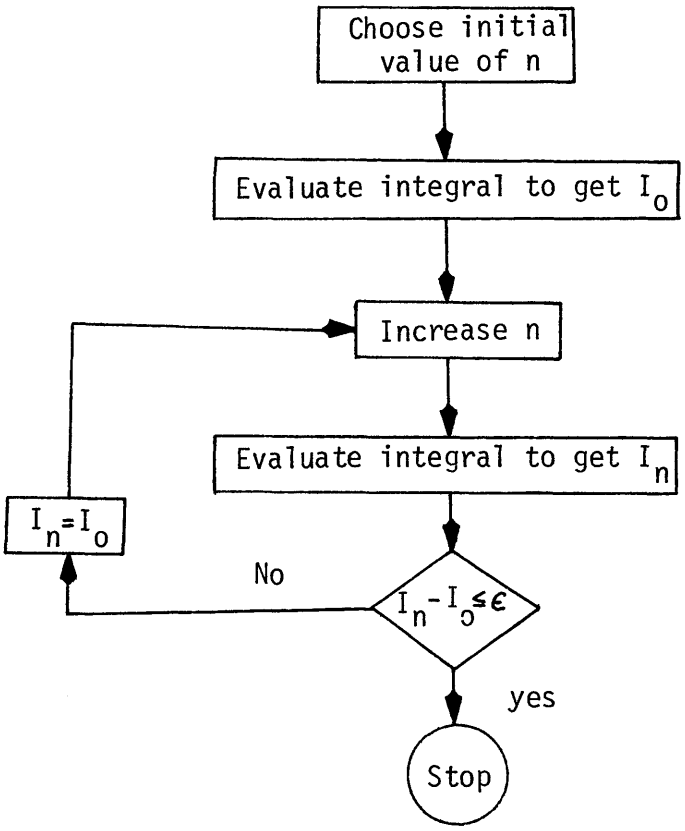

Figure E.2. Gaussian integration procedure

APPENDIX F

STABILITY ANALYSIS AND FREQUENCY LIMITATIONS

Weatherill et al. [55], deduced that relaxation techniques will be successful in analyzing flows about harmonically oscillating airfoils only if the reduced frequency satisfies the following inequality

$$k^2 + \frac{4\pi}{a_\xi} k \leq 4\pi^2 \frac{(1-m^2)}{m^2} \left[\frac{1}{a_\xi^2} + \frac{1}{(1-m^2) c_\eta^2} \right] \tag{F.1}$$

This relationship indicates that as the free stream Mach number increases toward unity and the extent of the computational region increases, the maximum reduced frequency of oscillation which leads to stable calculations is decreased.

The analysis which led to (F.1), was carried out on a uniformly spaced computational grid. However, irregular grids are generally applied to the type of problem treated in this work , and a relation that is applicable to those types of grids is needed. Assuming that for any nonuniform grid, I can write

$$\frac{\partial}{\partial x} = \frac{\partial \xi}{\partial x} \frac{\partial}{\partial \xi} = f \frac{\partial}{\partial \xi}$$

$$\frac{\partial}{\partial z} = \frac{\partial \eta}{\partial z} \frac{\partial}{\partial \eta} = h \frac{\partial}{\partial \eta}$$

Considering the case where the steady component of the flow is that past a nonlifting flat plate, (5.1) reduces to

$$(1-M^2)f(f\varphi_\xi)_\xi + h(h\varphi_\eta)_\eta - 2ikM^2 f\varphi_\xi + k^2M^2\varphi = 0 \qquad \text{(F.2)}$$

I should note that the properties of the fluid are not represented in (F.2). Since I only consider subsonic free stream Mach numbers, the finite difference representation of (F.2) becomes

$$(1-M^2)\frac{f_n}{\Delta\xi^2}\left\{f_{n+1/2}\varphi_{n+1,\ell} - (f_{n+1/2}+f_{n-1/2})\left[\frac{\varphi^+_{n,\ell}}{\omega} + \left(1-\frac{1}{\omega}\right)\varphi_{n,\ell}\right] + f_{n-1/2}\varphi^+_{n-1,\ell}\right\}$$

$$+\frac{h_\ell}{\Delta\eta^2}\left[h_{\ell+1/2}(\varphi^+_{n,\ell+1}-\varphi^+_{n,\ell}) - h_{\ell-1/2}(\varphi^+_{n,\ell}-\varphi^+_{n,\ell-1})\right] - \frac{ikM^2 f_n}{\Delta\xi}(\varphi_{n+1,\ell}-\varphi^+_{n-1,\ell})$$

$$+k^2M^2\left[\frac{\varphi^+_{n,\ell}}{\omega} + \left(1-\frac{1}{\omega}\right)\varphi_{n,\ell}\right] = 0 \qquad \text{(F.3)}$$

Each Fourier component of the potential may be written as

$$\varphi_{n,\ell} = G^K e^{i(n\theta_\xi + \ell\theta_\eta)} \qquad \text{(F.4)}$$

where

$$\theta_\xi = 2\pi\frac{\Delta\xi}{a_\xi}$$

$$\theta_\eta = 2\pi \frac{\Delta\eta}{c_\eta}$$

Writing $G^{k+1}=rG^k$, where r is an amplification factor, it becomes imperative that I require $|r| \leq 1$ if the solutions are to remain bounded.

The substitution of (E.4) into (E.3) leads to

$$(1-m^2)\frac{f_n}{\Delta\xi^2}\left\{f_{n+1/2}e^{i\theta_\xi} - (f_{n+1/2}+f_{n-1/2})\left[\frac{r}{\omega}+\left(1-\frac{1}{\omega}\right)\right] + f_{n-1/2}e^{-i\theta_\xi}\right\}$$

$$+\frac{r h_\ell}{\Delta\eta^2}\left[h_{\ell+1/2}(e^{i\theta_\eta}-1) - h_{\ell-1/2}(1-e^{-i\theta_\eta})\right] - \frac{ikm^2 f_n}{\Delta\xi}(e^{i\theta_\xi} - re^{-i\theta_\xi})$$

$$+k^2m^2\left[\frac{r}{\omega}+\left(1-\frac{1}{\omega}\right)\right] = 0$$

from which I obtain the amplification factor

$$r = \left\{-\left[(1-m^2)\frac{f_{n+1/2}}{\Delta\xi^2} - i\frac{km^2}{\Delta\xi}\right]f_n e^{i\theta_\xi} + \left[(1-m^2)\frac{f_n}{\Delta\xi^2}(f_{n+1/2}+f_{n-1/2}) - k^2m^2\right]\left(1-\frac{1}{\omega}\right)\right\}$$

$$\left\{\left[(1-m^2)\frac{f_{n-1/2}}{\Delta\xi^2} + i\frac{km^2}{\Delta\xi}\right]f_n e^{-i\theta_\xi} - (1-m^2)\frac{f_n}{\omega\Delta\xi^2}(f_{n+1/2}+f_{n-1/2}) + \frac{k^2m^2}{\omega}\right.$$

$$\left. + \frac{h_\ell}{\Delta\eta^2}\left[h_{\ell+1/2}(e^{i\theta_\eta}-1) - h_{\ell-1/2}(1-e^{-i\theta_\eta})\right]\right\}^{-1}$$

In the limit of vanishing grid spacing, I may assume

$$f_{n\pm1/2} \simeq f_n$$

$$h_{\ell\pm1/2} \simeq h_\ell$$

and the amplification factor reduces to

$$r = \left\{ -\left[(1-m^2)\frac{f_n}{\Delta\xi^2} - i\frac{km^2}{\Delta\xi} \right] f_n e^{i\theta_\xi} + \left[2(1-m^2)\frac{f_n^2}{\Delta\xi^2} - k^2m^2 \right]\left(1-\frac{1}{\omega}\right) \right\} \left\{ \frac{k^2m^2}{\omega} + \left[(1-m^2)\frac{f_n}{\Delta\xi^2} + i\frac{km^2}{\Delta\xi} \right] f_n e^{-i\theta_\xi} - 2(1-m^2)\frac{f_n^2}{\omega\Delta\xi^2} - 2\frac{h_\lambda^2}{\Delta\eta^2}(1-\cos\theta_\eta) \right\}^{-1} \quad \text{(F.5)}$$

Defining A and its conjugate, A^* , as

$$A \equiv \left[(1-m^2)\frac{f_n}{\Delta\xi^2} + i\frac{km^2}{\Delta\xi} \right] f_n e^{-i\theta_\xi} = m + ib$$

$$A^* \equiv \left[(1-m^2)\frac{f_n}{\Delta\xi^2} - i\frac{km^2}{\Delta\xi} \right] f_n e^{-i\theta_\xi} = m - ib$$

and p and d as

$$p \equiv \left[2(1-m^2)\frac{f_n^2}{\Delta\xi^2} - k^2m^2 \right]\left(1-\frac{1}{\omega}\right)$$

$$d \equiv -2(1-m^2)\frac{f_n^2}{\omega\Delta\xi^2} + \frac{k^2m^2}{\omega} - 2\frac{h_\lambda^2}{\Delta\eta^2}(1-\cos\theta_\eta)$$

the stability condition becomes p-d ≤ 2m or

$$k^2m^2 + 2km^2\frac{f_n}{\Delta\xi}\sin\theta_\xi \le 2(1-m^2)\frac{f_n^2}{\Delta\xi^2}(1-\cos\theta_\xi) + 2\frac{h_\lambda^2}{\Delta\eta^2}(1-\cos\theta_\eta)$$

Since I have assumed vanishing grid spacing, the definitions of θ_ξ and θ_η may be used to expand $\cos\theta_\xi$, $\cos\theta_\eta$ and $\sin\theta_\xi$ in in the form

$$\cos\theta_\xi = 1 - 2\pi^2 \frac{\Delta\xi^2}{a_\xi^2} + O(\Delta\xi^4)$$

$$\cos\theta_\eta = 1 - 2\pi^2 \frac{\Delta\eta^2}{c_\eta^2} + O(\Delta\eta^4)$$

$$\sin\theta_\xi = 2\pi \frac{\Delta\xi}{a_\xi} - O(\Delta\xi^3)$$

Employing the above expansions, the stability condition becomes

$$k^2 + 4\pi \frac{f_n}{a_\xi} k \leq 4\pi^2 \frac{(1-m^2)}{m^2} \left[\frac{f_n^2}{a_\xi^2} + \frac{h_c^2}{(1-m^2)c_\eta^2} \right] \qquad \text{(F.6)}$$

Since the steady, nonlinear effects are not included in the analysis, (F.6) only provides an estimate of the frequency limitation.

APPENDIX G

TRIDIAGONAL MATRIX SOLVER

At interior points of the computational domain, the finite difference equations are written in the tridiagonal form

$$-A_\ell q^+_{n,\ell-1} + B_\ell q^+_{n,\ell} - C_\ell q^+_{n,\ell+1} = D_\ell \tag{G.1}$$

where $1 \leq \ell \leq L$. If the grid column does not intersect the airfoil, I seek two vectors, E and F, such that solutions of (G.1) satisfy the relation

$$q^+_{n,\ell} = E_\ell q^+_{n,\ell+1} + F_\ell \tag{G.2}$$

Lowering the ℓ subscripts by one in (G.2), I obtain

$$q^+_{n,\ell-1} = E_{\ell-1} q^+_{n,\ell} + F_{\ell-1}$$

which when coupled with (G.1) leads to

$$(B_\ell - A_\ell E_{\ell-1}) q^+_{n,\ell} - C_\ell q^+_{n,\ell+1} = D_\ell + A_\ell F_{\ell-1} \tag{G.3}$$

When expressed in the form of (G.2), the interior point solution becomes

$$g^+_{n,\ell} = \frac{C_\ell}{B_\ell - A_\ell E_{\ell-1}} g^+_{n,\ell+1} + \frac{D_\ell + A_\ell F_{\ell-1}}{B_\ell - A_\ell E_{\ell-1}} \tag{G.4}$$

A comparison of (G.2) and (G.4) indicates that

$$E_\ell = \frac{C_\ell}{B_\ell - A_\ell E_{\ell-1}} \tag{G.5}$$

$$F_\ell = \frac{D_\ell + A_\ell F_{\ell-1}}{B_\ell - A_\ell E_{\ell-1}} \tag{G.6}$$

Once E_1 and F_1 are known, (G.5) and (G.6) are used to calculate, in succession, the values of E and F from $\ell = 2$ to $\ell = L-1$. E_1 and F_1 are easily determined by considering the solution of (G.1) at $\ell = 1$

$$g^+_{n,1} = E_1 g^+_{n,2} + F_1 \tag{G.7}$$

The value of $g^+_{n,1}$ is prescribed from the boundary conditions and is independent of the value of $g^+_{n,2}$. Therefore,

$$E_1 = 0 \tag{G.8}$$

$$F_1 = g^+_{n,1} \tag{G.9}$$

At ℓ =L-1, $g^{+}_{n,L}$ is inserted into (G.2) to initiate the calculation of g in the opposite direction.

If a grid column crosses the airfoil, I cannot compute the values of g along that column in a single sweep. Instead, I calculate the flow above and below the airfoil in separate operations. In calculating the flow field for $\ell \geq$ up, I use the procedure outlined above. E_{up} and F_{up}, now required to start the calculations, are found from (C.26)-(C.29). Utilizing (C.26)-(C.29), (G.1) takes the form

$$B_{up}\, g^{+}_{n,up} - C_{up}\, g^{+}_{n,up+1} = D_{up} \tag{G.10}$$

which is rearranged to read

$$g^{+}_{n,up} = \frac{C_{up}}{B_{up}}\, g_{n,up+1} + \frac{D_{up}}{B_{up}} \tag{G.11}$$

Equations (G.2) and(G.11) indicate that

$$E_{up} = \frac{C_{up}}{B_{up}} \tag{G.12}$$

$$F_{up} = \frac{D_{up}}{B_{up}} \tag{G.13}$$

Again, at ℓ =L-1, $g^+_{n,L}$ is used to initialize the calculation of g in the reverse direction. Also, when treating nonlifting flows, I compute only the flow above the airfoil, and (G.12) and (G.13) are used everywhere along ℓ =up.

In the lower portion of the flow field, we proceed from ℓ =low to ℓ =2 to determine the E and F vectors and in the opposite directions to calculate g. Because I march in the direction of decreasing ℓ, I seek solutions of the form

$$g^+_{n,\ell} = E_\ell g^+_{n,\ell-1} + F_\ell \tag{G.14}$$

which becomes at $\ell = \ell+1$

$$g^+_{n,\ell+1} = E_{\ell+1} g^+_\ell + F_{\ell+1} \tag{G.15}$$

Combining (G.15) and (G.1) yields

$$-A_\ell g^+_{n,\ell-1} + (B_\ell - C_\ell E_{\ell+1}) g^+_{n,\ell} = D_\ell + C_\ell F_{\ell+1} \tag{G.16}$$

Rewriting (G.16) as

$$g^+_{n,\ell} = \frac{A_\ell}{B_\ell - C_\ell E_{\ell+1}} g^+_{n,\ell-1} + \frac{D_\ell + C_\ell F_{\ell+1}}{B_\ell - C_\ell E_{\ell+1}} \tag{G.17}$$

shows that

$$E_\ell = \frac{A_\ell}{B_\ell - C_\ell E_{\ell+1}} \tag{G.18}$$

$$F_\ell = \frac{D_\ell + C_\ell F_{\ell+1}}{B_\ell - C_\ell E_{\ell+1}} \tag{G.19}$$

At points adjacent to the lower airfoil boundary, (C.30)-(C.35) indicate that the difference equations become

$$-A_{low}\, g^+_{n,low-1} + B_{low}\, g^+_{n,low} = D_{low} \tag{G.20}$$

Arranging (G.20) in the form

$$g^+_{n,low} = \frac{A_{low}}{B_{low}}\, g^+_{n,low-1} + \frac{D_{low}}{B_{low}} \tag{G.21}$$

reveals that

$$E_{low} = \frac{A_{low}}{B_{low}} \tag{G.22}$$

$$F_{low} = \frac{D_{low}}{B_{low}} \tag{G.23}$$

In the same manner as above, at $\ell = 2$, $g^+_{n,1}$ is utilized to begin the calculations of g.

APPENDIX H

FORTRAN PROGRAMS

```
C
C     ***************************************************************
C     *THIS PROGRAM COMPUTES THE STEADY LIFTING AND NONLIFTING TLOW     *
C     *FIELDS ABOUT AIRFOILS OF VARIOUS THICKNESS RATIOS AT VARIOUS     *
C     *ANGLES OF ATTACK.  THE INFINITE PHYSICAL DOMAIN IS MAPPED ONTO A *
C     *FINITE COMPUTATIONAL PLANE.  THE INPUTS ARE                      *
C     *      A1- DETERMINES THE SPACING IN THE LATERAL DIRECTION        *
C     *      A2- DETERMINES THE SPACING IN THE STREAMWISE DIRECTION     *
C     *      A3- DETERMINES THE SPACING IN THE STREAMWISE DIRECTION     *
C     *      M- FREE STREAM MACH NUMBER                                 *
C     *      PE- EXPONENT OF M IN THE NONLINEAR TERM IN THE POTENTIAL   *
C     *          EQUATION                                               *
C     *      X4- THE LOCATION OF THE BOUNDARY BETWEEN REGIONS I AND II  *
C     *          AND REGIONS II AND III                                 *
C     *      PSI4- DETERMINES THE SIZE OF THE COMPUTATIONAL REGION      *
C     *      DPSI- GRID SPACING IN THE STREAMWISE DIRECTION             *
C     *      DETA- GRID SPACING IN THE LATERAL DIRECTION                *
C     *      ANGO- INITIAL ANGLE OF ATTACK                              *
C     *      DANG- INCREMENT IN ANGLE OF ATTACK                         *
C     *      ANGMAX- MAXIMUM ANGLE AF ATTACK                            *
C     *      TO- INITIAL AIRFOIL THICKNESS RATIO                        *
C     *      DTAU- INCREMENT IN THE THICKNESS RATIO                     *
C     *      TAUMAX- MAXIMUM AIRFOIL THICKNESS RATIO                    *
C     *      GAM- RATIO OF SPECIFIC HEATS                               *
C     *      XTE- HALF OF THE CHORD LENGTH                              *
C     *      W- RELAXATION FACTOR                                       *
C     *      EPNL- CONVERGENCE CRITERIA FOR THICKNESS VARIATIONS        *
C     *      EPL- CONVERGENCE CRITERIA FOR ANGLE OF ATTACK VARIATIONS    *
C     *      EP- DETERMINES THE AMOUNT OF THE ADDITIONAL CROSS DERIVATIVE*
C     *          TERM TO BE ADDED TO THE SUPERSONIC DIFFERENCE EQUATION  *
C     *      WFAR- UNDERRELAXATION FACTOR USED TO SATISFY THE KUTTA AND  *
C     *            FAR FIELD CONDITIONS                                 *
C     *      IFLOW- DETERMINES TYPE OF FLOW TO BE COMPUTED              *
C     *             1- NONLIFTING                                       *
C     *             2- STEADY AND LIFTING                               *
C     *             3- UNSTEADY                                         *
```

```
C     *      IFOIL- THE TYPE OF AIRFOIL                                    *
C     *             1- PARABOLIC ARC                                       *
C     *             2- CIRCULAR ARC                                        *
C     *             3- NACA 00 SERIES                                      *
C     *      IPARM0- DETERMINES WHICH PARAMETER TO VARY FIRST              *
C     *              1- VARY THICKNESS RATIO FIRST                         *
C     *              2- VARY ANGLE OF ATTACK FIRST                         *
C     *      N1- THE NUMBER OF GRID SPACES IN THE PSI DIRECTION.  THIS     *
C     *          IS ONE LESS THAN THE TOTAL NUMBER OF GRID POINTS IN THE   *
C     *          PSI DIRECTION                                             *
C     *      L1- THE NUMBER OF GRID SPACES IN THE ETA DIRECTION.  THIS IS  *
C     *          ONE LESS THAN THE TOTAL NUMBER OF GRID POINTS IN THE ETA  *
C     *          DIRECTION                                                 *
C     *      IMAX- THE MAXIMUM NUMBER OF ITERATIONS                        *
C     *      K- THE NUMBER OF VALUES OF PHI AND G NEEDED TO EMPLOY THE     *
C     *         MOST ACCURATE PREDICTOR-CORRECTOR METHOD                   *
C     *      LLOW- THE GRID ROW ADJACENT TO  THE LOWER AIRFOIL BOUNDARY    *
C     *                                                                    *
C     *OTHER CONSTANTS ARE                                                 *
C     *      A4, B1- DETERMINE THE GRID SPACING IN THE STREAMWISE          *
C     *              DIRECTION IN REGION II OF THE FLOW FIELD              *
C     *      BM- PRANDTL-GLAURET CONSTANT                                  *
C     *      CRIT- CRITICAL PRESSURE COEFFICIENT                           *
C     *      NP1- MAXIMUM NUMBER OF GRID POINTS IN THE PSI DIRECTION       *
C     *      LP1- MAXIMUM NUMBER OF GRID POINTS IN THE ETA DIRECTION       *
C     *      KMAX- TOTAL NUMBER OF FLOW FIELDS STORED AT ANY TIME          *
C     ********************************************************************
C
      REAL M,MU,LOWCP,LOWSUR
      COMMON MU(51,22),PHI(51,22,5),G(51,22,5),UPSUR(51),LOWSUR(51),
     X       UPCP(51),LOWCP(51),DG(51),DPHI(51),XX(51),XP(51),F2(51)
      COMMON A1,A2,A3,A4,B1,X4,PSI4,DETA,DPSI,XTE,PSITE,FTE,DGT,DPHIT,
     X       M,BM,BBM,PE,GAM,THIK,ATTAK,TAUMAX,ANGMAX,EPL,EPNL,EP
      COMMON N1,L1,NP1,LP1,LUP,LLOW,NTE,IFLOW,IFOIL,IPARM0,IPARM,
     X       IMAX,KMAX
      DIMENSION A(22),B(22),C(22),D(22),E(22),F(22),ZZ(22),H(22),
```

```
     X          PRE(51,22),COR(51,22),ERR(51,22),GM(51,22)
      DATA PI/3.141593/
C
C     DEFINE STRETCHED COORDINATE FUNCTIONS
C
      X1(PSI)= -X4+ A2*TAN(.5*PI*(PSI+ PSI4))+
     X          A3*TAN(.5*PI*(PSI+ PSI4)**3)
      X2(PSI)= PSI*(A4+ B1*PSI**2)
      X3(PSI)= X4+ A2*TAN(.5*PI*(PSI-PSI4))+
     X          A3*TAN(.5*PI*(PSI- PSI4)**3)
C
      READ(5,101) A1
      READ(5,101) A2
      READ(5,101) A3
      READ(5,101) M
      READ(5,101) PE
      READ(5,101) X4
      READ(5,101) PSI4
      READ(5,101) DPSI
      READ(5,112) DETA
      READ(5,101) ANGO
      READ(5,101) DANG
      READ(5,101) ANGMAX
      READ(5,101) TO
      READ(5,101) DTAU
      READ(5,101) TAUMAX
      READ(5,101) GAM
      READ(5,101) XTE
      READ(5,101) W
      READ(5,101) EPNL
      READ(5,101) EPL
      READ(5,101) EP
      READ(5,101) WFAR
      READ(5,102) IFLOW
      READ(5,102) IFOIL
      READ(5,102) IPARMO
```

```
      READ(5,102) N1
      READ(5,102) L1
      READ(5,102) IMAX
      READ(5,102) K
      READ(5,102) LLOW
C
      A4= 1.5*X4/PSI4- .25*A2*PI
      B1= .25*PI*A2/(PSI4**2) - .5*X4/(PSI4**3)
C
      BM= SQRT(1.- M**2)
      BBM= 1.- M**2
      CRIT= -2.*BBM/((GAM+ 1.)*M**PE)
C
      NP1= N1+ 1
      LP1= L1+ 1
      KMAX= K+1
      LUP= LLOW+ 1
C
      IF(IFLOW .EQ. 1) WRITE(6,100)
      IF(IFLOW .EQ. 2) WRITE(6,104)
      IF(IFLOW .EQ. 3) WRITE(6,105)
      IF(IFOIL .EQ. 1) WRITE(6,106)
      IF(IFOIL .EQ. 2) WRITE(6,107)
      IF(IFOIL .EQ. 3) WRITE(6,108)
C
C     CHECK INPUT PARAMETERS
C
      WRITE(6,111)
      WRITE(6,109) A1,A2,A3,A4,B1,M,PE,X4,PSI4,DPSI,DETA,TO,DTAU,TAUMAX,
     X            ANGO,DANG,ANGMAX,GAM,XTE,W,EPL,EPNL,EP,WFAR,IFLOW,
     X            IFOIL,IPARMO,N1,L1,IMAX,K,LLOW
      WRITE(6,110) CRIT
C
C     INITIALIZE FLOW FIELD
C
      DO 2 KS= 1,KMAX
```

```
      DO 2 L= 1,LP1
      DO 2 N= 1,NP1
      PHI(N,L,KS)= 0.
    2 G(N,L,KS)= 0.
C
C     INITIALIZE SWITCHING FUNCTION AND PREDICTOR -CORRECTOR ERROR
C
      DO 3 L= 1,LP1
      DO 3 N= 1,NP1
      MU(N,L)= 0.
    3 ERR(N,L)= 0.
C
C     COMPUTE STRETCHED COORDINATES IN THE STREAMWISE DIRECTION
C
      PSI= -(1.+ PSI4)+ DPSI
      DO 1 N= 2,N1
      IF(PSI .LT. -PSI4) XX(N)= X1(PSI)
      IF(PSI .GE. -PSI4 .AND. PSI .LE. PSI4) XX(N)= X2(PSI)
      IF(PSI .GT. PSI4) XX(N)= X3(PSI)
      PSI= PSI+ DPSI
    1 CONTINUE
C
C     COMPUTE TRAILING EDGE LOCATION AND STRETCHING FACTOR AT THAT
C     LOCATION
C
      CALL TRAL(XT2)
C
      WRITE(6,103) PSITE,FTE,XT2,NTE
C
C     COMPUTE COORDINATE STRETCHING FACTORS IN THE STREAMWISE
C     DIRECTION
C
      CALL XGROW
C
      CALL   LIFT(A,B,C,D,E,F,ZZ,PRE,COR,ERR,GM,H,W,DTAU,K,DANG,ANGO,
     X            TO,WFAR)
```

```
C
  100 FORMAT('1','*************STEADY NONLIFTING FLOW PAST************')
  101 FORMAT(F8.5)
  102 FORMAT(I8)
  103 FORMAT(2X,'TRAILING EDGE PSI=',F8.5,2X,'STRETCHING=',F8.5,
     X       2X,'X TRAIL=',F8.5,2X,'N POINT=',I4//)
  104 FORMAT('1','*************STEADY LIFTING FLOW PAST*************')
  105 FORMAT('1','*************UNSTEADY MOTION OF*************')
  106 FORMAT('*************PARABOLIC ARC AIRFOILS*************'//)
  107 FORMAT('*************CIRCULAR ARC AIRFOILS*************'//)
  108 FORMAT('*************NACA 00 SERIES AIRFOILS*************'//)
  109 FORMAT(' A1=',F10.5/' A2=',F10.5/' A3=',F10.5/' A4=',F10.5/
     X       ' B1=',F10.5/' M=',F10.5/' PE=',F10.5/' X4=',F10.5/
     X       ' PSI4=',F10.5/' DPSI=',F10.5/' DETA=',F10.5/' T0=',F10.5/
     X       ' DTAU=',F10.5/' TAUMAX=',F10.5/' ANG0=',F10.5/
     X       ' DANG=',F10.5/' ANGMAX=',F10.5/' GAMMA=',F10.5/
     X       ' XTE=',F10.5/' W=',F10.5/' EPL=',F10.5/' EPNL=',F10.5/
     X       ' EP=',F10.5/' WFAR=',F10.5/' IFLOW=',I6/
     X       ' IFOIL=',I6/' IPARM0=',I6/
     X       ' N1=',I6/' L1=',I6/' IMAX=',I6/' K=',I6/' LLOW=',I6//)
  110 FORMAT('  CRITICAL PRESSURE COEFF=',F9.5//)
  111 FORMAT(30X,'CHECK OF INPUT PARAMETERS'/)
  112 FORMAT(F9.6)
      STOP
      END
```

```
      SUBROUTINE    LIFT(A,B,C,D,E,F,ZZ,PRE,COR,ERR,GM,H,W,DTAU,K,
     X                   DANG,ANGO,TO,WFAR)
C
C     ***************************************************************
C     *THE SUBROUTINE DEFINES THE TRIDIAGONAL COEFFICIENTS USED TO  *
C     *COMPUTE THE FLOW FIELD. THE COEFFICIENTS ARE DEFINED IN SUCH A*
C     *MANNER TO SATISFY THE TANGENCY, KUTTA, AND FAR FIELD CONDITIONS.*
C     *THE AIRFOIL LOADS ARE ALSO OUTPUTTED FROM THIS SUBROUTINE.   *
C     ***************************************************************
C
      REAL M,MU,LOWCP,LOWSUR
      COMMON MU(51,22),PHI(51,22,5),G(51,22,5),UPSUR(51),LOWSUR(51),
     X       UPCP(51),LOWCP(51),DG(51),DPHI(51),XX(51),XP(51),F2(51)
      COMMON A1,A2,A3,A4,B1,X4,PSI4,DETA,DPSI,XTE,PSITE,FTE,DGT,DPHIT,
     X       M,BM,BBM,PE,GAM,THIK,ATTAK,TAUMAX,ANGMAX,EPL,EPNL,EP
      COMMON N1,L1,NP1,LP1,LUP,LLOW,NTE,IFLOW,IFOIL,IPARM0,IPARM,
     X       IMAX,KMAX
      DIMENSION A(LP1), B(LP1), C(LP1), D(LP1), E(LP1), F(LP1), ZZ(LP1),
     X          PRE(NP1,LP1), COR(NP1,LP1), ERR(NP1,LP1), GM(NP1,LP1),
     X          H(LP1)
      DATA PI/3.141593/
C
      IPARM= IPARM0
C
      WRITE(6,112) LLOW,LUP
C
C     COMPUTE SPACING IN THE LATERAL DIRECTION
C
      ETA= -1.+ DETA
      DO 17 L= 2,L1
      ZZ(L)= A1*TAN(.5*PI*ETA)
      ETA= ETA+ DETA
   17 CONTINUE
C
C     CALCULATE GRID GROWTH FACTORS IN THE LATERAL DIRECTION
C
```

```
      CALL ZGROWU(H)
C
C     CHOOSE INITIAL THICKNESS RATIO AND ANGLE OF ATTACK
C
      TAU= TO
      ANG= ANGO
      THIK= TAU
      ATTAK= ANG
C
C     INITIALIZE FLAG CONDITIONS
      ITER= 1
C
C     DEFINE OFTEN USED CONSTANTS
      T1= (M**PE)*(GAM+ 1.)
      T2= 1./DPSI
      T3= 1./(DPSI**2)
      T4= 1./(DETA**2)
      T5= 1./W
      T6= 1.- 1./W
      T7= 1./DETA
      T8= ((PSI4+ DPSI- PSITE)/(PSITE- PSI4+ DPSI))**2
      T9= (PSITE- PSI4)/DPSI
      IF(IPARM .EQ. 1) EPS= EPNL
      IF(IPARM .EQ. 2) EPS= EPL
      INC= 2
C
C     SPECIFY BASE SOLUTION FROM FLAT PLATE OR INITIAL SINGULARITY
C     DISTRIBUTION
C
      CALL BASES(J1,ZZ,K,TAU,DTAU)
C
C     PRINT LINEARIZED PRESSURE DATA
C
      WRITE(6,100)
      WRITE(6,101) J1
      WRITE(6,102)
```

```
      WRITE(6,106)
      WRITE(6,110)
      WRITE(6,111)
      DO 1 N= 1,J1
      DCP= LOWCP(N)- UPCP(N)
    1 WRITE(6,103) XP(N),UPCP(N),LOWCP(N),DCP
C
    2 CALL DELG(H,T9,ANG,TAU,1)
      DGF= 0.
C
C     COMPUTE THE FLOW FIELD USING COLUMN RELAXATION AND MARCHING
C     FROM THE UPSTREAM BOUNDARY TO THE DOWNSTREAM BOUNDARY
C
      GL= -.75
      GU= -.25
    4 GLL= DGF*GL
      GUU= DGF*GU
      WRITE(6,114) DPHIT,DGT,DGF,GLL,GUU,IPARM
      DO 5 N= 2,N1
C
C     SET HALF-SPACE GRID GROWTH FACTORS IN THE STREAMWISE DIRECTION
C
      FF= .5*(F2(N+1)+ F2(N))
      FB= .5*(F2(N-1)+ F2(N))
      FH= 0.
      IF(N .GT. 2) FH= .5*(F2(N-2)+ F2(N-1))
C
C     COMPUTE THE FLOW FIELD ALONG N= CONSTANT COLUMNS
C
      DO 6 L= 2,L1
C
C     SET HALF-SPACE GRID GROWTH FACTORS IN THE LATERAL DIRECTION
C
      HF= .5*(H(L+1)+ H(L))
      HB= .5*(H(L-1)+ H(L))
C
```

```
C     SET TRIDIAGONAL COEFFICIENT ARRAYS
C
      AL1= F2(N)*FF*T3*(BBM- T1*FF*T2*(PHI(N+1,L,KMAX)-PHI(N,L,KMAX)))
      AL2= F2(N)*FB*T3*(BBM+ T1*FB*T2*(PHI(N-1,L,KMAX)-PHI(N,L,KMAX)))
C
C     CONDITIONS AT UPSTREAM INFINITY
C
      IF(N .NE. 2) GO TO 7
      A(L) = H(L)*HB*T4
      B(L) = H(L)*(HF+ HB)*T4+ AL1*T5
      C(L) = H(L)*HF*T4
      D(L) = AL1*(G(N+1,L,K)- T6*G(N,L,K))
      GO TO 6
C
C     CONDITIONS AT DOWNSTREAM INFINITY
C
    7 IF(N .NE. N1) GO TO 9
      A(L)= H(L)*HB*T4
      B(L) = H(L)*(HF+ HB)*T4+ AL2*T5
      C(L)= H(L)*HF*T4
      D(L) = AL2*(G(N-1,L,KMAX)-T6*G(N,L,K))
      GO TO 6
C
C     INTERIOR OF FLOW FIELD
C
    9 AL3= F2(N)*FH*T3*(BBM- T1*FH*T2*(PHI(N-1,L,KMAX)-PHI(N-2,L,KMAX)))
      A(L)= H(L)*HB*T4
      B(L)= H(L)*(HB+ HF)*T4+ (1.- MU(N,L))*T5*(AL1+ AL2)-
     X       EP*F2(N)*FB*T3*MU(N,L)
      C(L)= H(L)*HF*T4
      D(L)= (1.- MU(N,L))*AL1*G(N+1,L,K)+
     X       ((1.- MU(N,L))*AL2- EP*F2(N)*FB*T3*MU(N,L))*G(N-1,L,KMAX)-
     X       (MU(N-1,L)*(AL2+ AL3)- EP*F2(N)*FB*T3*MU(N,L))*
     X       G(N-1,L,K)- ((1.- MU(N,L))*(AL1+ AL2)*T6- MU(N-1,L)*AL2+
     X       EP*F2(N)*FB*T3*MU(N,L))*G(N,L,K)
      IF(MU(N-1,L) .GT. .5) D(L)= D(L)+ MU(N-1,L)*AL3*G(N-2,L,K)
```

```
C
    6 CONTINUE
C
C       SATISFY PROFILE TANGENCY CONDITIONS
C
        IF(XX(N) .LT. -XTE) GO TO 8
        IF(XX(N) .GT. XTE) GO TO 10
        B(LLOW)= B(LLOW)- .5*H(LLOW)*(H(LLOW) + H(LLOW+1))*T4
        C(LLOW)= 0.
        CALL PROTAN(GETA,N,1,TAU)
        D(LLOW)= D(LLOW)+ H(LLOW)*T7*GETA
C
        A(LUP)= 0.
        B(LUP)= B(LUP)- .5*H(LUP)*(H(LUP)+ H(LUP-1))*T4
        CALL PROTAN(GETA,N,2,TAU)
        D(LUP)= D(LUP)- H(LUP)*T7*GETA
        GO TO 8
C
C       SATISFY THE KUTTA CONDITION
C
   10 IF(MU(NTE,LUP) .GT. .5) GO TO 30
        IF(N .GT. NTE+1) GO TO 43
        CALL DELG(H,T9,ANG,TAU,1)
        DGF= DGF- WFAR*(DGF- DGT)
        DGN= T8*DG(NTE-1)+ (1.- T8)*DGT
C
   43 D(LLOW)= D(LLOW)- .5*H(LLOW)*(H(LLOW) + H(LUP))*T4*DGN
        D(LUP)= D(LUP)+ .5*H(LUP)*(H(LUP)+ H(LLOW))*T4*DGN
        GO TO 8
C
C       CONDITIONS AT SUPERSONIC TRAILING EDGES
C
   30 D(LLOW)= D(LLOW)- .5*H(LLOW)*(H(LLOW)+ H(LLOW+1))*T4*DG(NTE+1)
        D(LUP)= D(LUP)+ .5*H(LUP)*(H(LUP)+ H(LUP-1))*T4*DG(NTE+1)
C
C       APPLY THE CORRECT CONDITIONS ON THE UPPER AND LOWER BOUNDARIES
```

```
C      OF THE COMPUTATIONAL DOMAIN
C
    8 G(N,1,KMAX)= GLL
      G(N,LP1,KMAX)= GUU
C
      D(2)= D(2) + A(2)*G(N,1,KMAX)
      A(2)= 0.
      D(L1)= D(L1) + C(L1)*G(N,LP1,KMAX)
      C(L1)= 0.
      CALL TRISOL(A,B,C,D,E,F,N)
C
    5 CONTINUE
C
C     FIND THE MAXIMUM ERROR
C
      DO 11 L= 1,LP1
      DO 11 N= 2,N1
   11 GM(N,L)= ABS(T5*(G(N,L,KMAX)-G(N,L,K)))
C
      AM= GM(2,1)
      DO 29 L= 1,LP1
      DO 29 N= 2,N1
      IF(GM(N,L) .LE. AM) GO TO 29
      AM= GM(N,L)
      IN= N
      IL= L
   29 CONTINUE
C
C     TIME HISTORY OF CONVERGENCE
C
      WRITE(6,113) ITER,IN,IL,AM
C
      IF( AM .GT. EPS) GO TO 12
C
      GO TO 13
   12 ITER= ITER+ 1
```

```
C
C     IF FLAG CONDITIONS ARE MET, END THE COMPUTATIONAL PROCEDURE
C
      IF(ITER .GT. IMAX) GO TO 14
C
      DO 15 L= 1,LP1
      DO 15 N= 2,N1
   15 G(N,L,K)= G(N,L,KMAX)
      GO TO 4
C
   13 WRITE(6,104) TAU,ANG,ITER
      ITER= 1
C
C     CORRECT THE FLOW FIELD FOR THICKNESS RATIO VARIATIONS
C
      IF(IPARM .EQ. 2) GO TO 34
      IF(TAU .LT. TO+ .5*DTAU) GO TO 18
      CALL PREDCO(2,K,DTAU,PRE,COR,ERR,H,TAU,TO,TAU,ANG,CL,CMLE,J1,ZZ)
C
C     OUTPUT AIRFOIL LOADS
C
      WRITE(6,105)
      WRITE(6,102)
      WRITE(6,106)
      WRITE(6,110)
      WRITE(6,111)
      DO 19 N= 1,J1
      DCP= LOWCP(N)- UPCP(N)
   19 WRITE(6,103) XP(N),UPCP(N),LOWCP(N),DCP
      WRITE(6,108) CL,CMLE
      GO TO 18
C
   32 IF(TAUMAX .LT. TO+ .5*DTAU) GO TO 20
      EPS= EPNL
      INC= 1
C
```

```
   18 IPARM= 1
      THIK= TAU
      IF(INC .NE. 1) TAU= TAU+ DTAU
      ANG= ATTAK
      IF(TAU .GT. TAUMAX+ .5*DTAU .AND. IPARM0 .EQ. 2) GO TO 20
      IF(TAU .GT. TAUMAX+ .5*DTAU) GO TO 31
C
C     UPDATE AND PREDICT FLOW FIELD FOR THICKNESS  RATIO VARIATIONS
C
      DO 16 KS= 2,KMAX
      DO 16 L= 1,LP1
      DO 16 N= 1,NP1
   16 PHI(N,L,KS-1)= PHI(N,L,KS)
C
      DO 28 KS= 2,KMAX
      DO 28 L= 1,LP1
      DO 28 N= 2,N1
   28 G(N,L,KS-1)= G(N,L,KS)
C
      IF(INC .NE. 1)
     XCALL PREDCO(1,K,DTAU,PRE,COR,ERR,H,TAU,TO,TAU,ANG,CL,CMLE,J1,ZZ)
      INC= 2
      GO TO 2
C
C     CORRECT THE FLOW FIELD FOR ANGLE OF ATTACK VARIATIONS
C
   34 IF(ABS(ANG) .LT. ABS(ANGO+ .5*DANG)) GO TO 35
      CALL PREDCO(2,K,DANG,PRE,COR,ERR,H,ANG,ANGO,TAU,ANG,CL,CMLE,J1,ZZ)
C
C     OUTPUT AIRFOIL LOADS
C
      WRITE(6,105)
      WRITE(6,102)
      WRITE(6,106)
      WRITE(6,110)
      WRITE(6,111)
```

```
      DO 36 N= 1,J1
      DCP= LOWCP(N)- UPCP(N)
   36 WRITE(6,103) XP(N),UPCP(N),LOWCP(N),DCP
      WRITE(6,108) CL,CMLE
C
      GO TO 35
   31 IF(ABS(ANGMAX) .LT. ABS(ANGO+ .5*DANG)) GO TO 20
      EPS= EPL
      INC= 1
C
C     UPDATE AND PREDICT THE FLOW FIELD FOR ANGLE OF ATTACK VARIATIONS
C
   35 IPARM= 2
      ATTAK= ANG
      IF(INC .NE. 1) ANG= ANG+ DANG
      TAU= THIK
      AB1= ABS(ANG)
      AB2= ABS(ANGMAX+ .5*DANG)
      IF(AB1 .GT. AB2 .AND. IPARM0 .EQ. 1) GO TO 20
      IF(AB1 .GT. AB2) GO TO 32
C
      DO 37 KS= 2,KMAX
      DO 37 L= 1,LP1
      DO 37 N= 1,NP1
   37 PHI(N,L,KS-1)= PHI(N,L,KS)
C
      DO 38 KS= 2,KMAX
      DO 38 L= 1,LP1
      DO 38 N= 2,N1
   38 G(N,L,KS-1)= G(N,L,KS)
C
      IF(INC .NE. 1)
     XCALL PREDCO(1,K,DANG,PRE,COR,ERR,H,ANG,ANGO,TAU,ANG,CL,CMLE,J1,ZZ)
      INC= 2
      GO TO 2
C
```

```
 14 WRITE(6,107)
100 FORMAT('1',11X,'LINEARIZED PROFILE PRESSURE COEFFICIENTS'//)
101 FORMAT(2X,'NUMBER OF POINTS ON THE AIRFOIL PROFILE=',I4/)
102 FORMAT(15X,'X',14X,'UPPER',13X,'LOWER')
103 FORMAT(F18.3,3F18.5)
104 FORMAT('1','AIRFOIL THICKNESS RATIO=',F6.4,2X,
   X       'ANGLE OF ATTACK=',F12.5,2X,
   X       'SOLUTION CONVERGED IN',I5,' ITERATIONS'/)
105 FORMAT(6X,'     TRANSONIC PROFILE PRESSURE COEFFICIENTS'//)
106 FORMAT(15X,'-',13X,'PROFILE',11X,'PROFILE')
107 FORMAT('1','<<<<<<<<<<<<<SOLUTION DID NOT CONVERGE>>>>>>>>>>>>>')
108 FORMAT(/' LIFT COEFFICIENT= ',F10.5,2X,
   X          ' MOMENT COEFFICIENT ABOUT LEADING EDGE= ',F10.5/)
110 FORMAT(15X,'C',12X,'PRESSURE',10X,'PRESSURE',12X,'DELTA')
111 FORMAT(30X,'COEFF',13X,'COEFF',14X,'CP'/)
112 FORMAT(' LOWER PROFILE LINE=',I4,2X,' UPPER PROFILE LINE=',I4/)
113 FORMAT(1X,3I6,F18.6)
114 FORMAT(1X,5F18.6,I8)
 20 RETURN
    END
```

```
      SUBROUTINE TRISOL(A,B,C,D,E,F,N)
C
C
C     ***********************************************************************
C     *THIS SUBROUTINE SOLVES A SYSTEM OF TRIDIAGONAL EQUATIONS             *
C     ***********************************************************************
C
      REAL M,MU,LOWCP,LOWSUR
      COMMON MU(51,22),PHI(51,22,5),G(51,22,5),UPSUR(51),LOWSUR(51),
     X       UPCP(51),LOWCP(51),DG(51),DPHI(51),XX(51),XP(51),F2(51)
      COMMON A1,A2,A3,A4,B1,X4,PSI4,DETA,DPSI,XTE,PSITE,FTE,DGT,DPHIT,
     X       M,BM,BBM,PE,GAM,THIK,ATTAK,TAUMAX,ANGMAX,EPL,EPNL,EP
      COMMON N1,L1,NP1,LP1,LUP,LLOW,NTE,IFLOW,IFOIL,IPARM0,IPARM,
     X       IMAX,KMAX
      DIMENSION A(LP1),B(LP1),C(LP1),D(LP1),E(LP1),F(LP1)
C
C     COMPUTE THE FLOW FIELD OUT OF THE PLANE OF THE AIRFOIL
C
      L2= LP1- 2
C
      IF(ABS(XX(N)) .LT. XTE) GO TO 1
C
C     SATISFY FAR FIELD CONDITION
C
      E(1)= 0.
      F(1)= G(N,1,KMAX)
C
C     CALCULATE TRIDIAGONAL COEFFICIENTS
C
      DO 2 L= 2,L1
      DEN= B(L)- A(L)*E(L-1)
      E(L)= C(L)/DEN
    2 F(L)= (D(L)+ A(L)*F(L-1))/DEN
C
C     CALCULATE FLOW FIELD
C
```

```
      DO 3 L= 1,L2
      LL= LP1- L
    3 G(N,LL,KMAX)= E(LL)*G(N,LL+1,KMAX)+ F(LL)
      RETURN
C
C     CALCULATE THE FLOW FIELD IN THE PLANE OF THE AIRFOIL
C
    1 L3= LLOW- 1
      L2= LLOW+ 1
C
C     SATISFY THE LOWER BOUNDARY TANGENCY CONDITION
C
      E(LLOW)= A(LLOW)/B(LLOW)
      F(LLOW)= D(LLOW)/B(LLOW)
C
C     CALCULATE THE TRIDIAGONAL COEFFICIENTS BELOW THE AIRFOIL
C
      DO 5 L= 2,L3
      LL= L2- L
      DEN= B(LL)- C(LL)*E(LL+1)
      E(LL)= A(LL)/DEN
    5 F(LL)= (D(LL)+ C(LL)*F(LL+1))/DEN
C
C     CALCULATE THE FLOW FIELD BELOW THE AIRFOIL
C
      DO 6 L= 2,LLOW
    6 G(N,L,KMAX)= E(L)*G(N,L-1,KMAX)+ F(L)
C
      L3= LP1- LUP
      L2= LUP+ 1
C
C     SATISFY THE UPPER BOUNDARY TANGENCY CONDITION
C
      E(LUP)= C(LUP)/B(LUP)
      F(LUP)= D(LUP)/B(LUP)
C
```

```
C     CALCULATE THE TRIDIAGONAL COEFFICIENTS ABOVE THE AIRFOIL
C
      DO 7 L= L2,L1
      DEN= B(L)- A(L)*E(L-1)
      E(L) = C(L)/DEN
    7 F(L)= (D(L) + A(L)*F(L-1))/DEN
C
C     CALCULATE THE FLOW FIELD ABOVE THE AIRFOIL
C
      DO 8 L= 1,L3
      LL= LP1- L
    8 G(N,LL,KMAX) = E(LL)*G(N,LL+1,KMAX) + F(LL)
C
      RETURN
      END
```

```
      SUBROUTINE BASES(J1,ZZ,K,TAU,DTAU)
C
C     ******************************************************************
C     *THIS SUBROUTINE APPROXIMATES THE SOLUTION OF THE STEADY NONLIFT- *
C     *ING TRANSONIC FLOW PROBLEM WITH A DISTRIBUTION OF SOURCES AND    *
C     *SINKS ALONG THE AIRFOIL CHORD                                    *
C     ******************************************************************
C
      REAL M,MU,LOWCP,LOWSUR
      COMMON MU(51,22),PHI(51,22,5),G(51,22,5),UPSUR(51),LOWSUR(51),
     X       UPCP(51),LOWCP(51),DG(51),DPHI(51),XX(51),XP(51),F2(51)
      COMMON A1,A2,A3,A4,B1,X4,PSI4,DETA,DPSI,XTE,PSITE,FTE,DGT,DPHIT,
     X       M,BM,BBM,PE,GAM,THIK,ATTAK,TAUMAX,ANGMAX,EPL,EPNL,EP
      COMMON N1,L1,NP1,LP1,LUP,LLOW,NTE,IFLOW,IFOIL,IPARM0,IPARM,
     X       IMAX,KMAX
      DIMENSION ZZ(LP1)
      DATA PI/3.141593/
C
C     DEFINE OFTEN USED CONSTANTS
C
      J= 1
      A5= TAU/(BM*PI)
      A7= XTE**2
      A8= 1./(BM*PI)
C
      DO 1 N= 2,N1
C
C     DEFINE OFTEN USED CONSTANTS
C
      T1= XX(N)- XTE
      T2= T1**2
      T3= XX(N)+ XTE
      T4= T3**2
      T5= -XX(N)**2
C
C     PUT IN THE AIRFOIL PROFILE
```

```
C
      ZU= 2.*TAU*(XTE**2- XX(N)**2)
      ZL=-2.*TAU*(XTE**2- XX(N)**2)
      IF(ABS(XX(N)) .GE. XTE) ZU= 0.
      IF(ABS(XX(N)) .GE. XTE) ZL= 0.
C
      DO 2 L= 2,L1
      ZB= BM*ZZ(L)
      A6= ZB**2
      T6= (T5+ A7+ A6)*ALOG((T2+ A6)/(T4+ A6))- 4.*XX(N)*ZB*
     X     (ATAN(T1/ZB)- ATAN(T3/ZB))- 2.*XX(N)
C
C     COMPUTE THE POTENTIAL
C
      PHI(N,L,KMAX)= -A5*T6
C
C     COMPUTE LINEARIZED SURFACE PRESSURE COEFFICIENTS
C
      IF(L .NE. LUP .OR. ABS(XX(N)) .GT. XTE) GO TO 8
      XP(J)= .5*(XX(N)+ XTE)/XTE
      A9= BBM*ZU**2
      A10= BM*ZU
      IF(TAU .LT. .5*DTAU) UPCP(J)= 0.
      IF(TAU .LT. .5*DTAU) GO TO 5
      UPCP(J)= 2.*A5*(4.*A10*(ATAN(T3/A10)- ATAN(T1/A10))- 4.*
     X          2.*XX(N)*ALOG((T4+ A9)/(T2+ A9)))
    5 LOWCP(J)=  UPCP(J)
      J= J+1
C
C     SET INITIAL GUESS FOR G
C
    8 G(N,L,K)= -A8*T6
      IF(IPARM .EQ. 2) G(N,L,K)= 0.
C
    2 CONTINUE
    1 CONTINUE
```

```
J1= J-1
RETURN
END
```

```
      SUBROUTINE PROTAN(GETA,N,I,TAU)
C
C     ****************************************************************
C     *THIS SUBROUTINE DEFINES THE APPROPRIATE CONDITIONS ON THE      *
C     *BOUNDARY OF VARIOUS AIRFOILS                                   *
C     ****************************************************************
C
      REAL M,MU,LOWCP,LOWSUR
      COMMON MU(51,22),PHI(51,22,5),G(51,22,5),UPSUR(51),LOWSUR(51),
     X       UPCP(51),LOWCP(51),DG(51),DPHI(51),XX(51),XP(51),F2(51)
      COMMON A1,A2,A3,A4,B1,X4,PSI4,DETA,DPSI,XTE,PSITE,FTE,DGT,DPHIT,
     X       M,BM,BBM,PE,GAM,THIK,ATTAK,TAUMAX,ANGMAX,EPL,EPNL,EP
      COMMON N1,L1,NP1,LP1,LUP,LLOW,NTE,IFLOW,IFOIL,IPARM0,IPARM,
     X       IMAX,KMAX
C
      IF(IPARM .EQ. 2) GO TO 1
      IF(I .EQ. 1) GO TO 2
C     SET TANGENCY CONDITIONS FOR THICKNESS VARIATIONS
C
C
C     SET UPPER BOUNDARY TANGENCY CONDITIONS
C
C     DEFINE THE TANGENCY CONDITION FOR PARABOLIC ARC AIRFOILS
C
      IF(IFOIL .EQ. 1) GETA= -4.*XX(N)
C
C     DEFINE THE TANGENCY CONDITION FOR CIRCULAR ARC AIRFOILS
C
      IF(IFOIL .EQ. 2)
     X  GETA= -4.*XX(N)/(SQRT((1.+ TAU**2)**2- 16.*(TAU*XX(N))**2))+
     X         8.*XX(N)*TAU**2*(1.+ TAU**2- 8.*XX(N)**2)/
     X         ((SQRT((1.+ TAU**2)**2- 16.*(TAU*XX(N))**2))**3)
C
C     DEFINE THE TANGENCY CONDITION FOR NACA 00 SERIES AIRFOILS
C
      IF(IFOIL .EQ. 3)
```

```
     X  GETA= 5.*(.14845/SQRT(XX(N)+ .5) - 1.26 - .7032*(XX(N) + .5)+
     X         .8529*(XX(N)+ .5)**2- .406*(XX(N) + .5)**3)
      RETURN
C
C     SET LOWER BOUNDARY TANGENCY CONDITIONS
C
C     DEFINE TANGENCY CONDITION FOR PARABOLIC ARC AIRFOILS
C
    2 IF(IFOIL .EQ. 1) GETA=  4.*XX(N)
C
C     DEFINE TANGENCY CONDITION FOR CIRCULAR ARC AIRFOILS
C
      IF(IFOIL .EQ. 2)
     X  GETA=  4.*XX(N)/(SQRT((1.+ TAU**2)**2- 16.*(TAU*XX(N))**2))+
     X         8.*XX(N)*TAU**2*(1.+ TAU**2- 8.*XX(N)**2)/
     X         ((SQRT((1.+ TAU**2)**2- 16.*(TAU*XX(N))**2))**3)
C
C     DEFINE TANGENCY CONDITION FOR NACA 00 SERIES AIRFOILS
C
      IF(IFOIL .EQ. 3)
     X  GETA=-5.*(.14845/SQRT(XX(N)+ .5) - 1.26 - .7032*(XX(N) + .5)+
     X         .8529*(XX(N)+ .5)**2- .406*(XX(N)+ .5)**3)
      RETURN
C
C     SET TANGENCY CONDITION FOR ANGLE OF ATTACK VARIATIONS
C
    1 GETA= 1.
C
      RETURN
      END
```

```
      SUBROUTINE DELG(H,T1,ANG,TAU,IRET)
C
C     ****************************************************************
C     *THIS SUBROUTINE COMPUTES THE JUMP IN G ACROSS THE AIRFOIL, AND   *
C     *AN  ENTRAPOLATION PROCEDURE IS USED TO FIND THE JUMP AT THE      *
C     *TRAILING EDGE.                                                   *
C     ****************************************************************
C
      REAL M,MU,LOWCP,LOWSUR
      COMMON MU(51,22),PHI(51,22,5),G(51,22,5),UPSUR(51),LOWSUR(51),
     X       UPCP(51),LOWCP(51),DG(51),DPHI(51),XX(51),XP(51),F2(51)
      COMMON A1,A2,A3,A4,B1,X4,PSI4,DETA,DPSI,XTE,PSITE,FTE,DGT,DPHIT,
     X       M,BM,BBM,PE,GAM,THIK,ATTAK,TAUMAX,ANGMAX,EPL,EPNL,EP
      COMMON N1,L1,NP1,LP1,LUP,LLOW,NTE,IFLOW,IFOIL,IPARMU,IPARM,
     X       IMAX,KMAX
      DIMENSION H(LP1)
C
      T= 2./(H(LLOW) + H(LUP))
      NT= NTE+ 1
C
      DO 1 N= 2,N1
      IF(XX(N) .GT. XTE) GO TO 10
      IF(ABS(XX(N)) .GT. XTE) GO TO 1
      IF(IFOIL .NE. 1) GO TO 4
      IF(IPARM .EQ. 2) GO TO 2
C
C     DEFINE TANGENCY CONDITIONS IN PHYSICAL AND PARAMETER SPACE FOR
C     PARABOLIC ARC AIRFOILS
C
      GETAU= -4.*T*XX(N)
      GETAL= 4.*T*XX(N)
      GO TO 3
    2 GETAU= T
      GETAL= T
    3 PHETAU= -T*(4.*TAU*XX(N)- ANG)
      PHETAL= T*(4.*TAU*XX(N)+ ANG)
```

```
      GO TO 9
C
    4 IF(IFOIL .NE. 2) GO TO 7
      IF(IPARM .EQ. 2) GO TO 5
C
C     DEFINE TANGENCY CONDITIONS IN PHYSICAL AND PARAMETER
C     SPACE FOR CIRCULAR ARC AIRFOILS
C
      GETAU=  T*XX(N)*(-4./SQRT((1.+ TAU**2)**2- 16.*(TAU*XX(N))**2)+
     X        8.*TAU**2*(1.+ TAU**2- 8.*XX(N)**2)/
     X        ((SQRT((1.+ TAU**2)**2- 16.*(TAU*XX(N))**2))**3))
C
      GETAL= -T*XX(N)*(-4./SQRT((1.+ TAU**2)**2- 16.*(TAU*XX(N))**2)+
     X        8.*TAU**2*(1.+ TAU**2- 8.*XX(N)**2)/
     X        ((SQRT((1.+ TAU**2)**2- 16.*(TAU*XX(N))**2))**3))
      GO TO 6
    5 GETAU= T
      GETAL= T
    6 PHETAU= -T*(4.*TAU*XX(N)/SQRT((1.+ TAU**2)**2-
     X         16.*(TAU*XX(N))**2)- ANG)
      PHETAL=  T*(4.*TAU*XX(N)/SQRT((1.+ TAU**2)**2-
     X         16.*(TAU*XX(N))**2)+ ANG)
      GO TO 9
C
    7 IF(IPARM .EQ. 2) GO TO 8
C
C     DEFINE TANGENCY CONDITIONS IN PHYSICAL AND PARAMETER
C     SPACE FOR NACA 00 SERIES AIRFOILS
C
      GETAU=  5.*T*(.14845/SQRT(XX(N)+ XTE)- 1.26- .7032*(XX(N)+ XTE)+
     X        .8529*(XX(N)+ XTE)**2- .406*(XX(N)+ XTE)**3)
      GETAL= -5.*T*(.14845/SQRT(XX(N)+ XTE)- 1.26- .7032*(XX(N)+ XTE)+
     X        .8529*(XX(N)+ XTE)**2- .406*(XX(N)+ XTE)**3)
    8 GETAU= T
      GETAL= T
C
```

```
      PHETAU=  5.*T*TAU*(.14845/SQRT(XX(N)+ XTE)- 1.26- .7032*(XX(N)+
     X         XTE)+ .8529*(XX(N)+ XTE)**2- .406*(XX(N)+ XTE)**3)+
     X         T*ANG
      PHETAL= -5.*T*TAU*(.14845/SQRT(XX(N)+ XTE)- 1.26- .7032*(XX(N)+
     X         XTE)+ .8529*(XX(N)+ XTE)**2- .406*(XX(N)+ XTE)**3)+
     X         T*ANG
C
C     COMPUTE THE JUMPS ALONG THE AIRFOIL
C
    9 DG(N)= .125*(9.*(G(N,LUP,KMAX)- G(N,LLOW,KMAX))- G(N,LUP+1,KMAX)+
     X       G(N,LLOW-1,KMAX)- 3.*DETA*(GETAU+ GETAL))
C
      DPHI(N)= .125*(9.*(PHI(N,LUP,KMAX)- PHI(N,LLOW,KMAX))-
     X         PHI(N,LUP+1,KMAX)+ PHI(N,LLOW-1,KMAX)- 3.*DETA*
     X         (PHETAU+ PHETAL))
    1 CONTINUE
C
C     CALCULATE JUMPS AT THE TRAILING EDGE
C
   10 DPHIT= (1.+ 1.5*T1)*DPHI(NTE)- 2.*T1*DPHI(NTE-1)+
     X        .5*T1*DPHI(NTE-2)
      DGT= (1.+ 1.5*T1)*DG(NTE)- 2.*T1*DG(NTE-1)+ .5*T1*DG(NTE-2)
C
      IF(IRET .EQ. 1) RETURN
C
C     CALCULATE JUMPS JUST AFT OF THE TRAILING EDGE
C
      DPHI(NT)= 2.*(PHI(NT,LUP,KMAX)- PHI(NT,LLOW,KMAX))-
     X          .125*(-13.*(PHI(NT,LUP+1,KMAX)- PHI(NT,LLOW-1,KMAX))+
     X          6.*(PHI(NT,LUP+2,KMAX)- PHI(NT,LLOW-2,KMAX))-
     X          PHI(NT,LUP+3,KMAX)+ PHI(NT,LLOW-3,KMAX))
C
      DG(NT)= 2.*(G(NT,LUP,KMAX)- G(NT,LLOW,KMAX))-
     X        .125*(-13.*(G(NT,LUP+1,KMAX)- G(NT,LLOW-1,KMAX))+
     X        6.*(G(NT,LUP+2,KMAX)- G(NT,LLOW-2,KMAX))-
     X        G(NT,LUP+3,KMAX)+ G(NT,LLOW-3,KMAX))
```

```
C
      RETURN
      END
```

```
      SUBROUTINE PREDCO(IOPT,K,DTAU,PRE,COR,ERR,H,TAU,T0,TA,AN,CL,CMLE,
     X                  J1,ZZ)
C
C     ******************************************************************
C     *THIS SUBROUTINE PREDICTS THE NEW POTENTIALS AND THEN CORRECTS    *
C     *THEM.  AFTER THIS IS DONE, THE SURFACE POTENTIALS ARE FOUND USING*
C     *AN EXTRAPOLATION PROCEDURE AND THE FORCES AND MOMENTS ON THE     *
C     *AIRFOILS ARE COMPUTED.  THE PREDICTED AND CORRECTED SONIC LINES  *
C     *ARE ALSO COMPUTED.                                               *
C     ******************************************************************
C
      REAL M,MU,LOWCP,LOWSUR
      COMMON MU(51,22),PHI(51,22,5),G(51,22,5),UPSUR(51),LOWSUR(51),
     X       UPCP(51),LOWCP(51),DG(51),DPHI(51),XX(51),XP(51),F2(51)
      COMMON A1,A2,A3,A4,B1,X4,PSI4,DETA,DPSI,XTE,PSITE,FTE,DGT,DPHIT,
     X       M,BM,BBM,PE,GAM,THIK,ATTAK,TAUMAX,ANGMAX,EPL,EPNL,EP
      COMMON N1,L1,NP1,LP1,LUP,LLOW,NTE,IFLOW,IFOIL,IPARM0,IPARM,
     X       IMAX,KMAX
      DIMENSION PRE(NP1,LP1), COR(NP1,LP1), ERR(NP1,LP1), H(LP1),
     X          ZZ(LP1)
C
      K1= K- 1
      K2= K- 2
      K3= K- 3
C
      XX(1)= -9999.
      XX(NP1)= 9999.
C
C     PREDICT THE NEW POTENTIALS
C
      IF(IOPT .EQ. 2) GO TO 8
C
C     PREDICT THE POTENTIAL USING A SECOND ORDER PREDICTOR
C
      IF (ABS(TAU) .GT. ABS(T0+ 1.5*DTAU)) GO TO 2
      DO 1 L= 1,LP1
```

```
      DO 1 N= 2,N1
      PRE(N,L)= PHI(N,L,K)+ DTAU*G(N,L,K)
    1 PHI(N,L,KMAX)= PRE(N,L)+ .5*ERR(N,L)
      GO TO 38
C
C     PREDICT THE POTENTIAL USING A THIRD ORDER PREDICTOR
C
    2 IF(ABS(TAU) .GT. ABS(T0+ 2.5*DTAU)) GO TO 4
      DO 3 L= 1,LP1
      DO 3 N= 2,N1
      PRE(N,L)= PHI(N,L,K1)+ 2.*DTAU*G(N,L,K)
    3 PHI(N,L,KMAX)= PRE(N,L)+ .8*ERR(N,L)
      GO TO 38
C
C     PREDICT THE POTENTIAL USING A FOURTH ORDER PREDICTOR
C
    4 IF(ABS(TAU) .GT. ABS(T0+ 3.5*DTAU)) GO TO 6
      T= 8./9.
      DO 5 L= 1,LP1
      DO 5 N= 2,N1
      PRE(N,L)= PHI(N,L,K)+ PHI(N,L,K1)- PHI(N,L,K2)+
     X          2.*DTAU*(G(N,L,K)- G(N,L,K1))
    5 PHI(N,L,KMAX)= PRE(N,L)+ T*ERR(N,L)
      GO TO 38
C
C     PREDICT THE POTENTIAL USING A FIFTH ORDER PREDICTOR
C
    6 T1= 4./3.
      T2= 112./121.
      DO 7 L= 1,LP1
      DO 7 N= 2,N1
      PRE(N,L)= PHI(N,L,K3)+ T1*DTAU*(2.*G(N,L,K)- G(N,L,K1)+
     X          2.*G(N,L,K2))
    7 PHI(N,L,KMAX)= PRE(N,L)+ T2*ERR(N,L)
C
C     SATISFY THE UPSTREAM AND DOWNSTREAM CONDITIONS
```

```
C
   38 DO 28 L= 1,LP1
      PHI(1,L,KMAX)= PHI(2,L,KMAX)
   28 PHI(NP1,L,KMAX)= PHI(N1,L,KMAX)
C
      T= .5*(GAM+ 1.)*M**PE/DPSI
      DO 29 L= 1,LP1
      DO 29 N= 2,N1
      MU(N,L) = 0.
      IF(BBM- T*F2(N)*(PHI(N+1,L,KMAX) - PHI(N-1,L,KMAX)) .LT. 0.)
     X    MU(N,L) = 1.
   29 CONTINUE
C
C     CHECK FOR SONIC LINE
C
      DO 33 L= 2,L1
      ZSH= ZZ(L)
      DO 33 N= 2,N1
      XB= XX(N-1)
      XF= XX(N)
      XS= .5*(XX(N-1)+ XX(N))
      IF(MU(N,L) .GT. .5 .AND. MU(N-1,L) .LT. .5)
     X    WRITE(6,101) XB,XF,XS,ZSH
      IF(MU(N,L) .LT. .5 .AND. MU(N-1,L) .GT. .5)
     X    WRITE(6,102) XB,XF,XS,ZSH
   33 CONTINUE
      RETURN
C
C     CORRECT THE POTENTIAL USING A SECOND ORDER CORRECTOR
C
    8 IF(ABS(TAU) .GT. ABS(T0+ 1.5*DTAU)) GO TO 10
      DO 9 L= 1,LP1
      DO 9 N= 2,N1
      COR(N,L) = PHI(N,L,K)+ DTAU*G(N,L,KMAX)
      ERR(N,L)= COR(N,L)- PRE(N,L)
      PHI(N,L,KMAX)= COR(N,L)- .5*ERR(N,L)
```

```
    9 ERR(N,L) = 0.
      GO TO 16
C
C     CORRECT THE POTENTIAL USING A THIRD ORDER CORRECTOR
C
   10 IF(ABS(TAU) .GT. ABS(T0+ 2.5*DTAU)) GO TO 12
      DO 11 L= 1,LP1
      DO 11 N= 2,N1
      COR(N,L) = PHI(N,L,K) + .5*DTAU*(G(N,L,KMAX) + G(N,L,K))
      ERR(N,L) = COR(N,L) - PRE(N,L)
      PHI(N,L,KMAX)= COR(N,L)- .2*ERR(N,L)
   11 ERR(N,L) = 0.
      GO TO 16
C
C     CORRECT THE POTENTIAL USING A FOURTH ORDER CORRECTOR
C
   12 IF(ABS(TAU) .GT. ABS(T0+ 3.5*DTAU)) GO TO 14
      T1= 1./12.
      T2= 1./9.
      DO 13 L= 1,LP1
      DO 13 N= 2,N1
      COR(N,L) = PHI(N,L,K) + T1*DTAU*(5.*G(N,L,KMAX)+ 8.*G(N,L,K)-
     X           G(N,L,K1))
      ERR(N,L) = COR(N,L)- PRE(N,L)
      PHI(N,L,KMAX)= COR(N,L)- T2*ERR(N,L)
   13 ERR(N,L) = 0.
      GO TO 16
C
C     CORRECT THE POTENTIAL USING A FIFTH ORDER CORRECTOR
C
   14 T1= 1./3.
      T2= 1./36.
      T3= 9./121.
      DO 15 L= 1,LP1
      DO 15 N= 2,N1
      COR(N,L) = T1*(PHI(N,L,K) + PHI(N,L,K1) + PHI(N,L,K2)) +
```

```
     X           T2*DTAU*(13.*G(N,L,KMAX)+ 39.*G(N,L,K)+
     X           15.*G(N,L,K1)+ 5.*G(N,L,K2))
      ERR(N,L)= COR(N,L)- PRE(N,L)
      PHI(N,L,KMAX)= COR(N,L)- T3*ERR(N,L)
      IF(IPARM .EQ. 1 .AND. TAU .GT. TAUMAX- .5*DTAU) ERR(N,L)= 0.
      IF(IPARM .EQ. 2 .AND. ABS(TAU) .GT. ABS(ANGMAX- .5*DTAU))
     X   ERR(N,L)= 0.
   15 CONTINUE
C
C     SATISFY THE UPSTREAM AND DOWNSTREAM CONDITIONS
C
   16 DO 19 L= 1,LP1
      PHI(1,L,KMAX)= PHI(2,L,KMAX)
   19 PHI(NP1,L,KMAX)= PHI(N1,L,KMAX)
C
C     COMPUTE THE PROFILE POTENTIALS
C
      T= 2./(H(LLOW)+ H(LUP))
      DO 17 N= 2,N1
      PHETAU= (PHI(N,LUP,KMAX)- PHI(N,LLOW,KMAX))/DETA
      PHETAL= (PHI(N,LUP,KMAX)- PHI(N,LLOW,KMAX))/DETA
      IF(XX(N+1) .LT. -XTE) GO TO 17
      IF(XX(N) .LT. -XTE) GO TO 20
      IF(XX(N) .GT.  XTE) GO TO 22
      IF(IFOIL .NE. 1) GO TO 18
      PHETAU= -T*(4.*TA *XX(N)- AN )
      PHETAL=  T*(4.*TA *XX(N)+ AN )
      GO TO 20
C
   18 IF(IFOIL .NE. 2) GO TO 21
      PHETAU= -T*(4.*TA *XX(N)/SQRT((1.+ TA **2)**2-
     X          16.*(TA *XX(N))**2)- AN )
      PHETAL=  T*(4.*TA *XX(N)/SQRT((1.+ TA **2)**2-
     X          16.*(TA *XX(N))**2)+ AN )
      GO TO 20
C
```

```
   21 PHETAU=  5.*T*TA *(.14845/SQRT(XX(N)+ XTE)- 1.26- .7032*(XX(N)+
     X         XTE)+ .8529*(XX(N)+ XTE)**2- .406*(XX(N)+ XTE)**3)+
     X         T*AN
      PHETAL= -5.*T*TA *(.14845/SQRT(XX(N)+ XTE)- 1.26- .7032*(XX(N)+
     X         XTE)+ .8529*(XX(N)+ XTE)**2- .406*(XX(N)+ XTE)**3)+
     X         T*AN
C
   20 UPSUR(N) = .125*(9.*PHI(N,LUP,KMAX)- PHI(N,LUP+1,KMAX)-
     X          3.*DETA*PHETAU)
      LOWSUR(N)= .125*(9.*PHI(N,LLOW,KMAX)- PHI(N,LLOW-1,KMAX)+
     X          3.*DETA*PHETAL)
   17 CONTINUE
C
C     COMPUTE THE POTENTIAL ALONG THE FLOW FIELD CUT JUST AFT OF THE
C     TRAILING EDGE
C
   22 VAR= (PSITE- PSI4)/DPSI
      CALL DELG(H,VAR,AN,TA,1)
      UPSUR(N)= .125*(9.*PHI(N,LUP,KMAX)- PHI(N,LUP+1,KMAX)-
     X                3.*(PHI(N,LUP,KMAX)- PHI(N,LLOW,KMAX)- DPHIT))
      LOWSUR(N)= .125*(9.*PHI(N,LLOW,KMAX)- PHI(N,LLOW-1,KMAX)+
     X                3.*(PHI(N,LUP,KMAX)- PHI(N,LLOW,KMAX)- DPHIT))
C
      T= .5*(GAM+ 1.)*M**PE/DPSI
      DO 37 L= 1,LP1
      DO 37 N= 2,N1
      MU(N,L)= 0.
      IF(BBM- T*F2(N)*(PHI(N+1,L,KMAX)- PHI(N-1,L,KMAX)) .LT. 0.)
     X   MU(N,L)= 1.
   37 CONTINUE
C
C     CHECK FOR THE ACTUAL SONIC LINE
C
      DO 41 L= 2,L1
      ZSH= ZZ(L)
      DO 41 N= 2,N1
```

```
      XB= XX(N-1)
      XF= XX(N)
      XS= .5*(XX(N-1) + XX(N))
      IF(MU(N,L) .GT. .5 .AND. MU(N-1,L) .LT. .5)
     X   WRITE(6,103) XB,XF,XS,ZSH
      IF(MU(N,L) .LT. .5 .AND. MU(N-1,L) .GT. .5)
     X   WRITE(6,104) XB,XF,XS,ZSH
   41 CONTINUE
C
C     COMPUTE THE PROFILE PRESSURE DISTRIBUTION
C
      J= 1
      DO 24 N= 2,N1
      IF(XX(N) .LT. -XTE) GO TO 24
      IF(XX(N) .GT.  XTE) GO TO 43
      UPCP(J)= -F2(N)*(UPSUR(N+1)- UPSUR(N-1))/DPSI
      LOWCP(J)= -F2(N)*(LOWSUR(N+1)- LOWSUR(N-1))/DPSI
      J= J+ 1
   24 CONTINUE
C
C     COMPUTE THE LIFT COEFFICIENT, CL, AND THE MOMENT COEFFICIENT
C     ABOUT THE LEADING EDGE, CMLE.
C
   43 CL= XP(1)*(LOWCP(1)- UPCP(1))
      CMLE= XP(1)**2*(LOWCP(1)- UPCP(1))
      DO 42 N= 2,J1
      CL= CL+ .5*(XP(N)- XP(N-1))*(LOWCP(N)- UPCP(N)+
     X          LOWCP(N-1)- UPCP(N-1))
   42 CMLE= CMLE+ .5*(XP(N)- XP(N-1))*((LOWCP(N)- UPCP(N))*XP(N)+
     X              (LOWCP(N-1)- UPCP(N-1))*XP(N-1))
      CL= CL+ .5*(1.-XP(J1))*(LOWCP(J1)- UPCP(J1))
      CMLE= CMLE+ .5*(1.- XP(J1))*(LOWCP(J1)- UPCP(J1))*XP(J1)
C
  101 FORMAT(' PREDICTED SONIC LOCUS:',4X,'XBACK=',F10.4,2X,
     X       'XFOR=',F10.4,2X,'XSONIC=',F10.4,2X,'ZSONIC=',F10.4)
  102 FORMAT(' PREDICTED SHOCK LOCUS:',4X,'XBACK=',F10.4,2X,
```

```
     X        'XFOR=',F10.4,2X,'XSHOCK=',F10.4,2X,'ZSHOCK=',F10.4)
  103 FORMAT (' ACTUAL SONIC LOCUS:',4X,'XBACK=',F10.4,2X,
     X        'XFOR=',F10.4,2X,'XSONIC=',F10.4,2X,'ZSONIC=',F10.4)
  104 FORMAT (' ACTUAL SHOCK LOCUS:',4X,'XBACK=',F10.4,2X,
     X        'XFOR=',F10.4,2X,'XSHOCK=',F10.4,2X,'ZSHOCK=',F10.4)
C
       RETURN
       END
```

```
      SUBROUTINE TRAL(XT2)
C
C     ***************************************************************
C     *THIS SUBROUTINE LOCATES THE TRAILING EDGE AND COMPUTES THE    *
C     *STRETCHING FACTOR IN THE STREAMWISE DIRECTION AT THAT LOCATION*
C     ***************************************************************
C
      REAL M,MU,LOWCP,LOWSUR
      COMMON MU(51,22),PHI(51,22,5),G(51,22,5),UPSUR(51),LOWSUR(51),
     X       UPCP(51),LOWCP(51),DG(51),DPHI(51),XX(51),XP(51),F2(51)
      COMMON A1,A2,A3,A4,B1,X4,PSI4,DETA,DPSI,XTE,PSITE,FTE,DGT,DPHIT,
     X       M,BM,BBM,PE,GAM,THIK,ATTAK,TAUMAX,ANGMAX,EPL,EPNL,EP
      COMMON N1,L1,NP1,LP1,LUP,LLOW,NTE,IFLOW,IFOIL,IPARM0,IPARM,
     X       IMAX,KMAX
      DATA PI/3.141593/, TMIN/.00001/
C
      X3(PSI)= X4+ A2*TAN(.5*PI*(PSI-PSI4)) +
     X         A3*TAN(.5*PI*(PSI- PSI4)**3)
C
      SP= DPSI
      PSI= -(1.+ PSI4) + DPSI
      DO 1 N= 2,N1
      IF(XX(N+1) .LT. XTE) GO TO 8
      NTE= N
      XT1= X3(PSI)
      IF(X3(PSI+ DPSI) .GE. XTE) GO TO 2
    8 PSI= PSI+ DPSI
    1 CONTINUE
C
    2 SP= .5*SP
      PSI= PSI+ SP
      PSITE= PSI
    6 XT2= X3(PSI)
      IF(ABS(XT2- XTE) .LE. TMIN) GO TO 9
      IF(XT2 .GT. XTE) GO TO 4
      IF(XT1 .GT. XTE) GO TO 5
```

```
      PSI= PSI+ SP
      PSITE= PSI
      XT1= XT2
      GO TO 6
C
    5 SP= .5*SP
      PSI= PSI+ SP
      PSITE= PSI
      XT1= XT2
      GO TO 6
C
    4 IF(XT1 .GT. XTE) GO TO 7
      XT1= XT2
      SP= .5*SP
      PSI= PSI- SP
      PSITE= PSI
      GO TO 6
C
    7 PSI= PSI- SP
      PSITE= PSI
      XT1= XT2
      GO TO 6
C
    9 FTE= 2./(PI*(A2/((COS(.5*PI*(PSITE- PSI4)))**2)+
     X      3.*A3*(PSITE- PSI4)**2/((COS(.5*PI*(PSITE- PSI4)**3))**2)))
C
      RETURN
      END
```

```
      SUBROUTINE XGROW
C
C     ***************************************************************
C     *THIS SUBROUTINE CALCULATES THE GRID GROWTH FACTORS IN THE      *
C     *STREAMWISE DIRECTION                                          *
C     ***************************************************************
C
      REAL M,MU,LOWCP,LOWSUR
      COMMON MU(51,22),PHI(51,22,5),G(51,22,5),UPSUR(51),LOWSUR(51),
     X       UPCP(51),LOWCP(51),DG(51),DPHI(51),XX(51),XP(51),F2(51)
      COMMON A1,A2,A3,A4,B1,X4,PSI4,DETA,DPSI,XTE,PSITE,FIE,DGT,DPHIT,
     X       M,BM,BBM,PE,GAM,THIK,ATTAK,TAUMAX,ANGMAX,EPL,EPNL,EP
      COMMON N1,L1,NP1,LP1,LUP,LLOW,NTE,IFLOW,IFOIL,IPARM0,IPARM,
     X       IMAX,KMAX
      DATA PI/3.141593/
C
      PSI= -(1.+ PSI4)+ DPSI
      DO 1 N= 2,N1
      IF(PSI .LT. -PSI4)
     X  F2(N)= 2./(PI*(A2/((COS(.5*PI*(PSI+ PSI4)))**2)+
     X          3.*A3*(PSI+ PSI4)**2/((COS(.5*PI*(PSI+ PSI4)**3))**2)))
C
      IF(PSI .GE. -PSI4 .AND. PSI .LE. PSI4)
     X  F2(N)= 1./(A4+ 3.*B1*PSI**2)
C
      IF(PSI .GT. PSI4)
     X  F2(N)= 2./(PI*(A2/((COS(.5*PI*(PSI- PSI4)))**2)+
     X          3.*A3*(PSI- PSI4)**2/((COS(.5*PI*(PSI- PSI4)**3))**2)))
C
      PSI= PSI+ DPSI
    1 CONTINUE
C
      F2(1)= 0.
      F2(NP1)= 0.
C
      RETURN
```

END

```
      SUBROUTINE ZGROWU(H)
C
C     ***************************************************************
C     *THIS SUBROUTINE CALCULATES THE GRID GROWTH FACTORS IN THE      *
C     *LATERAL DIRECTION                                              *
C     ***************************************************************
C
      REAL M,MU,LOWCP,LOWSUR
      COMMON MU(51,22),PHI(51,22,5),G(51,22,5),UPSUR(51),LOWSUR(51),
     X       UPCP(51),LOWCP(51),DG(51),DPHI(51),XX(51),XP(51),F2(51)
      COMMON A1,A2,A3,A4,B1,X4,PSI4,DETA,DPSI,XTE,PSITE,FTE,DGT,DPHIT,
     X       M,BM,BBM,PE,GAM,THIK,ATTAK,TAUMAX,ANGMAX,EPL,EPNL,EP
      COMMON N1,L1,NP1,LP1,LUP,LLOW,NTE,IFLOW,IFOIL,IPARM0,IPARM,
     X       IMAX,KMAX
      DIMENSION H(LP1)
      DATA PI/3.141593/
C
      ETA= -1.+ DETA
      DO 1 L= 2,L1
      H(L)= (2.*(COS(.5*PI*ETA))**2)/(A1*PI)
      ETA= ETA+ DETA
    1 CONTINUE
C
      H(1)= 0.
      H(LP1)= 0.
C
      RETURN
      END
```

```
C
C     ***************************************************************
C     *THIS PROGRAM COMPUTES THE UNSTEADY LOADS ON AIRFOILS UNDERGOING  *
C     *HARMONIC OSCILLATIONS.  THE COMPUTATIONS ARE CARRIED OUT IN A    *
C     *COORDINATE SYSTEM WHICH IS STRETCHED TO INFINITY.  THE INPUTS ARE*
C     *      A1- DETERMINES THE SPACING IN THE LATERAL DIRECTION        *
C     *      A2- DETERMINES THE SPACING IN THE STREAMWISE DIRECTION     *
C     *      A3- DETERMINES THE SPACING IN THE STREAMWISE DIRECTION     *
C     *      PSI4- DETERMINES THE SIZE OF THE COMPUTATIONAL REGION      *
C     *      X4- THE LOCATION OF THE BOUNDARY BETWEEN REGIONS I AND II  *
C     *          AND REGIONS II AND III                                 *
C     *      M- FREE STREAM MACH NUMBER                                 *
C     *      PE- EXPONENT OF M IN THE NONLINEAR TERM IN THE POTENTIAL   *
C     *          EQUATION                                               *
C     *      XTE- HALF OF THE CHORD LENGTH                              *
C     *      W- RELAXATION FACTOR                                       *
C     *      TAU- AIRFOIL THICKNESS RATIO                               *
C     *      ANG- MEAN AIRFOIL ANGLE OF ATTACK                          *
C     *      DETA- GRID SPACING IN THE LATERAL DIRECTION                *
C     *      DPSI- GRID SPACING IN THE STREAMWISE DIRECTION             *
C     *      GAM- RATIO OF SPECIFIC HEATS                               *
C     *      AMP- AMPLITUDE OF THE UNSTEADY MOTION DIVIDED BY THE       *
C     *           AIRFOIL CHORD                                         *
C     *      FREQ- REDUCED FREQUENCY OF THE UNSTEADY MOTION             *
C     *      PER- PERCENT CHORD ABOUT WHICH THE AIRFOILPITCHES, OR THE   *
C     *           PERCENT CHORD AT WHICH THE FLAP HINGE IS LOCATED FOR   *
C     *           UNSTEADY FLAP MOTIONS                                 *
C     *      EPS- CONVERGENCE CRITERIA                                  *
C     *      EP- DETERMINES THE AMOUNT OF THE ADDITIONAL CROSS DERIVATIVE*
C     *          TERM TO BE ADDED TO THE SUPERSONIC DIFFERENCE EQUATION  *
C     *      MOTION- THE TYPE OF UNSTEADY MOTION TO BE CONSIDERED       *
C     *              1- HEAVE                                           *
C     *              2- PITCH                                           *
C     *              3- OSCILLATING FLAP                                *
C     *      N1- THE NUMBER OF GRID SPACES IN THE PSI DIRECTION.  THIS   *
C     *          IS ONE LESS THAN THE TOTAL NUMBER OF GRID POINTS IN THE *
```

```
C     *          PSI DIRECTION                                          *
C     *      L1- THE NUMBER OF GRID SPACES IN THE ETA DIRECTION.  THIS IS*
C     *          ONE LESS THAN THE TOTAL NUMBER OF GRID POINTS IN THE ETA*
C     *          DIRECTION                                              *
C     *      NS- THE NUMBER OF GRID SPACES TO MOVE THE UNSTEADY GRID     *
C     *          BOUNDARIES IN FROM THE UPSTREAM AND DOWNSTREAM STEADY   *
C     *          GRID BOUNDARIES                                        *
C     *      LS- THE NUMBER OF GRID SPACES TO MOVE THEUPPER AND LOWER    *
C     *          UNSTEADY GRID BOUNDARIES IN FORM THE STEADY BOUNDARIES  *
C     *      LLOW- THE GRID ROW ADJACENT TO  THE LOWER AIRFOIL BOUNDARY  *
C     *      K- THE NUMBER OF VALUES OF PHI AND G NEEDED TO EMPLOY THE   *
C     *         MOST ACCURATE PREDICTOR-CORRECTOR METHOD                *
C     *      IMAX- THE MAXIMUM NUMBER OF ITERATIONS                     *
C     *      IDATA- DETERMINES THE INPUT OF STEADY DATA                 *
C     *             1- STEADY DATA DETERMINED WITHIN THE PROGRAM        *
C     *             2- STEADY DATA READ IN FROM OUTSIDE OF THE PROGRAM  *
C     *                                                                 *
C     *OTHER CONSTANTS ARE                                              *
C     *      A4, B1- DETERMINE THE GRID SPACING IN THE STREAMWISE       *
C     *               DIRECTION IN REGION II OF THE FLOW FIELD          *
C     *      BM- PRANDTL-GLAURET CONSTANT                               *
C     *      CRIT- CRITICAL PRESSURE COEFFICIENT                        *
C     *      NP1- MAXIMUM NUMBER OF GRID POINTS IN THE PSI DIRECTION    *
C     *      LP1- MAXIMUM NUMBER OF GRID POINTS IN THE ETA DIRECTION    *
C     *      NMIN- THE GRID COLUMN AT THE UPSTREAM BOUNDARY             *
C     *      NMAX- THE GRID COLUMN AT THE DOWNSTREAM BOUNDARY           *
C     *      LMIN- THE GRID ROW AT THE LOWER BOUNDARY OF THE            *
C     *            COMPUTATIONAL DOMAIN                                 *
C     *      LMAX- THE GRID ROW AT THE UPPER BOUNDARY OF THE            *
C     *            COMPUTATIONAL DOMAIN                                 *
C     *      KMAX- TOTAL NUMBER OF FLOW FIELDS STORED AT ANY TIME       *
C     *      LUP- THE GRID ROW ADJACENT TO THE UPPER BOUNDARY OF THE     *
C     *           AIRFOIL AND WAKE                                      *
C     ************************************************************************
C
      REAL M,MU
```

```
      COMMON PHU(51,22,2), CPU(51),CPL(51), DEPHU(51), DPHUT
      COMMON XX(51), XP(51), F2(51), MU(51,22), PHI(51,22,1)
      COMMON A1,A2,A3,A4,B1,BM,BBM,M,PSI4,DPSI,DETA,X4,PER
      COMMON PSITE,XTE,FTE,GAM,PE,FREQ,AMP,EPS,EP
      COMMON NTE,KMAX,MOTION,IMAX,LUP,LLOW,N1,NP1,L1,LP1
      COMMON NMIN,NMAX,LMIN,LMAX
      COMPLEX PHU,CPU,CPL,DEPHU,DPHUT
      COMPLEX BB(22),DD(22),EE(22),FF2(22),PUP(22),PDOWN(22),UP(51),
     X        LOW(51),PTOP(51),PBOT(51),CZERO
      DIMENSION A(22),C(22),ZZ(22),H(22),GM(51,22)
      DATA PI/3.141593/, CZERO/(0.,0.)/
C
      X1(PSI)= -X4+ A2*TAN(PI*(PSI+ PSI4)/2.)+
     1 A3*TAN(PI*((PSI+ PSI4)**3)/2.)
      X2(PSI)= PSI*(A4+ B1*PSI**2)
      X3(PSI)= X4+ A2*TAN(PI*(PSI- PSI4)/2.)+
     1 A3*TAN(PI*((PSI- PSI4)**3)/2.)
C
      READ(5,100) A1
      READ(5,100) A2
      READ(5,100) A3
      READ(5,100) PSI4
      READ(5,100) X4
      READ(5,100) M
      READ(5,100) PE
      READ(5,100) XTE
      READ(5,100) W
      READ(5,100) TAU
      READ(5,100) ANG
      READ(5,100) DETA
      READ(5,100) DPSI
      READ(5,100) GAM
      READ(5,100) AMP
      READ(5,100) FREQ
      READ(5,100) PER
      READ(5,100) EPS
```

```
      READ(5,100) EP
      READ(5,101) MOTION
      READ(5,101) N1
      READ(5,101) L1
      READ(5,101) NS
      READ(5,101) LS
      READ(5,101) LLOW
      READ(5,101) K
      READ(5,101) IMAX
      READ(5,101) IDATA
C
      A4= 1.5*X4/PSI4- .25*A2*PI
      B1= .25*A2*PI/(PSI4**2)- .5*X4/(PSI4**3)
C
C     CHECK DATA
      WRITE(6,104) A1,A2,A3,A4,B1,PE,M,X4,PSI4,W,XTE,TAU,ANG,DETA,DPSI,
     X             GAM,EPS,EP,AMP,FREQ,N1,L1,NS,LS,LLOW,K,IMAX,IDATA
C
      NP1= N1+ 1
      LP1= L1+ 1
      NMIN= 1+ NS
      NMAX= NP1- NS
      LMIN= 1+ LS
      LMAX= LP1- LS
      KMAX= K+ 1
      LUP= LLOW+ 1
C
      BM= SQRT(1.- M**2)
      BBM= 1.- M**2
      CRIT= -2.*BBM/((GAM+ 1.)*M**PE)
C
C     COMPUTE THE STRETCHED COORDINATES IN THE STREAMWISE DIRECTION
C
      PSI= -(1.+ PSI4)+ DPSI
      DO 1 N= 2,N1
      IF(PSI .LT. -PSI4) XX(N)= X1(PSI)
```

```
      IF(PSI .GE. -PSI4 .AND. PSI .LE. PSI4) XX(N)= X2(PSI)
      IF(PSI .GT. PSI4) XX(N)= X3(PSI)
      PSI= PSI+ DPSI
    1 CONTINUE
C
C     INITIALIZE THE STEADY AND UNSTEADY FLOW FIELDS
C
      IF(IDATA .EQ. 1) GO TO 5
C
      DO 2 L= 1,LP1
      DO 2 N= 1,NP1
      MU(N,L)= 0.
    2 READ(5,106) PHI(N,L,KMAX)
      GO TO 6
C
    5 DO 7 L= 1,LP1
      DO 7 N= 1,NP1
      MU(N,L)= 0.
    7 PHI(N,L,KMAX)= 0.
C
    6 DO 3 KS= 1,2
      DO 3 L= 1,LP1
      DO 3 N= 1,NP1
    3 PHU(N,L,KS)= CZERO
C
C     COMPUTE THE TRAILING EDGE LOCATION IN STRETCHED COORDINATES
C
      CALL TRAIL(XT2)
      WRITE(6,102) PSITE,FTE,XT2,NTE
C
C    COMPUTE THE STRETCHING FACTORS IN THE STREAMWISE DIRECTION
C
      CALL GROWX
C
      T1= (GAM+ 1.)*M**PE
      DO 4 L= 2,L1
```

```
      DO 4 N= 2,N1
      IF(BBM- T1*F2(N)*(PHI(N+1,L,KMAX) - PHI(N-1,L,KMAX))/(2.*DPSI)
     X    .LT. 0.) MU(N,L)= 1.
    4 CONTINUE
C
      CALL UNSTDY(W,A,BB,C,DD,EE,FF2,GM,ZZ,H,PUP,PDOWN,UP,LOW,LS,
     X            PTOP,PBOT)
  100 FORMAT(F8.5)
  101 FORMAT(I8)
  102 FORMAT(1X,3F12.5,I6/)
  104 FORMAT(' A1=',F10.5/' A2=',F10.5/' A3=',F10.5/' A4=',F10.5/
     X       ' B1=',F10.5/' PE=',F10.5/' M=',F10.5/' X4=',F10.5/
     X       ' PSI4=',F10.5/' W=',F10.5/' XTE=',F10.5/' TAU=',F10.5/
     X       ' ANG=',F10.5/' DETA=',F10.5/' DPSI=',F10.5/
     X       ' GAMMA=',F10.5/' EPS=',F10.5/' EP=',F10.5/' AMP=',F10.5/
     X       ' FREQ=',F10.5/' N1=',I6/' L1=',I6/' NS=',I6/' LS=',I6/
     X       ' LLOW=',I6/' K=',I6/' IMAX=',I6/' IDATA=',I6//)
  106 FORMAT(F20.6)
      STOP
      END
```

```
      SUBROUTINE UNSTDY(W,A,B,C,D,E,F,GM,ZZ,H,PUP,PDOWN,UP,LOW,LS,
     X                  PTOP,PBOT)
C
C     ****************************************************************
C     *THIS SUBROUTINE DEFINES THE TRIDIAGONAL COEFFICIENTS USED TO  *
C     *COMPUTE THE UNSTEADY FLOW FIELD USING KLUNKER TYPE BOUNDARY   *
C     *CONDITIONS                                                    *
C     ****************************************************************
C
      REAL M,MU,KT,MUSTAR
      COMMON PHU(51,22,2), CPU(51),CPL(51), DEPHU(51), DPHUT
      COMMON XX(51), XP(51), F2(51), MU(51,22), PHI(51,22,1)
      COMMON A1,A2,A3,A4,B1,BM,BBM,M,PSI4,DPSI,DETA,X4,PER
      COMMON PSITE,XTE,FTE,GAM,PE,FREQ,AMP,EPS,EP
      COMMON NTE,KMAX,MOTION,IMAX,LUP,LLOW,N1,NP1,L1,LP1
      COMMON NMIN,NMAX,LMIN,LMAX
      COMPLEX PHU,CPU,CPL,DEPHU,DPHUT
      COMPLEX B(LMAX),D(LMAX),E(LMAX),F(LMAX),PUP(LMAX),PDOWN(LMAX),
     X        UP(NMAX),LOW(NMAX),PTOP(NMAX),PBOT(NMAX)
      COMPLEX T12,T14,T15,TANLOW,TANUP,TANUL,TANUT,TANLL,TANLT,
     X        JUMP,CIM,DPHU,DELTAN,CEX,COEFFU,COEFFL,CL,UNLIFT
      COMPLEX CZERO,SHOCK,EXCUR,AL4,AL5,CMLE,CML,KSTAR(22)
      DIMENSION A(LMAX),C(LMAX),ZZ(LMAX),H(LMAX),GM(NMAX,LMAX)
      DATA PI/3.141593/, CIM/(0.,1.)/, CZERO/(0.,0.)/
C
      ITER= 1
C
C     DEFINE OFTEN USED CONSTANTS
C
      NP= NMIN+ 1
      NM= NMAX- 1
      LP= LMIN+ 1
      LM= LMAX- 1
      ISHOCK= 0
      T1= (GAM+ 1.)*M**PE
      T2= 1./DPSI
```

```
      T3= 1./(DPSI**2)
      T4= 1./(DETA**2)
      T5= 1./W
      T6= 1.- 1./W
      T7= 1./DETA
      T8= ((PSI4+ DPSI- PSITE)/(PSITE- PSI4+ DPSI))**2
      T9= 2.*DPSI*SQRT(T8)
      T10= FREQ**2
      T11= (FREQ*DPSI)**2
      T12= CIM*FREQ*M**2/DPSI
      T13= M**2
      T14= CIM*FREQ*(GAM- 1.)/(DPSI**2)
      T15= CIM*FREQ*DPSI
      MUSTAR= (GAM- 1.+ 2./(M**2))/(GAM+ 1.)
C
      DO 2 L= 1,LP1
    2 KSTAR(L)= CZERO
C
C     COMPUTE THE SPACING IN THE LSTERAL DIRECTION
C
      ETA= -1.+ DETA
      DO 19 L= 2,L1
      ZZ(L)= A1*TAN(.5*PI*ETA)
      ETA= ETA+ DETA
   19 CONTINUE
C
C     COMPUTE THE STRETCHING FACTORS IN THE LATERAL DIRECTION
C
      CALL GROWZ(H)
C
C     COMPUTE THE FAR FIELD BOUNDARY CONDITIONS
C
      CALL WAKFIN(ZZ,WAKE1,WAKE2)
      CALL WAKINF(ZZ,WAKE3)
      CALL DELPHU(NP,NM,H)
    1 CALL INTEG(NP,NM,DPHU,DELTAN)
```

```
      CALL FARFLD(DPHU,DELTAN,WAKE1,WAKE2,WAKE3,ZZ,PUP,PDOWN,
     X            PTOP,PBOT,NP,NM)
C
C     SET TRIDIAGONAL COEFFICIENT ARRAYS
C
      DO 3 N= NP,NM
C
C     SET X STRETCHING FACTORS AT HALF SPACES
C
      FF= .5*(F2(N+1)+ F2(N))
      FB= .5*(F2(N)+ F2(N-1))
      FH= 0.
      IF(N .GT. NMIN+1) FH= .5*(F2(N-2)+ F2(N-1))
C
      DO 4 L= LP,LM
C
C     SET Z STRETCHING FACTORS AT HALF SPACES
C
      HF= .5*(H(L+1)+ H(L))
      HB= .5*(H(L)+ H(L-1))
C
      AL1= F2(N)*FF*T3*(BBM- T1*FF*T2*(PHI(N+1,L,KMAX)- PHI(N,L,KMAX)))
      AL2= F2(N)*FB*T3*(BBM+ T1*FB*T2*(PHI(N-1,L,KMAX)- PHI(N,L,KMAX)))
      AL4= T13*(T10- T14*F2(N)*(FF*(PHI(N+1,L,KMAX)- PHI(N,L,KMAX))-
     X                          FB*(PHI(N,L,KMAX)- PHI(N-1,L,KMAX))))
C
C     CONDITIONS AT THE UPSTREAM BOUNDARY
C
      IF(N .NE. NP) GO TO 5
      A(L)= H(L)*HB*T4
      B(L)= H(L)*(HF+ HB)*T4+ (AL1+ AL2- AL4)*T5-
     X      ((4.*FB**2- T11+ 4.*FB*T15)/(4.*FB**2+ T11))*(AL2+
     X      T12*F2(N))
      C(L)= H(L)*HF*T4
      D(L)= (AL1- T12*F2(N))*PHU(N+1,L,1)- (AL1+ AL2- AL4)*T6*PHU(N,L,1)
     X     -2.*DPSI*((2.*FB+ T15)/(4.*FB**2+ T11))*(AL2+ T12*F2(N))*
```

```
     X      PUP(L)
      GO TO 4
C
C     CONDITIONS AT THE DOWNSTREAM BOUNDARY
C
    5 IF(N .NE. NM) GO TO 6
      A(L)= H(L)*HB*T4
      B(L)= H(L)*(HF+ HB)*T4+ (AL1+ AL2- AL4)*T5
      C(L)= H(L)*HF*T4
      D(L)= -((AL1+ AL2- AL4)*T6- ((4.*FF**2- T11- 4.*T15*FF)/
     X       (4.*FF**2+ T11))*(AL1- F2(N)*T12))*PHU(N,L,1)+ (AL2+ F2(N)*
     X       T12)*PHU(N-1,L,2)- 2.*DPSI*((2.*FF- T15)/(4.*FF**2+ T11))*
     X       (AL1- T12)*PDOWN(L)
      GO TO 4
C
C     INTERIOR OF THE FLOW FIELD
C
    6 AL3= F2(N)*FH*T3*(BBM- T1*FH*T2*(PHI(N-1,L,KMAX)- PHI(N-2,L,KMAX
     X     )))
      AL5= T13*(T10- T14*F2(N)*(FB*(PHI(N,L,KMAX)- PHI(N-1,L,KMAX))-
     X                          FH*(PHI(N,L,KMAX)- PHI(N-2,L,KMAX))))
C
      A(L)= H(L)*HB*T4
      B(L)= H(L)*(HB+ HF)*T4+ (1.- MU(N,L))*(AL1+ AL2- AL4)*T5+
     X      EP*F2(N)*FB*T3*MU(N,L)
      C(L)= H(L)*HF*T4
      D(L)= (1.- MU(N,L))*(AL1- T12*F2(N))*PHU(N+1,L,1)+ ((1.- MU(N,L))*
     X      (AL2+ T12*F2(N))+ EP*F2(N)*FB*T3*MU(N,L))*PHU(N-1,L,2)-
     X      ((1.- MU(N,L))*(AL1+ AL2- AL4)*T6- MU(N-1,L)*(AL2- T12*F2
     X      (N))- MU(N,L)*(AL4+ EP*F2(N)*FB*T3))*PHU(N,L,1)- (MU(N-1,L)*
     X      (AL2+ AL3)+ EP*F2(N)*FB*T3*MU(N,L))*PHU(N-1,L,1)+ MU(N-1,L)*
     X      (AL3+ T12*F2(N))*PHU(N-2,L,1)
C
      IF(MU(N,L) .LT. .5 .AND. MU(N-1,L) .GT. .5) GO TO 20
C
      GO TO 4
```

```
C
C     SATISFY THE SHOCK BOUNDARY CONDITIONS
C
   20 KSTAR(L) =
     X       2.*DPSI*(T3*F2(N)*(FF*(PHI(N+1,L,KMAX)- PHI(N,L,KMAX))-
     X       FB*(PHI(N,L,KMAX)- PHI(N-1,L,KMAX)))- MUSTAR*F2(N-1)*T3*(
     X       FB*(PHI(N,L,KMAX)- PHI(N-1,L,KMAX))- FH*(
     X       PHI(N-1,L,KMAX)- PHI(N-2,L,KMAX)))+ 2.*CIM*FREQ*(GAM- 1.)/
     X       (GAM+ 1.)*F2(N-1)*.5*T2*(PHI(N,L,KMAX)- PHI(N-2,L,KMAX))-
     X       4.*CIM*FREQ/(GAM+ 1.))/(F2(N)*(PHI(N+1,L,KMAX)- PHI(N-1,L,
     X       KMAX))- F2(N-1)*(PHI(N,L,KMAX)- PHI(N-2,L,KMAX)))
      ISHOCK= 1
    4 CONTINUE
C
      IF(XX(N) .LT. -XTE) GO TO 18
      IF(XX(N) .GT. XTE) GO TO 23
C
C     UNSTEADY TANGENCY CONDITION
C
      B(LLOW) = B(LLOW)- .5*H(LLOW)*(H(LLOW)+ H(LUP))*T4
      C(LLOW)= 0.
      CALL TANGNT(N,TANLOW,TANUP,TANUL,TANUT,TANLL,TANLT)
      D(LLOW)= D(LLOW)+ H(LLOW)*T7*TANLOW
C
      A(LUP)= 0.
      B(LUP)= B(LUP)- .5*H(LUP)*(H(LLOW)+ H(LUP))*T4
      D(LUP)= D(LUP)- H(LUP)*T7*TANUP
      GO TO 18
C
   23 IF(MU(NTE,LUP) .GT. .5) GO TO 24
      IF(N .GT. NTE+1) GO TO 25
      CALL DELPHU(NP,NM,H)
   25 JUMP= (T8*DEPHU(NTE-1)+ (1.- T8- CIM*FREQ*T9/FTE)*DPHUT)*
     X       CEXP(-CIM*FREQ*(XX(N)- XX(NTE+1)))
C
C     INCORPORATE KUTTA AND WAKE CONDITIONS
```

```
C
      D(LLOW)= D(LLOW)- .5*H(LLOW)*(H(LLOW)+ H(LUP))*T4*JUMP
      D(LUP)= D(LUP)+ .5*H(LUP)*(H(LLOW)+ H(LUP))*T4*JUMP
      GO TO 18
C
C     SUPERSONIC TRAILING EDGE CONDITION
C
   24 D(LLOW)= D(LLOW)- .5*H(LLOW)*(H(LLOW)+ H(LUP))*T4*DEPHU(NTE+1)
      D(LUP)= D(LUP)+ .5*H(LUP)*(H(LLOW)+ H(LUP))*T4*DEPHU(NTE+1)
C
C     SATISFY THE CONDITIONS ON THE UPPER AND LOWER BOUNDARIES OF THE
C     COMPUTATIONAL REGION
C
   18 D(LMIN+1)= D(LMIN+1)+ A(LMIN+1)*PHU(N,LMIN,2)
      A(LMIN+1)= 0.
      D(LMAX-1)= D(LMAX-1)+ C(LMAX-1)*PHU(N,LMAX,2)
      C(LMAX-1)= 0.
C
      CALL TRISOV(A,B,C,D,E,F,N,LP,LM,LS,KSTAR,MUSTAR)
    3 CONTINUE
C
C     COMPUTE THE MAXIMUM ERROR
C
      DO 9 L= LMIN,LMAX
      DO 9 N= NP,NM
    9 GM(N,L)= CABS(T5*(PHU(N,L,2)- PHU(N,L,1)))
C
      AM= GM(NP,LMIN)
      DO 7 L= LMIN,LMAX
      DO 7 N= NP,NM
      IF(GM(N,L) .LE. AM) GO TO 7
      AM= GM(N,L)
      IN= N
      IL= L
    7 CONTINUE
C
```

```
C     WRITE THE CONVERGENCE HISTORY
C
      WRITE(6,100) ITER,IN,IL,AM
      IF(AM .GT. EPS) GO TO 13
      GO TO 14
C
C
C     CHECK FLAG CONDITIONS
C
   13 ITER= ITER+ 1
      IF(ITER .GT. IMAX) GO TO 14
C
C     IF THE SOLUTION HASN'T CONVERGED, UPDATE THE FLOW FIELD AND REPEAT
C     THE CALCULATIONS
C
      DO 16 L= LMIN,LMAX
      DO 16 N= NP,NM
   16 PHU(N,L,1)= PHU(N,L,2)
      GO TO 1
C
C     COMPUTE THE UNSTEADY PRESSURE AND LIFT COEFFICIENTS AND THE MOMENT
C     COEFFICIENT ABOUT THE LEADING EDGE
C
   14 CALL PRESS(UP,LOW,NP,NM,H,T8,T9,J,CL,CMLE)
      WRITE(6,105)
C
C     COMPUTE THE FORCE AND MOMENT COEFFICIENTS OVER ONE MOTION CYCLE
C
      KT= 0.
    8 WRITE(6,101) KT
      WRITE(6,106)
      WRITE(6,107)
      WRITE(6,108)
      CEX= CEXP(CIM*KT)
      DO 17 N= 1,J
      COEFFU= CEX*CPU(N)
```

```
      COEFFL= CEX*CPL(N)
      UNLIFT= COEFFL- COEFFU
   17 WRITE(6,102) XP(N),COEFFU,COEFFL,UNLIFT
      UNLIFT= CEX*CL
      CML= CEX*CMLE
      WRITE(6,104) UNLIFT,CML
      KT= KT+ PI/6.
      IF(KT .LT. 2.01*PI) GO TO 8
C
      KT= 0.
   10 WRITE(6,101) KT
      WRITE(6,106)
      WRITE(6,107)
      WRITE(6,108)
      CEX= CEXP(CIM*KT)
      DO 11 N= 1,J
      COEFFU= CEX*CPU(N)/AMP
      COEFFL= CEX*CPL(N)/AMP
      UNLIFT= COEFFL- COEFFU
   11 WRITE(6,102) XP(N),COEFFU,COEFFL,UNLIFT
C
      UNLIFT= CEX*CL/AMP
      CML= CEX*CMLE/AMP
      WRITE(6,104) UNLIFT,CML
      KT= KT+ PI/6.
      IF(KT .LT. 2.01*PI) GO TO 10
C
      IF(ISHOCK .EQ. 0) GO TO 12
      DO 21 L= LP,LM
      DO 21 N= NP,NM
      IF(MU(N,L) .GT. .5) GO TO 21
      IF(MU(N-1,L) .LT. .5) GO TO 21
      XSHOCK= .5*(XX(N)+ XX(N-1))
      WRITE(6,109) XX(N-1),XX(N),XSHOCK,ZZ(L)
      SHOCK= -(PHU(N,L,2)- PHU(N-1,L,2))/(F2(N)*T2*(PHI(N+1,L,KMAX)-
     X          PHI(N-1,L,KMAX))-  F2(N-1)*T2*(PHI(N,L,KMAX)-
```

```
     X          PHI(N-2,L,KMAX)))
      WRITE(6,110) SHOCK
C
C     FIND SHOCK MOTION OVER ONE MOTION CYCLE
C
      KT= 0.
   22 CEX= CEXP(CIM*KT)
      EXCUR= CEX*SHOCK
      POSIT= XSHOCK+ REAL(EXCUR)
      WRITE(6,111) KT,EXCUR,POSIT
      KT= KT+ PI/6.
      IF(KT .LT. 2.01*PI) GO TO 22
   21 CONTINUE
      GO TO 12
C
   15 WRITE(6,103)
  100 FORMAT(1X,3I6,F18.6)
  101 FORMAT(//' KT=',F10.5/)
  102 FORMAT(7F12.5)
  103 FORMAT('1','NO CONVERGENCE')
  104 FORMAT(/' REAL LIFT COEFF=',F12.5,2X,'IMAG LIFT COEFF=',F12.5/
     X        ' REAL MOMENT ABOUT LEADING EDGE=',F12.5,2X,
     X        ' IMAG MOMENT ABOUT LEADING EDGE=',F12.5)
  105 FORMAT('1',25X,'UNSTEADY PRESSURE DISTRIBUTIONS')
  106 FORMAT(8X,'X',9X,'REAL',8X,'IMAG',8X,'REAL',8X,'IMAG',8X,'REAL',
     X       8X,'IMAG')
  107 FORMAT(8X,'-',8X,'UPPER',7X,'UPPER',7X,'LOWER',7X,'LOWER',6X,
     X       'UNSTEADY',4X,'UNSTEADY')
  108 FORMAT(8X,'C',10X,'CP',10X,'CP',10X,'CP',10X,'CP',9X,'LIFT',8X,
     X       'LIFT'/)
  109 FORMAT(/2X,4F15.5/)
  110 FORMAT(' REAL SHOCK EXCURSION AMPLITUDE=',F12.5,2X,
     X       ' IMAG SHOCK EXCURSION AMPLITUDE=',F12.5/)
  111 FORMAT(' KT=',F10.5,2X,'REAL SHOCK MOTION=',F12.5,2X,'IMAG
     X SHOCK MOTION=',F12.5,2X,'SHOCK POSITION=',F12.5)
   12 RETURN
```

END

```
      SUBROUTINE DELPHU(NP,NM,H)
C
C     ****************************************************************
C     *THIS SUBROUTINE COMPUTES THE JUMP IN POTENTIAL ALONG THE AIRFOIL *
C     *AND AT THE TRAILING EDGE.  IF THE FLOW AT THE TRAILING EDGE IS   *
C     *SUPERSONIC, THE JUMP IN POTENTIAL IMMEDIATELY AFT OF THE TRAILING*
C     *EDGE IS ALSO COMPUTED.                                           *
C     ****************************************************************
C
      REAL M,MU
      COMMON PHU(51,22,2), CPU(51),CPL(51), DEPHU(51), DPHUT
      COMMON XX(51), XP(51), F2(51), MU(51,22), PHI(51,22,1)
      COMMON A1,A2,A3,A4,B1,BM,BBM,M,PSI4,DPSI,DETA,X4,PER
      COMMON PSITE,XTE,FTE,GAM,PE,FREQ,AMP,EPS,EP
      COMMON NTE,KMAX,MOTION,IMAX,LUP,LLOW,N1,NP1,L1,LP1
      COMMON NMIN,NMAX,LMIN,LMAX
      COMPLEX PHU,CPU,CPL,DEPHU,DPHUT
      COMPLEX TANLOW,TANUP,TANUL,TANUT,TANLL,TANLT
      DIMENSION H(LMAX)
C
C     COMPUTE THE JUMP IN POTENTIAL ALONG THE AIRFOIL
C
      DO 1 N= NP,NM
      IF(XX(N) .LT. -XTE) GO TO 1
      IF(XX(N) .GT. XTE) GO TO 2
      CALL TANGNT(N,TANLOW,TANUP,TANUL,TANUT,TANLL,TANLT)
      DEPHU(N)= .125*(9.*(PHU(N,LUP,2)- PHU(N,LLOW,2))-
     X          PHU(N,LUP+1,2)+ PHU(N,LLOW-1,2)-
     X          3.*DETA*2.*(TANUP+ TANLOW)/(H(LLOW)+ H(LUP)))
    1 CONTINUE
C
    2 T= (PSITE- PSI4)/DPSI
      DPHUT= (1.+ 1.5*T)*DEPHU(NTE)- 2.*T*DEPHU(NTE-1)+ .5*T*DEPHU(NTE-
     X       2)
C
      IF(MU(NTE,LUP) .LT. .5) RETURN
```

```
C
C     COMPUTE THE JUMP IN POTENTIAL IMMEDIATELY DOWNSTREAM OF THE
C     TRAILING EDGE
C
      NT= NTE+ 1
      DEPHU(NT) = 2.*(PHU(NT,LUP,2) - PHU(NT,LLOW,2))-
     X            .125*(-13.*(PHU(NT,LUP+1,2) - PHU(NT,LLOW-1,2))+
     X            6.*(PHU(NT,LUP+2,2) - PHU(NT,LLOW-2,2))-
     X            PHU(NT,LUP+3,2) + PHU(NT,LLOW-3,2))
C
      RETURN
      END
```

```
      SUBROUTINE TANGNT(N,TANLOW,TANUP,TANUL,TANUT,TANLL,TANLT)
C
C     ****************************************************************
C     *THIS SUBROUTINE DEFINES THE TANGENCY CONDITIONS FOR HEAVING,     *
C     *PITCHING, AND OSCILLATING FLAP MOTION.  THE NOMENCLATURE IS      *
C     *     TANUP- UPPER PROFILE TANGENCY CONDITION                     *
C     *     TANLOW- LOWER PROFILE TANGENCY CONDITION                    *
C     *     TANUL- TANGENCY CONDITION AT THE LEADING EDGE ON  THE UPPER *
C     *            PROFILE                                              *
C     *     TANUT- TANGENCY CONDITION AT THE TRAILING EDGE ON THE UPPER *
C     *            PROFILE                                              *
C     *     TANLL- TANGENCY CONDITION AT THE LEADING EDGE ON  THE LOWER *
C     *            PROFILE                                              *
C     *     TANLT- TANGENCY CONDITION AT THE TRAILING EDGE ON THE LOWER *
C     *            PROFILE                                              *
C     ****************************************************************
C
      REAL M,MU
      COMMON PHU(51,22,2), CPU(51),CPL(51), DEPHU(51), DPHUT
      COMMON XX(51), XP(51), F2(51), MU(51,22), PHI(51,22,1)
      COMMON A1,A2,A3,A4,B1,BM,BBM,M,PSI4,DPSI,DETA,X4,PER
      COMMON PSITE,XTE,FTE,GAM,PE,FREQ,AMP,EPS,EP
      COMMON NTE,KMAX,MOTION,IMAX,LUP,LLOW,N1,NP1,L1,LP1
      COMMON NMIN,NMAX,LMIN,LMAX
      COMPLEX PHU,CPU,CPL,DEPHU,DPHUT
      COMPLEX CIM,CZERO,TANLOW,TANUP,TANUL,TANUT,TANLL,TANLT,T2
      DATA CIM/(0.,1.)/, CZERO/(0.,0.)/
C
      IF(MOTION .NE. 1) GO TO 1
      T2= CIM*FREQ*AMP
C
C     HEAVING MOTION
C
      TANUP= T2
      TANLOW= T2
      TANUL= T2
```

```
      TANUT= T2
      TANLL= T2
      TANLT= T2
      RETURN
C
    1 IF(MOTION .NE. 2) GO TO 2
      T1= TAN(AMP)
      T2= CIM*FREQ*TAN(AMP)
C
C     PITCHING MOTION
C
      TANUP= -T1+ T2*((2.*PER- 1.)*XTE- XX(N))
      TANLOW= -T1+ T2*((2.*PER- 1.)*XTE- XX(N))
      TANUL= -T1+ 2.*T2*PER*XTE
      TANUT= -T1+ 2.*T2*XTE*(PER- 1.)
      TANLL= -T1+ 2.*T2*PER*XTE
      TANLT= -T1+ 2.*T2*XTE*(PER- 1.)
      RETURN
C
    2 IF(MOTION .NE. 3) RETURN
C
C     MOVING FLAP
C
      IF(XX(N) .GE. 2.*XTE*(PER- .5)) GO TO 3
      TANUP= CZERO
      TANLOW= CZERO
      TANUL= CZERO
      TANUT= CZERO
      TANLL= CZERO
      TANLT= CZERO
      RETURN
C
    3 T1= TAN(AMP)
      T2= CIM*FREQ*TAN(AMP)
      TANUP= -T1+ T2*((2.*PER- 1.)*XTE- XX(N))
      TANLOW= -T1+ T2*((2.*PER- 1.)*XTE- XX(N))
```

```
      TANUL= -T1+ 2.*T2*PER*XTE
      TANUT= -T1+ 2.*T2*XTE*(PER- 1.)
      TANLL= -T1+ 2.*T2*PER*XTE
      TANLT= -T1+ 2.*T2*XTE*(PER- 1.)
C
      RETURN
      END
```

```
      SUBROUTINE TRISOV(A,B,C,D,E,F,N,LP,LM,LS,KSTAR,MUSTAR)
C
C     ****************************************************************
C     *THIS SUBROUTINE SOLVES A SYSTEM OF TRIDIAGONAL EQUATIONS       *
C     ****************************************************************
C
      REAL M,MU,MUSTAR
      COMMON PHU(51,22,2), CPU(51),CPL(51), DEPHU(51), DPHUT
      COMMON XX(51), XP(51), F2(51), MU(51,22), PHI(51,22,1)
      COMMON A1,A2,A3,A4,B1,BM,BBM,M,PSI4,DPSI,DETA,X4,PER
      COMMON PSITE,XTE,FTE,GAM,PE,FREQ,AMP,EPS,EP
      COMMON NTE,KMAX,MOTION,IMAX,LUP,LLOW,N1,NP1,L1,LP1
      COMMON NMIN,NMAX,LMIN,LMAX
      COMPLEX PHU,CPU,CPL,DEPHU,DPHUT,KSTAR(LMAX),CIM
      COMPLEX CZERO,B(LMAX),D(LMAX),E(LMAX),F(LMAX),DEN
      DIMENSION A(LMAX),C(LMAX)
      DATA CZERO/(0.,0.)/,CIM/(0.,1.)/
C
C     COMPUTE THE FLOW FIELD OUT OF THE PLANE OF THE AIRFOIL
C
      IF(ABS(XX(N)) .LT. XTE) GO TO 1
      L2= LMAX- 2
C
C     SATISFY FAR FIELD CONDITION
C
      E(LMIN)= CZERO
      F(LMIN)= PHU(N,LMIN,2)
C
C     CALCULATE TRIDIAGONAL COEFFICIENTS
C
      DO 2 L= LP,LM
      DEN= B(L)- A(L)*E(I-1)
      E(L)= C(L)/DEN
    2 F(L)= (D(L)+ A(L)*F(L-1))/DEN
C
C     CALCULATE FLOW FIELD
```

```
C
      DO 3 L= LMIN,L2
      LL= LP1- L
      PHU(N,LL,2) = E(LL)*PHU(N,LL+1,2) + F(LL)
C
C     SATISFY UNSTEADY SHOCK CONDITIONS
C
      IF(MU(N,LL) .LT. .5 .AND. MU(N-1,LL) .GT. .5) PHU(N,LL,2)=
     X   1./(F2(N)- 2.*DPSI*KSTAR(LL))*(-(2.*DPSI*KSTAR(LL)+ MUSTAR*
     X   F2(N-1)+ 4.*CIM*FREQ*DPSI*(GAM- 1.)/(GAM+ 1.))*PHU(N-1,LL,2)+
     X   F2(N)*PHU(N-2,LL,2)+ MUSTAR*F2(N-1)*PHU(N-3,LL,2))
    3 CONTINUE
      RETURN
C
C     CALCULATE THE FLOW FIELD IN THE PLANE OF THE AIRFOIL
C
    1 L3= LLOW- 1
      L2= LUP+ LS
C
C     SATISFY THE LOWER BOUNDARY TANGENCY CONDITION
C
      E(LLOW) = A(LLOW)/B(LLOW)
      F(LLOW) = D(LLOW)/B(LLOW)
C
C     CALCULATE THE TRIDIAGONAL COEFFICIENTS BELOW THE AIRFOIL
C
      DO 5 L= LP,L3
      LL= L2- L
      DEN= B(LL) - C(LL)*E(LL+1)
      E(LL)= A(LL)/DEN
    5 F(LL)= (D(LL)+ C(LL)*F(LL+1))/DEN
C
C     CALCULATE THE FLOW FIELD BELOW THE AIRFOIL
C
      DO 6 L= LP,LLOW
      LL= L
```

```
     X    F2(N)*PHU(N-2,LL,2)+ MUSTAR*F2(N-1)*PHU(N-3,LL,2))
    8 CONTINUE
C
      RETURN
      END
```

```
      PHU(N,L,2) = E(L)*PHU(N,L-1,2) + F(L)
C
C     SATISFY UNSTEADY SHOCK CONDITIONS
C
      IF(MU(N,LL) .LT. .5 .AND. MU(N-1,LL) .GT. .5) PHU(N,LL,2) =
     X   1./(F2(N)- 2.*DPSI*KSTAR(LL))*(-(2.*DPSI*KSTAR(LL) + MUSTAR*
     X   F2(N-1) + 4.*CIM*FREQ*DPSI*(GAM- 1.)/(GAM+ 1.))*PHU(N-1,LL,2) +
     X   F2(N)*PHU(N-2,LL,2) + MUSTAR*F2(N-1)*PHU(N-3,LL,2))
    6 CONTINUE
C
      L3= LP1- LUP
      L2= LUP+ 1
C
C     SATISFY THE UPPER BOUNDARY TANGENCY CONDITION
C
      E(LUP) = C(LUP)/B(LUP)
      F(LUP) = D(LUP)/B(LUP)
C
C     CALCULATE THE TRIDIAGONAL COEFFICIENTS ABOVE THE AIRFOIL
C
      DO 7 L= L2,LM
      DEN= B(L)- A(L)*E(L-1)
      E(L)= C(L)/DEN
    7 F(L)= (D(L) + A(L)*F(L-1))/DEN
C
C     CALCULATE THE FLOW FIELD ABOVE THE AIRFOIL
C
      DO 8 L= LMIN,L3
      LL= LP1- L
      PHU(N,LL,2)= E(LL)*PHU(N,LL+1,2) + F(LL)
C
C     SATISFY UNSTEADY SHOCK CONDITIONS
C
      IF(MU(N,LL) .LT. .5 .AND. MU(N-1,LL) .GT. .5) PHU(N,LL,2) =
     X   1./(F2(N)- 2.*DPSI*KSTAR(LL))*(-(2.*DPSI*KSTAR(LL) + MUSTAR*
     X   F2(N-1) + 4.*CIM*FREQ*DPSI*(GAM- 1.)/(GAM+ 1.))*PHU(N-1,LL,2) +
```

```
      SUBROUTINE PRESS(UP,LOW,NP,NM,H,T8,T9,J,CL,CMLE)
C
C     ****************************************************************
C     *THIS SUBROUTINE COMPUTES THE UNSTEADY PRESSURE AND LIFT        *
C     *COEFFICIENTS AND THE UNSTEADY MOMENT COEFFICIENT ABOUT THE     *
C     *LEADING EDGE                                                   *
C     ****************************************************************
C
      REAL M,MU
      COMMON PHU(51,22,2), CPU(51),CPL(51), DEPHU(51), DPHUT
      COMMON XX(51), XP(51), F2(51), MU(51,22), PHI(51,22,1)
      COMMON A1,A2,A3,A4,B1,BM,BBM,M,PSI4,DPSI,DETA,X4,PER
      COMMON PSITE,XTE,FTE,GAM,PE,FREQ,AMP,EPS,EP
      COMMON NTE,KMAX,MOTION,IMAX,LUP,LLOW,N1,NP1,L1,LP1
      COMMON NMIN,NMAX,LMIN,LMAX
      COMPLEX PHU,CPU,CPL,DEPHU,DPHUT
      COMPLEX CIM,UP(NMAX),LOW(NMAX),TANLOW,TANUP,TANUL,TANUT,
     X        TANLL,TANLT,JUMP,T2,CL,CMLE
      DIMENSION H(LMAX)
      DATA CIM/(0.,1.)/
C
C     COMPUTE THE UPPER AND LOWER PROFILE POTENTIALS, UP AND LOW
C
      T= .5*(H(LLOW)+ H(LUP))
      DO 1 N= NP,NM
      IF(XX(N+1) .LT. -XTE) GO TO 1
      IF(XX(N-1) .GT. XTE) GO TO 4
      IF(XX(N) .GT. -XTE) GO TO 2
      UP(N)= .125*(9.*PHU(N,LUP,2)- PHU(N,LUP+1,2)-
     X             3.*(PHU(N,LUP,2)- PHU(N,LLOW,2)))
      LOW(N)= .125*(9.*PHU(N,LLOW,2)- PHU(N,LLOW-1,2)-
     X              3.*(PHU(N,LUP,2)- PHU(N,LLOW,2)))
      GO TO 1
C
    2 IF(XX(N) .GT. XTE) GO TO 3
      CALL TANGNT(N,TANLOW,TANUP,TANUL,TANUT,TANLL,TANLT)
```

```
      UP(N)= .125*(9.*PHU(N,LUP,2) - PHU(N,LUP+1,2)-
     X              3.*DETA*TANUP/T)
      LOW(N)= .125*(9.*PHU(N,LLOW,2) - PHU(N,LLOW-1,2)-
     X               3.*DETA*TANLOW/T)
      GO TO 1
C
    3 JUMP= T8*DEPHU(NTE-1)+ (1.- T8- CIM*FREQ*T9/FTE)*DPHUT
      UP(N)= .125*(9.*PHU(N,LUP,2) - PHU(N,LUP+1,2)-
     X              3.*(PHU(N,LUP,2) - PHU(N,LLOW,2)- JUMP))
      LOW(N)= .125*(9.*PHU(N,LLOW,2) - PHU(N,LLOW-1,2)-
     X               3.*(PHU(N,LUP,2) - PHU(N,LLOW,2)- JUMP))
    1 CONTINUE
C
C     COMPUTE THE UPPER AND LOWER PRESSURE COEFFICIENTS, CPU AND CPL
C
    4 J= 1
      T1= 1./(2.*DPSI)
      T2= CIM*FREQ
      DO 5 N= NP,NM
      IF(XX(N) .LT. -XTE) GO TO 5
      IF(XX(N) .GT. XTE) GO TO 6
      XP(J)= XX(N)+ XTE
      CPU(J)= -2.*(F2(N)*T1*(UP(N+1)- UP(N-1))+ T2*UP(N))
      CPL(J)= -2.*(F2(N)*T1*(LOW(N+1)- LOW(N-1))+ T2*LOW(N))
      J= J+ 1
    5 CONTINUE
    6 J= J-1
C
C     COMPUTE THE UNSTEADY LIFT COEFFICIENT, CL, AND MOMENT COEFFICIENT
C     ABOUT THE LEADING EDGE, CMLE
C
      CL= XP(1)*(CPL(1)- CPU(1))
      CMLE= XP(1)**2*(CPL(1)- CPU(1))
      DO 7 N= 2,J
      CMLE= CMLE+ .5*(XP(N)- XP(N-1))*((CPL(N)- CPU(N))*XP(N)+
     X               (CPL(N-1)- CPU(N-1))*XP(N-1))
```

```
    7 CL= CL+ .5*(XP(N)- XP(N-1))*(CPL(N)- CPU(N)+ CPL(N-1)- CPU(N-1))
      CL= CL+ .5*(1.- XP(J))*(CPL(J)- CPU(J))
      CMLE= CMLE+ .5*(1.- XP(J))*(CPL(J)- CPU(J))*XP(J)
C
      RETURN
      END
```

```
      SUBROUTINE INTEG(NP,NM,DPHU,DELTAN)
C
C     ****************************************************************
C     *THIS SUBROUTINE INTEGRATES THE JUMP IN POTENTIAL AND THE JUMP IN *
C     *THE TANGENCY CONDITION ALONG THE AIRFOIL CHORD                   *
C     ****************************************************************
C
      REAL M,MU
      COMMON PHU(51,22,2), CPU(51),CPL(51), DEPHU(51), DPHUT
      COMMON XX(51), XP(51), F2(51), MU(51,22), PHI(51,22,1)
      COMMON A1,A2,A3,A4,B1,BM,BBM,M,PSI4,DPSI,DETA,X4,PER
      COMMON PSITE,XTE,FTE,GAM,PE,FREQ,AMP,EPS,EP
      COMMON NTE,KMAX,MOTION,IMAX,LUP,LLOW,N1,NP1,L1,LP1
      COMMON NMIN,NMAX,LMIN,LMAX
      COMPLEX PHU,CPU,CPL,DEPHU,DPHUT
      COMPLEX DPHU,DELTAN,TANLOW,TANUP,TANUL,TANUT,TANLL,TANLT,
     X        TLOW,TUP,TUL,TUT,TLL,TLT
C
      DO 1 N= NP,NM
      IF(XX(N) .LT. -XTE) GO TO 1
      T= .5*(XX(N)- XTE)
      CALL TANGNT(N,TANLOW,TANUP,TANUL,TANUT,TANLL,TANLT)
      DPHU= T*DEPHU(N)
      DELTAN= T*(TANUP+ TANUL- TANLOW- TANLL)
      GO TO 2
    1 CONTINUE
C
    2 DO 3 I= N,NM
      II= I+1
      T= .5*(XX(II)- XX(I))
      CALL TANGNT(I,TLOW,TUP,TUL,TUT,TLL,TLT)
      CALL TANGNT(II,TANLOW,TANUP,TANUL,TANUT,TANLL,TANLT)
      IF(XX(II) .LT. XTE) GO TO 4
      DPHU= DPHU+ .5*(XTE- XX(I))*(DEPHU(I)+ DPHUT)
      DELTAN= DELTAN+ .5*(XTE- XX(I))*(TANUP+ TANUT- TANLOW- TANLT)
      RETURN
```

```
    4 DPHU= DPHU+ T*(DEPHU(I)+ DEPHU(II))
    3 DELTAN= DELTAN+ T*(TANUP+ TUP- TANLOW- TLOW)
C
      RETURN
      END
```

```
      SUBROUTINE WAKFIN(ZZ,WAKE1,WAKE2)
C
C     ****************************************************************
C     *THIS SUBROUTINE COMPUTES THE VALUE OF THE WAKE INTEGRALS, WAKE1  *
C     *AND WAKE2, THAT ARE TO BE INTEGRATED OVER THE INTERVAL 0 TO .5PI.*
C     *LEGENDRE-GAUSS QUADRATURE IS USED TO EVALUATE THE INTEGRALS      *
C     ****************************************************************
C
      REAL M,MU
      COMMON PHU(51,22,2), CPU(51),CPL(51), DEPHU(51), DPHUT
      COMMON XX(51), XP(51), F2(51), MU(51,22), PHI(51,22,1)
      COMMON A1,A2,A3,A4,B1,BM,BBM,M,PSI4,DPSI,DETA,X4,PER
      COMMON PSITE,XTE,FTE,GAM,PE,FREQ,AMP,EPS,EP
      COMMON NTE,KMAX,MOTION,IMAX,LUP,LLOW,N1,NP1,L1,LP1
      COMMON NMIN,NMAX,LMIN,LMAX
      COMPLEX PHU,CPU,CPL,DEPHU,DPHUT
      DIMENSION ZZ(LMAX)
      DATA PI/3.141593/
C
      IER= 0
      MIN= 8
      MAX= 20
      INCR= 4
      T1= .25*PI
      T2= FREQ*ZZ(LMAX)/BM
      T3= M*T2
      T4= 2./PI
C
      WAKE1= 0.
      WAKE2= 0.
      TEMP1= WAKE1
      TEMP2= WAKE2
      DO 1 N= MIN,MAX,INCR
      DO 2 I= 1,N
      READ(5,100) XG
      IF(N .LE. 16) READ(5,101) WG
```

```
      IF(N .GT. 16) READ(5,100) WG
      THETA= T1*(XG+ 1.)
      CALL BJY1(T3*SIN(THETA),RJ1,RY1,IER)
      CALL BK1(T3*SINH(THETA),RK1,IER)
      WAKE1= WAKE1+ WG*EXP(-T2*COS(THETA))*RJ1
    2 WAKE2= WAKE2+ WG*(EXP(-T2*COS(THETA))*RY1+ T4*EXP(-T2*COSH(
     X                    THETA))*RK1)
      WAKE1= T1*WAKE1
      WAKE2= T1*WAKE2
      IF(ABS(WAKE1- TEMP1) .LT. EPS .AND. ABS(WAKE2- TEMP2) .LT. EPS)
     X   GO TO 3
      WRITE(6,102) N,WAKE1,WAKE2
      TEMP1= WAKE1
      TEMP2= WAKE2
      WAKE1= 0.
      WAKE2= 0.
    1 CONTINUE
      N= N- INCR
C
    3 WRITE(6,103) N,WAKE1,WAKE2
      IF(N .EQ. MAX) RETURN
      N= N+ INCR
      DO 4 J= N,MAX,INCR
      DO 4 I= 1,J
      READ(5,100) XG
      IF(J .LE. 16) READ(5,101) WG
    4 IF(J .GT. 16) READ(5,100) WG
C
  100 FORMAT(F40.15)
  101 FORMAT(F39.15)
  102 FORMAT(' NUMBER OF POINTS=',I4,2X,'WAKE1=',F12.6,2X,'WAKE2=',
     X         F12.6)
  103 FORMAT(' NUMBER OF POINTS=',I4,2X,'CONVERGED WAKE1=',F12.6,2X,
     X         'CONVERGED WAKE2=',F12.6/)
      RETURN
      END
```

```
      SUBROUTINE WAKINF(ZZ,WAKE3)
C
C     ****************************************************************
C     *THIS SUBROUTINE COMPUTES THE VALUE OF THE WAKE INTEGRAL, WAKE3,  *
C     *THAT IS TO BE EVALUATED OVER THE INTERVAL .5PI TO INFINITY.      *
C     *GAUSS-LAGUERRE QUADRATURE IS USED TO CARRY OUT THE INTEGRATION   *
C     ****************************************************************
C
      REAL M,MU
      COMMON PHU(51,22,2), CPU(51),CPL(51), DEPHU(51), DPHUT
      COMMON XX(51), XP(51), F2(51), MU(51,22), PHI(51,22,1)
      COMMON A1,A2,A3,A4,B1,BM,BBM,M,PSI4,DPSI,DETA,X4,PER
      COMMON PSITE,XTE,FTE,GAM,PE,FREQ,AMP,EPS,EP
      COMMON NTE,KMAX,MOTION,IMAX,LUP,LLOW,N1,NP1,L1,LP1
      COMMON NMIN,NMAX,LMIN,LMAX
      COMPLEX PHU,CPU,CPL,DEPHU,DPHUT
      DIMENSION ZZ(LMAX)
      DATA PI/3.141593/
C
      IER= 0
      MIN= 24
      MAX= 32
      INCR= 4
      T1= .5*PI
      T2= FREQ*ZZ(LMAX)/BM
      T3= COSH(T1)
      T4= (SINH(T1))**2
      T5= M*T2
      T6= 2.*T2
      T7= (1./T2)**2
C
      WAKE3= 0.
      TEMP= WAKE3
      DO 1 N= MIN,MAX,INCR
      DO 2 I= 1,N
      READ(5,100) XG
```

```
      READ(5,100) WG
      CALL BK1(T5*SQRT(T7*XG*(XG+ T6*T3)+ T4),RK1,IER)
    2 WAKE3= WAKE3+ WG*RK1/SQRT(XG*(XG+ T6*T3)+ T4*T2**2)
      WAKE3= EXP(-T2*T3)*WAKE3
      IF(ABS(WAKE3- TEMP) .LT. EPS) GO TO 3
      WRITE(6,101) N,WAKE3
      TEMP= WAKE3
      WAKE3= 0.
    1 CONTINUE
      N= N- INCR
C
    3 WRITE(6,102) N,WAKE3
      IF(N .EQ. MAX) RETURN
      N= N+ INCR
      DO 4 J= N,MAX,INCR
      DO 4 I= 1,J
      READ(5,100) XG
    4 READ(5,100) WG
C
  100 FORMAT(F16.12)
  101 FORMAT(    ' NUMBER OF POINTS=',I4,2X,'INFINITE INTEGRAL HAS
     X       A VALUE=',F12.6)
  102 FORMAT(' NUMBER OF POINTS=',I4,2X,'CONVERGED VALUE OF INFINITE
     X         INTEGRAL=',F12.6/)
      RETURN
      END
```

```
      SUBROUTINE FARFLD(DPHU,DELTAN,WAKE1,WAKE2,WAKE3,ZZ,PUP,PDOWN,
     X                  PTOP,PBOT,NP,NM)
C
C     ****************************************************************
C     *THIS SUBROUTINE DEFINES THE FAR FIELD CONDITIONS                *
C     ****************************************************************
C
      REAL M,MU,LAMDA
      COMMON PHU(51,22,2), CPU(51),CPL(51), DEPHU(51), DPHUT
      COMMON XX(51), XP(51), F2(51), MU(51,22), PHI(51,22,1)
      COMMON A1,A2,A3,A4,B1,BM,BBM,M,PSI4,DPSI,DETA,X4,PER
      COMMON PSITE,XTE,FTE,GAM,PE,FREQ,AMP,EPS,EP
      COMMON NTE,KMAX,MOTION,IMAX,LUP,LLOW,N1,NP1,L1,LP1
      COMMON NMIN,NMAX,LMIN,LMAX
      COMPLEX PHU,CPU,CPL,DEPHU,DPHUT
      COMPLEX CIM,CZERO,DPHU,DELTAN,PUP(LMAX),PDOWN(LMAX),PTOP(NMAX),
     X        PBOT(NMAX),T1,T2,T3,T6,T7,H0,H1,PTRALU,PTRALL,PHUP,PHUL
      DIMENSION ZZ(LMAX)
      DATA PI/3.141593/, CIM/(0.,1.)/, CZERO/(0.,0.)/
C
      LAMDA= FREQ*M/BBM
      T1= .5*CIM*PI
      T2= CIM*LAMDA*M
      T3= CIM*FREQ/BBM
      T4= LAMDA**2*BBM
      T5= 2.*LAMDA*BBM
      T6= CIM*LAMDA*FREQ
      T7= T1*T4
      IER= 0
C
      X= .5*(XX(NMIN)+ XX(NMIN+1))
      X2= X**2
      DO 1 L= LMIN,LMAX
      T8= SQRT(X2+ BBM*ZZ(L)**2)
      T9= LAMDA*T8
      CALL BJY0(T9,RJ0,RY0,IER)
```

```
      CALL BJY1(T9,RJ1,RY1,IER)
      H0= RJ0- CIM*RY0
      H1= RJ1- CIM*RY1
      PUP(L)= T1*CEXP(T2*X)/BM*((-T4*X*ZZ(L)*H0/(T8**2)+
     X         (T5*X*ZZ(L)/(T8**3)- T6*ZZ(L)/T8)*H1)*DPHU+
     X         (T3*H0- LAMDA*X*H1/T8)*DELTAN+ H0*DPHUT)
      IER= 0
    1 CCNTINUE
C
      T8= SQRT(XTE**2+ BBM*ZZ(LMAX)**2)
      T9= LAMDA*T8
      CALL BJY0(T9,RJ0,RY0,IER)
      CALL BJY1(T9,RJ1,RY1,IER)
      H0= RJ0- CIM*RY0
      H1= RJ1- CIM*RY1
      PTRALU= T1*CEXP(T2*XTE)/BM*((-T4*XTE*ZZ(LMAX)*H0/(T8**2)+
     X         (T5*XTE*ZZ(LMAX)/(T8**3)- T6*ZZ(LMAX)/T8)*H1)*DPHU+
     X         (T3*H0- LAMDA*XTE*H1/T8)*DELTAN+ H0*DPHUT)
C
      X= .5*(XX(NM)+ XX(NMAX))
      X2= X**2
      DO 2 L= LMIN,LMAX
      T8= SQRT(X2+ BBM*ZZ(L)**2)
      T9= LAMDA*T8
      CALL BJY0(T9,RJ0,RY0,IER)
      CALL BJY1(T9,RJ1,RY1,IER)
      H0= RJ0- CIM*RY0
      H1= RJ1- CIM*RY1
      PDOWN(L)= T1*CEXP(T2*X)/BM*((-T4*X*ZZ(L)*H0/(T8**2)+
     X          (T5*X*ZZ(L)/(T8**3)- T6*ZZ(L)/T8)*H1)*DPHU+
     X          (T3*H0- LAMDA*X*H1/T8)*DELTAN+ H0*DPHUT)
      IER= 0
    2 CONTINUE
C
      T8= SQRT(XTE**2+ BBM*ZZ(LMIN)**2)
      T9= LAMDA*T8
```

```
      CALL BJY0(T9,RJ0,RY0,IER)
      CALL BJY1(T9,RJ1,RY1,IER)
      H0= RJ0- CIM*RY0
      H1= RJ1- CIM*RY1
      PTRALL= T1*CEXP(T2*XTE)/BM*((-T4*XTE*ZZ(LMIN)*H0/(T8**2)+
     X        (T5*XTE*ZZ(LMIN)/(T8**3)- T6*ZZ(LMIN)/T8)*H1)*DPHU+
     X        (T3*H0- LAMDA*XTE*H1/T8)*DELTAN+ H0*DPHUT)
C
      IER= 0
      L= LMAX
      DO 3 N= NP,NM
      T8= SQRT(XX(N)**2+ BBM*ZZ(L)**2)
      T9= LAMDA*T8
      CALL BJY0(T9,RJ0,RY0,IER)
      CALL BJY1(T9,RJ1,RY1,IER)
      H0= RJ0- CIM*RY0
      H1= RJ1- CIM*RY1
      PTOP(N)= T1*CEXP(T2*XX(N))/BM*((-T4*XX(N)*ZZ(L)*H0/(T8**2)+
     X         (T5*XX(N)*ZZ(L)/(T8**3)- T6*ZZ(L)/T8)*H1)*DPHU+
     X         (T3*H0- LAMDA*XX(N)*H1/T8)*DELTAN+ DPHUT*H0)
      IER= 0
    3 CONTINUE
C
      L= LMIN
      DO 4 N= NP,NM
      T8= SQRT(XX(N)**2+ BBM*ZZ(L)**2)
      T9= LAMDA*T8
      CALL BJY0(T9,RJ0,RY0,IER)
      CALL BJY1(T9,RJ1,RY1,IER)
      H0= RJ0- CIM*RY0
      H1= RJ1- CIM*RY1
      PBOT(N)= T1*CEXP(T2*XX(N))/BM*((-T4*XX(N)*ZZ(L)*H0/(T8**2)+
     X         (T5*XX(N)*ZZ(L)/(T8**3)- T6*ZZ(L)/T8)*H1)*DPHU+
     X         (T3*H0- LAMDA*XX(N)*H1/T8)*DELTAN+ DPHUT*H0)
      IER= 0
    4 CONTINUE
```

```
C
      T8= SQRT(XTE**2+ BBM*ZZ(LMAX)**2)
      T9= LAMDA*T8
      CALL BJY0(T9,RJ0,RY0,IER)
      CALL BJY1(T9,RJ1,RY1,IER)
      H0= RJ0- CIM*RY0
      H1= RJ1- CIM*RY1
      PHUP= T1*CEXP(T2*XTE)/BM*(-T4*ZZ(LMAX)*H1*DPHU/T8+ H0*DELTAN)+
     X      FREQ*M*T1*ZZ(LMAX)*DPHUT*(CIM*WAKE1+ WAKE2+ 2.*WAKE3/PI)/BM
      IER= 0
C
      T8= SQRT(XTE**2+ BBM*ZZ(LMIN)**2)
      T9= LAMDA*T8
      CALL BJY0(T9,RJ0,RY0,IER)
      CALL BJY1(T9,RJ1,RY1,IER)
      H0= RJ0- CIM*RY0
      H1= RJ1- CIM*RY1
      PHUL= T1*CEXP(T2*XTE)/BM*(-T4*ZZ(LMIN)*H1*DPHU/T8+ DELTAN*H0)+
     X      ZZ(LMIN)*FREQ*M*T1*DPHUT/BM*(CIM*WAKE1+ WAKE2+ 2.*WAKE3/PI)
C
      PHU(NTE,LMAX,2)=PHUP*CEXP(CIM*FREQ*(XTE- XX(NTE)))- .5*(XTE-
     X                XX(NTE))*(PTRALU*CEXP(CIM*FREQ*(XTE- XX(NTE)))+
     X                PTOP(NTE))
C
      PHU(NTE,LMIN,2)= PHUL*CEXP(CIM*FREQ*(XTE- XX(NTE)))- .5*(XTE-
     X                 XX(NTE))*(PTRALL*CEXP(CIM*FREQ*(XTE- XX(NTE)))+
     X                 PBOT(NTE))
C
      PHU(NTE+1,LMAX,2)=PHUP*CEXP(-CIM*FREQ*(XX(NTE+1)- XTE))+
     X                  .5*(XX(NTE+1)- XTE)*(PTOP(NTE+1)+ PTRALU*
     X                  CEXP(-CIM*FREQ*(XX(NTE+1)- XTE)))
C
      PHU(NTE+1,LMIN,2)= PHUL*CEXP(-CIM*FREQ*(XX(NTE+1)- XTE))+
     X                   .5*(XX(NTE+1)- XTE)*(PBOT(NTE+1)+ PTRALL*
     X                   CEXP(-CIM*FREQ*(XX(NTE+1)- XTE)))
C
```

```
      NT= NTE+ 2
      DO 5 N= NT,NM
      PHU(N,LMAX,2)= PHU(N-1,LMAX,2)*CEXP(-CIM*FREQ*(XX(N)- XX(N-1)))+
     X              .5*(XX(N)- XX(N-1))*(PTOP(N)+ PTOP(N-1)*CEXP(-CIM*
     X              FREQ*(XX(N)- XX(N-1))))
C
      PHU(N,LMIN,2)= PHU(N-1,LMIN,2)*CEXP(-CIM*FREQ*(XX(N)- XX(N-1)))+
     X               .5*(XX(N)- XX(N-1))*(PBOT(N)+ PBOT(N-1)*CEXP(-CIM*
     X              FREQ*(XX(N)- XX(N-1))))
    5 CONTINUE
C
      NT= NTE- NMIN- 1
      DO 6 I= 1,NT
      N= NTE- I
      PHU(N,LMAX,2)= PHU(N+1,LMAX,2)*CEXP(CIM*FREQ*(XX(N+1)- XX(N)))-
     X              .5*(XX(N+1)- XX(N))*(PTOP(N+1)*CEXP(CIM*FREQ*
     X              (XX(N+1)- XX(N)))+ PTOP(N))
C
      PHU(N,LMIN,2)= PHU(N+1,LMIN,2)*CEXP(CIM*FREQ*(XX(N+1)- XX(N)))-
     X               .5*(XX(N+1)- XX(N))*(PBOT(N+1)*CEXP(CIM*FREQ*
     X               (XX(N+1)- XX(N)))+ PBOT(N))
    6 CONTINUE
C
      RETURN
      END
```

```
      SUBROUTINE TRAIL(XT2)
C
C     ****************************************************************
C     *THIS SUBROUTINE LOCATES THE TRAILING EDGE AND COMPUTES THE      *
C     *STRETCHING FACTOR IN THE STREAMWISE DIRECTION AT THAT LOCATION  *
C     ****************************************************************
C
      REAL M,MU
      COMMON PHU(51,22,2), CPU(51),CPL(51), DEPHU(51), DPHUT
      COMMON XX(51), XP(51), F2(51), MU(51,22), PHI(51,22,1)
      COMMON A1,A2,A3,A4,B1,BM,BBM,M,PSI4,DPSI,DETA,X4,PER
      COMMON PSITE,XTE,FTE,GAM,PE,FREQ,AMP,EPS,EP
      COMMON NTE,KMAX,MCTION,IMAX,LUP,LLOW,N1,NP1,L1,LP1
      COMMON NMIN,NMAX,LMIN,LMAX
      COMPLEX PHU,CPU,CPL,DEPHU,DPHUT
      DATA PI/3.141593/, TMIN/.00001/
C
      X3(PSI)= X4+ A2*TAN(.5*PI*(PSI-PSI4))+
     X         A3*TAN(.5*PI*(PSI- PSI4)**3)
C
      SP= DPSI
      PSI= -(1.+ PSI4)+ DPSI
      DO 1 N= 2,N1
      IF(XX(N+1) .LT. XTE) GO TO 8
      NTE= N
      XT1= X3(PSI)
      IF(X3(PSI+ DPSI) .GE. XTE) GO TO 2
    8 PSI= PSI+ DPSI
    1 CONTINUE
C
    2 SP= .5*SP
      PSI= PSI+ SP
      PSITE= PSI
    6 XT2= X3(PSI)
      IF(ABS(XT2- XTE) .LE. TMIN) GO TO 9
      IF(XT2 .GT. XTE) GO TO 4
```

```
      IF(XT1 .GT. XTE) GO TO 5
      PSI= PSI+ SP
      PSITE= PSI
      XT1= XT2
      GO TO 6
C
    5 SP= .5*SP
      PSI= PSI+ SP
      PSITE= PSI
      XT1= XT2
      GO TO 6
C
    4 IF(XT1 .GT. XTE) GO TO 7
      XT1= XT2
      SP= .5*SP
      PSI= PSI- SP
      PSITE= PSI
      GO TO 6
C
    7 PSI= PSI- SP
      PSITE= PSI
      XT1= XT2
      GO TO 6
C
    9 FTE= 2./(PI*(A2/((COS(.5*PI*(PSITE- PSI4)))**2)+
     X      3.*A3*(PSITE- PSI4)**2/((COS(.5*PI*(PSITE- PSI4)**3))**2)))
C
      RETURN
      END
```

```
      SUBROUTINE GROWX
C
C     ****************************************************************
C     *THIS SUBROUTINE CALCULATES THE GRID GROWTH FACTORS IN THE      *
C     *STREAMWISE DIRECTION                                           *
C     ****************************************************************
C
      REAL M,MU
      COMMON PHU(51,22,2), CPU(51),CPL(51), DEPHU(51), DPHUT
      COMMON XX(51), XP(51), F2(51), MU(51,22), PHI(51,22,1)
      COMMON A1,A2,A3,A4,B1,BM,BBM,M,PSI4,DPSI,DETA,X4,PER
      COMMON PSITE,XTE,FTE,GAM,PE,FREQ,AMP,EPS,EP
      COMMON NTE,KMAX,MOTION,IMAX,LUP,LLOW,N1,NP1,L1,LP1
      COMMON NMIN,NMAX,LMIN,LMAX
      COMPLEX PHU,CPU,CPL,DEPHU,DPHUT
      DATA PI/3.141593/
C
      PSI= -(1.+ PSI4)+ DPSI
      DO 1 N= 2,N1
      IF(PSI .LT. -PSI4)
     X  F2(N)= 2./(PI*(A2/((COS(.5*PI*(PSI+ PSI4)))**2)+
     X          3.*A3*(PSI+ PSI4)**2/((COS(.5*PI*(PSI+ PSI4)**3))**2)))
C
      IF(PSI .GE. -PSI4 .AND. PSI .LE. PSI4)
     X  F2(N)= 1./(A4+ 3.*B1*PSI**2)
C
      IF(PSI .GT. PSI4)
     X  F2(N)= 2./(PI*(A2/((COS(.5*PI*(PSI- PSI4)))**2)+
     X          3.*A3*(PSI- PSI4)**2/((COS(.5*PI*(PSI- PSI4)**3))**2)))
C
      PSI= PSI+ DPSI
    1 CONTINUE
C
      F2(1)= 0.
      F2(NP1)= 0.
C
```

```
RETURN
END
```

```
      SUBROUTINE GROWZ(H)
C
C     ***************************************************************
C     *THIS SUBROUTINE CALCULATES THE GRID GROWTH FACTORS IN THE      *
C     *LATERAL DIRECTION                                              *
C     ***************************************************************
C
      REAL M,MU
      COMMON PHU(51,22,2), CPU(51),CPL(51), DEPHU(51), DPHUT
      COMMON XX(51), XP(51), F2(51), MU(51,22), PHI(51,22,1)
      COMMON A1,A2,A3,A4,B1,BM,BBM,M,PSI4,DPSI,DETA,X4,PER
      COMMON PSITE,XTE,FTE,GAM,PE,FREQ,AMP,EPS,EP
      COMMON NTE,KMAX,MOTION,IMAX,LUP,LLOW,N1,NP1,L1,LP1
      COMMON NMIN,NMAX,LMIN,LMAX
      COMPLEX PHU,CPU,CPL,DEPHU,DPHUT
      DIMENSION H(LMAX)
      DATA PI/3.141593/
C
      ETA= -1.+ DETA
      DO 1 L= 2,L1
      H(L)= (2.*(COS(.5*PI*ETA))**2)/(A1*PI)
      ETA= ETA+ DETA
    1 CONTINUE
C
      H(1)= 0.
      H(LP1)= 0.
C
      RETURN
      END
```

REFERENCES

1. Guderley, G. and Yoshihara, H., "The Flow over a Wedge Profile at Mach Number 1," Journal of the Aeronautical Sciences, Vol. 17, No. 11, pp. 723-735,1950.

2. Cole, J. D., "Drag of a Finite Wedge at High Subsonic Speeds," Journal of Mathematics and Physics, Vol. 30, No. 2, pp. 79-93, 1951.

3. Guderley, G. and Yoshihara, H., "Two Dimensional Unsymmetric Flow Patterns at Mach Number 1," Journal of the Aeronautical Sciences, Vol. 20, No. 11, pp. 757-768, 1953.

4. Nieuwlang, G. Y. and Spee, B. M.,"Transonic Airfoils: Recent Developments in Theory, Experiment and Design," Annual Review of Fluid Mechanics, Vol. 5, pp. 119-150, 1973.

5. Boerstoel, J. W., "Review of the Application of Hodograph Theory to Transonic Aerofoil Design and Theoretical and Experimental Analysis of Shock-Free Aerofoils," IUTAM Symposium Transsonicum, pp. 109-133, 1975.

6. Spreiter, J. R. and Alksne, A. Y., "Thin Airfoil Theory Based on Approximate Solutions of the Transonic Flow Equation," NACA Report 1359, 1958.

7. Landahl, M. T., Unsteady Transonic Flow, Pergamon Press, New York, 1961.

8. Magnus, R. and Yoshihara, H., "Inviscid Transonic Flow over Airfoils," AIAA Paper 70-47, 1970.

9. Murman, E. M. and Cole, J. D., "Calculation of Plane Steady Transonic Flows," AIAA Journal, Vol. 9, No. 1, pp. 114-121, 1971.

10. Murman, E. M., "Analysis of Embedded Shock Waves Calculated by Relaxation Methods," AIAA Computational Fluid Dynamics Conference. pp. 27-40, 1973.

11. Landahl, M. T., "Some Recent Developments in Unsteady Transonic Flow Research," IUTAM Symposium Transsonicum, pp. 1-32, 1975.

12. McCroskey, W. J., "Some Current Research in Unsteady Fluid Dynamics," Transactions of the ASME, pp. 8-38, 1977.

13. Jameson, A., "Transonic Flow Calculations," Von Karman Institute Lectures, 1976.

14. Ballhaus, W. F., "Some Recent Progress in Unsteady Transonic Flow Computations," Von Karman Institute Lectures, 1976.

15. Jameson, A., "Iterative Solutions of Transonic Flows over Airfoils and Wings, Including Flows at Mach 1," Communications on Pure and Applied Mathematics, Vol. 27, pp. 283-309, 1974.

16. Jameson, A., "Transonic Potential Flow Calculations using Conservation Form," AIAA Computational Fluid Dynamics Conference, pp. 148-161, 1975.

17. Ballhaus, W. F. and Goorjian, P. M., "Implicit Finite-Difference Computations of Unsteady Transonic Flows about Airfoils," AIAA Journal, Vol. 15. No. 12, pp. 1728-1735, 1977.

18. Stahara, S. S. and Spreiter, J. R., "Unsteady Local Linearization Solution for Pulsating Bodies at M = 1, AIAA Journal, Vol. 14. No. 7, pp. 990-992, 1976.

19. Stahara, S. S. and Spreiter, J. R., "Unsteady Local Linearization Solution for Pitching Bodies of Revolution at M = 1: Stability Derivative Analysis," AIAA Journal, Vol. 14, No. 10, pp. 1402-1408, 1976.

20. Isogai, K., "Unsteady Transonic Flow over Oscillating Circular-Arc Airfoils," AIAA Paper 74-360, 1974.

21. Ehlers, F. E., "A Finite Difference Method for the Solution of the Transonic Flow around Harmonically Oscillating Wings," NASA CR-2257, 1974.

22. Traci, R. M., Farr, J. L., and Albano, E. D., "Perturbation Method for Transonic Flows about Oscillating Airfoils," AIAA Paper 75-877, 1975.

23. Traci, R. M., Albano, E. D., and Farr, J. L., "Small Disturbance Transonic Flows about Oscillating Airfoils and Planar Wings," AFFDL-TR-75-100, 1975.

24. Tijdeman, H. and Zwaan, R. J., "On the Prediction of Aerodynamic Loads on Oscillating Wings in Transonic Flow," NLR MP 73026 U, 1973.

25. Tijdeman, H., "High Subsonic and Transonic Effects in Unsteady Aerodynamics," NLR TR 75079 U, 1975.

26. Nixon, D., "Perturbations of a Discontinuous Transonic Flow," AIAA Journal, Vol. 16, No. 1, pp. 47-52, 1978.

27. Nixon, D., "Perturbations in Two and Three Dimensional Transonic Flows," AIAA Journal, Vol. 16, No. 7, pp. 699-709, 1978.

28. Rubbert, P. E. and Landahl, M. T., "Solution of the Transonic Airfoil Problem through Parametric Differentiation," AIAA Journal, Vol. 5, No. 3, pp 470-479, 1967.

29. Yu, N. J. and Seebass, A. R., "Inviscid Transonic Flow Computations with Shock Fitting," IUTAM Symposium Transsonicum, pp. 449-456, 1975.

30. Hafez, M. M. and Cheng, H. K., "Shock Fitting Applied to Relaxation Solutions of Transonic Small Disturbance Equations," AIAA Journal, Vol. 15, No. 6, pp. 786-793, 1977.

31. Ashley, H. and Landahl, M. T., Aerodynamics of Wings and Bodies, Addison-Wesley, Reading, MA, 1965.

32. Liepmann, H. W. and Roshko, A., Elements of Gasdynamics, John Wiley and Sons, Inc., New York, 1967.

33. Krupp, J. A., "The Numerical Calculation of Plane Steady Transonic Flows past Thin Lifting Airfoils," Boeing Scientific Research Laboratory Document D180-12958-1. 1971.

34. Satyanarayana, B. and Davis, S., "Experimental Studies of Unsteady Trailing Edge Conditions," AIAA Journal, Vol. 16, No. 2, pp. 125- 129, 1978.

35. Archibald, F. S., "Unsteady Kutta Condition at High Values of the Reduced Frequency Parameter," Journal of Aircraft, Vol. 12, No. 6, pp. 545-550, 1975.

36. Rubbert, P. E. and Landahl, M. T., "Solution of Nonlinear Flow Problems through Parametric Differentiation," Physics of Fluids, Vol. 10, No. 4, pp. 831-835, 1967.

37. Whitlow, W., "Inviscid, Unsteady, Non-Linear, Internal Transonic Flow," MIT S.M. Thesis, 1975.

38. Whitlow, W. and Harris, W. L., "Solutions to Internal Transonic Flows via Parametric Differentiation," Transonic Flow Problems in Turbomachinery, Hemisphere Publishing Corp., Washington, D. C., p. 346, 1977.

39. Jischke, M. C. and Baron, J. R., "Application of Parametric Differentiation to Radiative Gasdynamics," AIAA Journal, Vol. 7, No. 7, pp. 1326-1335, 1969.

40. Harris, W. L., Sr., "Farfield Viscous Effects in Nonlinear Noise Propagation," Journal of the Acoustical Society of America, Vol. 56, No. 2, pp. 313-322, 1974.

41. Hamming, R. W., Numerical Methods for Scientists and Engineers, McGraw-Hill, New York, 1962.

42. Miles, J. W., "Linearization of the Equations of Non-Steady Flow in a Compressible Fluid," Journal of Mathematics and Physics, Vol. 33, No. 2, pp. 135-143, 1954.

43. Lin, C. C., Reissner, E., and Tsien, H., "On Two-Dimensional Non-Steady Motion of a Slender Body in a Compressible Fluid," Journal of Mathematics and Physics, Vol. 27, No. 3, pp. 220-231, 1948.

44. Carlson, L. A., "Transonic Airfoil Flow Field Analysis Using Cartesian Coordinates, NASA CR-2577, 1975.

45. Ballhaus, W. F. and Bailey, F. R., "Numerical Calculation of Transonic Flow about Swept Wings," AIAA Paper 72-677, 1972.

46. Rubbert, P. E.,"Analysis of Transonic Flow by means of Parametric Differentiation," MIT FDRL Report No. 65-2, 1965.

47. Knechtel, E. D., "Experimental Investigation at Transonic Speeds of Pressure Distributions over Wedge and Circular-Arc Airfoil Sections and Evaluation of Perforated-Wall Interference," NASA TN D-15, 1959.

48. Ogana, W., "Numerical Solution for Subcritical Flows by a Transonic Integral Equation Method," AIAA Journal, Vol. 15, No. 3, pp. 444-446, 1977.

49. Sivaneri, N. T., "Transonic Flows by Parametric Differentiation and Integral Equation Techniques," MIT S.M. Thesis, 1978.

50. Weatherill, W. H., Ehlers, F. E., and Sebastian, J. D., "Computation of the Transonic Perturbation Flow Fields around Two and Three Dimensional Oscillating Wings," NASA CR-2599, 1975.

51. Cunningham, A. M., Jr., "A Steady and Oscillatory Kernal Function Method for Interfering Surfaces in Subsonic, Transonic, and Supersonic Flow," NASA CR-144895, 1976.

52. Weatherill, W. H., Sebastian, J. D., and Ehlers, F. E., "Application of a Finite Difference Method to the Analysis of Transonic Flow over Oscillating Airfoils and Wings," AGARD-CP-226, p. 17, 1977.

53. Ballhaus, W. F., Jameson, A., and Albert, J., "Implicit Approximate Factorization Schemes for the Efficient Solution

of Steady Transonic Flow Problems," NASA TMX-73,202, 1977.

54. Carrier, G. F., Krook, M., and Pearson, C. E., Functions of a Complex Variable, McGraw-Hill, New York, 1966.

55. Williams, M. H., "Linearization of Unsteady Transonic Flows Containing Shocks," AIAA Journal, Vol. 17, No. 4, pp. 394-397, 1979.

BIOGRAPHY

Woodrow Whitlow, Jr. was born to Woodrow and Willie Mae Whitlow on December 13, 1952 in Inkster, Michigan. He was enrolled in Carver Elementary School in September 1957 and later attended Fellrath Junior High School, both in Inkster. In June 1970, he graduated from Inkster High School as valedictorian.

In September 1970, Mr. Whitlow enrolled in the Massachusetts Institute of Technology (MIT) where he majored in Aeronautics and Astronautics. On January 6, 1971, he married Michele Carnita Wimberly, and two children, Mary Annessa and Natalie Michele, were born into that marriage. Woodrow received his Bachelor of Science degree in Aeronautics and Astronautics in May 1974. That year, he was also awarded the Department of Aeronautics and Astronautics James Means Memorial Prize and won first prize in the American Institute of Aeronautics and Astronautics (AIAA) New England Section Student Awards Program.

Mr. Whitlow began graduate study at MIT in September 1974 and received the Master of Science degree in Aeronautics and Astronautics in June 1975. His Master's thesis, entitled "Inviscid, Unsteady, Nonlinear, Internal Transonic Flow," was supervised by Professor Wesley L. Harris. In September 1975, Mr. Whitlow entered the doctoral program in the MIT Department of Aeronautics and Astronautics and was supported by a departmental research assistantship.

Mr. Whitlow is a member of the AIAA, Sigma Xi and the National

Society of Black Engineers. His puplications are:

Whitlow, W. and Harris, W. L., "Sonic Boom Propagation through Nonuniform Flow Fields," AIAA Paper 76-586, 1976.

Whitlow, W. and Harris, W. L., "Solutions to Internal Transonic Flows via Parametric Differentiation," Transonic Flow Problems in Turbomachinery, T. C. Adamson and M. F. Platzer, Eds., Hemisphere Publishing Corp., Washington, D. C., p. 346, 1977.

Mr. Whitlow is a sports enthusiast who enjoys baseball, football, basketball, tennis and bowling. His hobbies include building model airplanes and building and flying model rockets. Mr. Whitlow has accepted a position at the National Aeronautics and Space Administration's Langley Research Center. There, he will begin his career by doing research on unsteady aerodynamics.